MECHANISMS INVOLVED IN HUMAN THERMOGENESIS

Dr Fleur Talbot

Department of Clinical Biochemistry

University of Cambridge

This dissertation is submitted for the degree of *Doctor of Philosophy*

Wolfson College **January 2018**

Declaration

I declare that this dissertation is the result of my own work and includes nothing which is the outcome of work done in collaboration except as declared in the Preface and specified in the text.

I declare that this dissertation is not substantially the same as any that I have submitted, or, is being concurrently submitted for a degree or diploma or other qualification at the University of Cambridge or any other University or similar institution except as declared in the Preface and specified in the text. I further state that no substantial part of my dissertation has already been submitted, or, is being concurrently submitted for any such degree, diploma or other qualification at the University of Cambridge or any other University of similar institution except as declared in the Preface and specified in the text.

I declare this dissertation does not exceed the prescribed limit of length, being less than 60,000 words.

To my family

For their love, support and laughter

Acknowledgements

This PhD is not “mine”, it’s “ours”. Without any of the people listed below, I would not have a thesis for submission. I am so grateful to have had you all as colleagues, and I hope to long cherish our friendships.

Firstly I would like to thank my mentor, supervisor and friend, Prof Sadaf Farooqi, the fiercest, most loyal and hilarious person I know. Thank you for everything: the mentorship, the pep talks, for believing in me when I didn’t believe in myself. Not to mention the parties and the samosas…! You are the best role model I could have asked for, and the past three years have been completely brilliant. I am going to miss working with you a lot.

Thank you to Elana Henning for everything. You have been a serene and calming presence in a very intense study, and I couldn’t have got through it without your kindness, common sense and determination, not to mention sense of humour and hard work. I feel very lucky to know you.

Thank you to Julia Keogh for being the world’s best ethics committee negotiator, and for your support. We will always have Newcastle…! Thank you also to Zoe Humphries for her persistence in contacting patients, and to the TRF team for making it such a fantastic working environment.

Thank you to Dr Jacek Mokrosinski for the lab tutorials, endless (endless!) patience, kindness and understanding. And bread. The world’s best bread. You’ve been a great mentor.

Thank you to Dr Agatha Van der Klaauw for your help with getting to grips with clinical data analysis, and your ongoing enthusiasm and guidance, and “hypothalamic tea”! And for the second mortgage I nearly had to take out after our Copenhagen shopping trip!

Thank you to Dr Edson de Mendes and Dr Matthew Banton for confocal expertise (and friendship), and to Dr Lukas Stadler for ImageJ analysis (and sarcasm).

Thank you to Dr Albert Koulman and Larissa Richardson for all their help with the metabolomics data. I really appreciated how quickly you managed to turn the samples around.

Thank you to Dr Birgitta Olofsson for her help with *C. elegans*. It was lovely working with you.

Thank you to Dr Tak Sonoyama and Dr Katherine Lawler for the work analysing the metabolomics data.

Thank you to Vikram Ayinampudi for assay support and Jenny Backhaus for cooling suit training.

Thank you to The Evelyn Trust and The Wellcome Trust for funding this work.

Thank you to family, and especially my lovely Mum for all the babysitting.

Thank you to Barney for the endless support and cups of tea. And for being the love of my life.

And especially thank you to Frida and Henry for being the naughtiest, loveliest and most brilliant kids anyone could ever wish for. This is for you. I love you more than I can ever tell you.

Summary

Energy expenditure in humans is partially understood. Sympathetic drive is an important stimulator of brown-adipose tissue-mediated increases in energy expenditure, and it is known that leptin-mediated pathways in part contribute to this.

This thesis has sought to understand human energy expenditure further by two different methods. Firstly, we have characterised the first rare human mutations in G protein-coupled receptor 10 (GPR10), a G protein coupled receptor expressed in key brain areas associated with energy homeostasis. GPR10-mediated signalling in the dorsomedial hypothalamus is necessary for the thermogenic effects of leptin. We have undertaken a detailed functional study of the mutations found from the whole exome and targeted resequencing of patients with severe early onset obesity, recruited to the Genetics of Obesity Study (GOOS). We have demonstrated that thirteen of the fifteen mutations found result in a complete or partial loss of function *in vitro*. We have additionally demonstrated that the mutations resulting in a complete loss of function on wild type receptor. This is important because the human mutations are found in heterozygous form.

Secondly, we have conducted a randomised cross-over study of the effects of mild cooling on healthy lean men. We have demonstrated that exposure to temperatures of 16^{o}C for two hours results in an increase in systolic blood pressure and pulse rate, relative to thermoneutral conditions. Cold exposure resulted in a drop in circulating leptin, which in common with previous studies on macronutrient preference in patients with disrupted leptin-melanocortin signalling, is associated with an increase in consumption of high fat food.

Cooling is known to be neuroprotective in acute brain injury, and recent published data suggests a protective effect in chronic neurodegenerative conditions by improvements in synaptic plasticity. We have demonstrated an improvement in neurocognition after two hours of mild cooling. We have additionally shown increases in docoshexaenoic acid, a polyunsaturated fatty acid known to play a role in neuroprotection, with a role in maintaining membrane fluidity.

These studies broaden our knowledge of human energy homeostasis. They provide evidence for the role of GPR10 in human energy homeostasis, and a rationale for the targeting of GPR10-mediated signalling pharmacologically, and provide some evidence for a role in improved neurocognition in humans.

Table of contents

List of figures

List of tables

Abbreviations

A1	Alpha-1 noradrenergic receptor
A2	Alpha-2 noradrenergic receptor
AAV	Adeno-associated virus
ACE-III	Addenbrooke's Cognitive Examination III
ACTH	Adrenocorticotrophic hormone
ADP	Adenosine diphosphate
ANCOVA	Analysis of covariance
ANOVA	Analysis of variance
AP-1	Activator-protein 1
AVP	Arginine vasopressin
B3	Beta-3 adrenergic receptor
BARCIST	Brown Adipose Reporting Criteria in Imaging STudies
BAT	Brown adipose tissue
BDNF	Brain-derived neurotrophic factor
BDZ	Benzodiazepine
BEH	Bridged Ethylsiloxane hybrid
$B_{max,}$	Maximal binding
BMI	Body mass index
BMR	Basal metabolic rate
BRET	Bioluminescent resonance energy transfer
BRET	Bioluminescent resonance energy transfer

BSA	Bovine serum albumin
cAMP	Cyclic adenosine monophosphate
CARS	Coherent anti-Stokes Raman scattering
CBAL	Core Biochemical Assay Laboratory
CCK	Cholecystokinin
CCK	Cholecystokinin
cDNA	Complementary deoxyribonucleic acid
Cer	Ceramides
cm	centimetres
COS-7	C V-1 in Origin with S V40 genes-7
CRH	Corticotrophin releasing hormone
CT	Computer tomography
CXCR	Chemokine receptor
DAGs	Diacylglycerols
DAPI	4',6-diamidino-2-phenylindole
dBP	Diastolic blood pressure
DEXA	Dual X-ray Absorptiometry
DHA	Docosahexaenoic acid
DIHRMS	Direct infusion high resolution mass spectrometry
DIO	Diet induced obesity
DIO2	Deiodinase-2 enzyme
DMEM	Dulbecco’s modified eagles medium
DMH	Dorsomedial hypothalamus
DMN	Dorsomedial nucleus

DNA	Deoxyribonucleic acid
DREADD	Designer receptors exclusively activated by designer drugs
dv	Dependent variable
EDTA	Ethylenediaminetetraacetic acid
EE	Energy expenditure
EEG	Electroencephalogram
ELISA	Enzyme-linked immunosorbent assay
EMG	Electromyogram
EMG	Electromyogram
ERK	Extracellular signal-regulated kinase
FAHFAs	Fatty acid ester of hydroxyl fatty acids
FDG	Fludeoxyglucose
FDG-PET	Fludeoxyglucose-positron emission tomography
FFAs	Free fatty acids
FIA	Flow-injection analysis mass spectrometry
FLAG	FLAG octapeptide
FRET	Fluorescent resonance energy transfer
g	Grams
GABA	Gamma amino-butyric acid
GEM	Gas exchange monitor
Gi	G alpha i protein (inhibitory)
GOOS	Genetics of Obesity Study
GPCR	G protein coupled receptor
GPR10	G protein coupled receptor 10

Gq	G alpha q protein
Gs	G alpha s protein (stimulatory)
GWAS	Genome-wide association study
H_2O	Water
HBSS	Hanks balanced salt solution
HEK293	Human embryonic kidney-293 cell line
HEPES buffer	4-(2-hydroxyethyl)-1-piperazineethanesulfonic acid buffer
HFD	High fat diet
HPA	Hypothalamo-pituitary-adrenal
HR	Heart rate
IBMX	3 isobutyl-1-methylxanthine
IC_{50}	Inhibitory concentration 50%
icv	Intra-cerebroventricular
ip	Intraperitoneal
IP1	Inositol monophosphate
IP3	Inositol triphosphate
IPA	Isopropyl alcohol
JNK	Jun kinase
kcal	Kilocalorie
KCl	Potassium chloride
KD	Dissociation constant
K_D	Dissociation constant
KEGG	Kyoto Encyclopaedia of Genes and Genomes
KG	Kilogram

KO	Knockout
LepR	Leptin receptor
LepRb	Leptin receptor
LIMMA	Linear Models for Microarrays
LOF	Loss of function
LPE	Lysophosphatidylethanolamines
LPS	Lipopolysaccharide
LPXRFa	LPXRFamide
LS	Least squares
MAF	Minor allele frequency
MAGs	Monoacylglycerols
MAP	Mean arterial pressure
MAPK	Mitogen activated protein kinase
MC4R	Melanocortin 4 receptor
MeOH	Methanol
MgCl2	Magnesium chloride
MJ	Megajoule
ML	Millilitre
mM	Millimolar
mmHG	Millimeters of mercury
MRM	Multiple reaction monitoring
mRNA	Messenger RNA
MS	Mass spectrometry
MSH	Melanocyte stimulating hormone

MS-mix	Mass spectrometry mix
MT	Mutant
MTBE	Methyl tert-butyl ether
N2 strain	Wild type *C. elegans* strain
NaCl	Sodium chloride
NaOH	Sodium hydroxide
NF-kB	Nuclear factor-kappa B
ng	Nanograms
NH_4Ac	Ammonium acetate
NIHR	National Institute for Health Research
nMOL	Nanomolar
NPFF	Neuropeptide FF
NPFFR2	Neuropeptide FF receptor 2
npr-6	Neuropeptide receptor 6
NTS	Nucleus of the tractus solitarius
ob gene	Obese gene, encodes leptin
OLETF	Otsuka Long Evans Tokushima Fatty
OP-50	Wormbase ID of *E. Coli* strain
OPO	Optical parametric oscillator
PBS	Phosphate buffered saline
pCMV-Tag2B	Cytomegalovirus-Tag2B vector
PIP2	Phosphoinositol diphosphate
POMC	Pro-opiomelanocortin
PRLHR	Prolactin releasing peptide hormone receptor

PrRP	Prolactin releasing peptide
pSTAT3	Phosphorylated Signal transducer and activator of transcription 3
PVN	Paraventricular nucleus
QFRP	pyroglutamylated RFamide peptide
RANOVA	Repeated measures analysis of variance
RAVLT	Rey auditory verbal learning test
RBM3	RNA Binding Protein 3
RBM-3	RNA binding protein 3
RCT	Random controlled trials
RPM	Rotations per minute
RQ	Respiratory quotient
RTP	Room temperature and pressure
sBP	Systolic blood pressure
SD	Standard deviation
SEM	Standard error of mean
SNS	Sympathetic nervous system
SRC-1	Steroid receptor complex-1
SS	Sum of squares
T3, fT3	Triiodothyronine
T4, fT4	Thyroxine
TAGs	Triacylglycerols
Tc	Core temperature
TH	Tyrosine hydroxylase
TPEF	Two photon excitation fluorescence

tRNA	Transfer ribonucleic acid
TSH	Thyroid stimulating hormone
UCP-1	Uncoupling protein 1
ug	Microgram
uL	Microlitre
uM	Micromolar
UPLC	Ultra-performance liquid chromatography
V1-R	Vasopressin 1 receptor
VAS	Visual analogue scale
VLM	Ventrolateral medulla
VO2	Volume of oxygen
WAT	White adipose tissue
WT	Wild type
YSi SPA	Yttrium coated scintillation proximity assay beads

CHAPTER ONE: INTRODUCTION

1.1. Obesity

1.1.1. The rising prevalence of obesity in society and its associated health consequences

Obesity is defined as an increase in fat mass sufficient to adversely affect health (Kuri-Morales, Emberson et al. 2009). Body mass index (BMI, weight/height^2 (kg/m^2) is used as a surrogate marker for fat mass, and the World Health Organisation categorises obesity as a BMI >30 kg/m^2. Using this definition, the prevalence of obesity has increased dramatically in developed countries over the past three decades. In 2008, 10% of men and 14% of women in the world were obese (BMI ≥30 kg/m^2), compared with 5% for men and 8% for women in 1980 (www.who.int), a near-doubling in the prevalence of obesity.

Being overweight or obese is associated with excessive morbidity and mortality. Obesity is associated with increased blood pressure, dyslipidaemia and insulin resistance. Risks of coronary heart disease, ischemic stroke and type 2 diabetes mellitus increase with increasing BMI, as does the risk of cancers of the breast, colon, prostate, endometrium, kidney and gall bladder. At an individual level, obesity also incurs significant social stigma, and has been associated with lower self-esteem and educational attainment (Gavrilova, Leon et al. (1999)).

1.1.2. Aetiology of obesity: genetic and environmental contributors

Evidence for the environmental influence on obesity prevalence is provided by the inverse relationship between BMI and social class and the trend for an increase in BMI in developing countries undergoing industrialisation and urbanisation. Whilst sedentary lifestyles and ready access to highly palatable, energy dense foods, are undoubtedly significant factors, there is considerable variability between individuals in body weight and fat mass within a given environment, suggesting a complex interaction between genetic, environmental and behavioural influences.

Direct evidence for the role of genetics is provided by a number of seminal studies looking at BMI in twins, between family members and in adopted children. Analysis of waist circumference and BMI in over 5000 UK twin pairs growing up during the obesity epidemic demonstrated a heritability of 77% for both (Wardle, Carnell et al. 2008). A similar estimate of heritability was found in analysis of 53 twin pairs reared apart (Allison, Kaprio et al. 1996). Furthermore, a study comparing the degree of obesity in adopted children with those in their full or half siblings raised by the biological parent found an increase in BMI of the full sibling when the adoptee was overweight or obese (Sorensen, Holst et

al. 1998). These studies support the contribution of genetics to obesity, and make a genetic approach to the delineation of molecular pathways controlling energy homeostasis feasible.

Several genome-wide association studies (GWAS) have been performed to identify common variants (minor allele frequency (MAF) > 5%) associated with BMI or obesity. For example, the GIANT consortium identified 97 BMI-associated loci (P < 5 × 10(-8)), 56 of which were novel, accounting for approximately 2.7% of BMI variation (Locke, Kahali et al. 2015). However, using common variants to dissect the pathways governing energy homoeostasis is challenging as the effect size associated with variants is invariably small, and because variants are often in noncoding regions of the genome. The largest GWAS signal for obesity has consistently come from an area upstream of the *FTO* gene; possession of two copies of the obesity associated allele increases mean BMI by 2.7kg/m^2 (Frayling, Timpson et al. 2007).

It has been shown that the characterisation of rare obesity-associated human variants can provide information about the molecular pathways controlling body weight. To date such approaches have provided important evidence for the role of the leptin-melanocortin pathway in energy homeostasis. The majority of these monogenic disorders result in hyperphagia, but there are a small number of genetic disorders, involving *KSR2* and *GNAS1* where obesity may also arise as a result of reduced energy expenditure (Chan, Heist et al. 2003, Pearce, Atanassova et al. 2013).

1.1.3. Homeostatic regulation of body weight

Obesity arises from the persistent imbalance between energy intake and energy expenditure which leads to weight gain. In humans, at thermoneutrality, approximately 70% of energy expenditure is accounted for by basal metabolic rate (the metabolic cost of processes such as the maintenance of transmembrane ion gradients and resting cardiopulmonary activity), with the thermic effect of food contributing ~10% and physical activity ~20%. The dissection of the mechanisms underlying human energy expenditure therefore has the potential to reveal novel targets that could be exploited for weight loss. Additionally, homeostatic physiological mechanisms compensate for any reduction in energy intake. For example, caloric restriction results in a reduction in total daily energy expenditure in overweight participants under free living conditions of up to 633 kcal/day with severe caloric restriction (890 kcal/day) (Redman, Heilbronn et al. 2009). The targeting of mechanisms that contribute to this adaptive response could provide a useful adjunct to dieting to improve the likelihood of successful long-term weight loss. Therefore, the focus of this thesis is on understanding the molecular and physiological mechanisms involved in human energy expenditure.

1.2. Leptin

1.2.1. The discovery of leptin as a pivotal regulator of energy homeostasis

The discovery of leptin in 1994 paved the way for the understanding of the molecular mechanisms involved in the regulation of energy balance (Zhang, Proenca et al. 1994). Leptin was discovered through the study of the severely obese *ob/ob* mouse, which occurred as a spontaneous mutation in an inbred strain of mice (Ingalls, Dickie et al. 1950). These mice gained weight rapidly, and were distinguishable by 4-6 weeks from their wild type littermates, eventually weighing up to four times that of a normal mouse. They developed diabetes mellitus and were sterile. Parabiosis experiments had demonstrated that *ob/ob* mice were deficient for a blood-borne factor, and it was initially hypothesised that this was cholecystokinin (CCK) (Pelleymounter, Cullen et al. 1995). In 1994 Friedman and colleagues used positional cloning to demonstrate that the *ob* gene and the *CCK* gene mapped to different chromosomes. They then showed, using northern blot analysis, that the *ob* gene encodes an mRNA product found exclusively in adipose tissue. They named the *ob* gene product leptin (Zhang, Proenca et al. 1994). Experiments comparing the effects of saline vs leptin in *ob/ob* mice proved that leptin was a circulating factor that reversed the obesity of these mice (Halaas, Gajiwala et al.). There was no effect administering leptin to obese *db/db* diabetic mice who were subsequently found to harbour mutations in the leptin receptor (Halaas, Gajiwala et al. 1995, Tartaglia, Dembski et al. 1995). Subsequent studies in rodents showed that in the arcuate nucleus of the hypothalamus, leptin stimulates the expression of pro-opiomelanocortin (POMC) (Schwartz, Seeley et al. 1997), and increases the activity of POMC neurons, resulting in the release of POMC peptides (α,β,γ melanocyte stimulating hormone (MSH), adrenocorticotrophic hormone (ACTH) and β-endorphin) (Schwartz, Seeley et al. 1997). Stimulation of the melanocortin-4 receptor by α-MSH in the paraventricular nucleus of the hypothalamus increases sympathetic nervous system (SNS) activity, and together with converging signals from multiple other pathways, signals the fed state (Fan, Boston et al. 1997).

Leptin additionally acts as a potent signal to defend against starvation. The absence of leptin is a potent orexigen and results in reduction in energy expenditure. It also has an important role in coordinating the neuroendocrine response to starvation. Prevention of starvation-induced falls in leptin by exogenous administration blunts the gonadal, thyroid and adrenal axis changes in male mice, and prevents the starvation-induced delay in ovulation in female mice. Leptin administration did not have significant effects on weight loss, blood glucose or ketone production (Ahima, Prabakaran et al. 1996).

The effects of leptin on hunger has also been explored in obese subjects, who had undergone a 10% reduction in body weight, who were treated with either subcutaneous leptin or placebo, showed leptin-reversible increases in neural activity in response to visual food cues in the brainstem, parahippocampal gyrus, inferior and middle frontal gyri, middle temporal gyrus, and lingual gyrus. There were also leptin-reversible decreases in activity in response to food cues in the hypothalamus, cingulate gyrus, and middle frontal gyrus (Rosenbaum, Sy et al. 2008). This study illustrates that many of the neurobehavioral changes induced by caloric restriction are secondary to this partial leptin deficiency, and are reversed by restoration of plasma leptin levels.

The first leptin-deficient humans were described by in 1997 (Montague, Farooqi et al. 1997). These two children, who were first cousins from a highly consanguineous pedigree, were homozygous for a frameshift mutation in the LEP gene that led to undetectable leptin levels. They had a normal birth weight but developed severe early onset obesity, with marked hyperphagia and hyperinsulinaemia. They additionally had normal basal metabolic rate and total energy expenditure (after adjusting for age and body composition), hypothalamic hypothyroidism and hypogonadotrophic hypogonadism. In subsequent studies, treatment with recombinant human leptin resulted in a reduction in hyperphagia and significant weight loss (Farooqi, Matarese et al. (2002).

1.2.2. The role of leptin in the regulation of energy intake and energy expenditure

Negative energy balance secondary to caloric restriction results in an acute reduction in circulating leptin levels, and thus a state of partial leptin deficiency (Chan, Heist et al. 2003). Studies in rodents and humans demonstrate that this fall in leptin drives the homeostatic response. Studies of obese subjects who had undergone a 10% reduction in body weight, who were treated with either subcutaneous leptin or placebo, have shed light on the homeostatic role of leptin. The weight-reduced state was associated with increased hunger and changes in neural activity in response to visual food cues in several brain regions. These phenotypes were reversed by the administration of leptin (Rosenbaum, Sy et al. 2008). This study illustrated that many of the neurobehavioural changes induced by caloric restriction are secondary to partial leptin deficiency, and are reversed by restoration of plasma leptin levels.

In studies conducted in congenital leptin deficiency, whilst unable to detect a significant difference in basal metabolic rate (using indirect calorimetry) or total energy expenditure (using the double-labelled water method) compared to weight matched controls (Farooqi, Matarese et al. 2002), weight loss is usually associated with reductions in energy expenditure, and this is not seen in leptin-treated

individuals with leptin deficiency (Galgani, Greenway et al. 2010). Furthermore, leptin deficient humans have impaired sympathetic tone (Ozata, Ozdemir et al. 1999), consistent with defects in the efferent limb of thermogenesis. Additionally there is some evidence that leptin deficiency may alter thyroid function; in one study on the effects of recombinant human leptin administration on three children with congenital leptin deficiency, fT4 was significantly increased after two months of therapy and subsequently remained constant (Farooqi, Matarese et al. 2002). A second study looked at TSH pulsatility in a single homozygous leptin-deficient adult and found that it was highly disorganised when compared to healthy controls (Mantzoros, Ozata et al. 2001). In rodents, leptin stimulates fatty acid oxidation in skeletal muscle via the stimulation of AMP kinase activity (Minokoshi, Kim et al. 2002). In leptin-deficient adults, impaired fat oxidation has been measured by chamber calorimetry (Galgani, Greenway et al. 2010).

Ob/ob mice develop obesity when pair-fed to their wild-type littermates, accumulating up to twice as much subcutaneous fat (Alonso and Maren 1955). Mature *ob/ob* mice are unable to maintain their body weight when exposed to cold, and will die if exposed to temperatures of 4^{o}C (Davis and Mayer 1954). Previous studies have suggested that this thermoregulatory defect is caused by inadequate thermogenesis, rather than a failure of heat conservation (Trayhurn, Thurlby et al. 1977). BAT is known to be activated by the sympathetic nervous system, with inputs from the dorsomedial hypothalamus, possibly via relay in the rostral raphe nucleus (Dib, Rompre et al. 1994). There is also evidence that the brown adipose tissue mass can expand in response to demand, and that there are “beige/brite” adipose tissue cells that are phenotypically distinct from both brown and white adipose tissue cells, can be induced to transform into brown adipose tissue (Young, Arch et al. 1984). “Browning” of these cells is an adaptable and reversible process induced by cold and B3-agonism, and inhibited by thermoneutrality and high fat diets (Cousin, Cinti et al. 1992, Giralt and Villarroya 2013) .

Brown adipose tissue has long been known to play a role in protection from hypothermia in neonates, but it has only been recently that a role for active brown tissue has been proposed in adults. The presence of BAT in adults was identified from the retrospective analysis of 3640 FDG-PET scans performed for other diagnostic purposes. Tissue, more than 4mm in diameter and of the same density as adipose tissue was seen and found to be highly metabolically active, with an uptake of FDG of at least 2g per millilitre. This tissue was located in the intrascapular, neck and supraclavicular regions. Tissue from this region had multiloculated, UCP-1 immunopositive adipocytes, indicating that this was brown adipose tissue (Cypess, Lehman et al. 2009).

Furthermore, leptin stimulates CART expressing neurones and inhibits the action of neuropeptide Y-expressing neurones in the in the arcuate nucleus.

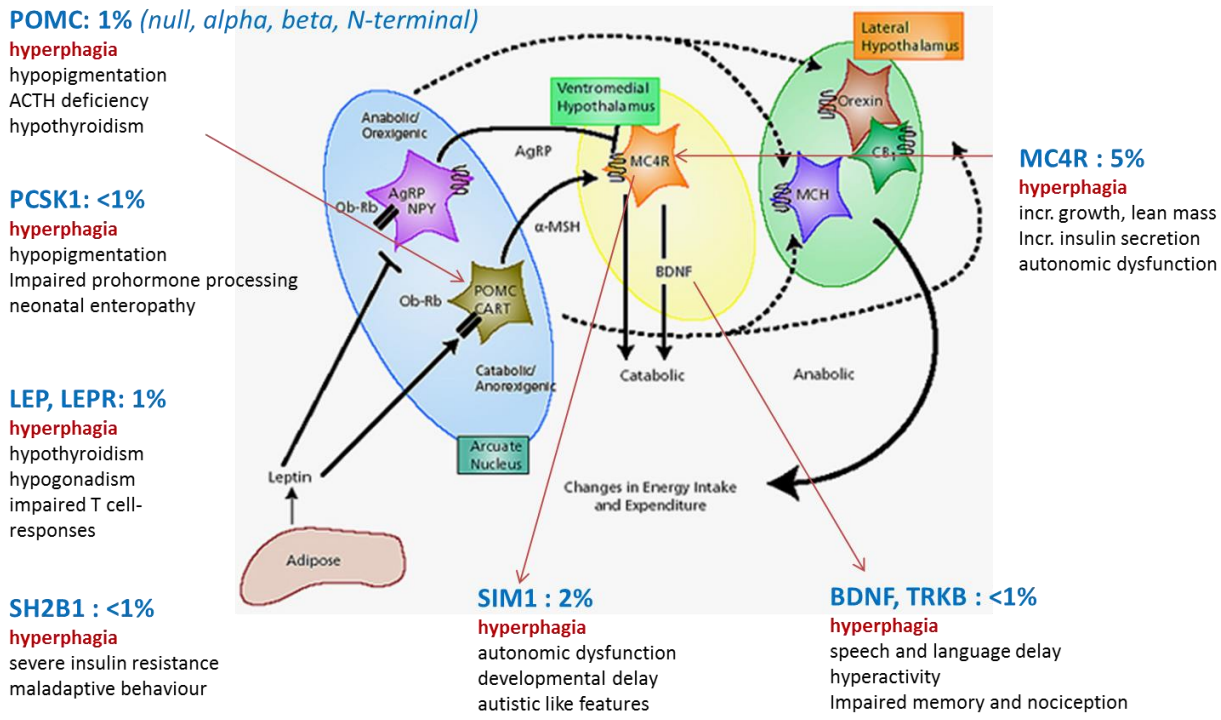

Figure 1. Mutations in the leptin-melanocortin pathway result in hyperphagia and severe obesity

1.2.3. The homeostatic response to temperature change in humans

Homeothermic animals (those that maintain a constant core body temperature) have the advantage of being able to survive in a wide variety of terrains. However, this comes at a significant energy cost, and the efficient maintenance of core body temperature is therefore essential to survival. Brown adipose tissue defends ore body temperature, whilst minimising energy expenditure. Human brown fat mass can be expanded and this has beneficial metabolic consequences (Labbe, Mouchiroud et al. 2016).

Initial research into the homeostatic mechanisms involved in the maintenance of body temperature were performed with the aim of defining human physiology (Pembrey MS, 1904). He defined that a normal core body temperature for humans can range from 36°C to 37.8°C, and noted that this did not change if the human lived in the tropics or the Artic. He also noted that "cold is a stimulant more powerful in its effect on metabolism than any drug", noting an increase in CO_2 output of 50-60% on cold exposure.

In the 1960s the focus of research was on the ability of research and military workers to operate in extreme cold (Davis TR, 1961). They compared the effect of exposure to an air temperature of 11.8°C

for 8 hours per day for 31 days on 10 nude men in March to the effect of an air temperature of 13.5°C for 8 hours per day for 31 days in 6 nude men in September. He noted by day 14 there was a significant decrease in shivering, and a decrease in heat production on the winter group but not the summer group. They did not find an effect on basal metabolic rate. Metabolism was estimated by measuring the amount of oxygen in the expired air, and the presence of shivering by surface electrodes.

More recently interest has focussed on the possibility of using BAT activation as a tool for weight loss. The demonstration of cold-induced brown adipose tissue in adult men was first described in 2009 (Van Marken Lichtenbelt, NEJM 2009). They compared both lean and obese men when exposed to thermoneutral conditions and mild cold (16°C). They used (18)FDG-PET and indirect calorimetry to measure putative BAT activation and energy expenditure, respectively. They showed that BAT activity was observed in 23/24 individuals, but that this effect was lower in obese subjects.

1.2.4. Mechanisms of cold detection and physiological response

Changes in environmental temperature are detected by thermoreceptors in the skin. Thermoneutrality is defined as the environmental temperature that keeps bodily temperature at an optimal point at which the least amount of oxygen is consumed by metabolism. In humans this is a temperature of 25°C, in mice it is 26-28 °C in adult mice weighing >25g.

Afferent signals are detected by temperature sensitive neurons in the lateral preoptic area that feed into the median preoptic area. A coordinated response is then produced. Glutaminergic signals relayed via the lateral parabrachial nucleus to the spinal intermediolateral nucleus control the innervation of brown adipose tissue (Hinuma, Habata et al. (1998). GABAergic signals to the dorsomedial hypothalamus control both homeostatic and pyretic prostaglandin E2-mediated changes in temperature, and in turn communicate with seratonergic neurons in the rostral raphe pallidus that also relay with the spinal intermediolateral nucleus. This area additionally relays, via the thalamus, to the cerebral cortex to stimulate behavioural change in response to changes in environmental temperature.

The complex coordinated metabolic response to cold has only been partially elucidated. Cold exposure has been shown to reduce leptin expression in rodents. Mice exposed to 4°C for between 2-18h showed a reduction in *ob* gene expression in their white adipose tissue (Trayhurn, Thomas et al. 1995). There is also some published data that suggests a similar response in humans. Cold air exposure (6.3°C) in adult females for 30, 60 or 90 minutes resulted in a reduction in circulating leptin of 14%, 17% and 22% respectively, with corresponding increases in norepinephrine levels (Ricci, Fried et al. 2000). The

relationship between cold-induced BAT activation and circulating leptin levels has been further explored in rodents; in lean Sprague Dawley rats hypothermia-induced increases in sympathetic nervous system drive to intrascapular BAT were significantly augmented by leptin (Hausberg, Morgan et al. 2002). These data suggest a circuitry by which cold exposure results in a drop in circulating plasma leptin levels, resulting in an increased sympathetic drive and consequent BAT activation.

1.2.5. Central pathways that mediate the effects of leptin on thermogenesis

As leptin appears to play a role in the coordinated response to cold, it is important to consider the mechanisms by which it may be acting. Central leptin-melanocortin signalling has a direct effect on sympathetic tone, and has been implicated as the link between fat mass and blood pressure in mice (Hall, Ferrario et al. 1997) and due to the observations that obese subjects with defects in these signalling pathways have much lower than expected levels of hypertension, lower systolic blood pressures and evidence of impaired sympathetic tone (Greenfield, NEJM, 2009). The neurocircuitry responsible for these observations were dissected by Simonds and colleagues (Simonds, Pryor et al. 2014), who demonstrated that C57BL/6J mice fed a high fat diet (43% fat) had a significantly increased heart rate by 4 weeks, and blood pressure by 12 weeks of feeding, when compared to chow-fed littermates (4.3% fat), which paralleled the increase in circulating leptin concentrations seen with their weight gain. Comparison of this phenotype to obese mice lacking leptin (*ob/ob*) or the leptin receptor (*db/db)* showed that only mice with DIO developed the increases in HR and BP, and showed that obesity alone was not enough to drive this change. Treatment of *ob/ob* mice with leptin (30ug per day via osmotic mini-pump) resulted in decreased food intake and body weight, but despite this increases in HR, sBP and to a lesser extent dBP were seen. Peripheral administration of a leptin antibody or central administration of a leptin receptor antagonist significantly reduced heart rate, systolic and diastolic blood pressure in mice with DIO, compared to those treated with vehicle alone. To locate the precise site of action, both leptin receptor antagonist and AAV-expressing short hairpin RNA directed against the leptin receptor via a catheter into the DMH, resulting in a decrease in sBP within 7 days and 4 weeks, respectively. Selective LepR deletion in the DMH also reduced systolic BP. Reactivation of LepR here rapidly increased both sBP and HR. Measurement of BP in the fasted, rested state in 8 children with homozygous loss of function mutations in the leptin gene (with undetectable levels of circulating leptin) showed a significantly lower systolic BP (but no difference in dBP) when compared to 42 age- and BMI-matched controls, whose circulating leptin levels were appropriate for their degree of adiposity.

The role of leptin in activating the sympathetic nervous system has consequences for energy expenditure and non-shivering thermogenesis. The leptin receptor expressing population in the dorsomedial hypothalamus increases sympathetic outflow to brown adipose tissue. A DREADD system designed to selectively activate DMH LepRb receptors also stimulated BAT thermogenesis, and the increased energy expenditure was partially blocked by the administration of a B3 antagonist. Use of a virally driven cre-recombinase to selectively delete the LepRb in the DMH resulted in acute impairment of the thermoregulatory response and an overall impairment of energy expenditure (Rezai-Zadeh, Yu et al. 2014). The downstream targets of these leptin effects are therefore of interest as they have the potential for pharmacological manipulation.

Prolactin releasing peptide (PrRP) is an endogenous ligand for G protein-coupled receptor 10 (GPR10), a G protein coupled receptor (GPCR) expressed in brain areas involved in energy homeostasis and subsequently shown to play a role in mediating the thermogenic effects of leptin (Dodd, Worth et al. 2014). Prolactin releasing peptide is a member of the RFamide family, a group of neuropeptides defined by their carboxy terminal arginine (R) and aminidated phenylalanine (F) residues (hence RFamides) (Osugi, Ukena et al. 2006). These highly evolutionarily-conserved peptides (PrRP, kisspeptin, QFRP, LPXRFa and Neuropeptide FF (NPFF)) are involved in a wide range of biological functions, from muscle contraction to neuroendocrine function. A role in eating behaviour was proposed when FMRFamide was shown to be anorexigenic in mice (Kavaliers and Hirst 1985). Several members of the RFamide family have been shown to play a role in energy homeostasis; centrally administered NPFF and PrRP reduce food intake (Sunter, Hewson et al. 2001, Bechtold and Luckman 2006), whilst 26aRF and QRFP stimulate food intake and energy expenditure (Takayasu, Sakurai et al. 2006).

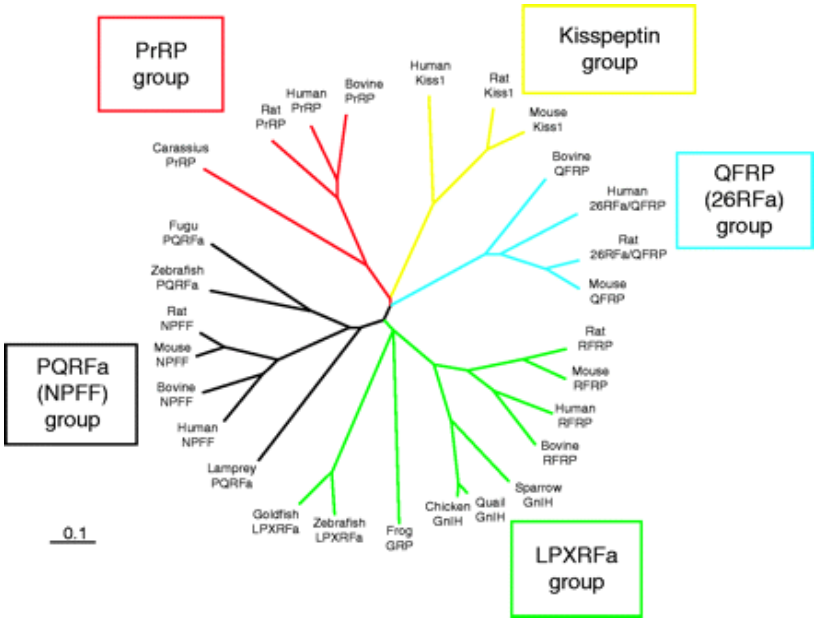

Figure 2. Unrooted phylogenetic tree of the identified and the putative RFamide peptides in mammals and other vertebrates. (Bechtold and Luckman 2007)

PrRP is a promiscuous ligand, binding with high affinity to both GPR10 and neuropeptide FF receptor 2 (NPFFR2) (KD 0.4nM and 5.9nM, respectively (Gu, Geddes et al. 2004)), but experiments indicate that its central effects are mediated through GPR10, as PrRP does not bind to cell membranes extracted from the brains of GPR10 null mice (Gu, Geddes et al. 2004). Furthermore, PrRP does not reduce food intake or increase energy expenditure in GPR10 -/- mice (Bechtold and Luckman 2006), indicating that these effects are not mediated via signalling through an alternative receptor.

Several studies have demonstrated that GPR10-mediated signalling plays a role in energy homeostasis. Both receptor and ligand are highly expressed in the dorsomedial and paraventricular nuclei of the hypothalamus, the brainstem, ventrolateral medulla and nucleus of the tractus solitarius (NTS) (Maruyama, Matsumoto et al. 1999). Colocalisation studies have shown that in the brainstem, PrRP-containing neurons colocalise with tyrosine hydroxylase, the rate-limiting enzyme for catecholamine biosynthesis, indicating that these likely relate to the A1 (VLM) and A2 (NTS) noradrenergic cell populations (Ellacott, Lawrence et al. 2002). Double immunohistochemistry has shown that PrRP colocalises with the leptin receptor in the dorsomedial hypothalamus, suggesting that it may mediate its effects at this site. Expression of PrRP mRNA is highly sensitive to feeding status as rats fasted for 48 hours showed reductions of PrRP mRNA of 32% in the DMH, 34% in the NTS and 55% in the ventrolateral medulla (Ellacott, Lawrence et al. 2002). Furthermore, PrRP mRNA is reduced by other states of negative energy balance, such as lactation (Lawrence, Celsi et al. 2000). Central administration of PrRP leads to reduced post-fast refeeding and increases core body temperature (Lawrence, Celsi et al. 2000). This effect is seen in both fasted and *ad libitum* fed rats, and the observed effect is not altered by the timing of injection (light vs dark phase). Central injection of PrRP-31 (4nmol) also resulted in an increase in VO2 and induced UCP-1 expression in brown adipose tissue in rats, before any effects are seen on body weight (Lawrence, Celsi et al. 2000, Lawrence, Liu et al. 2004).

1.2.7. Disruption of PrRP/GPR10 signalling results in late-onset obesity in mice

PrRP null mice generated on a C57BL/6 background fed *ad libitum* with standard chow (13% fat) develop late onset obesity, with female mice gaining weight earlier than male (females significantly heavier by 14 weeks, males by 22 weeks, (Mochiduki, Takeda et al. 2010)). This weight gain was largely due to increased white adipose tissue, although increases in brown adipose tissue were also seen

(Takayanagi, Matsumoto et al. 2008, Mochiduki, Takeda et al. 2010). A similar picture was seen in the GPR10 -/- mice generated on a C57BL/6 background (Gu, Geddes et al. 2004).

Cumulative food intake was increased in the PrRP knockout mice, but this was only significant from the age of 18 weeks, and this was secondary to increased meal size and not meal frequency (measured by minute-by-minute recordings of food intake by an automated food counter) (Takayanagi, Matsumoto et al. 2008). Food intake in the GPR10 knockout mice was also increased, with null animals consuming 22% more per week than their wild-type littermates (Gu, Geddes et al. 2004). Knockouts were also more susceptible to a high fat diet (30% fat): PrRP -/- mice gained significantly more weight than their wild type littermates within 2 weeks on this diet. Mice show increased leptin in keeping with their increased WAT mass. Both hepatic and plasma triglyceride levels were increased (20% higher than WT mice), as were insulin (increased 350%), and glucose levels in a glucose tolerance test (Takayanagi, Matsumoto et al. 2008). Similar results were seen in the GPR10 -/- mouse (Gu, Geddes et al. 2004).

Experiments in pair-fed animals treated with PrRP indicate that PrRP plays a role in energy expenditure as well as food intake. Animals treated with PrRP have a reduction in weight gain of 42%, compared to 30% for pair fed littermates (Lawrence, Celsi et al. 2000). However, pair-feeding experiments in 12 week old single-housed male PrRP-null mice do not show a difference in body weight gain in either chow of high fat diet-fed mice (Takayanagi, Matsumoto et al. 2008). No change in locomotor activity is seen in the PrRP knockout mice (Takayanagi, Matsumoto et al. 2008). This group also reported no change in energy expenditure as measured by indirect cage calorimetry in 11 week old wild-type, null and knockdown animals (following *icv* injection of an anti-PrRP monoclonal antibody). Bjurstell (Bjursell, Lenneras et al. 2007) found a reduction in energy expenditure in female 21 week old GPR10 null mice, compared to wild-type littermates, but the difference did not reach significance in the male mice. Dodd (Dodd, Worth et al. 2014) showed 10-11 week old PrRP null mice had a lower VO2 than wild-type littermates. These data support a possible role for both increased food intake and reduced energy expenditure in the obesity observed in mice with disrupted GPR10-mediated signalling.

1.2.8. PrRP/GPR10 expressing neurons modulate energy homeostasis in response to peripheral hormones

Cholecystokinin is released from the enteroendocrine cells (I cells) in the duodenum in response to food ingestion, particularly of lipids. CCK has local effects on the gut, inhibiting gastric emptying, decreasing gastric acid secretion, and stimulating the acinar cells of the pancreas to release pancreatic

enzymes. It also increases the production of bile, and stimulates gall bladder contraction, and relaxation of the sphincter of Oddi. Central effects of CCK are largely mediated via the vagal nerve and direct action on central CCK receptors distributed widely throughout the CNS, including in the brainstem. Administration of CCK reduces meal size and increases energy expenditure via stimulation of BAT via the CCK-1R (King, Yang et al. 2015). Mice deficient in CCK are resistant to high fat diet-induced obesity (HFD for 10 weeks) and have increased energy expenditure (King, Yang et al. 2015 2010).

Centrally administered PrRP (4nmol, *icv*) reduced the latency period in the rodent behavioural satiety sequence in Sprague Dawley rats, suggesting that it may be a satiety factor. Male rats treated *ip* with CCK show *c-fos* activation of PrRP-containing neurons in the VLM and NTS of the brainstem (Lawrence, Ellacott et al. 2002). GPR10 -/- mice fail to reduce food intake when treated with CCK, in contrast to wild type mice (Bechtold and Luckman 2006). Further work by the same group has used targeted deletion and rescue experiments in mice to show that the PrRP neurons in the brainstem are required for the satiating effects of CCK, likely acting via vagal afferents on these centres (Dodd, Worth et al. 2014).

PrRP is also expressed at high levels in a small subregion posterior to the compact zone of the dorsomedial nucleus of the hypothalamus. 100% of PrRP-expressing neurons here also express the signalling form of the leptin receptor (LepRb) (Dodd, Worth et al. 2014), whereas the PrRP-positive neurons only account for 10% of the LepRb neurons here (Ellacott, Lawrence et al. 2002). PrRP expression in the NTS and DMH (but not the VLM) is responsive to energy status (Dodd, Worth et al. 2014). Administration of PrRP and leptin led to 24% and 18% reduction in food intake respectively, with resultant reductions in body weight gain of 56% and 55%. Coadministration of leptin and PrRP resulted in a 54% reduction in food intake, resulting in a net loss in body weight (Ellacott, Lawrence et al. 2002).

Administration of the same doses of leptin and PrRP resulted in increases in core body temperature when given singly, *icv*, to adult male Sprague Dawley rats. Again an additive effect was seen when they were given in combination (Ellacott, Lawrence et al. 2002). Takayanagi (Takayanagi, Matsumoto et al. 2008) investigated the effects of both ip (2.5mg/kg body weight) and icv (0.2ug) leptin in PrRP null mice, when compared to wild type littermates in male 16 week old and 18-19 week old mice, respectively. They found that both methods of administration resulted in pSTAT3 expression in PrRP-expressing neurons in the NTS and DMN of the hypothalamus. Wild-type littermates showed significant reductions in both food intake and body weight with both the centrally and peripherally administered leptin, whereas in the null mice this effect was attenuated. Interestingly, blockade of the

melanocortin 3/4 receptors with a centrally administered antagonist (SHU-9119, 0.1nmol icv) did not blunt the effects of centrally administered PrRP-31 (Lawrence, Liu et al. 2004). Collectively, these data point to a role for PrRP-expressing neurons in leptin-mediated anorexia, but indicate that these effects may not be mediated via classical melanocortin signalling.

1.2.9. The thermogenic effects of leptin are mediated by the DMH population of PrRP neurons

Dodd (Dodd, Worth et al. 2014) defined a population of PrRP expressing cells in the DMH that were activated by leptin. Transgenic mice created using the *lox*-STOP-*lox* method to globally delete PrRP were significantly heavier than wild type littermates from 18 weeks. A similar phenotype was achieved by a brain-specific knockout of PrRP. Both failed to increase core body temperature or induce BAT UCP-1 in response to intraperitoneal leptin. They additionally did not reduce their food intake in response to leptin or CCK.

Selective rescue of PrRP in *TH*-positive cells in the NTS and VLM of the brainstem rescued the obese phenotype, the satiating effects of CCK, and reduced hyperphagia, but did not rescue leptin's effects on energy intake or thermogenesis. It can therefore be concluded that the PrRP cell populations in the brainstem are necessary for the satiating effects of CCK, and do not mediate the PrRP-dependent effects of leptin. Growth curves for GPR10 +/- mice are identical to the wild-type (Gu, Geddes et al. 2004), as are those for PrRP +/- mice, both on standard chow, and a high fat diet (Takayanagi, Matsumoto et al. 2008).

1.3.1. GPR10 signalling is involved in other physiological processes

GPR10 signalling plays a role in several other physiological systems including the stress response and blood pressure regulation. OLETF rats, which lack functional GPR10, display a less anxious phenotype when tested using different rodent behavioural models. They visit a novel, aversively-lit area more frequently than controls in the open field test, they spend longer in the open arms of the elevated plus maze test and they spend more time in the open (rather than the more secure tube) in the defensive withdrawal test (Watanabe, Okuno et al. 2007). A similar trend was explored in GPR10 null mice, but it did not reach statistical significance (Laurent, Becker et al. 2005).

Baroreceptors in the great vessels, activated by hypotension, transmit signals to the NTS of the brainstem, prompting a homeostatic neuroendocrine response. PrRP-expressing neurons in the

brainstem became *c-fos* immunopositive within two hours of hypotensive haemorrhage, as do vasopressin and CRH neurones in the PVN. Retrograde tracer studies indicate that PrRP-containing neurones deliver the signal from the brainstem to the cells in the paraventricular nucleus (Uchida, Kobayashi et al. 2010). Bacterial lipopolysaccharide reduces feeding through activation of the hypothalamo-pituitary-adrenal (HPA) axis. Administration of LPS (125-500ug, *ip*) in conjunction with PrRP (4nmol, *icv*) reduced feeding in a dose-dependent manner, and caused a dramatic rise in plasma corticosterone 90 minutes after injection. However, there was no significant difference in the response between wild-type and GPR10 null mice.

In support of a role of GPR10-PrRP signalling in regulating the HPA axis, Laurent (Laurent, Becker et al. 2005) found that GPR10 null mice had lower circulating corticosterone levels, and a blunted corticosterone response to hypoglycaemic stress. However, Mochiduki (Mochiduki, Takeda et al. 2010) demonstrated that PrRP knockout mice (C57BL/6 background) exposed to 1 hour of restraint stress using a wire mesh had an increase in plasma corticosterone compared to wild-type littermates. Plasma ACTH levels were unchanged, as was *c-fos* expression in the paraventricular hypothalamus. There are therefore mixed data on the role of GPR10-PrRP signalling on the modulation of the HPA axis.

Icv PrRP raises blood pressure and heart rate, with readings peaking 5 minutes after central administration. Yamada (Yamada, Mochiduki et al. 2009) further investigated the role of these neuroendocrine neurones (vasopressin and CRH) in executing the effects of PrRP. They found that while V1-R antagonists administered before PrRP did not attenuate the effects of PrRP (4nmol, *icv*), the effects of PrRP on MAP and heart rate were significantly reduced by pre-treatment with α-helical CRH, a CRH receptor antagonist (Yamada, Mochiduki et al. 2009). Coadministration of PrRP with the central CRH receptor antagonist astressin (7.5 mg/kg or 20ug *icv*) significantly reduces PrRP-induced anorexia in 18 week old male C57BL/6J mice (Lawrence, Liu et al. 2004, Bechtold and Luckman 2006). There are also effects on pain sensation and sleep.

Both isoforms of PrRP (PrRP-20 and PrRP-31 at concentrations of 0.4nmol or 4nmol) were found to increase mean arterial pressure (external carotid artery pressure measured by an external pressure transducer attached to an implanted indwelling catheter) in conscious, unrestrained adult male Sprague Dawley rats when administered *icv*. Results were comparable to 0.1nmol (a pressor dose) of angiotensin II (Samson, Resch et al. 2000).

1.3.1 Evidence for the role of GPR10 signalling in human energy homeostasis

Previously, using a candidate gene approach to sequence 94 patients with severe, early-onset obesity from the Genetics of Obesity (GOOS) cohort, a common polymorphism in GPR10, P305L, was described, which was shown to result in a partial loss of function. Genotyping this variant in 1084 participants from the Ely study found that whilst there was no significant association with obesity, subjects possessing the variant had on average a 5mmHg reduction in both systolic and diastolic blood pressure.

To date, the variants in this project are the first rare human obesity-associated variants in GPR10 to be described.

1.3. Hypotheses and aims

1.3.1. Hypotheses

1. Novel and rare human mutations in GPR10 result in a loss of function and contribute to the subject's obesity.
2. Cooling in humans results in a coordinated metabolic response, some of which is leptin mediated.

1.3.2. Aims

1. To functionally characterise human mutations in GPR10 identified in a severely obese cohort.
2. To examine the effects of mild cooling on healthy, normal weight adult males and to characterise their impact on metabolism, food preference, neurocognition and lipidomic profile.

CHAPTER TWO: METHODS

2.1 Functional characterisation of human mutations in GPR10

Mutations identified from the whole exome and targeted resequencing of a population of subjects with severe early onset obesity were taken forwards for functional characterisation. Constructs were created using site-directed mutagenesis and placed in a plasmid vector. These were transfected into cell lines for further study as described below. The cell surface expression, ligand binding and signalling of ach of the receptors was assessed. As the mutations are found in heterozygous form, and heterozygous-knockout mice are not known to be obese, the possibility of a dominant-negative effect was explored.

2.1.1. Identification of mutations in GPR10

The whole exome sequencing of 737 Caucasian patients with severe, early onset obesity, and subsequent targeted resequencing of 1,811 patients was performed in collaboration with Dr Ines Barroso at the Wellcome Trust Sanger Institute, as previously described (Hendricks, Bochukova et al. 2017).

2.1.2. Creation of Constructs

Mutant receptors were constructed using mutant primers (Sigma Aldrich) and the Quikchange II XL site directed mutagenesis kit (Agilent) as per kit instructions. The engineered cDNAs were cloned into the eukaryotic expression vector pCMV-Tag2B (Stratagene) encoding N-terminal FLAG tag. All constructs were verified by DNA sequencing.

2.1.3. Cell culture and transfection

Cos-7 and HEK293 cells were grown in Dulbecco's modified Eagle's medium (DMEM, Life Technologies) supplemented with 10% fetal bovine serum (Thermo Fischer), 2mM L-glutamine (Sigma Aldrich) and penicillin and streptomycin antibiotics (Sigma Aldrich). Cells were removed by trypsinisation or incubation with 10mmol EDTA, and counted with a haemocytometer before seeding into 96 well plates previously coated in poly-D-lysin (Sigma Aldrich). Transfection was performed using Lipofectamine 2000 (Invitrogen) in Optimem medium (Life Technologies). Transfection was stopped

the next day by substituting Optimem medium for DMEM, and were grown for 24 h before further experiments were performed.

2.1.4. Enzyme-linked Immunosorbent Assay (ELISA)

Cos-7 cells were seeded in poly-D-Lysin coated 96 well plates at a density of 20,000 cells per well and were transfected the next day with 5ng FLAG-tagged receptor DNA/well as described above. Following incubation, cells were placed on ice and washed twice with ice-cold PBS containing magnesium and calcium (Sigma Aldrich). Cells were blocked for 30 minutes with 3% dry milk blocking buffer containing 5% 50mM Tris pH 7.4 in phosphate buffered saline (PBS, Sigma Aldrich) on ice. Blocking buffer was substituted for primary antibody (anti-FLAG M2, Sigma Aldrich), diluted 1:1000 in blocking buffer for 2h on ice. Cells were washed twice with ice-cold PBS containing calcium and magnesium on ice for 10 minutes, and were then fixed with 3.7% formaldehyde for 10 minutes on ice and then 10 minutes at room temperature. Cells were washed 4 times using a plate washer (AquaMax), using standard PBS. Cells were again blocked with blocking buffer for 30 minutes at room temperature with gentle shaking at 300rpm. Cells were treated with secondary antibody (Goat anti-mouse with conjugated horse-radish peroxidase, BioRad), diluted 1:1250 in 1.5% dry milk buffer and incubated for 1h at RTP with shaking at 300rpm. Cells were washed 4 times using the plate washer. The ELISA was developed by adding 100ul per well of Quanta Blu Fluorogenic Peroxidase substrate (Thermo Scientific) for 20 minutes with shaking at 350rpm, before the reaction was stopped as per kit instructions. 150ul of solution was transferred to a black 96 well plate and fluorescence measured. Results were analysed using GraphPad Prism 6.0.

2.1.5. Confocal microscopy visualisation of fluorescently-tagged constructs

150,000 HEK293 cells were seeded onto sterile 19mm glass coverslips in 12 well plates and were coated in poly-D-lysin. 24 hours later cells were transfected with 300ng/well of receptor DNA using lipofectamine 2000. Transfection was stopped after 5 hours by substitution of lipofectamine-DNA media with HEK media (high glucose DMEM supplemented as described), and cells were incubated overnight (37^{o}C, 5% CO_2). Cells were washed in PBS and fixed for 10 minutes with 4% formaldehyde in PBS. Cells were washed twice before application of 100ul Alexa 647-tagged wheat germ agglutinin (Life Technologies) diluted in HBSS (Sigma Aldrich) to 10ul/ml for 10 minutes. Cells were washed 3 times with HBSS, before permeabilisation for 5 minutes with 0.1% Triton-x100 (Sigma Aldrich). Cells

were washed twice for 5 minutes with PBS. Non-specific binding was blocked by incubation with 3% BSA (Sigma Aldrich, diluted in PBS) for 1 hour. 150ul of anti-FLAG-M2 antibody (Sigma Aldrich), diluted 1:100 in blocking buffer, was added and cells incubated for 1 hour. Cells were washed three times with PBS. 1ml of DAPI (Invitrogen), diluted 1:1000 in PBS was added and incubated for 10 minutes. Cells were washed again twice with PBS. 150ul of Alexa 488 anti-mouse antibody (Life Technologies) was added dropwise to the coverslips, diluted 1:200 in PBS, and incubated for 1h in the dark. Cells were washed 3 times, before mounting onto cells using DAPI-containing mounting medium (Vectashield H-1200, Vector), and sealing with clear nail varnish. Cells were visualised using the Leica SP8 confocal microscope.

2.1.6. Inositol Monophosphate Accumulation Assay

COS-7 cells were seeded at a density of 20,000 cells per well as described. Cells were transfected with 5ul/well of DNA using lipofectamine 2000. Transfection was stopped the next morning by substituting optimem medium with 100ul/well of low glucose DMEM, supplemented with Myo-[2-^{3}H]-inositol (5ul/ml, Perkin-Elmer) and cells were cultured overnight. The next morning cells were washed with 200ul plain HBSS, and then 100ul HBSS containing 10mM LiCl was dispensed per well. Cells were stimulated with 5ul/well of ligand (PrRP-31, Bachem, concentration $1x10^{-6}$ – $1x10^{-12}$, or diluent alone), and incubated for 1 hour at 37^{o}C, 5% CO2. Cells were then placed on ice and assay buffer substituted with 50ul/well ice cold 10mM formic acid, for at least 1 hour. 20ul of cell lysate was transferred to a white 96-well plate containing polylysine YSi SPA bead suspension (Perkin Elmer). Plates were sealed with Topseal (Perkin Elmer), and manually shaken for 10-15 seconds. Radioactivity was counted using a microplate scintillation counter (Topcount) after an 8h delay to stabilise the signal. Remaining lysate in the assay plate was frozen at -20^{o}C, in case reanalysis was desired. Results were analysed using GraphPad Prism 6.0.

2.1.7. Generation of stably transfected cell line

pCMV-Tag2B plasmid, resistant to kanamycin and neomycin antibiotics, and containing wild type GPR10 DNA was transiently transfected into HEK293 cells in T75 flasks (10ug/flask) using lipofectamine 2000 (1.5ml optimem medium supplemented with 30ul lipofectamine). The following day, plain high glucose DMEM medium was substituted for that supplemented with genectacin

(G418). Killing curve experiments were first done to identify the optimal dose of genectacin, for selection of stably transfected cells; a dose of 250ug/ml was chosen.

Pooled clones of stably transfected cells were grown in T75 flasks, in standard high glucose DMEM medium supplemented with 250ug/ml genectacin. Cells were harvested by trypsinisation as previously described, and seeded in white 96-well plates at a density of 20,000 cells per well for the cAMP accumulation assay.

2.1.8. cAMP accumulation assay

Measurement of ligand-induced cAMP generation in HEK 293 cells stably transfected with GPR10 wild type construct (one day after transfection) was done using HitHunter cAMP assay (DiscoverX, 90-0075SM) according to manufacturer's protocol with modifications. Cells were washed with PBS and incubated in 30 µL PBS supplemented with 0.5 mM 3isobutyl-1-methylxanthine (IBMX, Cayman Chemical, 13347) for 30 min prior to stimulation with agonist. Cells were stimulated with forskolin (20mM) and serial dilutions of agonist (1.5 µL/well, 20x dilution) for further 30 min at 37°C. Intracellular cAMP detection was carried out directly after the ligand stimulation. 10 µL anti-cAMP antibody followed by 40 µL chemiluminescent substrate/lysis buffer/enzyme donor-cAMP complex mix prepared according to manufacturer's protocol were added and plates were incubated shaking for 1 hour at ambient temperature. Finally, 40 µL enzyme acceptor was dispensed and chemiluminescent signal was quantified after 4-5 hours in a TopCount Microplate Scintillation Counter (Packard).

2.1.9. Radioligand Binding Assay

COS-7 cells were seeded in plain white 96-well plates at a density of 20,000 cells per well and transfected with 5ul/well receptor DNA. The next day transfection was stopped by substituting the lipofectamine-DNA complex solution with fresh COS-7 media (low glucose DMEM supplemented as previously described). After overnight incubation (37^{o}C, 5% CO_2) the cells were washed with 200ul assay buffer (20mM HEPES buffer pH7.4 containing 119mM NaCl, 4.7mM KCl, 5mM MgCl2, 5.5mM glucose, 1mg/ml BSA) and placed on wet ice. 5ul/well cold ligand was dispensed ($1x10^{-6}$ – $1x10^{-12}$ concentrations used), swiftly followed by 50ul of "hot" ligand solution (5ul/ml of ^{125}I-PrRP-31 diluted in binding buffer, Perkin Elmer) and plates were stored at 4^{o}C for 5h. Plates were washed with

200ul/well buffer solution twice. 25ul/well 0.1M NaOH was dispensed and cells were shaken at 1000rpm for 2 minutes. 100ul/well scintillant (Microscint TM-20, Perkin Elmer) was added, plates were sealed (Topseal, Perkin Elmer), and again shaken x1000rpm for 5 minutes. Radioactivity was counted using a microplate scintillation counter (Topcount) after a 3h delay to stabilise the signal. Results were analysed using GraphPad Prism 6.0.

2.1.10. Dominant Negative Experiments

Cos-7 cells were seeded in poly-D-Lysin coated 96 well plates at a density of 20,000 cells per well and were transfected the next day with 2.5ng/well of wild-type receptor DNA, plus mutant DNA. The following ratios of WT:MT DNA were explored: 1:3, 1:2, 1:1, 1:0.5, 1:0.2. Transfection with additional empty pCMV DNA was performed to keep the total concentration of DNA across experiments constant. Lipofectamine 2000 was used for all transfections. Inositol monophosphate accumulation was measured as previously described.

2.2. *C. elegans* strains and growing conditions

Worm strains were maintained at 20^{o}C on nematode growth medium (Langmead, Szekeres et al.) plates seeded with E. Coli OP-50. The N2 strain, wildtype control, and npr-6 (tm1497) mutant worms were carefully synchronised from time of egg laying to ensure uniformity of stage (in collaboration with Dr Birgitta Olofsson). They were individually picked and mounted on a 2% agarose patch using M-9 C. elegans buffer. Sodium azide was used to anaesthetise and immobilise the worms. Three worms of each genotype were mounted on slides alternately to ensure accurate synchronisation. L4 larvae and young adults were imaged and analysed independently.

2.2.1. CARS microscopy set up

Lipid was visualised using coherent anti-Stokes Raman scattering (CARS) microscopy in conjunction with the Dr Lorraine Berry and Dr Stefanie Reichelt at the Light Microscopy Core Facility at Cancer Research UK, Cambridge Biomedical Campus.

A ti:sapphire laser and an optical parametric oscillator (OPO) laser were synchronized to each other through an electronic module controller. The two parallel-polarized laser beams, pump and Stokes, were collinearly combined and sent into a laser scanning confocal microscope. Pump and Stokes lasers were tuned to 836 nm and 1104 nm, respectively, to be in resonance with the CH_2 symmetric stretch vibration at 2845 cm^{-1}. The combined beams were focused into the sample through a 40x water immersion microscope objective with a 1.0 numerical aperture. Forward-detected CARS signal was collected by an air condenser with a 0.55 numerical aperture, transmitted through a 675/67 nm bandpass filter, and detected by a photomultiplier tube. Simultaneously, back-reflected TPEF signal was collected by the same illuminating objective, spectrally separated from the excitation source, transmitted through a 525/50 nm bandpass filter, and detected by a photomultiplier tube mounted at the back port of the microscope. To obtain Raman spectra of lipid droplets, the Stokes beam was blocked and the pump-laser induced Raman scattering signal was directed toward a spectrometer to permit spectral analysis from 642 cm^{-1} to 709cm^{-1}, which covers the CH-stretch vibration regions. The combined Stokes and pump laser power was kept constantly at 40 mW. For all Raman spectral measurements, pump laser power was reduced to 10 mW.

2.2.2. CARS imaging conditions and data analysis

To evaluate the levels of lipids and auto-fluorescent bodies, a probe volume with dimensions of 102 µm×102 µm was defined covering the intestinal cells most proximal to the worm pharynx of wild type or mutant worms. Simultaneous depth imaging with CARS and TPEF along the vertical (z) axis was performed at 1 µm step size. Total CARS and TPEF signal arising from worms were integrated over the frames and divided by the worm volumes to obtain average pixel intensity values. Thus, the average pixel intensity values were not affected by size variability among worms. Background CARS and TPEF signal were defined as those arising from the worm bodies devoid of lipid droplets or auto-fluorescent granules. Background CARS and TPEF pixel intensity were subtracted from the average pixel intensity of CARS and TPEF signal to obtain CARS signal for fat stores and TPEF signal for auto-fluorescent granules, respectively.

ImageJ software was used for particle analysis; all the droplets in the field of view were measured, and this total was divided by the number of droplets counted. To measure average lipid droplet density (the number of droplets per defined area), a defined area proximal to the pharynx was chosen with a diameter of 15,000 pixels. The total number of droplets in this area was then counted. The average of two separate comparisons was made.

2.3. Cooling study

Lean, healthy men were recruited to the cooling study. Consent was taken along with baseline bloods at the screening visit. They all attended for two overnight visits which were identical with the exception of the temperature intervention. Core body and skin temperature was measured, together with energy expenditure, changes in hunger, fat preference and neurocognition. Bloods were taken and analysed as described.

2.3.1. Cooling study protocol

All studies were approved by the Cambridge Local Research Ethics Committee (17/EE/0069) and undertaken with informed consent. Lean individuals were recruited from the local population by advertisement. Exclusion criteria were use of any medication, any medical or psychiatric disease, shift work, regular cold exposure (for instance, cold water swimming), excessive caffeine use and smoking.

Screening visits were conducted at 9am on the Wellcome Trust Translational Research Facility after an overnight fast. An ACE-III questionnaire was performed, to screen for pre-existing cognitive impairment; a score <88 was used as a cut off for study exclusion. A fasting blood screen was taken; any significant abnormality resulted in study exclusion. Subjects were familiarised with the unit and the equipment used, including the Gas Exchange Monitor (GEM) and the cooling suit.

A fat preference test was then administered, as described in our previous paper (van der Klaauw, Keogh et al. 2016). Briefly, we developed a three choice, ad libitum meal paradigm (Quorn Korma and Rice) in which fat content was covertly manipulated (by adding rapeseed oil) to provide 20 (low), 40 (medium) and 60% (high) of the total caloric content, without altering appearance, texture or taste. Participants were initially provided with 'tasters' (15 g) of the three meals and liking/disliking ratings obtained using VAS before meal consumption. We then provided large dishes containing the low/medium/high fat quorn korma curry and rice (finely chopped and mixed to prevent selection of specific components) in excess (10 MJ; ~2,390 kcal). Participants were encouraged to try the three dishes without explicitly stating that the three meals were different and instructed to eat until they were comfortably full. The amount consumed was covertly weighed. After the meal, liking ratings were measured as before.

If participants met eligibility criteria, they were invited to attend the Wellcome Trust Translational Research Facility for two study visits, spaced two weeks apart. The study visits were identical, with the exception of the temperature intervention (thermoneutral visit (visit A), temperature 25^{o}C; cooling

study visit (visit B), temperature 16°C). The order of the visits was randomised, and participants were not informed of the study order before the temperature intervention.

Participants arrived at 3pm on the first study visit day. Two actiheart heart rate monitors (Camntech) were fitted. Participants were given a fixed amount of water, and a fixed evening meal and snack. Consumption of food and drink not directly administered by the study team was prohibited.

Participants were woken at 0700h the next morning, and a set of observations were taken. Subjects were asked to pass urine and dress in standardised light clothing. Digital skin temperature monitors (iButtons, Maxim Integrated), set up in accordance with the manufacturer's instructions, and was taped bilaterally to the patient's skin in seven locations (forearm, supraclavicular fossa, chest, abdomen, thigh, calf and foot). The EMG recording was set up in accordance with the manufacturer's instructions (BrainAmp EMG); electrodes were taped bilaterally to the chest and abdomen. Continuous recording was made in both study arms until the end of temperature intervention.

18 gauge cannulae were inserted into each antecubital fossae. A blood pressure cuff was applied on one side, and the subject put on the water-perfused cooling suit, which was then connected to a Julabo cooling unit. The temperature of the perfused water was set to 25°C, and the room was dimly lit and quiet.

After 1 hour (Tn60 time point) blood samples were taken with minimal disturbance (for a full list of samples taken please refer to table 1). Basal metabolic rate and respiratory quotient were determined by indirect calorimetry using an open circuit, ventilated, canopy measurement system (Europa Gas Exchange Monitor; NutrEn Technology), and a set of observations was taken. The skin temperature measured by one of the foot iButtons was recorded, and a visual analogue scale performed. A brief set of cognitive tasks, comprising a verbal fluency test and a digit span was performed. The temperature of the cooler unit was then set in accordance with the study arm (either 16°C or 25°C); on reaching the temperature intervention the time was recorded (Ti0). The room was kept quiet and dimly lit throughout. Bloods, observations and skin temperature were taken according to the sample sheet, Table 1, and processed as standard: EDTA and lithium heparin samples were placed on wet ice immediately, and spun straight away (3,000rpm for 10 minutes at 4°C), before snap-freezing on dry ice. Serum sample were left to clot for 30 minutes before being processed in the same way. PAXgene samples for RNA were left at room temperature before being placed in a -80°C freezer. All samples were carefully labelled with barcode and stored at -80°C.

After 2 hours of temperature intervention a further gas exchange monitor reading was performed to measure energy expenditure, and the visual analogue scale was repeated. The cooling unit was

switched off, but cognitive tasks were performed with the patient remaining in the suit. These comprised a RAVLT test, Hayling sentence completion task, verbal fluency, trails test, digit span and Rey diagram test. Copies of these tests are provided below.

2.3.1.1 Copies of cognitive tasks

The digit span test

FTD Core Test Booklet Patient ID: _____ Date: _____ RA: _____

Digit Span (WMS-III)

"I am going to say some numbers. Listen carefully, and when I am through, I want you to say them right after me. Just say what I say."

Forwards

Item	Trial	Response	Score 0 or 1
1	1-7		
	6-3		
2	5-8-2		
	6-9-4		
3	6-4-3-9		
	7-2-8-6		
4	4-2-7-3-1		
	7-5-8-3-6		
5	6-1-9-4-7-3		
	3-9-2-4-8-7		
6	5-9-1-7-4-2-8		
	4-1-7-9-3-8-6		
7	5-8-1-9-2-6-4-7		
	3-8-2-9-5-1-7-4		
8	2-7-5-8-6-2-5-8-4		
	7-1-3-9-4-2-5-6-8		

Raw: _____ **Max Digits Forwards:** _____

"Now I am going to say some more numbers. But this time when I stop, I want you to say them backward. For example, if I say 7-1-9, what would you say?"

If correct: "That's right".

If incorrect: "No you would say 9-1-7. I said 7-1-9, so to say it backward you would say 9-1-7. Now try these numbers. Remember, you are to say them backward: 3-4-8."

Backwards

Item	Trial	Response	Score 0 or 1
1	2-4		
	5-7		
2	6-2-9		
	4-1-5		
3	3-2-7-9		
	4-9-6-8		
4	1-5-2-8-6		
	6-1-8-4-3		
5	5-3-9-4-1-8		
	7-2-4-8-5-6		
6	8-1-2-9-3-6-5		
	4-7-3-9-1-2-8		
7	9-4-3-7-6-2-5-8		
	7-2-8-1-9-6-5-3		

Raw: _____ **Max Digits Backwards:** _____

Total Raw: _____

The Hayling sentence completion test

FTD Core Test Booklet Patient ID: _____ Date: _____ RA: _____

Hayling Sentence Completion Test (Burgess & Shallice, 1997)

"In a moment I am going to read you a series of sentences, each of which has the last word missing from it. I want you to listen carefully to each sentence, and when I have finished each one, your job is to give me a word which completes the sentence. Do you understand?" [Repeat instructions if needed]

"Before we start, I'll give you a couple of practice sentences so you can get the hang of it. Are you ready?"

Administer the two Practice Items for Section 1. Do not time these.

Item	Sentence	Response	Time
P1	The rich child attended a private...		N/A
P2	The crime rate has gone up this...		N/A

"OK, that's the end of the practice items. The next few sentences I'll read aren't really any more difficult than the two you've just done. But the important thing is that I want you to give me your answer as quickly as you can – the faster the better. Is that clear?" [Give as much further explanation as necessary]

NOTE: Record time in whole second units which *are not rounded up*. Max time for each trial is 60 seconds; record time latency as 60.

Section 1

Item	Sentence	Response	Time
1	He posted a letter without a...		
2	In the first space, enter your...		
3.	The old house will be torn...		
4.	It's hard to admit when one is...		
5.	The job was easy most of the...		
6.	When you go to bed turn off the...		
7.	The game was stopped when it started to...		
8.	He scraped the cold food from his...		
9.	The dispute was settled by a third...		
10.	Three people were killed in a major motorway...		
11.	The baby cried and upset her...		
12.	George could not believe that his son had stolen a...		
13.	He crept into the room without a...		
14.	Billy hit his sister on the...		
15.	Too many men are out of...		

Raw Score	Scaled Score	Comment
0	7	High Average
1-9	6	Average
10-18	5	Moderate Average
19-22	4	Low Average
23-50	3	Poor
51-60	2	Abnormal
>60	1	Impaired

Total Time:

Raw Score _____

Scaled Score _____ (A)

NOTE:

1. Change of mind – If the patient changes their mind and gives two responses, record the response and time for their first answer.
2. Multi-word answers – Score the first multi-word answer as it stands but before giving the next item, say "You've just given me an answer which was more than one word. This doesn't matter too much, but I would prefer it if you would try to keep your answers to just one word." Correct them once only.
3. Mishearing – If patients mishear, ask them to repeat the sentence back to you first. If it is incorrect, then repeat the item to them again.
4. Strategy development – Some patients may repeat the same word to all trials. This is not permitted. "You've already used that answer. Repeating the same word to each sentence is a good way of approaching this test, but it makes it too easy, so I'm afraid that I'm going to have to ask you not to use it. From now on I want a different word each time." [Score further repeats as Category A responses].

Always administer Section 2 *immediately after* Section 1.

Section 2

"Now we are going to move onto the second section of the test. In this section, I will read you a set of sentences with the last word missing just like the ones you have already done, but this time I want you to give me a word which does **NOT** fit at the end of the sentence – I want the word you give me to be completely unconnected to the sentence in every way. Do you understand?"

"Before we start, I'll give you a couple of practice sentences so that you can get the hang of what is required."

The RAVLT test

FTD Core Test Booklet Patient ID: _____ Date: _____ RA: _____

RAVLT

Trial 1 - **I am going to read a list of words. Listen carefully, for when I stop, you are to repeat back as many words as you can remember. It doesn't matter in what order you repeat them. Just try to remember as many as you can.** Read list 1, with a 1 sec interval between each word. Give no feedback.

Trial 2 – 5 - **Now I am going to read the same words again, and once again when I stop, I want you to tell me as many words as you can remember, including words you said the first time. It doesn't matter in what order you say them. Just say as many words as you can remember, whether or not you said them before.**

List B Trial - Now I am going to read a second list of words. This time, again, you are to say back as many words of the second list as you can remember. Again, the order in which you say the words does not matter. Just try to remember as many as you can

Trial 6 - **Now I want you to tell me as many words as you can from the first list of words that I asked you to remember.**

Trial 7 - After 20-30 mins **A short while ago I read a list of words to you several times, and you were trying** to learn these words. Tell me the words from that first list again **(that is, the list that we went through several times).**

	Recall Trials					LIST B	Recall Trials			
	A1	A2	A3	A4	A5		B1	A6	A7	
Drum						Desk				Drum
Curtain						Ranger				Curtain
Bell						Bird				Bell
Coffee						Shoe				Coffee
School						Stove				School
Parent						Mountain				Parent
Moon						Glasses				Moon
Garden						Towel				Garden
Hat						Cloud				Hat
Farmer						Boat				Farmer
Nose						Lamb				Nose
Turkey						Gun				Turkey
Colour						Pencil				Colour
House						Church				House
River						Fish				River
SCORE						SCORE				

The Rey diagram

This figure is placed horizontally in front of the participant. The time taken to copy the figure is recorded. The diagram and the subject's drawing are then removed and 1 minute is times. The subject is then asked to draw what they can remember of the diagram.

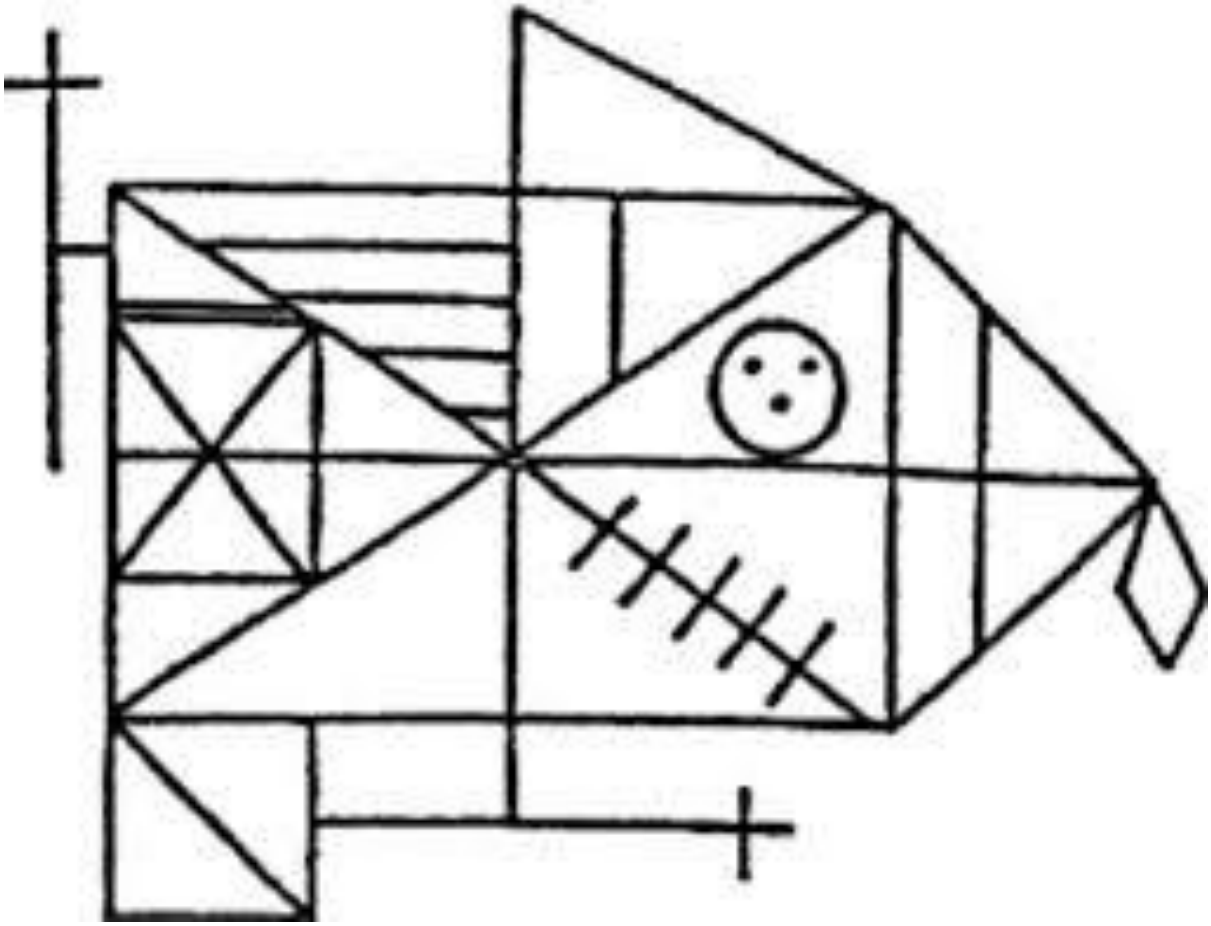

The trail making test

FTD Core Test Booklet ID: _____ Date: _____ RA: ____

Trail Making Test

PART A

Sample
"On this page (point) are some numbers. Begin at number 1 (point) and draw a line from one to two, (point), two to three (point) three to four (point) and so on, in order, until you reach the end (point) Draw the lines as fast as you can. Do not lift the pencil from the paper. Ready! Begin!"

Test
"On this page are numbers from 1 to 25. Do this the same way. Begin at number one (point) and draw a line from one to two (point) two to three (point), three to four (point) and so on, in order until you reach the end (point). Remember work as fast as you can. Ready! Begin!".

[If subject makes a mistake, call it to his/her attention immediately, do not stop timing.]

PART B

Sample
"On this page are some numbers and letters. Begin at number one (point) and draw a line from one to A (point), A to two (point), two to B (point) B to three (point), three to C (point) and so on, in order until you reach the end (point). Remember first you have a number (point 1) then a letter (point A), then a number (point 2) then a letter (point B), and so on. Draw the line as fast as you can. Ready! Begin!"

Test
"Good, let's try the next one. On this page are both numbers and letters. Do this the same way. Begin at number one (point) and draw a line from one to A (point), A to two (point) two to B (point) B to three (point), three to C (point) and so on, in order until you reach the end (point). Remember first you have a number (point 1) then a letter (point A), then a number (point 2) then a letter (point B), and so on. Do not skip around, but go from one circle to the next in the proper order. Draw the lines as fast as you can. Ready! Begin!"

Corrections:

- You started with the wrong circle. This is where you start (point)
- Please keep the pencil on the paper, and continue right on to the next circle.
- You only went as far as this circle (point). You should have gone to the circle marked END (point). Go on from here.
- You skipped this circle (point) You should go from number one (point) to two (point) two to three (point) and so on, until you reach the circle marked "END" (point)

  OR

  You skipped this circle (point) You should go from number one (point) to A (point) A to two (point), two to B (point), B to three (point) and so on, until you reach the circle marked "END" (point)

If patient can't complete Sample A with corrections, take the person's hand and guide the pencil (eraser end down) through the trail, then say ask them to try it, repeating the instructions.

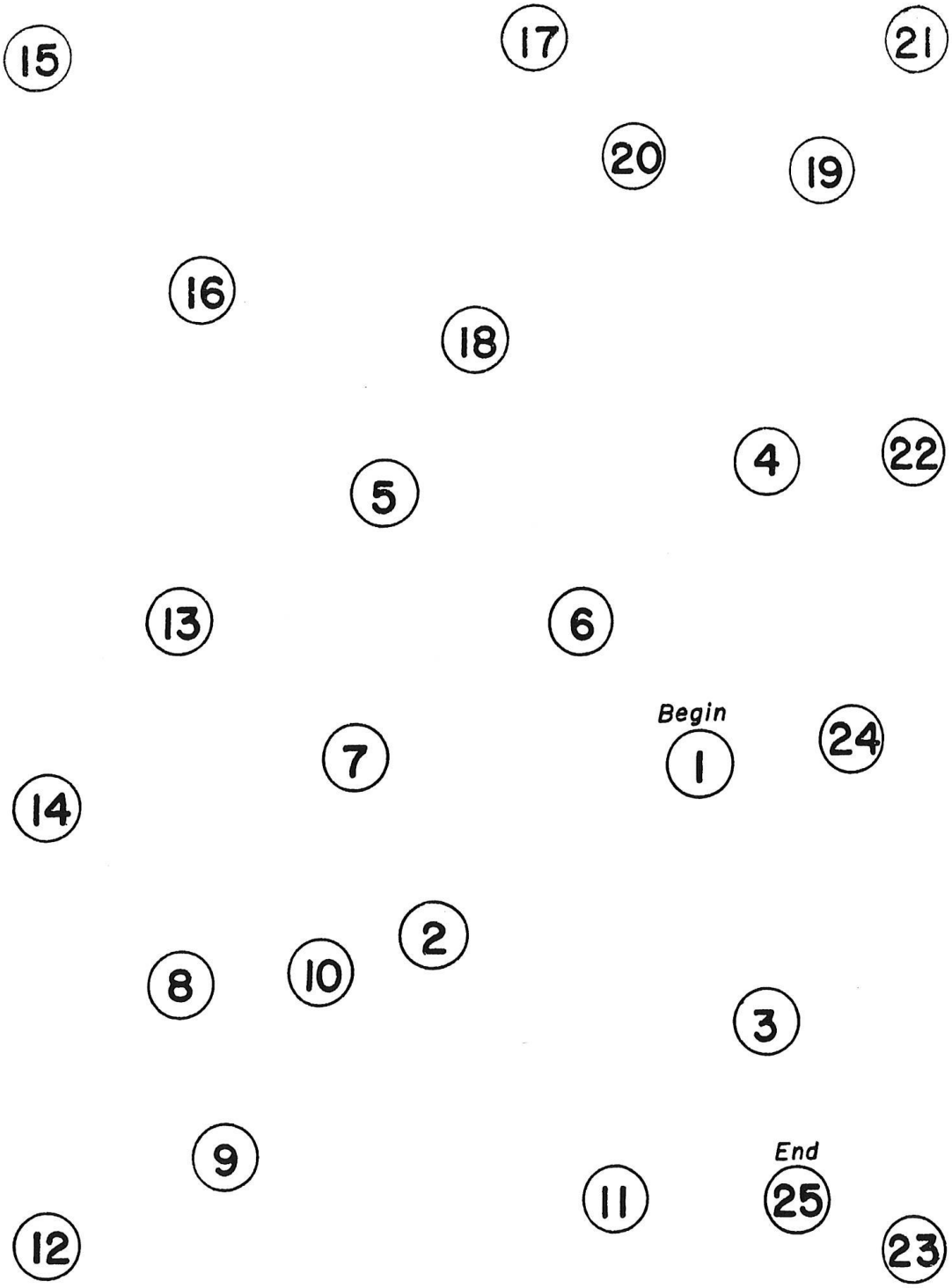
15
17
21
20
19
16
18
4
22
5
13
6
Begin
24
7
1
14
2
8
10
3
9
End
11
25
12
23

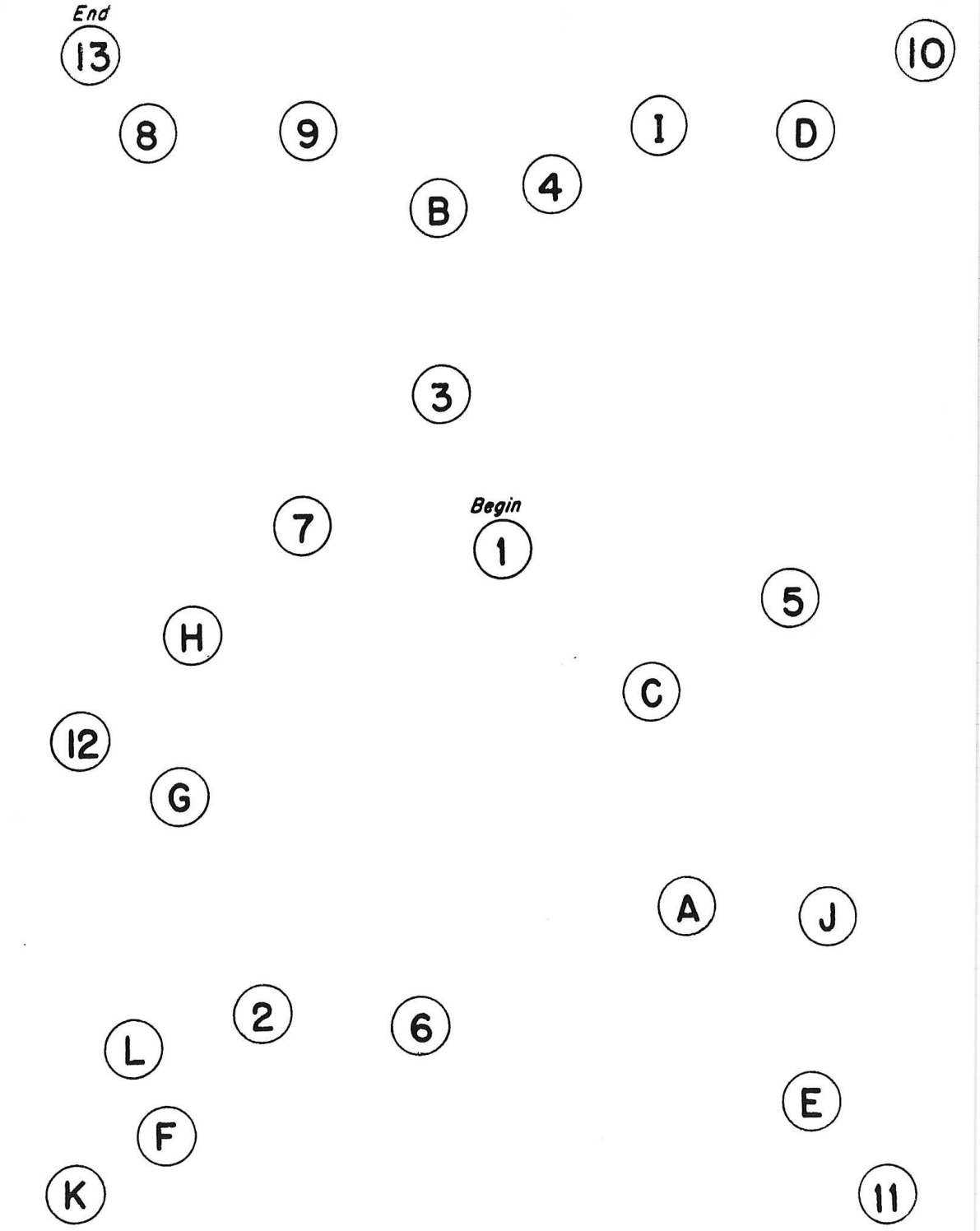
End
13
10
8
9
1
D
4
B
3
7
Begin
1
5
H
C
12
G
A
J
2
6
L
E
F
K
11

The verbal fluency test

FTD Core Test Booklet ID: _____ Date: _____ RA: ____

Verbal Fluency

I will say a letter of the alphabet then I want you to give me as many words that begin with that letter as quickly as you can. For instance, if I say "B", you might give me "bad", "battle" "bed".. I do not want you to use words that are proper names such as "Brisbane" or "Bob" and no numbers. Also, do not use the same word again but with a different ending such as "eat", "eating". Any questions?

Begin when I say a letter. The first letter is "F". Go ahead.

F	A	S
Total Correct:	**Total Correct:**	**Total Correct:**

Once this was complete the time was recorded (Tp0). Subjects were allowed to dress, and light levels were returned to normal. After 60 minutes, a further fasting blood sample was taken, and participants were taken for a fat preference meal (procedure as described above). Further blood samples were taken through the cannula at 2, 3, and 4 hours. The cannula was removed and the patient sent home.

TIME POINT	BLOODS					OBSERVATIONS					Skin Tem	VAS	GEM	Cog. task	Fat pref
	EDTA	LiHEP	Serum	Gluc	PAX	EMG	sBP	dBP	P	Tc					
On waking															
1h (Tn 60)	X3	X2	X2	X1	X1										
Ti 10’	X3	X2	X2		X1										
Ti 20’		X2	X2												
Ti 30’	X3	X2	X2		X1										
Ti 60’	X3	X2	X2		X1										
Ti 90’		X2	X2												
Ti 120’	X3	X2	X2	X1	X1										
Tp 0’															
Tp 60’	X3	X2	X2		X1										
Tp 120’	X3	X2	X2		X1										
Tp 180’	X3	X2	X2		X1										
Tp 240’	X3	X2	X2		X1										

Table 1. Sample sheet illustrating blood sampling and interventions. Taken on the second study day of both study arms. EMG, electromyogram; sBP, systolic blood pressure; dBP, diastolic blood pressure; P, pulse; Tc, core temperature (measured tympanically); skin temp, skin temperature (iButton measurement from foot); VAS, visual analogue scale; GEM, gas exchange monitor; cog task, cognitive tasks; fat pref, fat preference meal.

2.3.2. Sample Analysis

Biochemistry samples were sent to, and processed by Dr Keith Burling, Core Biochemical Assay Laboratory (CBAL), Addenbrooke's Hospital, Cambridge. Lipidomic and metabolomic samples were sent to and processed by Dr Albert Koulman, NIHR BRC Core Metabolomics and Lipidomics Laboratory, Department of Biochemistry, Addenbrooke's Hospital, Cambridge. The assays utilised are listed here: FT3 was assayed using the QPulse human FT3 Diasorin Liaison kit, and FT4 using the QPulse Human Diasorin Liaison FT4 kit, both of which utilise the solid phase antigen linked technique (SPALT). TSH was analysed using the Diasorin TSH liaison kit, using a sandwich chemiluminescent immunoassay technique. These used the Advia Centaur machine. Insulin was assayed using Diasorin Liaison insulin kit, utilising a sandwich chemiluminescence assay. Leptin was measured using an in-house two-site microtitre plate-based DELFIA assay which has been automated on the Perkin Elmer AutoDELFIA analyser. Glucagon was measured using a solid-phase two-site enzyme immunoassay (ELISA), using a kit from Mercodia AB, Sweden. Glucose was measured using a kit by Siemens Healthcare on the Siemens Dimension EXL analyser, which utilises an adaption of the hexokinase-glucose-6-phosphate dehydrogenase method. Cortisol was assayed using the Diasorin cortisol kit, based on the SPALT principle. BDNF (Brain-Derived Neurotrophic Factor) was measured using an in-house two-site plate-based assay on the MesoScale Discovery platform, using antibodies and standards from R&D systems.

2.3.3. Data analysis

Data was analysed using GraphPad Prism 6.0 and XLSTAT add-in for Excel software. Statistical tests were applied as stated in the thesis. Further details of analysis for the cooling study are given in chapter 4.

2.3.4. Lipidomics sample extraction

We adapted a method for open profiling of lipids by DIHRMS (Han and Gross 2003, Graessler, Schwudke et al. 2009). An automated method for the extraction of lipids was developed using an automated liquid handler (Integra Viaflo96, SLS, Nottingham, UK). Eighty samples, four blanks, and 12 QC samples in 1.2 mL Cryovials were randomized to 96-wells plate format, 100 µL of MilliQ H_2O was added to each of the wells and mixed, and then 100 µL of the mixture was transferred to a glass coated 2.4 mL deep well plate (Plate+™, Esslab, Hadleigh, UK). Next, 250 µL of MeOH was added containing

17 internal standards, followed by 500 µL of methyl tert-butyl ether (MTBE). The plates were then sealed (using Corning aluminium micro-plate sealing tape [Sigma Aldrich Company, UK]) and shaken for 10 min at 600 rpm, after which the plate was transferred to a centrifuge and spun for 10 min at 6,000 rpm. Each well in the resulting plate had two layers, with an aqueous layer at the bottom and an organic layer on top, from which 25 µL of the organic layer was transferred to a glass coated 240 µL low well plate (Plate+™, Esslab, Hadleigh, UK), and 90 µL of MS-mix (7.5 mM NH_4Ac IPA:MeOH [2:1]) was added using a Hydra Matrix, after which the plate was sealed and stored at –20 °C until analysis.

2.3.5. Direct infusion high-resolution mass spectrometry

All samples were infused into an Exactive Orbitrap (Thermo, Hemel Hampstead, UK), using a Triversa Nanomate (Advion, Ithaca, US). The Nanomate infusion mandrel was used to pierce the seal of each well before analysis, after which, with a fresh tip, 5 µL of sample was aspirated, followed by an air gap (1.5 µL). The tip was pressed against a fresh nozzle and the sample was dispensed using 0.2 psi nitrogen pressure. Ionization was achieved with a 1.2 kV voltage. The Exactive started acquiring data 20 seconds after sample aspiration began. The Exactive acquired data with a scan rate of 1 Hz (resulting in a mass resolution of 65,000 full width at half maximum [fwhm] at 400 m/z). After 72 seconds of acquisition in positive mode the Nanomate and the Exactive switched over to negative mode, decreasing the voltage to –1.5 kV. The spray was maintained for another 66 seconds, after which the analysis was stopped, and the tip discarded, before the analysis of the next sample began. The sample plate was kept at 15 °C throughout the analysis. Samples were run in row order and repeated multiple times if necessary to ensure accuracy.

2.3.6. Lipidomics data processing and peak picking

The resulting mass spectrometry data files were decompressed and converted to mzXML format using the “msconvert” tool in ProteoWizard (Chambers MC, Nature Biotechnology, 2012). For each infusion, an average spectrum was calculated from the user-defined time window. The R package “xcms” (Smith, Want et al. 2006) was used to average fifty spectra per mode using an m/z window of 185–1,000 and a retention time window of 20–70 seconds for positive ionization mode and 95–145 seconds for negative ionization mode.

A list of m/z identity pairs, based on expected and possible lipids in human serum, was used to extract small windows of data around the target m/z in the average spectrum. The peak maximum was measured and the two closest points to the half-height on either side were found, resulting in four points. The points with which a horizontal line at half-height intersected a line connecting the two points on either side of the peak (one above the half-height and one below) was used for a peak-width calculation (distance of the line) and a more accurate m/z value for the peak maximum (midpoint of the line). For all m/z identity pairs, the maximum intensity was recorded as well as the deviation of the peaks' accurate m/z. The final step was the combination of all the signals and deviations into their respective files. The technical set-up yielded average deviations of less than 4 ppm for the detected lipid species.

2.3.7. Metabolomics measurements

The levels of 175 metabolites were measured across samples in both study arms by the AbsoluteIDQ® Biocrates p180 Kit (Biocrates Life Sciences AG, Innsbruck, Austria) as reported elsewhere in detail (Illig, Gieger et al. 2010, Walsh, Broadhurst et al. 2012). We used a Waters Acquity UPLC (Waters ltd, Manchester, UK) system coupled to ABSciex 5500 Qtrap (Sciex ltd, Warrington, UK). In short: samples were derivatised and extracted using a Hamilton STAR liquid handling station (Hamilton Robotics Ltd, Birmingham, UK). Flow injection analysis coupled with tandem mass spectrometry (FIA-MS/MS) using multiple reaction monitoring (MRM) in positive mode ionisation was performed to measure the relative levels of acylcarnitines, phosphatidylcholines, lysophosphatidylcholines and sphingolipids; in negative ionisation mode the level of hexose was measured. Liquid chromatography coupled with tandem mass spectrometry (UPLC-MS/MS) using multiple reaction monitoring (MRM) was performed to measure the absolute concentration of amino acids and biogenic amines. The chromatography consisted of a 5 minute gradient starting at 100% aqueous (0.2% Formic acid) increasing to 95% acetonitrile (0.2% Formic acid) over a Waters Acquity UPLC BEH C18 column (2.1 x 50 mm, 1.7 µm, with guard column). Isotopically labelled internal standards are integrated with in the Biocrates p180 Kit for quantification. Data was processed in the Biocrates MetIDQ software.

2.3.8. Analysis of metabolomic data

Metabolomic data was first analysed using Metaboanalyst software to examine hierarchical clustering of the data. LIMMA, a program that was devised to fit linear models to microarray data, was used to fit a linear model to both lipidomic and metabolomic data. KEGG pathway analysis was conducted on amino acid measurements. An equivalent was not available for the analysis of lipid data, which was therefore analysed by examining species enrichment in cooling in order of significance.

CHAPTER THREE: IDENTIFICATION AND FUNCTIONAL CHARACTERISATION OF HUMAN MUTATIONS IN GPR10

3.1. Summary

GPR10 is a G protein coupled receptor expressed in key brain areas involved in the regulation of energy homeostasis, including the brainstem, and the dorsomedial nucleus and paraventricular nucleus of the hypothalamus. We hypothesised that disruption of GPR10 signalling may contribute to human obesity based on the phenotype of GPR10 null mice, which have are obese with reduced energy expenditure. The whole exome sequencing of 737 patients with severe early onset obesity, and the targeted resequencing of a set of obesity genes in a further 1811 patients identified 15 heterozygous variants in 17 patients. Identical methods applied to control exomes from the UK10K identified 5 heterozygous variants in 1117 subjects. These variants were taken forward for functional characterisation.

An enzyme-linked immunosorbent assay showed that none of the mutations significantly reduced cell surface expression. Second messenger assays, conducted with and without chimeric G protein to allow the detection of Gi-coupled pathways, demonstrated that the receptor signalled through Gq- and Gi-coupled pathways, and the mutations had a spectrum of effect, with three of those found in cases resulting in a complete loss of function. Radioligand binding assays, testing the ability of unlabelled PrRP to displace a radiolabelled version of the ligand, showed a similar range of effect, with the aforementioned three loss of function receptors failing to bind ligand. Collectively, these experiments showed that none of the mutations reduced cell surface expression. Thirteen of the 15 variants found in cases, and 4 of the 5 found in controls showed a degree of functional impairment, with 3 of each showing complete loss of function.

As the heterozygous-null mice appear to have a wild type-like phenotype on standard chow, it was hypothesised that the GPR10 variants might exert a dominant negative effect on the wild type receptor. Second messenger accumulation in cells co-transfected with varying doses of both wild type and selected mutant receptor DNA showed a dose-dependent inhibition of wild type signal by the mutant receptor, without alteration of wild type cell surface expression. Additionally, the viability of exploring mutation effect on fat accumulation was explored in a *C. elegans* model system.

3.2. Introduction

GPR10 is a G protein coupled receptor, and is stimulated by the RFamide, prolactin releasing peptide (PrRP). GPR10 and PrRP are expressed in key brain areas involved in the regulation of mammalian energy homeostasis, including the nucleus tractus solitarius and ventrolateral medulla in the brainstem, where PrRP colocalises with A1 and A2 noradrenergic neurons (Uchida, Kobayashi et al. 2010), the dorsomedial nucleus of the hypothalamus, where both GPR10 and PrRP colocalises with the leptin receptor (Dodd, Worth et al. 2014) , and in the paraventricular nucleus. GPR10 null mice on a C57BL/6 background are obese, with increased food intake and reduced energy expenditure (measured by cage calorimetry on a normal chow diet) (Takayanagi, Matsumoto et al. 2008). The biological basis of this phenotype has only been partially explained. Neurons in the brainstem are responsive to the gut hormone cholecystokinin, whilst neurons in the dorsomedial hypothalamus are necessary for the thermogenic effects of leptin ((Dodd, Worth et al. 2014) and unpublished data) and project to a number of key brain areas, including the medial preoptic area and the paraventricular nucleus (unpublished data from Professor Luckman's group has shown that these are not oxytocin neurons). Additionally, intact GPR10-mediated signalling contributes to the anorectic effects of leptin (Ellacott, Lawrence et al. 2002).

PrRP was first discovered using a reverse pharmacology approach (Hinuma, Habata et al. 1998). They identified a pituitary-expressed orphan receptor which they termed hGR3, which showed sequence homology to the previously described GPCR UHR-1. They then applied bovine hypothalamic extract and purified the ligand that resulted in its stimulation. They termed this protein prolactin-releasing peptide, because it seemed to release prolactin from when applied to a cell culture of the anterior pituitary cells of lactating rats. However other groups were unable to replicate this data, and there is a lack of staining of PrRP in the median eminence of the anterior pituitary. It is now accepted that release of prolactin is not the primary effect of PrRP.

GPR10 signalling has been implicated in modulating the stress response. Hypotensive haemorrhage causes *c*-fos activation in PrRP immunoreactive neurones in the nucleus tractus solitarius, and in CRH and vasopressin immunopositive neurons in the paraventricular nucleus of the hypothalamus. Injection of a retrograde tracer into these cells in the PVN showed that the brainstem PrRP-containing neurons conveyed this signal (Uchida, Kobayashi et al. 2010). They have impaired nociception, and PrRP can reverse opioid-induced analgesia (Laurent, Becker et al. 2005). Centrally administered PrRP promotes wakefulness and can suppress sleep oscillations on EEG and EMG (Lin, Arai et al. 2002). Additionally, injection of PrRP into the ventrolateral medulla results in dose-dependent increases in mean arterial blood pressure, heart rate and renal sympathetic nerve activity (Horiuchi, Saigusa et al.

2002). Interestingly it has been shown that the increase in blood pressure associated with obesity is mediated through the population of leptin receptors that reside in the dorsomedial hypothalamus, and proportion of which colocalise with PrRP-containing neurons (Simonds, Pryor et al. 2014).

The precise molecular mechanisms through which GPR10 mediates its effects have only partially been explored prior to this study. Langmead has previously demonstrated that GPR10 has both high and low affinity binding sites for PrRP (K_D 0.026 ± 0.006 and 0.57 ± 0.14 nM, respectively), and that both isoforms of PrRP (PrRP-20 and PrRP-31) are potent full agonists and result in calcium release from the endoplasmic reticulum, indicating Gq-coupled signalling. They additionally showed that PrRP does not increase basal cAMP levels (and therefore does not signal through Gs-coupled pathways), and in contrast to our findings does not reduce forskolin-stimulated cAMP levels (therefore concluding that there was no evidence of signalling through Gi-coupled mechanisms) (Langmead, Szekeres et al. 2000).

Biased signalling, rather than a complete disruption of signalling is another mechanism by which mutations in GPCRs may exert an effect. GPCRs may couple to more than one secondary messenger pathway, and the "tone" between these signalling pathways may be affected by mutations carried by the receptor. An example of this is the distinct roles attributed to different second messenger pathways stimulated by MC4R activation; disruption of Gq-mediated pathways in the paraventricular nucleus result in hyperphagic obesity, increased linear growth and hypothalamo-pituitary-adrenal inactivation, whereas inactivation of Gs-coupled pathways outside the PVN is responsible for the impairments of glucose metabolism and energy expenditure seen in MC4R deficiency (Li, Shrestha et al. 2016). As a result we explored the roles of Gs, Gq and Gi-coupled pathways in both the wild-type receptor and in all the mutations.

There was no segregation with gender. Insufficient family data was available to fully determine segregation with phenotype. However as the phenotype of these patients is severe, and all the GPR10 mutations are found in heterozygous form, it raises the possibility of either haploinsufficiency or a dominant negative effect.

It has been well established that rhodopsin-like group A GPCRs can form both homodimers and heterodimers by using molecular tools such as immunoprecipitation, enzyme complementation assays and bioluminescent resonance energy transfer (BRET); for example the alpha1-adrenoceptor has been shown to dimerize with the chemokine receptor, CXCR (Milligan, Wilson et al. 2005). There are also examples where this interaction has been shown to have a dominant negative effect, for example mutant forms of the TSH receptor can dimerize with the wild type receptor, resulting in a dominantly inherited form of TSH resistance (Calebiro, de Filippis et al. 2005). This is therefore a feasible

explanation for the severe phenotype we observe in our patients with heterozygous GPR10 variants, and was explored further here.

While no rare human variants in GPR10 have been described, our group has previously detailed a common variant, P305L (Bhattacharyya, Luan et al. 2003). 94 patients with severe early onset obesity were screened for variants in GPR10. Two non-synonymous variants were found, one of which, P305L, had functional consequences and reduced endoplasmic calcium release on ligand stimulation relative to wild type. This was typed in 1084 UK Caucasians, and was found to have a MAF 7%. While this variant was not associated with an increase in BMI, it was associated with a lower systolic blood pressure (5mmHg, $p<0.05$) and diastolic blood pressure (4mmHg, $p<0.01$).

In this study we examined whether GPR10 is involved in human energy homeostasis by testing whether rare variants in GPR10 are associated with severe human obesity, and secondly by ascertaining whether these variants affect the function of GPR10 *in vitro*.

3.3. Methods

The human GPR10 gene (Genbank Association number NM_004248.2) comprises 2 exons located on chromosome 10. In collaboration with Prof Ines Barroso at the Wellcome Trust Sanger Institute, the whole exome and targeted resequencing was undertaken of 2548 patients with severe early onset obesity, and a further 1118 subjects sequenced using the same methods as art of the UK10K project. This identified 15 variants in 17 cases, and 5 variants in controls. Having identified rare variants in GPR10 we undertook functional studies in order to ascertain whether these mutations disrupted the function of GPR10 protein.

We firstly created the mutants with N-terminal FLAG in a pCMV-Tag2B construct by site-directed mutagenesis using the Quikchange II kit. We then set out to define the function of wild type GPR10, determining the signalling pathways triggered by ligand application by using second messenger assays. Stimulation of GPR10 failed to increase cAMP, indicating that GPR10 is not a Gs-coupled receptor. Stimulation of GPR10 did increase the cellular concentration of inositol monophosphate, a breakdown product of inositol triphosphate, indicating that GPR10 signals through Gq-coupled pathways. Gi-coupled signalling was explored in to ways; firstly the inositol monophosphate accumulation assay was repeated in cells co-transfected with GαΔ6qi4myr, a chimeric G protein that couples Gi binding residues to Gq signalling, allowing for a readily detectable response. This showed a dose-dependent increase in IP1, indicating signalling through Gi-coupled residues. However, this is an artificial system. To further test whether wild type GPR10 does signal through Gi-coupled pathways a HEK293 cell line stably transfected with wild type GPR10 was stimulated with forskolin, a receptor-independent stimulator of adenylate cyclase. Stimulation with ligand resulted in a dose-dependent reduction in cAMP, thereby confirming that the receptor signals via Gi-coupled mechanisms, in addition to Gq. The IP1 assay, performed with and without GαΔ6qi4myr therefore formed the basis of the functional characterisation of mutation impact on signalling.

An in-house ELISA, with primary antibody directed at N-terminal FLAG, was used to assess the cell surface expression of mutants. This demonstrated that none of the mutations reduced cell surface expression. Results were confirmed by confocal microscopy in HEK293 cells, with anti-FALG antibody used to localise GPR10 and wheat germ agglutinin to show cell membrane.

A competition radioligand binding assay was used to explore the effect of the mutations on radioligand binding. As all the variants were found in heterozygous form, and the heterozygous-null mouse is not known to be obese we tested the possibility of the mutant receptor exerting a dominant negative effect on the wild type receptor by measuring IP1 accumulation in cells co-transfected with varying

doses of wild type and mutant cDNA in COS7 cells. A second wildtype construct tagged with c-myc was created to allow differentiation of their relative levels of cell surface expression by ELISA assay. The three complete loss of function variants found in cases (A121D, P193S, P237R) were selected for testing. All methods are described in detail in Chapter 2.

3.4. Results

3.4.1. Identification of rare variants in GPR10 in the GOOS cohort

3.4.1.1. Genetic studies

In collaboration with Dr Ines Barroso at the WT Sanger Institute, we performed exome sequencing of 737 UK GOOS patients in whom known causes of obesity have been excluded. Using the Agilent Sure-Select Human All Exon 50Mb array followed by Illumina HiSeq, high quality sequence data was obtained. These data were compared to 1,117 exomes from the UK10K exomes, comprised of DNA from patients with other diseases, and consented controls, analysed using the same multiple sample calling techniques. This identified one heterozygous mutation in GPR10, L350S. The targeted resequencing of a set of obesity genes in a further 1,811 patients was then undertaken (Hendricks AE, Science reports, 2017), identified a further 13 heterozygous GPR10 mutations in 15 patients. Sanger sequencing failed to confirm three of these mutations, resulting in a total of 11 mutations in 13 patients, and no mutations in control exomes. Based on the statistically significant enrichment in the GOOS cohort, compared to the ExAC database, these mutations were taken forward for further study. However, in 2015, a second data release was made, where data had been analysed using a different multiple sample calling algorithm; four additional mutations were identified in cases and five in controls. The prevalence of non-synonymous mutations was no longer enriched in the GOOS cohort, when compared to UK10K controls (Table 2). It should be noted that the control exomes in the UK10K cohort are taken from patients with other diseases, who were included in the UK10K project. No BMI data are available for these patients, so it is possible that these individuals may also be obese. Insufficient family data was available to state whether they segregated with phenotype. Both males and females were seemingly affected equally.

	GOOS			UK10K controls		
	Variants	Cohort size	% variants cohort	Variants	Cohort size	% variants cohort
	17	2,548	0.67	5	1,117	0.447
OR			1.5			
p value			0.5			

Table 2. Analysis of GPR10 variants found in the GOOS cohort in comparison with controls. Comparison of variant frequency between the GOOS cohort and the UK10K controls.

3.4.1.2. Location of mutations within the GPR10 molecule

Mutations were located throughout the GPR10 molecule, with no clustering in any one region. Some of the mutations found affected highly conserved residues (P193S, P237R). The functional characterisation of 15 variants in cases and 5 variants in controls are presented here.

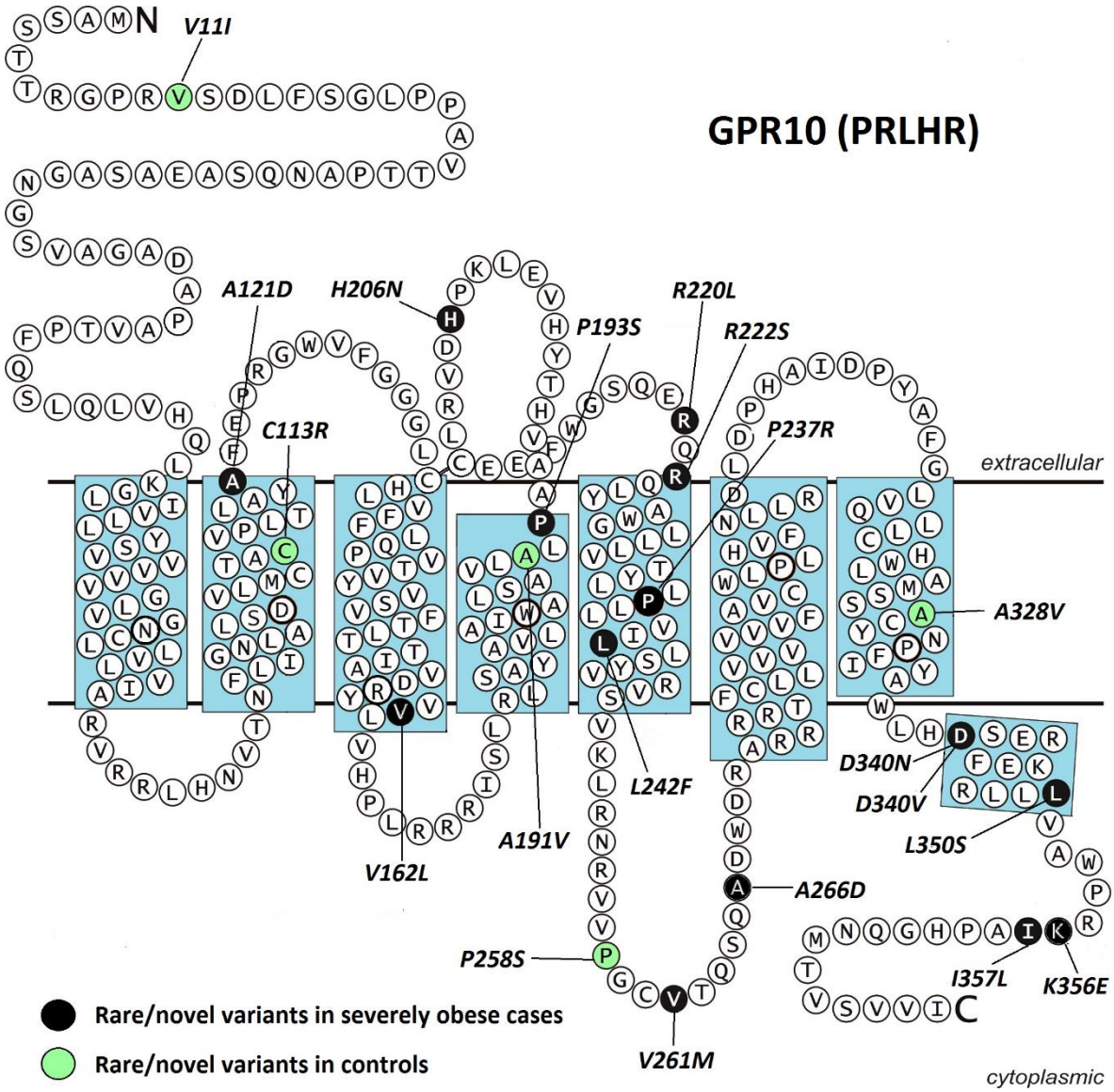

Figure 3. Two dimensional model of GPR10. ENSG00000119973 (GPR10), showing its seven trans-membrane structure. Mutations found in cases are shown in black, and those found in controls are in green. This was constructed using homology modelling of other GPCRs, based on the alignment of the highly conserved residues.

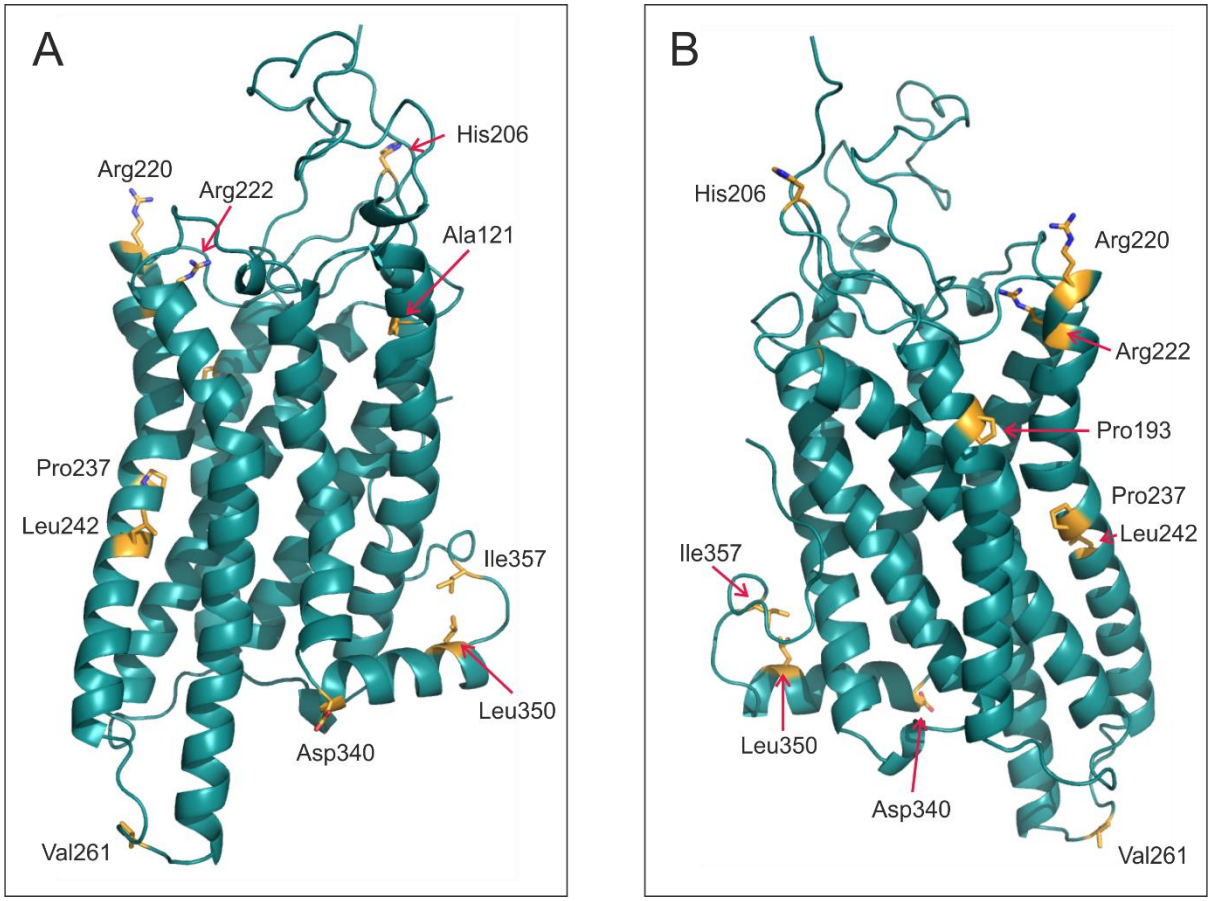

Figure 4. Molecular structure of GPR10 generated by homology modelling with protein structure prediction server Robetta. Secondary structure represented by ribbons is shown as parallel to the membrane plane, with extracellular side of the receptor on top and cytoplasmic side on the bottom, respectively. In the front plane from left to right, in panel A, transmembrane (TM) domain V, TM-VI, TM-VII with helix 8 and TM-I, whereas in panel B, TM-II, TM-IV, TM-V with TM-III going across behind TM-IV from extracellular end of TM-II towards intracellular end of TM-V. Amino acid residues affected by mutation are presented in orange.

3.4.2. Functional characterisation of rare variants in GPR10

Functional studies were performed on 15 variants in GPR10 found in cases and 5 in controls to test whether these genetic changes have functional consequences on the protein. Mutations were created by site-directed mutagenesis using the Quikchange II kit, and successful mutagenesis was confirmed by Sanger sequencing (Methods, chapter 2).


V11I
Homo sapiens_PRLHR
Macaca mulatta_PRLHR
Canis lupus familiaris_PRLHR
Danio rerio_prlhr2a
Drosophila melanogaster_sNPF-R
Caenorhabditis elegans_npr-6
C113R
A121D
V162L
A191V
P193S
H206N
R220L
R222S
P237R
L242F
P258S
V261M
A266D
P305L
A328V
D340V
D340N
L350S
K356E
I357L
Homo sapiens_PRLHR
Macaca mulatta_PRLHR
Canis lupus familiaris_PRLHR
Danio rerio_prlhr2a
Drosophila melanogaster_sNPF-R
Caenorhabditis elegans_npr-6

Figure 5. Sequence alignment of variants found in the GOOS cohort and UK10K controls. A species alignment of GPR10 proteins was performed using Geneious software. All variants occurred in residues conserved across mammals, and in some cases (V162L, P193S, R222S, P237R, D340V/N) to the level of the nematode Caenorrhabditis elegans. GOOS cohort shown in red and UK10K controls in green. A previously published common variant, P305L (add ref), is shown in orange.

3.4.2.1. Cell surface expression of mutant forms of GPR10

To test the levels of cell surface expression of variants relative to wild type receptor an in house enzyme-linked immunosorbent assay was established in which FLAG-tagged variants were detected with a primary anti-FLAG murine antibody, which was then in turn detected by a goat anti-mouse antibody conjugated to horseradish peroxidase allowing for its detection. Initially a gene-dosing experiment (5 - 200ng cDNA/well) was performed to validate the assay and define the optimal gene dose for future experiments (1-25ng/well; 5ng/well was selected).

Cell surface expression was studied in COS7 cells (35,000 cells/well) transiently transfected with FLAG-tagged constructs encoding wild type or mutant GPR10 or empty pCMV-Tag2B vector DNA. These experiments showed that none of the mutations reduced cell surface expression compared to the wild-type receptor. Two of the mutations (V261M, I357L) were expressed at a higher level than the wild type receptor (Figure 5). This was an unexpected result, further experiments were therefore undertaken to test the effect of the mutations on cell surface expression. Firstly, it was proposed that the result of the ELISA may in part be down to the protocol; cells are fixed before the application of the primary antibody, and it was proposed that this may make cells permeable to the antibody, allowing for detection of intracellular FLAG. This possibility was explored using an alternate ELISA protocol, where the primary antibody was applied before cell fixation, and cells were kept on ice until after fixation to slow cellular metabolism. The results from these experiments were similar to those of the standard ELISA technique, and it was therefore concluded that the standard ELISA results were not secondary to detection of intracellular antigen.

A. Cell surface expression of variants found in cases relative to wild type.

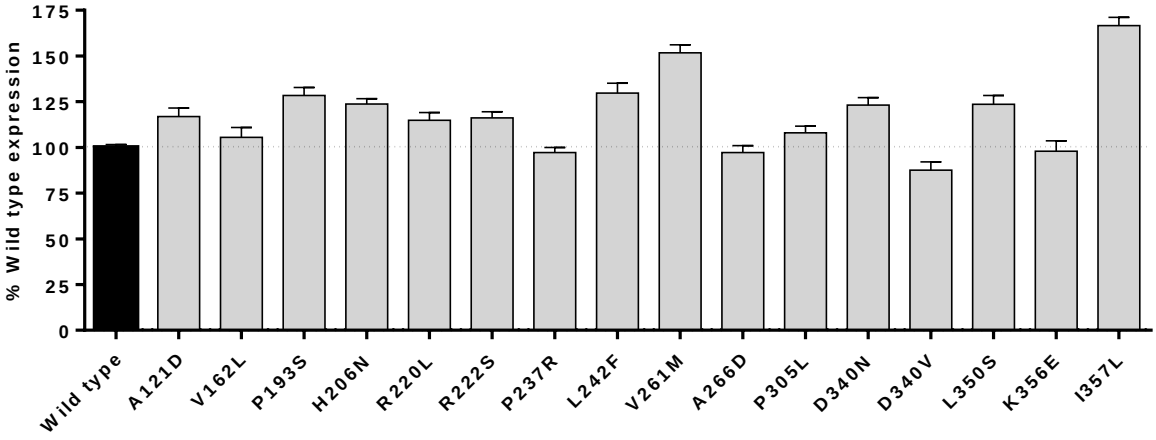

B. ELISA demonstrating cell surface expression of variants found in controls relative to wild type.

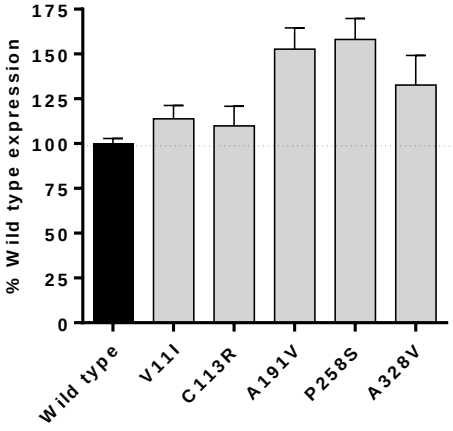

Figure 6. Mutations in GPR10 do not reduce the cell surface expression of receptor, relative to wild type. COS 7 cells were seeded at a density of 25,000 cells per well into 96-well plates and transiently transfected with 5ng/well of either mutant or wild type GPR10 in a pCMV-Tag2B construct. After 24 hours cells were fixed and an enzyme-linked immunosorbent assay (ELISA) performed to determine relative levels of cell surface expression. Results were fitted to a non-linear regression curve and normalised relative to wild type in GraphPad Prism 6.0. An unpaired T test was performed for each variant; after a Bonferroni correction, none of the variants were expressed at significantly different levels than wild type ($P<0.0025$).

3.4.2.2. Cellular localisation of GPR10 using confocal microscopy

Confocal microscopy of cells transiently transfected with selected mutants was performed to ascertain cellular localisation. A HEK 293 cell line (University of Dundee) was used, as the high ratio of cytoplasm to cell volume in this cell line allows for easier visualisation of the cellular sublocalization of fluorescent signal. Wheat germ agglutinin and DAPI were used to stain cell membranes and nuclei, respectively. FLAG-tagged mutant or wild type GPR10 was targeted with an Alexa 488 anti-FLAG M2 antibody. For each mutation, 20 representative images were taken. Images were viewed and analysed using ImageJ software.

Cells transfected with the empty vector, pCMV-Tag2B were used as a negative control, and did not show any Alexa 488 signal. Cells transfected with wild type receptor showed clear signal at the cell membrane. Three loss of function mutations, A121D, P193S and P237R were tested for comparison to wild type together with selected other mutants. All showed receptor present at the cell membrane, and not in the cytoplasm (Figure 6). These data concur with the findings of the ELISA.

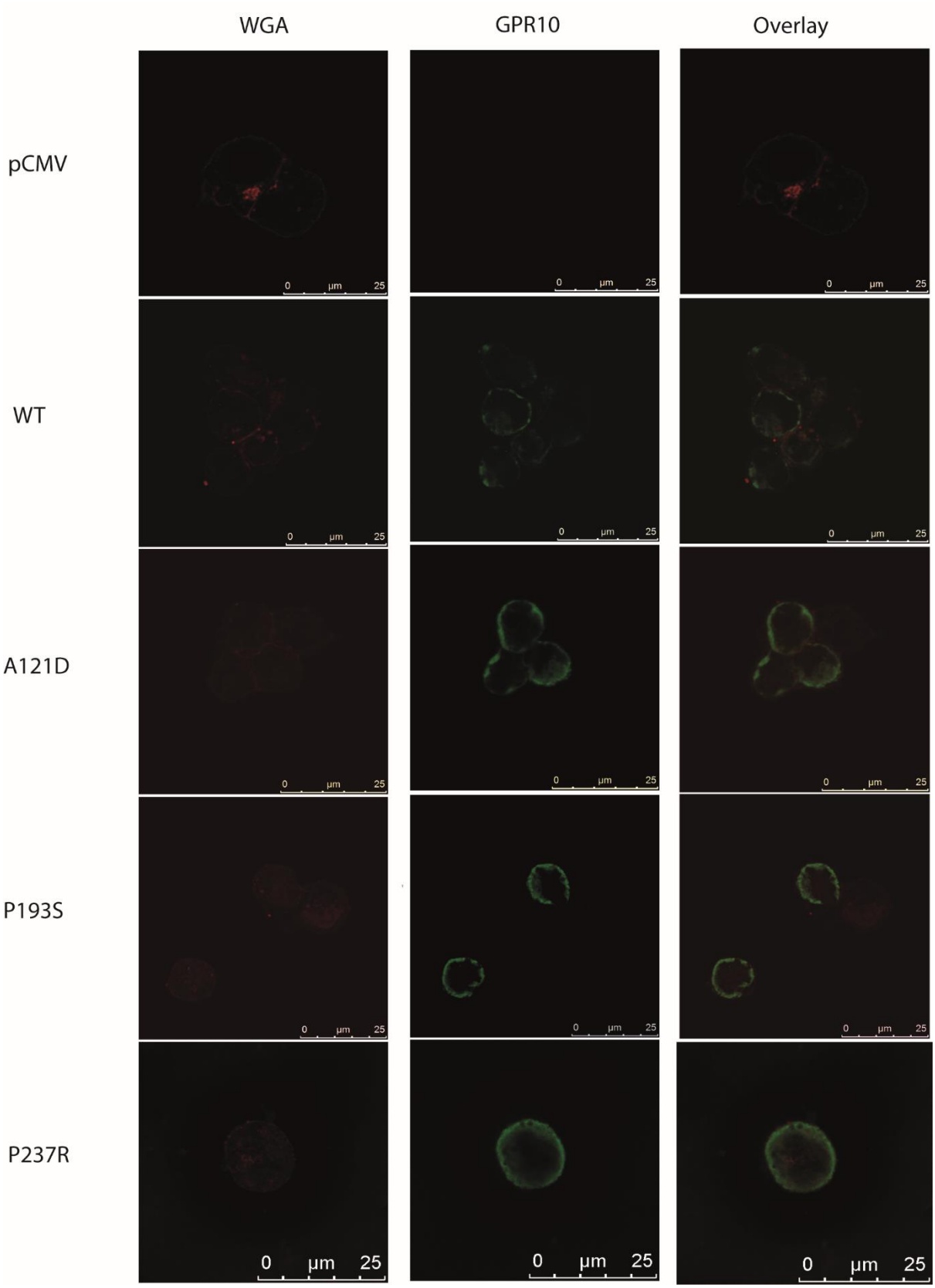
WGA
GPR10
Overlay
pCMV
WT
A121D
P193S
P237R
0 µm 25

Figure 7. Cellular localisation of FLAG-tagged mutant GPR10. FLAG-tagged GPR10 was visualised in HEK293 cells with the anti-FLAG antibody seen in green. Wheat germ agglutinin shows cell membranes in red. DAPI nuclear staining was performed, but has been removed from these images for ease of visualisation. Wild type GPR10 was seen at the cell membrane, and little cytoplasmic staining was seen. GPR10 loss of function mutations were all seen at the membrane, as were selected other mutations tested, with little or no mutant seen at other cellular locations.

3.4.2.3. GPR10 signals through both Gi and Gq pathways

GPR10 mediates signalling by prolactin-releasing peptide (PrRP). Based on studies in rodents, two PrRP isoforms exist: PrRP-31 and a truncated form, PrRP-20. Existing literature indicates that these ligands bind to GPR10 with comparable affinity, and no significant difference in potency has been demonstrated. For my initial experiments I tested the signalling response to stimulation with both ligands at a concentration of $20x10^{-6}$M and found no difference in potency. All subsequent experiments were performed with a range of $20x10^{-12}$ - $20x10^{-6}$ M concentration of PrRP-31.

To test the signalling profile of WT human GPR10, a series of assays were performed. To test Gαs mediated signalling, a cAMP accumulation assay using the HitHunter assay platform in HEK293 cells transiently transfected with WT GPR10 was used, and found that there was no evidence of cAMP accumulation.

To test Gq-coupled signalling, COS 7 cells transfected with wild type GPR10 and stimulated with PrRP-31 were assessed using an inositol monophosphate accumulation assay which measures activity of the IP3/calcium coupled intracellular pathway. Dose-dependent accumulation of IP1 was demonstrated.

Gi signalling is challenging to assay, as it results in a reduction in cAMP, which is difficult to measure. Gi signalling was therefore explored using two methods. Firstly, cells were co-transfected with both wild-type receptor and a promiscuous chimeric G protein, GαΔ6qi4myr, which couples Gi binding residues on the internal surface of the GPCR to a Gq signalling pathway, allowing for a detectable response. This assay showed a dose-dependent increase in IP1 with increasing concentrations of PrRP-31 (Figure 9).

The use of chimeric G protein is an artificial system, and therefore it was important to test the PrRP-stimulated activity of Gi-coupled pathways by an independent method. COS-7 cells were stably transfected and stimulated with forskolin, a receptor-independent stimulator of adenylyl cyclase. The

reduction in cAMP was then measured on stimulation with PrRP-31, which occurred in a dose-dependent manner, thereby confirming the results of the chimeric G protein assay (Figure 7). This resulted in dose-dependent accumulation of IP1 on stimulation with PrRP-31.

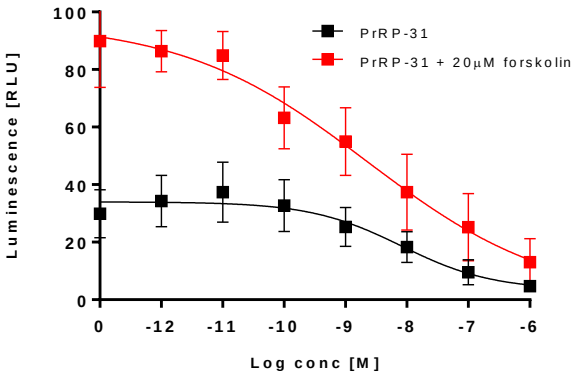

Figure 8. Stimulation of HEK293 cells stably transfected with GPR10, with and without forskolin. The data in black shows inhibition of intrinsic cAMP levels with increasing doses of PrRP-31. The data in red demonstrates inhibition of forskolin-stimulated levels of cAMP. Data was fitted to a non-linear regression curve and normalised in GraphPad Prism 6.0. Cumulative data from 4 individual experiments is shown with mean and standard deviation.

3.4.2.4. GPR10 mutants impair signalling through Gq pathways when stimulated with PrRP-31

To test the effects of GPR10 mutant on signalling, mutant constructs were transiently transfected into COS7 cells. An inositol monophosphate assay was used to assess signalling through the Gq receptor. Cells cultured in medium supplemented with myo-[^{3}-H]-inositol were treated with lithium chloride to prevent the dephosphorylation of inositol monophosphate into myoinositol. Cells were stimulated with varying doses of PrRP-31, and a scintillation proximity assay was performed to measure the relative amounts of radiolabelled IP1 that accumulated.

Of the 15 variants found in cases that were tested on the Gq assay platform, four showed a complete loss of function (A121D, P193S, P237R, A266D), with a further six showing a partial loss of function. Of the five variants found in controls, three showed a complete loss of function, one a partial loss of function, and one demonstrated a wild type-like response. An additional common variant, P305L,

reported previously was tested in addition to wild type receptor and mock transfected cells as a further control. This is a common variant previously described by our group, that is associated with a lower blood pressure that weight-matched controls, but not with obesity. This showed a partial loss of Gq signalling (Figure 9).

A. Normalised response of COS-7 cells transiently transfected with variants found in cases, relative to wild type receptor (n=3-8)

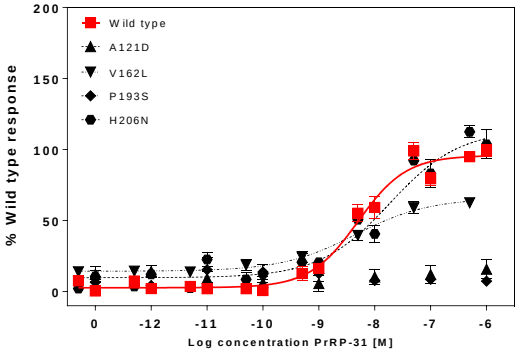

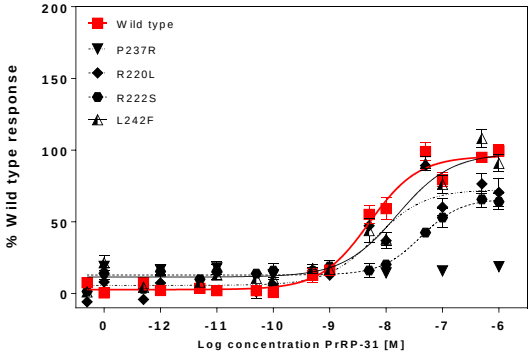

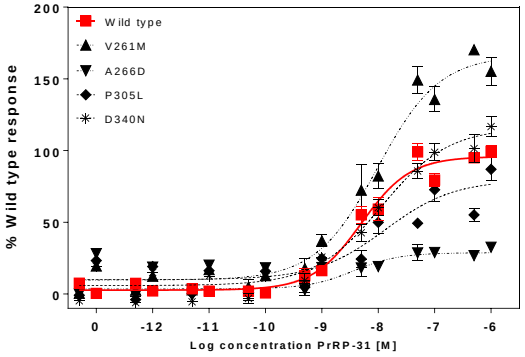

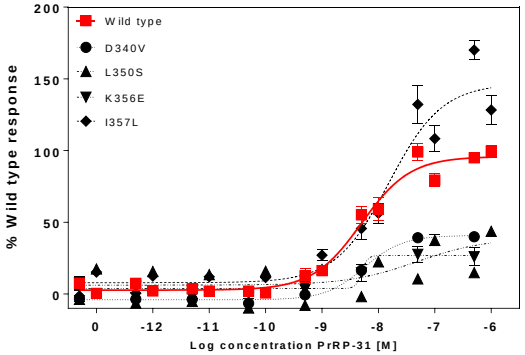

B. Normalised response of COS7 cells transiently transfected with variants found in controls, relative to wild type (n=3)

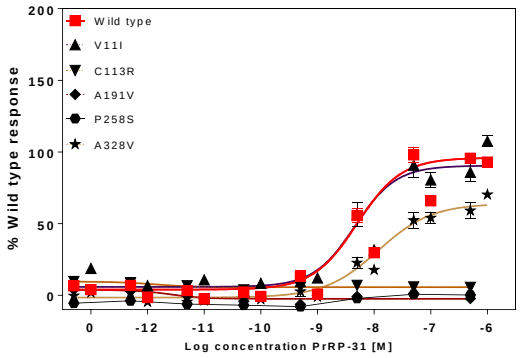

Figure 9. GPR10 mutations found in cases (A) or controls (B) impair signalling through Gq pathways when stimulated with PrRP-31. COS7 cells transiently transfected with either mutant or wild type DNA were cultured in media supplemented with myo-[^{3}-H]-inositol. Cells were treated with 10mM lithium to prevent degradation of inositol monophosphate, and were stimulated with PrRP-31. Inositol monophosphate accumulation was measured using a scintillation proximity assay. Three variants found in cases resulted in a complete loss of function (A121D, P193S, P237R), with a further nine causing a partial loss of function. Of the variants found in controls, three resulted in a complete loss of function. One caused a partial loss of function, and one had no effect. Each graph represents the normalisation of a minimum of three independent experiments and is plotted showing the standard error of mean (Castellano, Navarro et al.). The potency (IC50) and efficacy (Emax) with standard error of mean were calculated from normalised data fitted to a non-linear regression curve in GraphPad Prism 6.0.

3.4.2.5. GPR10 mutants impair signalling through Gi pathways when stimulated with PrRP-31

Cells co-transfected with either wild type or mutant DNA and GαΔ6qi4myr chimeric G protein were assessed for they ability to generate inositol monophosphate as previously described. Three of the variants found in cases demonstrated a complete loss of function (A121D, P193S, P237R), with a further 10 showing a partial loss of function. One mutation, I357L, which demonstrated a gain of function of both Gq and Gi signalling (Figure 9). Interestingly this receptor also showed an increase in cell surface expression on the ELISA, and so it may be that the increase in IP1 accumulation is due to an increased presence of receptor at the cell membrane, rather than an increased ability of the receptor to signal.

Of the four mutations that showed a complete loss of function on the Gq platform, three showed a complete loss of Gi signalling too, with one showing a partial loss of function (A266D). Two of the mutations that had shown wild type-like signalling on the Gq platform showed a partial loss of Gi signalling (H206N, D340N), thereby providing a possible explanation as to their pathogenicity. One mutation that had shown a partial loss of Gq signalling showed wild type-like levels of Gi signalling. These data indicate that some mutations in GPR10 result in a signalling bias towards either Gi or Gq signalling.

A. Gi-coupled signalling of variants found in cases. Data is normalised relative to wild type and shows inositol monophosphate accumulation in COS7 cells co-transfected with receptor and chimeric G protein (n=3-8).

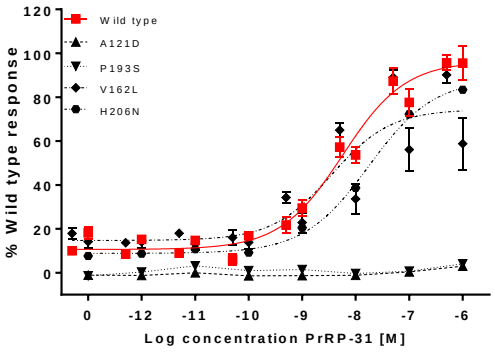

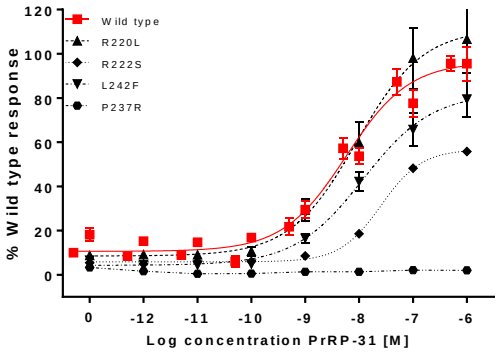

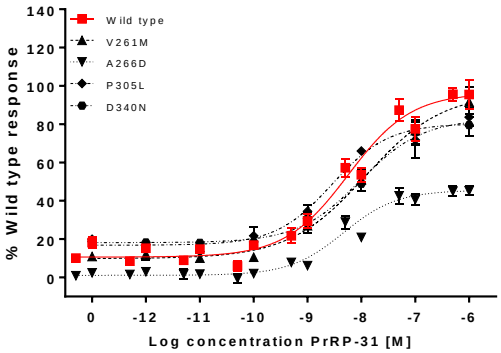

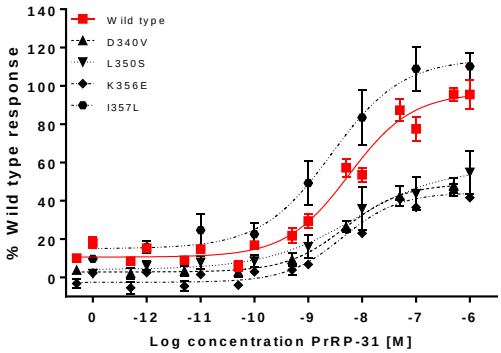

B. Gi-coupled signalling of variants found in controls. Data is normalised relative to wild type and shows inositol monophosphate accumulation in COS7 cells cotransfected with receptor and chimeric G protein

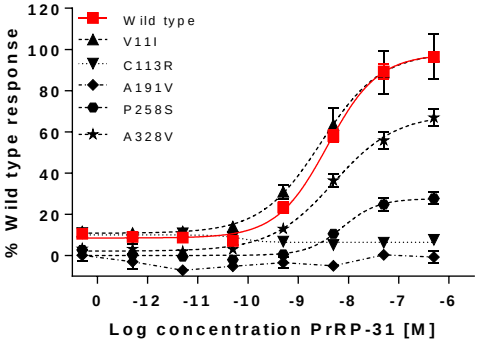

Figure 10. GPR10 mutations found in cases (A) or controls (B) impair signalling through Gi pathways when stimulated with PrRP-31. COS7 cells transiently transfected with either mutant or wild type DNA plus the chimeric G protein, GαΔ6qi4myr, and were cultured in radiolabelled myoinositol. Cells were treated with lithium to prevent degradation of inositol monophosphate, and were stimulated with PrRP-31. Inositol monophosphate accumulation was measured using a scintillation proximity assay. The potency (IC50) and efficacy (Emax) with standard error of mean were calculated from normalised data fitted to a non-linear regression curve in GraphPad Prism 6.0.

Three of the mutations found in cases demonstrated a complete loss of function (A121D, P193S, P237R), with a further 10 showing a partial loss of function. Some of the results were discordant with the findings of the IP1 assay conducted without chimeric G protein; mutations H206N, R220L, L242F showed a partial loss of function in the Gi assay, whereas signalling through Gq was comparable to wild type. Conversely mutations V162L and L350S appeared wild type like in the Gi assay, but caused a partial loss of function in the Gq assay. These are examples of mutations causing a signalling bias.

3.4.2.6. Human mutations in GPR10 impair binding of PrRP-31

To examine the functional consequences of the mutations on the binding of ligand, we performed a competition binding assay where the displacement of radioactive ^{125}-I-PrRP-31 by non-radioactive (cold) PrRP-31 was measured in a scintillation proximity assay. All three of the mutations found in cases that showed a complete lack of ability to generate inositol monophosphate either with or without the use of chimeric G protein also failed to bind ligand. All of the remaining mutations, with the exception of variants V162L and I357L, showed a partial reduction in their ability to bind ligand. Of the three loss of function variants found in controls, two failed to bind ligand, with the remaining three showing wild type levels of binding (Figure 12).

A. Competition binding assay showing normalised data of variants found in cases relative to wild type (n=4)

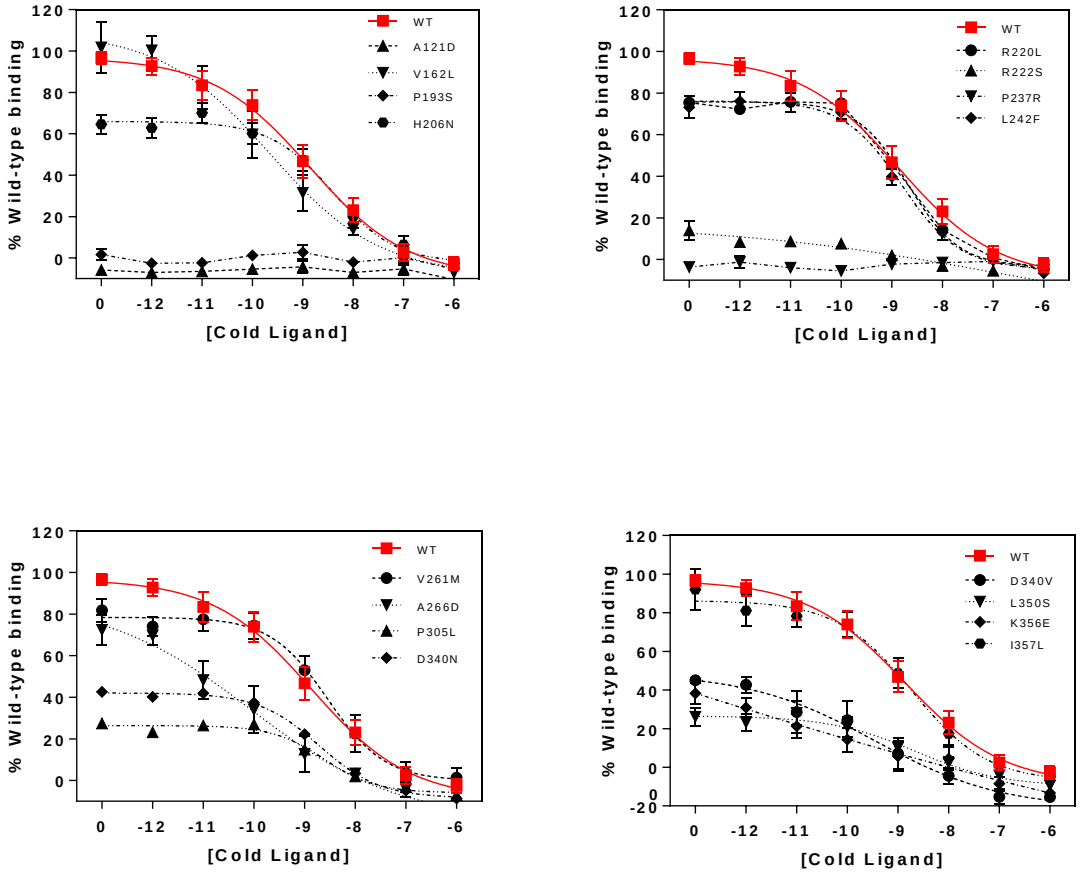

B. Competition binding assay showing normalised data of variants found in controls relative to wild type (n=4)

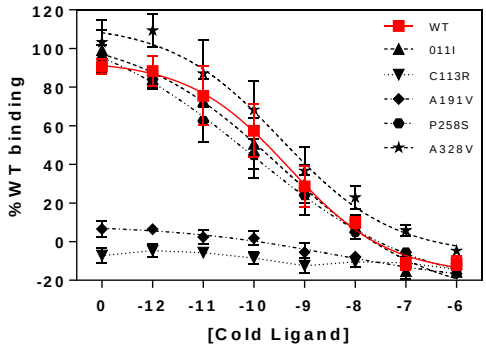

Figure 11. GPR10 mutations found in cases (A) or controls (B) impair ligand binding.

COS7 cells were transiently transfected with either FLAG-tagged mutant or wild type DNA in a pCMV-Tag2B construct. ^{125}I-PrRP-31 was applied, followed by varying doses of unlabelled PrRP-31. Radioactivity was measured using scintillation. Three mutations fond in cases showed a complete impairment of binding, with a further ten showing a partial loss of binding. Two of the variants found in controls showed impaired binding, with three responding in a manner comparable to wild type. The

potency (IC50) and efficacy (Bmax) with standard error of mean, were calculated from normalised data fitted to a non-linear regression curve in GraphPad Prism 6.0.

Summary Data: Impact of Human GPR10 mutations on receptor function

GPR10 variant	Cell surface expression [%WT]			Ligand binding (radioligand competition)							
				Affinity (IC_{50}) (Locke, Kahali et al.)			F_{mut} (var_{IC50}/WT_{IC50})	Number of binding sites (B_{max}) [%WT]			
Cases	**Mean**	**SEM**	**n**	**Mean**	**SEM**	**n**		**Mean**	**SEM**	**n**	
WT	100	N/D	12	2.2	± 1.0	6	N/D	100	± N/D	8	
A121D	117	± 7.4	4	N/D (cLoF)		4	N/D	N/D (cLoF)		4	
V162L	108	± 15	4	1.3	± 0.2	3	0.6	91	± 10	3	
P193S	129	± 7.6	4	N/D (cLoF)		4	N/D	N/D (cLoF)		3	
H206N	124	± 1.7	4	1.6	± 0.5	4	0.7	65	± 6.2	4	
R220L	116	± 8.9	4	1.0	± 0.3	4	0.5	81	± 7.8	4	
R222S	115	± 5.1	4	1.0	± 0.5	3	0.5	13	± 3.2	4	
P237R	97	± 3.5	4	N/D (cLoF)		4	N/D	N/D (cLoF)		3	
L242F	129	± 14	4	0.9	± 0.2	4	0.4	80	± 9.2	4	
V261M	152	± 7.9	4	1.0	± 0.2	3	0.5	86	± 6.0	4	
A266D	98	± 7	4	1.3	± 0.5	3	0.6	63	± 3.7	3	
D340N	123	± 11	4	1.0	± 0.1	3	0.5	46	± 4.2	3	
D340V	87	± 12	4	1.8	± 0.5	3	0.8	46	± 3.3	3	
L350S	123	± 9.2	4	1.3	± 0.3	4	0.6	30	± 6.1	4	
K356E	97	± 17	4	3.8	± 2.0	3	1.7	26	± 4.1	3	
I357L	167	± 7.6	4	0.5	± 0.04	4	0.2	99	± 23	4	
Controls											
V011I	102	± 7.8	4	1.7	± 0.4	3	0.8	85	± 4.7	3	
C113R	91	± 20	4	N/D (cLoF)		3	N/D	N/D (cLoF)		3	
A191V	124	± 9.8	4	6.9	± 0.3	3	3.1	11	± 3.0	4	
P258S	138	± 20	4	1.4	± 0.8	3	0.6	84	± 3.5	3	
A328V	93	± 11	4	1.6	± 0.4	3	0.7	108	± 3.9	4	
Common variant											
P305L	108	± 4.0	4	1.3	± 0.4	3	0.6	36	± 2.2	3	

Table 3. Mutation impact on receptor cell surface expression and radioligand binding. Cell surface expression of mutant receptor relative to wild type was calculated from normalised data using GraphPad Prism 6.0. The number of receptor binding sites and affinity were calculated with standard error of mean from normalised non-linear regression curves using GraphPad Prism 6.0.

GPR10 variant	Gq signalling (IP-1 accumulation)								Gi/o signalling (IP-1 accumulation with $G\alpha_{\Delta 6qi4myr}$)							
	Potency (EC_{50}) (Locke, Kahali et al.)				F_{mut} (var_{EC50}/WT_{EC50})	Efficacy (E_{max}) [%WT]			Potency (EC_{50}) (Locke, Kahali et al.)				F_{mut} (var_{EC50}/WT_{EC50})	Efficacy (E_{max}) [%WT]		
Cases	**mean**		**SEM**	**n**		**mean**	**SEM**	**n**	**mean**		**SEM**	**n**		**mean**	**SEM**	**n**
WT	9.4	±	4.0	7	N/D	100	N/D	7	6.7	±	2.25	7	N/D	100	N/D	7
A121D	N/D (cLoF)			5	N/D	N/D (cLoF)		5	112	±	17	4	17	17	± 4.8	4
V162L	5.0	±	1.2	4	0.5	71	± 6.5	4	6.3	±	3.9	3	0.9	92	± 1.6	3
P193S	N/D (cLoF)			5	N/D	N/D (cLoF)		5	N/D (cLoF)			3	N/D	N/D (cLoF)		3
H206N	16	±	3.9	4	1.8	125	± 13	4	14	±	8.6	3	2.1	123	± 13	3
R220L	10	±	3.8	3	1.1	126	± 22	3	5.7	±	3.2	3	0.8	128	± 17	3
R222S	53	±	29	3	5.7	64	± 10.0	3	34	±	19	3	5.0	86	± 10	3
P237R	N/D (cLoF)			5	N/D	N/D (cLoF)		5	N/D (cLoF)			3	N/D	N/D (cLoF)		3
L242F	14	±	3.8	4	1.5	105	± 6.5	4	11.3	±	7.3	4	1.7	95	± 15	4
V261M	8.3	±	2.5	4	0.9	175	± 6.4	4	15	±	4.8	2	2.2	108	± 4.5	2
A266D	7.4	±	3.4	5	0.8	34	± 6.6	5	6.9	±	2.6	4	1.0	45	± 2.4	4
D340N	16	±	7.4	5	1.7	115	± 9.4	5	7.3	±	2.2	4	1.1	100	± 11	4
D340V	5.3	±	1.5	4	0.6	64	± 14	4	7.6	±	2.5	3	1.1	56	± 8.3	3
L350S	20	±	5.5	4	2.1	32	± 9.6	4	5.2	±	3.1	4	0.8	56	± 8.5	4
K356E	10	±	5.4	5	1.1	32	± 8.7	5	6.7	±	1.9	4	1.0	44	± 0.9	4
I357L	20	±	5.6	5	2.1	149	± 16	5	4.5	±	2.2	4	0.7	132	± 3.4	4
Controls																
V11I	4.9	±	0.7	4	0.5	93	± 17	4	12	±	9.7	3	1.8	127	± 3.3	3
C113R	N/D (cLoF)			6	N/D	N/D (cLoF)		6	N/D (cLoF)			3	N/D	N/D (cLoF)		3
A191V	N/D (cLoF)			6	N/D	N/D (cLoF)		6	N/D (cLoF)			3	N/D	N/D (cLoF)		3
P258S	N/D (cLoF)			6	N/D	N/D (cLoF)		6	22	±	17	3	3.3	33	± 0.7	3
A328V	13	±	4.6	5	1.3	76	± 14	5	8.7	±	3.8	5	1.3	72	± 3.3	5
Common variant																
P305L	9.1	±	3.3	4	1.0	77	± 14	4	2.8		N/D	1	0.4	80	N/D	1

Table 4. Mutation impact on receptor ability to trigger Gq and Gi-coupled pathways. Potency and efficacy with standard error of mean were calculated from normalised non-linear regression curves, using GraphPad Prism 6.0.

3.4.2.7. Human mutations in GPR10 impair the function of wild type receptor in a cell system co-transfected with both wild type and mutant receptor

All of the human variants in GPR10 are found in heterozygous form. The limited amount of data in GPR10/PrRP heterozygous null mice suggests they do not develop obesity. To explore whether heterozygous mutations in GPR10 might exert a dominant negative effect, c-myc tagged wild type receptor was created from the FLAG-tagged wild type receptor using a restriction endonuclease approach. This allowed for the relative levels of expression of wild type and mutant receptor to be distinguished. 20,000 cells/well were co-transfected with varying doses of c-myc-tagged wild type receptor (1-5ng/well) and FLAG-tagged mutant DNA (1-5ng/well). The ability of wild type GPR10 to generate IP1 in the presence of increasing doses of mutant DNA was tested. Cell surface expression levels were assayed to determine whether any observed effects were due to alterations in cell surface expression. The three complete loss of function mutations A121D, P193S and P237R were tested for a possible dominant negative effect. Total concentration of DNA transfected was kept constant by supplementation with empty vector to ensure this did not affect results.

At all concentrations of wild type receptor, increasing concentrations of mutant receptors reduced the amount of inositol monophosphate accumulation (Figure 11), and this reached statistical significance for A121D and P237R. An ELISA using a primary antibody targeting c-myc confirmed that increasing doses of mutant receptor did not reduce the expression of the wild type receptor. We therefore conclude that for the three mutants tested, the presence of the mutant receptors tested exerted a dominant negative effect on the ability of the wild type receptor to signal, and this reached statistical significance with the mutations A121D and P237R.

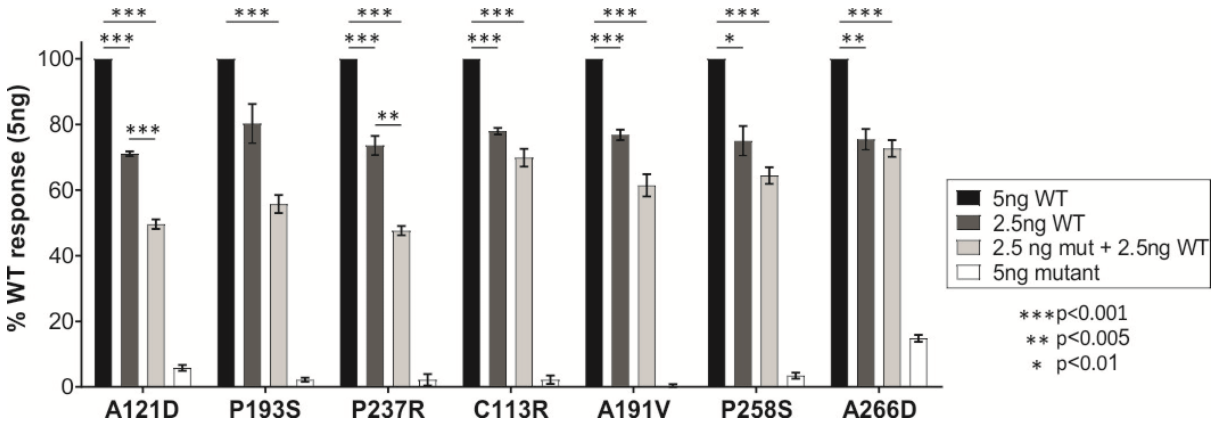

Figure 12. Mutations in GPR10 exert a dominant negative effect on the wild type receptor: cases and controls.

An inositol monophosphate assay was performed to assess the effect of varying concentrations of c-myc-tagged wild type and FLAG-tagged mutant DNA on the signal generated. Increasing doses of mutant DNA reduced IP1 accumulation on stimulation with 20x10-6M PrRP-31, independent of cell surface expression. Results show normalised values of three independent experiments, with error bars showing standard error of mean on cases (A121D, P193S, P237R) and controls (C113R, A191V, P258S, A266D). This shows that the reduction in receptor signalling was significantly reduced in the cases, but not the controls.

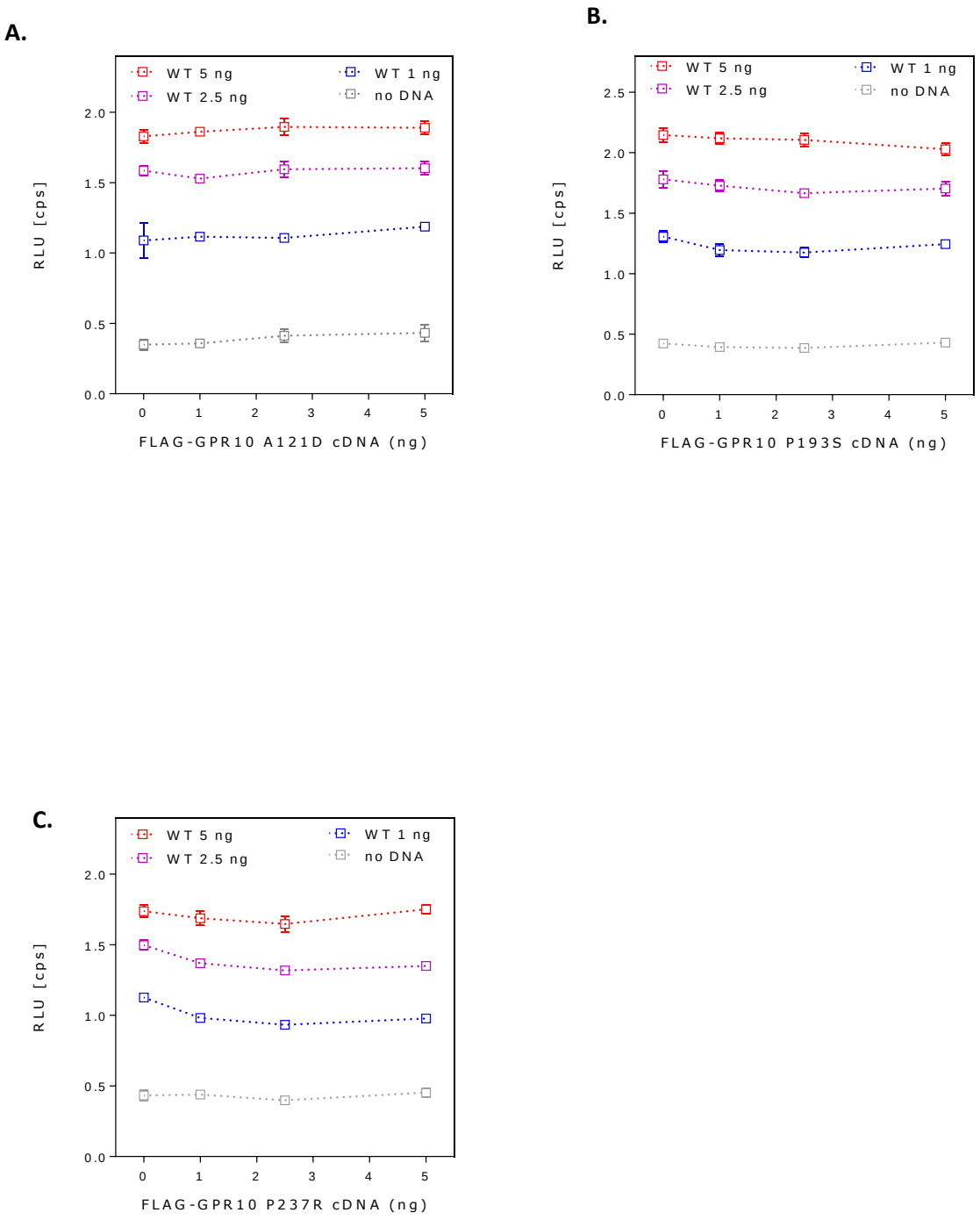

Figure 13. Expression of wild type receptor is not affected by cotransfection of increasing doses of variants A121D (A), P193S (B), P237R (C). An in house ELISA using a primary antibody directed at the wild type c-myc tag showed no reduction in signal when COS7 cells were co-transfected with doses (0-5ng/well) of variant GPR10.

3.4.3. *Caenorhabditis elegans* as a model for studying the effects of GPR10 on fat accumulation

Demonstrating that the described variants result in the patient phenotype is a problem common to all rare variant work. We were interested in exploring model organism systems to test this association. *Caenorhabditis elegans* has an orthologue similar to GPR10, neuropeptide receptor 6 (*npr6).* We explored the use of wild type and *npr6* null worms to quantify fat accumulation, with the plan to create quantify lipid droplet accumulation in heterozygous null variants of our complete loss of function variants if this proved to be a viable method.

Different methods of lipid droplet visualisation and quantification were explored. We performed 2 coherent anti-Stokes Raman scattering (CARS) microscopy, rather than the more commonly used Sudan black or Nile red stains, as there is evidence that these may stain gut granules in addition to lipid droplets, and can therefore provide misleading results. As such, CARS microscopy is the gold standard for lipid droplet quantification in *C. elegans* (Yen, Le et al. 2010). Worms were controlled for larval stage, and the area immediately distal to the pharynx to prevent any variability arising from different sections.

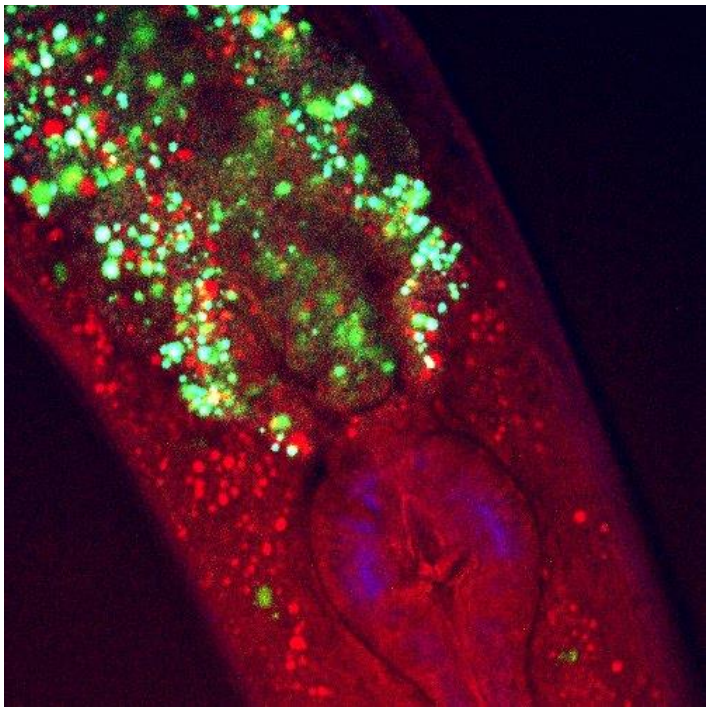

Figure 14. Sample image from CARS microscopy, demonstrating a wild type worm. Lipid droplets are shown in red, gut granules in green, and muscle fibres in blue.

A.

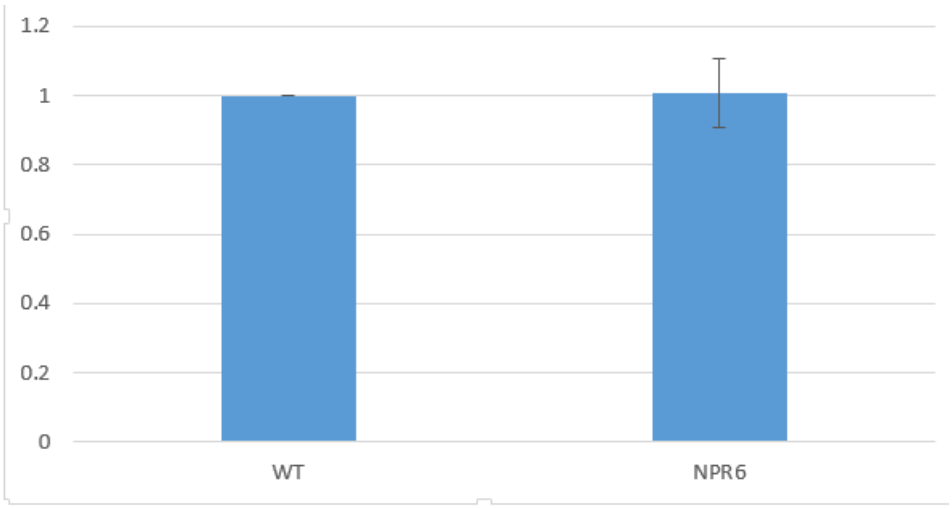

B.

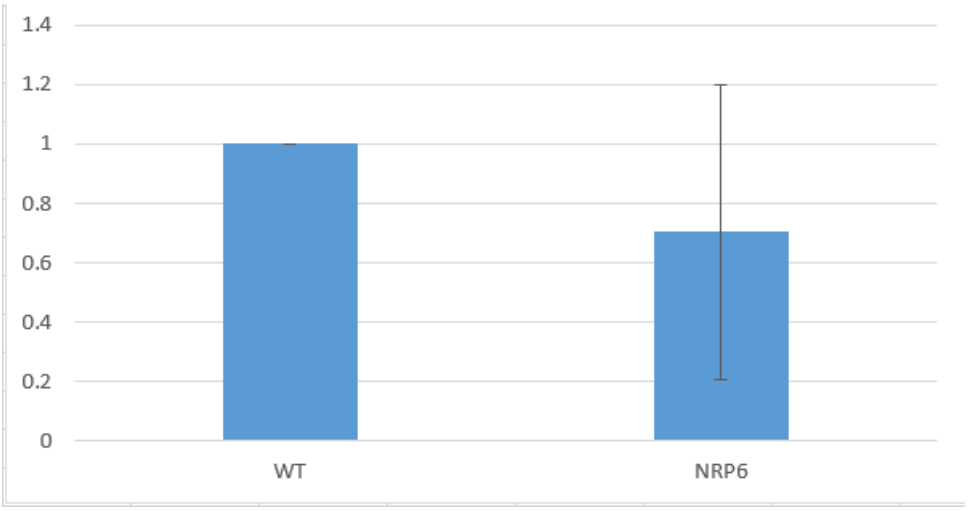

Figure 15. Lipid content analysis of C. elegans. (A). demonstrates average lipid droplet size, normalised to the wild type worm. All the droplets in the field of view were measured, and this total was divided by the number of droplets counted. **(B)** shows average lipid droplet density (the number of droplets per defined area) normalised to the wild type worm. A defined standardized area bordering the larynx measuring 15,000 pixels in diameter was used. The total number of droplets in this area was then counted. The npr-6 null worms tended to have a smaller amount of droplets.

Both graphs show the lipid droplet size or density of NPR6 null worms normalised to the wild type. The average of two separate comparisons was made. Results show mean with standard deviation. There was no significant difference for either of the two metrics.

There was a high degree of variability in the lipid droplet density and size, indicating that this was not an ideal platform for determining fat content. Additionally the NPR-6 null worms had a lower lipid droplet density than their wild type counterparts. This may be because the knockout worms were not as healthy as the wild type worms, but it suggests that the npr6 null worms are not an ideal orthologue for assessment of obesity-associated variants in GPR10.

As these experiments have not proved consistent enough to test whether the mutations in GPR10 result in an increase in fat accumulation *in vivo*, we have proceeded to collaborate with Professor Simon Luckman to create a mouse model of the heterozygous P193S mutation. This was chosen as it is highly conserved between species, and functional studies demonstrate a complete loss function and a dominant negative effect *in vitro*. The mutations A121D and P237R were additionally considered; however one of these patients was not Caucasian, raising the possibility of an ethnic variant, and the other patient also had an *SRC-1* mutation, which makes it difficult to be sure of the contribution of GPR10 in this individual's weight.

3.5 Discussion

3.5.1. Identification of rare and novel mutations in GPR10 in the GOOS cohort

A common polymorphism in GPR10, P305L, which was associated with lower blood pressure than age and weight-matched controls, but not obesity has previously been described. This work therefore constitutes the first study of rare variants in GPR10. Fifteen heterozygous variants were identified from the whole exome sequencing of 2,548 patients with severe early onset obesity recruited to the GOOS cohort. A further 5 mutations were found in 1,117 "control" exomes as part of the UK10K project, sequenced using the same methods; these exomes comprise of DNA from healthy volunteers, and disease exomes from other patients undergoing sequencing. No BMI data is available on the subjects used as controls, and it is therefore not possible to exclude that they are not obese. Whilst these variants are rare, the enrichment of variants in the GOOS cohort, and the conservation across species indicated that there was a reasonable probability that some of the variants would have functional consequences, and an *in vitro* functional characterisation was therefore justified.

3.5.2. Functional characterisation of rare variants in GPR10 identified in the GOOS cohort and control exomes

In this study we have sought to explore mechanisms by which variants may exert an effect on receptor function. We have shown that none of the variants found in cases or controls results in a significant reduction in cell surface expression. This finding is unusual as approximately 60% of disease-causing human mutations in the melanocortin 4 receptor result in a reduction in cell surface expression (Tan, Pogozheva et al. 2009). Additionally, intracellular retention of the TSH receptor is a documented method by which these mutations may cause congenital hypothyroidism (Labadi, Grassi et al. 2015).

We have shown that the receptor signals through both Gi and Gq-coupled mechanisms, and that three variants found in cases, and two in controls results in a complete reduction in Gq-coupled signalling. These same variants, when tested with a competition radioligand binding assay showed an absence of ligand binding, and it is therefore logical to assume that it is through a lack of ligand binding that they fail to signal.

We have also shown a partial loss of function in all but two of the variants found in cases. Additionally two of the variants found in controls had no impact on any of the assays tested. To summarise,

functional studies of mutant GPR10 in cases and controls showed that 13 of 15 variants in cases and 3 of 5 variants in controls resulted in a LOF by effecting ligand binding and/or signalling.

3.5.3. Limitations of the methods used

We then progressed to performing a series of second messenger assays. A cAMP assay showed no signal, indicating that the receptor does not couple with Gs proteins, whereas an inositol monophosphate assay gave a clear dose-dependent response to ligand, both with and without chimeric G protein, indicating coupling to both Gi and Gq proteins. The use of chimeric G protein was further validated by testing Gi coupling by creating a cell line that was stably transfected with GPR10, stimulating it with forskolin and then treating it with PrRP; a dose dependent reduction in cAMP was observed. The IP1 assay, used both with and without chimeric G protein to assay Gq and Gi pathways, therefore formed the basis of our characterisation of variant impact on intracellular signalling.

Other groups frequently use alternative methods to look at these pathways. Intracellular calcium assays, using a fluorescent calcium binding dye are a common method of assessing Gq-coupled activity, and were considered for this study. However, the results from the IP1 assay were extremely consistent and as this is a well validated method of assessing Gq-coupled pathway activity we did not proceed to corroborate these results with a second assay. Additionally the signal readout from the calcium assay is one step further removed from the interaction of interest, and increasing levels of intracellular calcium can reflect intracellular stress, so on balance it was felt that there would be little extra gained from the additional use of this assay.

A competition binding assay was used to assess the binding of ligand to the receptor; in this assay radioactive ligand is applied to cells transfected with receptor, which is then displaced by increasing doses of “cold” (i.e. non-radioactive) ligand. This assay therefore measures the equilibrium binding of a single concentration of radioligand at various concentrations of an unlabelled competitor. This primarily gives information on the affinity of the receptor for the competitor. There are limitations to this assay; it does not take into account the possibility of non-specific binding and it assumes that the radioactive label does not interfere in any way with the binding of the ligand and that labelled and non-labelled ligand have equal receptor affinity. It also has limitations when compared to a saturation binding assay in that it cannot be used directly to calculate K_D by plotting a Scatchard plot. However, the main advantage of the competition binding assay over a saturation assay is that considerably less radioligand is used, resulting in a cheaper and safer experiment with fewer issues surrounding disposal

of waste. It also provides considerable useful information on ligand binding, allowing determination of IC_{50}, and estimation of $B_{max,}$ and is sufficient for the purposes of this characterisation.

3.5.3.1. Other GPCR-mediated mechanisms through which mutation effect has not been assessed

β-arrestin recruitment is necessary for receptor internalisation, and has its own well-defined signalling pathways. Recruitment allows the response of the activated receptor to be turned off, and allows persistent signals to be adapted. The first step to β-arrestin recruitment is phosphorylation of specific residues on the activated G protein by specific serine/threonine kinases, called G protein receptor kinases (GRKs), preparing the GPCR for β-arrestin recruitment. The β-arrestin molecule then binds, inactivating the receptor by blocking further G protein-mediated signalling (it blocks the binding site of the heterotrimeric G protein) and signals the receptor for internalisation by linking it to clathrin and the clathrin adaptor protein, AP2, promoting the internalisation of the receptor into endosomes. β-arrestins are now known to also function as scaffold proteins that link GPCR activation to several downstream effectors such as the MAPK cascade (ERK [extracellular signal-regulated kinase] and JNK), Src, and calmodulin.

We have not explored β-arrestin recruitment or signalling in this study, and it is possible that some of the effects exerted by the variants utilise these pathways, and this is an area where future work in needed. It is interesting to note the two variants found in cases for which we have no evidence of functional impact on ligand binding or signalling are expressed at significantly higher levels that the wild type receptor, and this may be consistent with impaired β-arrestin recruitment.

3.5.5. Further characterisation of dominant negative effect

We have demonstrated in this study that co-expression of wild type GPR10 with A121D and P237R variants found in cases results in an *in vitro* loss of function results in a dose-dependent reduction in inositol monophosphate accumulation from the stimulated receptor. We have shown that this effect is not caused by a reduction in the expression of the wild type receptor; however we have not provided a conclusive mechanism by which the observed effect occurs.

To explore this further it would first be important to test whether the wild type and mutant receptors have a direct physical interaction. Practically, this could be done using an enzyme complementation

assay, or by using wither bioluminescent or fluorescent resonance energy transfer (BRET/FRET), which would provide direct information about receptor interaction.

It is possible that the observed dominant negative effect on signalling is a result of altered ligand interaction. None of the three mutants that were selected for coexpression studies binds ligand when tested alone, and we know from the ELISA studies that coexpression of wild type and mutant receptor does not reduce the wild type expression. It would therefore be possible to compare the competition binding curves of wild type receptor expressed alone to that when it is expressed with mutant receptor. However this method could not be used more generally to explore the effects on binding with other mutants that themselves bind radioligand.

We know from the inositol monophosphate assay that the downstream effect of co-expression is a reduction in signalling, but we have not explored the upstream cause of this. A possible mechanism by which the mutant receptor might exert its effect is by altering interaction of the wild type receptor with its cytosolic targets. This could either be through steric hindrance by physically making its binding sites inaccessible, or by altering the receptor conformation in a way that changes the binding sites of cytosolic proteins. This could affect the recruitment of phospholipase C, thereby hindering the degradation of PIP2 into IP3 and the triggering of intracellular signalling cascades. Again, this is not something that we have explored in this study, but could be approached using an enzyme complementation assay.

We have only tested 3 of the loss of function variants found in cases. However, all variants are found in heterozygous form, and it therefore important to test whether they too exert a dominant negative effect on the wild type receptor.

3.5.6. Final conclusions

Described here are the first rare human mutations in GPR10, a molecule known to play a key role in energy expenditure in rodents. We have demonstrated that the wild type receptor signals through Gi and Gq-coupled pathways, and that the described mutations have variable impact, with three mutations resulting in a complete loss of signalling and ligand binding. As the mutations are found in heterozygous form in humans we have explored and demonstrated a dominant negative effect of mutant receptor on wild type function. We have explored *C. elegans* as a model system for directly testing the effect of mutations on lipid accumulation, but rejected it on the basis of too much variability.

The characterisation of rare obesity-associated GPR10 variants provides some evidence for its role in human disease. Further exploration of GPR10 signalling and its pharmacological manipulation has potential in the search for anti-obesity drugs.

CHAPTER FOUR: THE PHYSIOLOGICAL, METABOLIC, AND NEUROCOGNITIVE EFFECTS OF COOLING

4.1. Summary

We hypothesised that energy deficit, regardless of cause (whether secondary to caloric restriction, exercise or increased expenditure from cold exposure) is detected and responded to by a central mechanism, and this mechanism is leptin-mediated.

To test this hypothesis, we recruited 15 healthy, normal weight (BMI 18.5-26) male volunteers. Subjects were screened for pre-existing medical conditions, medication use, neurocognitive dysfunction and biochemical abnormalities. Successful subjects were then invited to participate in a randomised cross-over trial involving two overnight study visits, each identical with the exception of the temperature intervention, which was exposure to either 25^{o}C or 16^{o}C for two hours via a specialised cooling suit (*Chapter 2, Methods)*. We assessed heart rate variability, skin and core body temperature and energy expenditure in response to the temperature intervention, using validated methods. Additionally we assessed the effect on the participant's biochemistry and metabolomics profile. As defects in leptin signalling are known to increase preference for high fat foods, we included a fat preference meal to determine whether altered food preference was induced by cold exposure, a state of partial leptin deficiency.

As cooling has been associated with long term neuroprotection as a result of improved synaptic plasticity secondary to RBM3 induction, we undertook studies into the short term neurocognitive effects of cooling. In collaboration with Professor Malluci's lab we measured participant RBM3 levels and conducted standardised validated tests to assess whether if there were short term effects of cooling on neurocognition.

4.2. Introduction

Hibernation is characterized by a reduction in metabolic rate (by as much as 90%) and body temperature set point to maximize energy savings during times of low food availability and unfavourable environmental conditions, and may last from days to months, with severe drops in body temperature (as low as 1^{o}C above ambient temperatures when in the range of 5 – 15^{o}C). Metabolic suppression and cell-level adjustments to manage limited food intake are common themes among species. Small-bodied mammalian hibernators in temperate climates suppress metabolic, respiratory and heart rates to 1–9 % of basal rates while lowering body temperature to enter a state called torpor (Ruf and Geiser 2015). Larger mammals, such as bears also vary metabolism, reaching 25 % of basal values (Toien, Blake et al. 2011) and adopting mass-specific metabolic rates that approach those of torpor in small mammals (Geiser and Heldmaier 1995, Heldmaier, Ortmann et al. 2004). Mice and other very small mammals enter torpor, rather than hibernation, possibly because they cannot store enough fuel for an extended hibernation.

Mice can enter torpor when there is a quiet environment, reduced food availability, and a low ambient temperature. During deep torpor, mice will maintain their body temperature at 1–2°C above ambient temperature, down to a minimum of 16–19°C. Because of plentiful food and adequate room temperatures, deep torpor is infrequently seen in laboratory mice. The *ob/ob* mice are an exception, entering deep torpor upon fasting and occasionally entering torpor even when well-fed and housed at room temperature (Webb, Jagot et al. 1982). In a study examining the effects of leptin on torpor, it was found that wild-type mice entered torpor and dropped their core body temperature by 4^{o}C on fasting, and that leptin did not affect this. However, leptin replacement in *ob/ob* not only prevented the deep torpor, but also the modest 4°C fall. These data demonstrate that leptin plus large energy stores (i.e., leptin-treated *ob/ob* mice) prevents both deep torpor and the modest hypothermic state (Gavrilova, Leon et al. 1999).

While reductions in energy expenditure have not been demonstrated in humans when tested using the double-labelled water method (Farooqi, Matarese et al. 2002), it is interesting that leptin-treated individuals do not display a metabolic adaptation to weight loss i.e. the reduction in energy expenditure seen in weight-matched controls on weight loss (Galgani, Greenway et al. 2010). Additionally, there is evidence that leptin-deficient adults have impaired sympathetic function (Ozata, Ozdemir et al. 1999). Furthermore, whilst humans do not hibernate, they do have to defend against low ambient temperatures, and do reduce their metabolic rate in response to caloric restriction (Collet, Sonoyama et al. 2017). Therefore studies of human physiology in response to cold exposure may yield new insights into this adaptation.

There is evidence in rodents that acute cold exposure reduces *ob* gene expression in white adipose tissue (Trayhurn, Thomas et al. 1995), and some evidence of a similar response in humans (Ricci, Fried et al. 2000). Many mammals enter a state of cold-induced torpor or hibernation in the winter months, which is characterised by significant reductions in energy expenditure. Additionally the picture is further complicated by the cold-induced activation of brown adipose tissue (BAT) (Enriori, Sinnayah et al. 2011). Collectively these findings lead us to hypothesise that energy deficit, irrespective of cause, is detected and responded to by a common mechanism, and this is leptin-mediated. We hypothesise that this cold-induced reduction in circulating leptin will be reflected in altered fat preference, energy expenditure, and circulating markers of sympathetic activation.

The acute neuroprotective effects of cooling have long been observed, and therapeutic hypothermia is standard practice under many clinical scenarios where acute neuroprotection is required; for example, cardiothoracic surgery. Recent work in rodents has shown that cold exposure may have the potential to induce more long-term neuroprotection. In mouse models of Alzheimer's disease, Parkinson's disease and prion disease cold exposure results in a marked improvement in the histological change of the disease. The underlying mechanism behind this finding is the induction of a cold shock protein, RNA Binding Protein 3 (RBM3), which appears to promote synaptic plasticity (Peretti, Bastide et al. 2015). RBM3 is widely expressed in the brain, spinal cord and in peripheral tissues including the gut and adipose tissue. Loss of synaptic plasticity is an upstream event in many neurodegenerative diseases, occurring before symptom onset. The mechanism underlying the loss of synaptic plasticity has not yet been elucidated, but it may be secondary to change in lipid membrane content. It is interesting to note that high fat diets, especially those that induce ketogenesis, the preference for which may be induced by impairment of leptin-melanocortin signalling, may also be neuroprotective (Maalouf, Rho et al. 2009, Rahman, Muhammad et al. 2014). It is known that humans who are repeatedly exposed to cold (for instance, cold water swimmers) have elevated levels of RBM3 (Mallucci, unpublished), although the dynamics of this (for instance the frequency and duration of cold exposure) in humans has not been defined. We therefore sought to explore the dynamics of RBM3 with mild cold exposure, and to define if there were any acute effects on neurocognition.

4.3. Methods

4.3.1. Cooling study overview

Healthy, normal weight (BMI 18.5 – 25.9) men age 18-50 years, with no past medical history and who were not taking any medications were invited to attend the Wellcome Trust Clinical Research Facility or the Wellcome Trust Translational Research Facility for clinical studies. An initial screening visit, consisting of anthropometric measurements, fasting bloods, DEXA scan to assess body composition, and fat preference meal were administered. Subjects were asked to complete the ACE-III questionnaire in order to identify any pre-existing neurocognitive deficit.

Participants with normal results were then invited to participate in two overnight studies, a fortnight apart. The studies were identical, with the exception of the temperature of the temperature intervention (either 16°C or 25°C), and measurements included skin temperature, core body temperature, pulse and blood pressure, heart rate variability, energy expenditure, blood parameters, and neurocognitive function. Participants were dressed in standardised light clothing before putting the cooling suit on, room temperature was controlled at 22°C, and lights were dimmed at a consistent setting. The order of study visits was randomised.

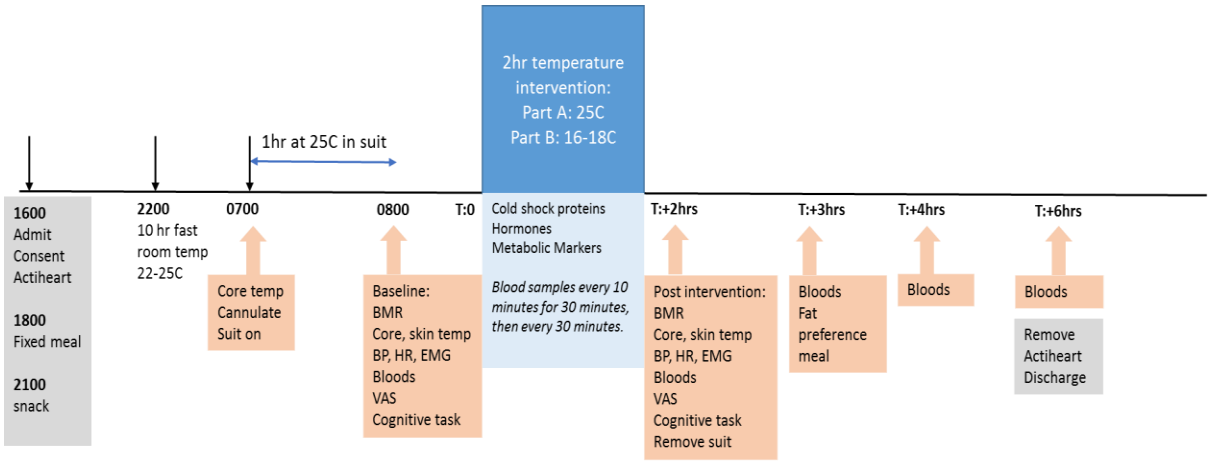

Figure 16. Schematic of the cooling study protocol. T0 is the start of the temperature intervention (either at 25°C or 16°C). Once post temperature intervention measurements were taken, the time was recorded and this was used as a "second T0" (labelled Tp, "time post") as a benchmark for post-intervention time points and measurements. Clinical data is represented as mean ± standard deviation. Differences between groups were studied using the unpaired student's t-test.

4.3.2. Statistical analysis and terminology

These experiments are observational studies of the effects of cooling on a chosen set of physiological, biochemical, and neuropsychological parameters. All individuals underwent two identical experiments with the exception of whether they were cooled or not cooled (referred to as 'thermoneutral' and 'cooling' groups), and these experiments were two weeks apart with subjects randomly allocated to which they had first.

Table 5 shows a typical data set generated from this experiment, using leptin concentration as an example. One can see several potential problems with this type of data set. A two-tailed test on the mean value or percentage change of the treatment groups loses any potential time interval differences, but performing these calculations at each time point will also not be sufficient as this will not properly take into account any baseline differences between individuals and/or baseline differences between means. Table 5 and its corresponding figure 20 show that there is a wide variation in values between subjects, and this in itself is interesting (see discussion). Mean values for group 1 (thermoneutral) and group 2 (cooling) are 3.5 and 3.7, respectively, and given the small variance in means over time, it is likely this would confound analysis. Theoretically, the means at time zero should be identical, especially as the two groups actually contain the same individuals. There are several reasons why this could be, but most importantly regression to the mean will mean that the two groups are likely to be different on repeated measurements. In addition, the fact that the two experiments took place sequentially will mean that conditions and participant behaviour will not be identical. It is therefore vital to take into account baseline differences between subjects when analysing pre- and post-test scores for both treatment interventions, and using change scores alone will not always correct for regression to the mean (Bland and Altman 1994).

		Leptin concentration (ng/ml)					
		Pre-test	Post-test				
Individual	Group	0 min	30 min	60 min	90 min	120 min	180 min
1	1	7.9	7.5	7.5	7	6.6	6.2
2	1	0.2	0.1		0.1	0	0
3	1	3.4	3.1	3	2.9	2.7	2.5
4	1	7.1	6.2	6.3	6.5	6	5.1
5	1		1.9	1.8	1.6	1.6	1.2
6	1	5.2	5	4.8	4.4	4.8	4.6
7	1	6.5	5.4	5.6	5.4	5.3	4.9
8	1	3.1	3.1	2.8	2.6	2.6	2.4
9	1	1.2	1.1	1	0.9	0.9	0.8
10	1	4.7	4.2	3.9	3.7	3.5	3.3
11	1	0.9	0.8	0.7	0.7	0.7	0.6
12	1	0.3	0.3	0.3	0.2	0.2	0.3
13	1	1.7		1.5	1.4	1.4	
14	1	3.1	2.9	2.9	2.8	2.7	2.4
	Mean	**3.5**	**3.2**	**3.2**	**2.9**	**2.8**	**2.6**
	SD	**2.6**	**2.4**	**2.3**	**2.3**	**2.2**	**2.0**
1	2	10.4	9.4	9.3			7.4
2	2	0.2	0.2	0.1			0.2
3	2	2.9	2.6	2.4	2.4	2.2	1.9
4	2	9.2	8.4	7.3	7	6.4	5.1
5	2	1.5	1.7	1.5	1.4	1.5	0.8
6	2	6.3	5.9	5	4.9	4.6	4.4
7	2	6.6	5.8	5.2	4.8	4.8	4.1
8	2	3.3	2.9	2.6	2.5	2.4	2.2
9	2	1.3	1.2	1.1	1.1		1.1
10	2	3.1	2.7	2.9	2.4	2.5	2.1
11	2	0.7		0.6	0.6	0.6	
12	2	0.8	0.6	0.6	0.6	0.5	0.4
13	2	1.7	1.3	1.3	1.2	1.4	
14	2	3.8	3.8	3.6	3.4	3.4	2.8
	Mean	**3.7**	**3.6**	**3.1**	**2.7**	**2.8**	**2.7**
	SD	**3.2**	**2.9**	**2.7**	**2.0**	**1.9**	**2.2**

Table 5. Leptin concentration measured during the cooling experiment. Group 1, thermoneutral; group 2, cooling. Missing values are due to technical failure. Mean and standard deviation (SD) at each time point given per group.

4.3.2.1. Different methods of data analysis

Although it appears logical to adjust for baseline data of the dependant variable, many large multi-centre randomly controlled trials (RCTs) do not do this, and interestingly the Consolidated Standards of Reporting Trials (CONSORT) guidance on RCT reporting does not cover this issue at all (Twisk, Bosman et al. 2018), leaving researchers to decide amongst themselves whether to control for baseline differences, and if so, which method to use.

Analysis of the data in this chapter also needs to take into account overall trends in post-test repeated measures at multiple time points, and be able to detect the extent to which time influences variance, both independently and as an interaction with group (referred to as the interaction factor group*time). In other words, what independent effect does the treatment group have on the dependant variable (dv)? What effect does time have irrespective of treatment? And does treatment *over time* influence variance?

The final problem encountered is that measurements were not achievable for every single data point. There are inherent risks in imputing data for these missing values and if possible, is best not performed. Most statistical packages are unable to perform analysis of variance (ANOVA) with missing values, paired t tests performed on areas under the curve (AUC) with missing values is likely to omit important information generating misleading results, and analysis of change is not possible if a missing value happens to be the pre-test measure.

There appears to be a consensus amongst researchers that if baseline differences exist, then in a repeated measures ANOVA (RANOVA) with a pre-test score and multiple post-test scores, the indication of whether a treatment has an effect is not just the presence of a group factor, but also the presence of a significant group and time *interaction*. This overrides any pre-test differences by testing whether the pattern of change differs between groups; a proper adjustment is not achieved by performing a regular RANOVA or analysis of change alone (Twisk, Bosman et al. 2018).

Analysis of change involves the calculation of a gain score by subtraction of the pre-test value from every subsequent time point as a way to cancel out the baseline differences (effectively converting the pre-test score to zero). This is a useful way to estimate differences between groups, and can also be used in ANOVAs and ANCOVAs if the raw data does not fit into a valid model, but is generally not used in isolation because of the problem of not correcting for regression to the mean.

Alternatively, if the pre-test score is used as a quantitative covariate (in addition to using qualitative categorical covariates such as group and time), then ANCOVA modelling of post-test scores (referred to in this chapter as 'ANCOVA-POST') can take place. This allows one to test whether the pre-test

score predicts any change over subsequent readings, rather than just controlling for the pre-test (baseline difference) score.

4.3.2.2. Statistical methods used for this study

Data modelling was performed using the XLSTAT add-on for Microsoft Excel (Addinsoft 2017). For repeated measures ANOVA modelling, two fixed factors (time and group) were used as explanatory variables and one interaction factor (time*group) was investigated. For ANCOVA modelling, pre-test scores (0 minutes data) were moved from the dependant variable (dv) portion of results to become a fixed covariate for the post-test outcomes for each subject. Full Factorial used analysis was selected. Model validity was determined using goodness of fit statistics (R^2) and F value of analysis of variance, with its corresponding p value.

For RANOVA, XLSTAT uses a mixed effect model, and output tables include an analysis of variance that determines whether the explanatory variables brings significant information to the model, in other words it asks whether it is valid to use the mean to describe the whole population. A Z test on the covariance parameters shows whether the modelling is appropriate for the data (providing significance levels for variance and sigma 1). The model is further tested using a null model likelihood ratio test on the compound symmetry structure used, again providing a significance level for this. Type III tests of fixed effects investigate whether the covariate factors have a significant effect on the dv (replacing the type III sum of squares of the classical ANOVA and ANCOVA models.

For all models used, missing values were excluded from the analysis, but all remaining data for that subject was included. Subjects were only excluded in their entirety if no data was available, and this was usually because no blood was available to measure that variable. No data was excluded for reasons of outlie. This is likely in some data sets to lose some signal and reduce power, but subject-to-subject variability appeared evenly spread with no clear outlier 'cut offs' apparent.

The dependent variable (dv) at the zero time point (t_0) is referred to as the 'pre-test' value or score for both thermoneutral and cooling groups. All dependent variables at subsequent time points are referred to as the 'post-test' values or scores, although it is acknowledged that thermoneutral and cooling treatments continue at 30 min (t_{30}), 60 min (t_{60}), 90 min (t_{90}), and 120 min (t_{120}). The treatment ends at t_{120}, and so the final time point (180 min, t_{180}) occurs 60 minutes after the end of treatment. The terms 'treatment' and 'treatment groups' refer to both thermoneutral and cooling interventions, and it is important to note that subjects within both treatment groups have also been fasted overnight

and any effects seen (especially in the thermoneutral group) may naturally arise as a result of this fixed intervention, which is not taken into account in the modelling as there are no control groups that have not been fasted.

4.4. Results

4.4.1. Demographics of participants recruited to the cooling study

Healthy, non-smoking males aged 18-50 years were recruited to the cooling study. All participants had normal serum cholesterol, thyroid function, liver and renal function and full blood count. BMI ranged from 18.69 – 25.84 kg/m^2. No participants had any significant past medical history or took any prescribed medications. All participants had normal neurocognitive function, defined as a score >88 on the ACE-III questionnaire. The average total percentage body fat, determined by Dual X Ray Absorptiometry (DEXA), average was 22.1% (range from 12.6% to 33.5%). Baseline observations of the participants are outlined in Table 6.

Subject	Height (m)	Age (years)	Weight (kg)	BMI (kg/m^2)	sBP (mm Hg)	dBP (mm Hg)	Pulse rate (bpm)	Temperature (^{o}C)
1	1.782	19	65.85	20.73	112	67	59	36.5
2	1.879	24	84.2	23.84	121	77	50	35.9
3	1.785	23	80.2	25.17	131	72	82	36.6
4	1.929	24	92.1	24.75	124	70	61	36.5
5	1.757	33	79.8	25.84	116	56	50	36.7
6	1.751	19	60	19.56	112	66	64	36.3
7	1.74	19	56.6	18.69	111	68	78	36.3
8	1.791	24	64.3	20.04	117	63	71	36.1
9	1.879	19	82.8	23.45	120	77	68	36.1
10	1.786	20	64.8	20.31	120	77	75	36.2
11	1.884	18	74.4	20.96	119	73	55	36
12	1.887	21	70.2	19.71	124	64	62	36.1
13	1.834	19	75.75	22.52	118	71	82	36.2
14	1.74	21	61.4	20.28	116	62	53	35.7
15	1.739	23	60.2	19.90	119	69	61	35.8

Table 6. Baseline observations of participants recruited to the cooling study. Measures of height, weight, systolic and diastolic blood pressure, pulse and temperature are shown for the 15 participants who underwent both study arms of the cooling study. Body mass index of the participants is additionally shown.

4.4.2. Physiological response to cooling

4.4.2.1. Skin temperature response to cooling

iButtons are digital sensors that are taped to the skin. They record temperature in Celcius to two decimal places. The ibuttons were set to record skin temperature every two minutes. Sensors were placed bilaterally in seven different sites; the forearms, supraclavicular fossa, chest, abdomen, thighs, calves and feet. iButton temperature measurements demonstrated a significant drop in peripheral skin temperature in response to cooling. However, there was no change in supraclavicular temperature, measured using the same methods.

(a)

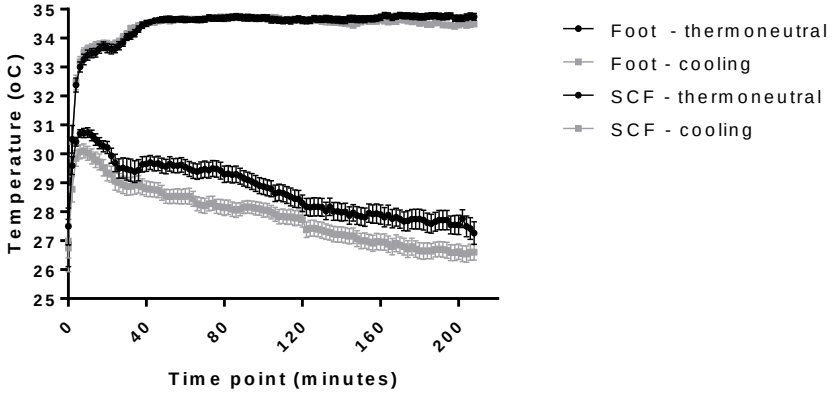

(b)

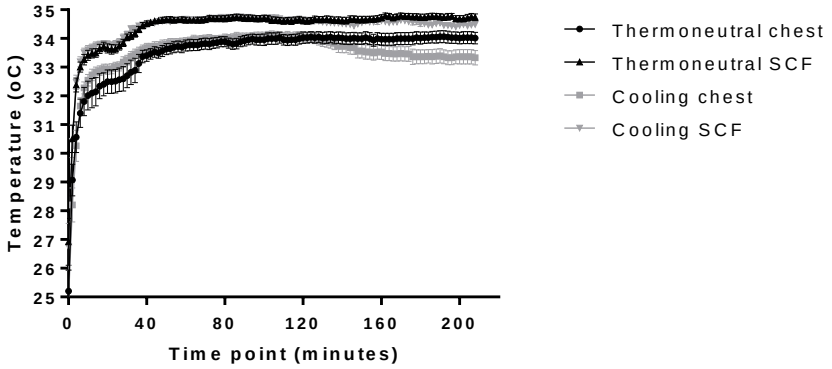

Figure 17. Alteration of temperature in response to cooling. Peripheral (a) and chest (b) temperature relative to supraclavicular fossa temperature in response to exposure to 16oC or 25oC (n=15). Complete iButton data was available on all 15 participants. An EMG was used to ensure that the subjects did not shiver; electrodes were places bilaterally over the pectoral muscles and the rectus abdominis as the shivering response starts centrally and spreads peripherally. This confirmed that there was no evidence of shivering in any of the participants.

iButton recordings showed that there was a difference between the cooling and thermoneutral study arms in peripheral skin temperature ($p = 0.0048$). However this difference was not seen with supraclavicular temperature recordings. Supraclavicular and chest temperature recordings were compared to see if this difference was caused by activation of supraclavicular BAT stores, or whether the difference was secondary to peripheral vasoconstriction. The difference between supraclavicular and chest temperatures were compared at 200 minutes, and they were significant ($p = 0.001$).

4.4.2.2. Pulse

Blood pressure and pulse rate were measured after an overnight fast in the semi-recumbent position, in a dimly lit, quiet room before the temperature intervention, and every 30 minutes during it. There were no statistically significant differences at any time point between the thermoneutral and cooling groups (figure 18a), and this was also so for gain score analysis of the data (figure 18b). ANCOVA analysis using pre-test scores as a quantitative covariate to adjust for baseline differences (see workings and discussion for leptin, section 4.4.3.1) does not show any significance for the group or time factors (p values 0.858 and 0.468, respectively). The least squares (LS) means derived from this modelling is shown in figure 18c, and t tests performed on individual time points are not significant.

(a)

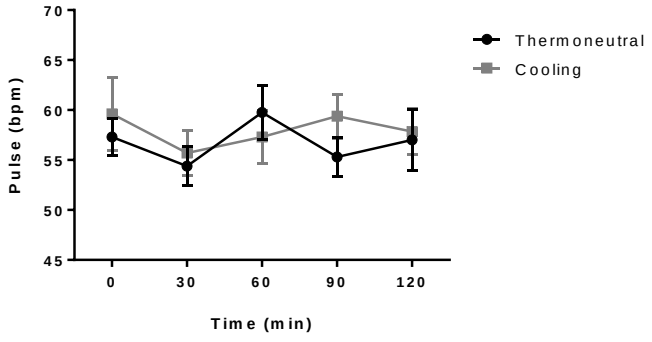

(b)

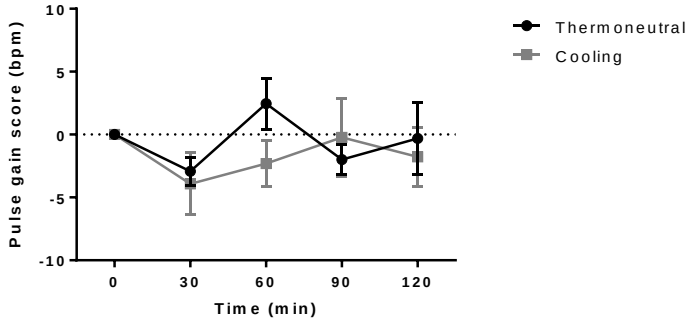

(c)

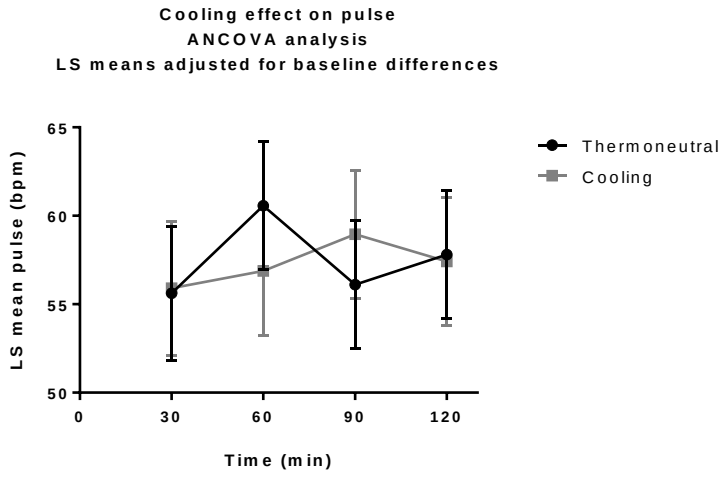

Figure 18. Effect of temperature intervention on pulse. Complete pulse rate data was available on 13 of the study participants. (a) Results show mean pulse with standard error of the mean, with thermoneutral study arm in black and cooling arm in grey. There were no apparent differences between the temperature intervention groups at any time point after a two-tailed paired t test analysis. (b) Gain scores for pulse at each time point with no significant differences at any time point. (c) ANCOVA analysis adjusting for baseline differences between groups did not show any group or time differences and multiple t tests of LS means also did not show any differences.

4.4.2.3. Blood pressure

The raw data shows a trend for an increasing blood pressure (BP) in the cooling temperature intervention group as time progresses (figure 19a). Individual time points were not significant. Adjusting for individual participant baseline differences using ANCOVA analysis shows that this

observed difference is real. Analysis was undertaken separately for systolic and diastolic BP (but shown together for illustrative purposes in figure 19b). The systolic BP ANCOVA model was significant (R^2 0.562 and p <0.0001) and showed statistically significant differences between groups (p = 0.001) and over time (p = 0.039). The diastolic BP ANCOVA model was significant (R^2 0.550 and p <0.0001) but showed no statistically significant differences between groups (p = 0.624) nor over time (p = 0.898). The least squares (LS) means are shown in figure 19b, and two-tailed paired t tests on individual time points were significant for systolic BP at 60 min and 120 min (p values 0.033 and 0.020, respectively). This could be in keeping with an increased sympathetic drive during the cooling intervention when compared to the thermoneutral arm of the study.

(a)

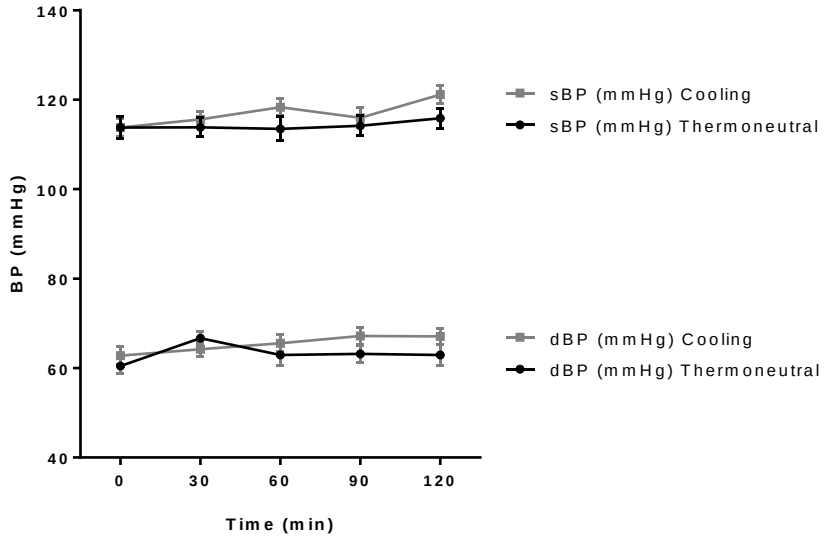

(b)

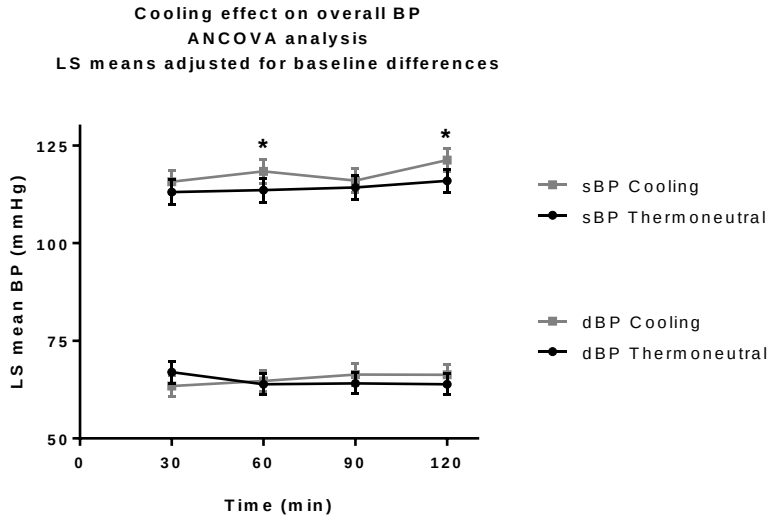

Figure 19. Effect of temperature intervention on blood pressure. Complete blood pressure data was available on 13 participants. (a) Mean systolic and diastolic blood pressure at each time point with error bars (SEM) suggesting a trend for higher BP in the cooling group. (b) Least squares mean systolic and diastolic BP derived from ANCOVA modelling adjusting for individual participant baseline differences, showing an overall significant difference between systolic BP thermoneutral and cooling groups. Error bars (SEM) also shown. Post-analysis t tests on individual time points of the least squares means shows significance at 60 min and 120 min (p values 0.033 and 0.020, respectively).

4.4.2.4. Power spectral analysis of Actiheart data

A sample of actiheart data taken during the gas exchange monitor at the end of the temperature intervention (when patients were at rest, under standardised quiet, light-dimmed conditions) was chosen for analysis (table 7). Independent sample t tests were performed; heart rate was significantly different between the two study intervention arms (p = 0.0318). Other measurements did not reach significance.

	Thermoneutral	Cooling
Mean HR (bpm)	55.5 ± 13.7	57.4 ± 14.5
Log10 RMSSD	1.77 ± 0.46	1.77 ± 0.53
Log10 LF power (ms2)	1.73 ± 0.18	1.73 ± 0.19
Log10 HF power (ms2)	1.62 ± 0.37	1.61 ± 0.36
Log10 LFHF ratio	-0.11 ± 0.54	0.12 ± 0.55

Table 7. Comparison of temperature interventions on power spectral analysis of actiheart data. Mean Actiheart data taken during the gas exchange monitor at the end of the temperature intervention. Two-tailed paired t test analysis showed a statistically significant difference between the two study intervention arms (p = 0.0318).

4.4.3. Biochemical response to cooling

4.4.3.1. Leptin

Plasma leptin concentration was measured at all time points. All subject/group rows passed D'Agostino & Pearson omnibus and Shapiro-Wilk normality tests and so the data was not log transformed. The data set acquired is shown in table 5. Figure 20 shows this data as a scatter plot so that the variability and spread of individual data points can be seen (figure 20a). Ordinary means of these values are shown in figure 20b and suggest that leptin concentration decreases over time for both treatment groups, without any discernible difference between groups (a decrease potentially due to the ongoing fasting state). However, it can also be seen that the baseline means are different between groups, and so gain scores were calculated (shown in table 8) and plotted (figure 20c).

		Leptin concentration (ng/ml)					
		Pre-test	**Post-test**				
Individual	**Group**	**0 min**	**30 min**	**60 min**	**90 min**	**120 min**	**180 min**
1	1	0	-0.4	-0.4	-0.9	-1.3	-1.7
2	1	0	-0.1		-0.1	-0.2	-0.2
3	1	0	-0.3	-0.4	-0.5	-0.7	-0.9
4	1	0	-0.9	-0.8	-0.6	-1.1	-2
5	1	0					
6	1	0	-0.2	-0.4	-0.8	-0.4	-0.6
7	1	0	-1.1	-0.9	-1.1	-1.2	-1.6
8	1	0	0	-0.3	-0.5	-0.5	-0.7
9	1	0	-0.1	-0.2	-0.3	-0.3	-0.4
10	1	0	-0.5	-0.8	-1	-1.2	-1.4
11	1	0	-0.1	-0.2	-0.2	-0.2	-0.3
12	1	0	0	0	-0.1	-0.1	0
13	1	0		-0.2	-0.3	-0.3	
14	1	0	-0.2	-0.2	-0.3	-0.4	-0.7
	Mean	**0.00**	**0.33**	**0.40**	**0.52**	**0.61**	**0.88**
	SD	**0.00**	**0.35**	**0.29**	**0.34**	**0.44**	**0.65**
1	2	0	-1	-1.1			-3
2	2	0	0	-0.1			0
3	2	0	-0.3	-0.5	-0.5	-0.7	-1
4	2	0	-0.8	-1.9	-2.2	-2.8	-4.1
5	2	0	0.2	0	-0.1	0	-0.7
6	2	0	-0.4	-1.3	-1.4	-1.7	-1.9
7	2	0	-0.8	-1.4	-1.8	-1.8	-2.5
8	2	0	-0.4	-0.7	-0.8	-0.9	-1.1
9	2	0	-0.1	-0.2	-0.2		-0.2
10	2	0	-0.4	-0.2	-0.7	-0.6	-1
11	2	0		-0.1	-0.1	-0.1	
12	2	0	-0.2	-0.2	-0.2	-0.3	-0.4
13	2	0	-0.4	-0.4	-0.5	-0.3	
14	2	0	0	-0.2	-0.4	-0.4	-1
	Mean	**0.00**	**0.35**	**0.59**	**0.74**	**0.87**	**1.41**
	SD	**0.00**	**0.35**	**0.60**	**0.70**	**0.87**	**1.23**

Table 8. Leptin concentration temperature intervention data set. Including 14 participants in two groups (thermoneutral and cooling), with leptin concentrations taken at 0 mins, and 30 min intervals up to 120 min. A final level was taken an hour after treatment cessation at 180 min.

This shows a considerably more discernible pattern of decrease in leptin concentration, which is more marked for the cooling group. A two-tailed t test was not significant at any time point, however. It does appear that the gain score means are showing a biological effect, and so the data was next analysed using an ANCOVA-POST model.

(a)

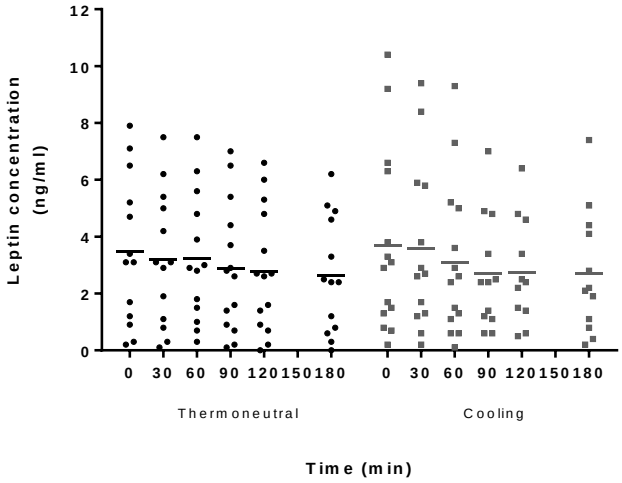

(b)

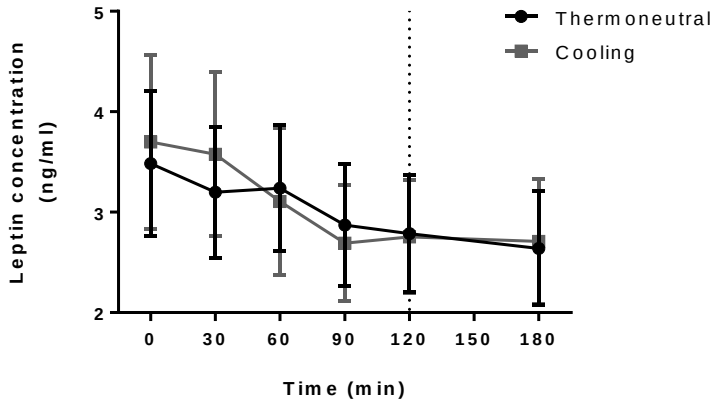

(c)

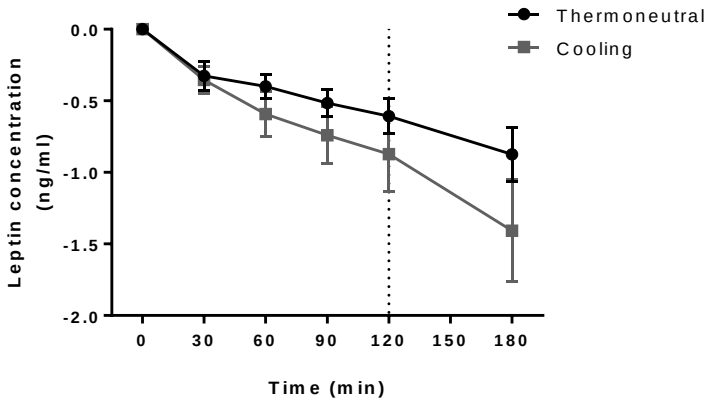

Figure 20. Effect of temperature intervention on leptin concentration. (a) All data points for thermoneutral (black) and cooling (grey) groups with lines at each time point to denote corresponding means. It can be seen that there is a large degree of variability between subjects in both groups. (b) Group means with error bars (SEM); it is clearly seen that the cooling group baseline mean (t_0) starts at a higher value than that of the thermoneutral mean. (c) Group means of gain scores (calculations shown in table 8) with error bars (SEM). No group differences at any time point was significant for (b) or (c) using multiple two-tailed paired t tests. Vertical dotted line denotes treatment cessation at t_{120}.

4.4.3.1.1. ANCOVA analysis using pre-test as a quantitative covariate (ANCOVA-POST)

Goodness of fit statistics for the dependent variable gives an R^2 value of 0.986, suggesting that almost all of the variability is explained by the model parameters included. Analysis of leptin variance gives an F value of 535.07 for the model with $p < 0.0001$, suggesting that the model fits well. Model parameters reveal that post-test scores after adjusting for pre-test scores reflect a very strong overall effect due to time (F-test $p<0.0001$), and this is also strongly significant at each individual time point. Importantly, analysis shows that the treatment group has a statistically significant effect on overall leptin concentration, albeit weaker than for time ($p = 0.002$).

The ANCOVA modelling output also produces least squares means (also known as the estimated population marginal means), which represent the means of each group once the covariate has been controlled for and are derived from the regression intercept B0. In other words, they are within-group means appropriately adjusted for the other quantitative effects in the model, namely the pre-test score, and are shown in table 9 and figure 21 along with their standard error and 95% confidence intervals. Both thermoneutral and cooling groups show a reduction in leptin concentration over time

(highly significant, p<0.0001), and an overall group effect is also seen (p = 0.002) with the cooling arm showing lower leptin concentrations at all time points, with an increasing difference as time progresses, even 60 minutes after cessation of treatment at t_{180}. Multiple two-tailed paired t tests on LS mean differences at each time point show that the group difference at t_{180} is significant (p = 0.003).

Group	Time	LS mean	Standard error	Lower bound (95%)	Upper bound (95%)
1	30	3.373	0.084	3.207	3.539
1	60	3.298	0.084	3.132	3.464
1	90	3.102	0.081	2.942	3.262
1	120	3.018	0.080	2.858	3.177
1	180	2.791	0.084	2.625	2.957
2	30	3.372	0.081	3.213	3.532
2	60	3.098	0.078	2.944	3.251
2	90	2.867	0.084	2.700	3.033
2	120	2.785	0.088	2.612	2.959
2	180	2.404	0.084	2.237	2.571

Table 9. Treatment group effect on leptin concentration LS means using ANCOVA-POST analysis. LS means shown at post-test time points, adjusted by ANCOVA-POST modelling on the pre-test values as a covariate using the XLSAT package for Microsoft Excel. Group 1, thermoneutral and group 2, cooling.

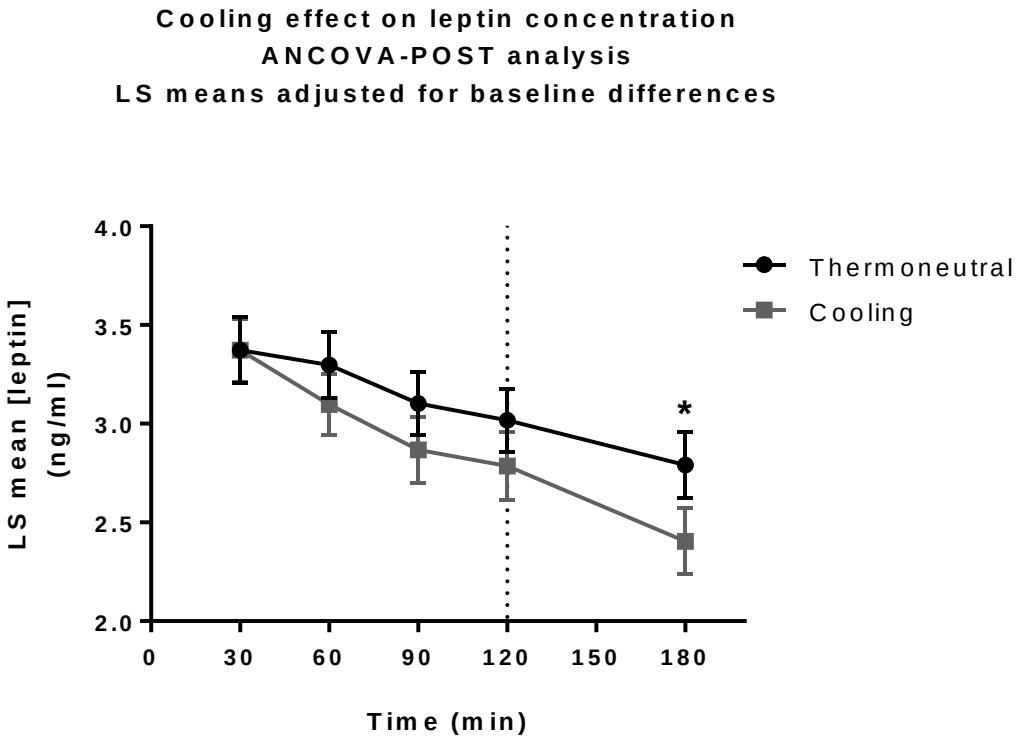

Figure 21. Effect of temperature on LS means of leptin concentration (ANOVA-POST). LS means shown with error bars (SEM 95% CI) at post-test time points, adjusted for the pre-test covariate by ANCOVA-POST modelling. Overall effect of time and group statistically significant (see main text). A two-tailed paired t test was also performed between groups on each individual time point (30, 60, 90, 120, and 180 min) giving p values of 0.993, 0.093, 0.054, 0.061, and 0.003, respectively. Vertical dotted line denotes treatment cessation at t_{120}.

4.4.3.1.2. ANCOVA analysis using dv subtracted from baseline value (ANCOVA-CHANGE)

Rather than using raw pre-test scores as a covariate for raw post-test scores, this model incorporates analysis of change values to the model. The pre-test score is a subtraction of the baseline value from t30, and post-test scores are derived from baseline subtractions from subsequent time points, as illustrated in table 10 for the first 4 subjects in group 1 below (for illustrative purposes).

Group	Subject	pre-test	post-test			
			t1	t2	t3	t4
		(t_{30}-t_0)	(t_{60}-t_0)	(t_{90}-t_0)	(t_{120}-t_0)	(t_{180}-t_0)
1	1	-0.4	-0.4	-0.9	-1.3	-1.7
1	2	-0.1		-0.1	-0.2	-0.2
1	3	-0.3	-0.4	-0.5	-0.7	-0.9
1	4	-0.9	-0.8	-0.6	-1.1	-2

Table 10. Gain score method for ANCOVA-CHANGE analysis.

Goodness of fit statistics for the dependent variable gives an R^2 value of only 0.644, suggesting that this method may indeed be inferior to the ANCOVA-POST method. The analysis of leptin variance gives an F value of 18.99, but still with a highly significant p value (<0.0001). Model parameters reveal that time still has a highly significant effect on leptin concentration overall (p<0.0001), and also at each time point. Again, a significant overall effect of group on leptin concentrations is observed (p = 0.01). The LS means adjusted for baseline differences are shown in figure 22 along with 95% confidence intervals.

As with analysis using ANOVA-POST, both thermoneutral and cooling groups show a statistically significant reduction in leptin concentration over time with the cooling group exhibiting lower concentrations than in the thermoneutral group and with increasing differences as time progresses. Multiple two-tailed paired t tests on LS mean differences at each time point show significance for the difference at t4 ($p = 0.014$).

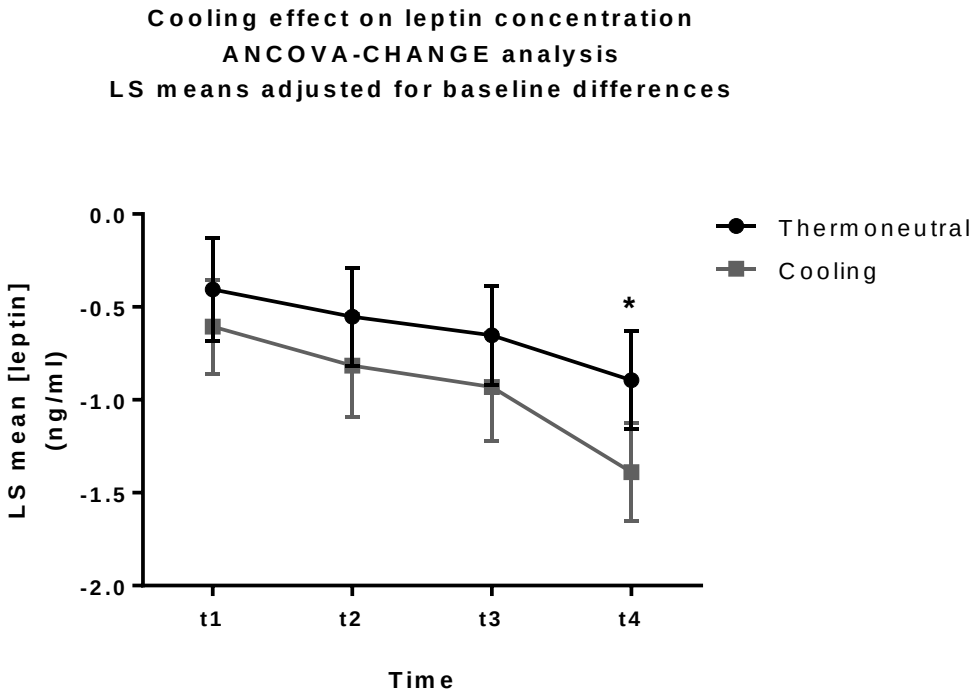

Figure 22. Effect of temperature on LS means of leptin concentration (ANOVA-CHANGE). LS means shown with error bars (SEM 95% CI) at post-test time points, adjusted for the pre-test covariate by ANCOVA-CHANGE modelling. The overall effect of group with time is statistically significant (see main text). A two-tailed paired t test was also performed between groups on each individual time point, giving p=0.300 at t1, p=0.183 at t2, p=0.170 at t3, and p=0.014 at t4.

4.4.3.1.3. Repeated measures ANOVA

As discussed, repeated measures ANOVA (RANOVA) does not take into account baseline differences between subjects, and so for the model to have practical use with this data, the critical indication of a differential effect of the group (treatment) factor is the presence of a significant interaction between groups and time. In other words, the group*time interaction tests whether the pattern of change is different between groups over time. RANOVA analysis of leptin concentration was performed and showed that the covariance parameters (variance and sigma 1) were highly significant (both $p<0.0001$ with Z test scores of 7.681 and 3.591, respectively) and the null model likelihood ratio test was also highly significant ($p<0.0001$ with chi-square of 407.2), both suggesting that the model was valid for the data. Type III tests of fixed effects show that time has a significant effect on the data ($p<0.0001$) but not the group ($p=0.905$) or group*time interaction overall ($p=0.167$). However, the individual group2*time interaction at 180 minutes was significant ($p=0.017$) suggesting that the strong signal at the last time point found by the other analyses was also seen using RANOVA.

4.4.3.1.4. Repeated measures ANOVA using mixed models

This analysis takes into account both fixed and random effects in a single general linear model (GLM), and is able to incorporate repeated measures in a similar way to RANOVA. Its output includes type I, II, and III tests of the fixed effects. Running this model gives similar results to the RANOVA shown above, observing that time has a significant effect on the data ($p<0.0001$) but not the group ($p=0.901$) or group*time interaction overall ($p=0.133$). The individual group2*time interaction at 180 minutes is again significant ($p=0.013$). Unsurprisingly, both RANOVA analyses do not show any significant effect of group on the overall variance of leptin concentration as the derived group*time means used are not corrected for baseline.

4.4.3.2. BDNF

The study sought to test whether a cooling-induced calorie deficit would have any effect on circulating BDNF levels, by measuring it at 30 minute intervals during the temperature intervention and 60 minutes after. Raw data suggested an overall trend in greater BDNF concentration in the cooling group, with an increase at 90 minutes of cooling (figure 23b). However, two-tailed paired t tests on means at each time point were not significant. Adjusting for baseline differences, ANCOVA-POST analysis gave an R^2 value of only 0.121, and the analysis of variance showed that the validity of the model was not significant ($p = 0.426$). Due to these results suggesting that the model was not valid, the assumptions of the ANCOVA model were subsequently tested firstly by running an ANOVA to check that there were no significant differences in the pre-test values between groups, and secondly running an ANCOVA on post-test scores using pre-test and group covariates to check that the group*pre-test interaction had no significant between-subject effects (thereby testing the assumption of homogeneity of regression correlation). The first test showed that there were between-group differences in pre-test scores ($p = 0.001$), but the second test showed that the assumption of homogeneity was valid (group*pre-test interaction $p = 0.609$). As there were statistically significant differences in the pre-test scores between groups, running these checks on a gain score transformation of the data set (figure 23d) showed that there were no differences between groups in the pre-test scores ($p = 0.268$) and also that the assumption of homogeneity was valid in this data format.

An ANCOVA-CHANGE analysis was therefore performed and showed that the R^2 value was better at 0.380, and the validity of the model was highly significant ($p < 0.0001$). This analysis showed that there were no significant effects of group overall on BDNF levels (although did approach significance, $p = 0.080$). The least squares means derived from this analysis did, however, suggest that there was a nominally statistically significant difference in BDNF levels at the t4 timeframe (figure 23e).

(a)

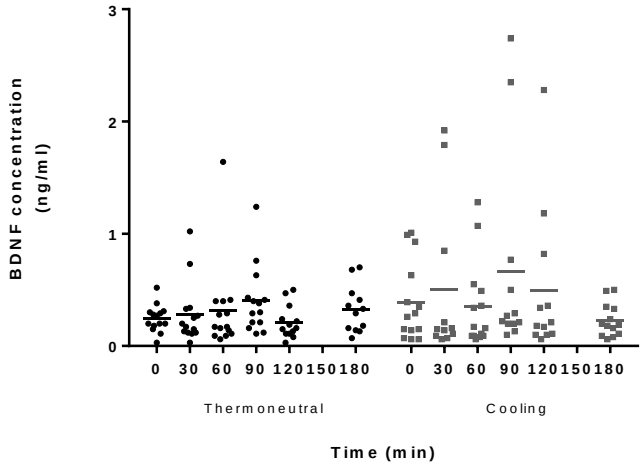
BDNF concentration (ng/ml)
3
2
1
0
0 30 60 90 120 150 180 0 30 60 90 120 150 180
Thermoneutral
Cooling
Time (min)

(b)

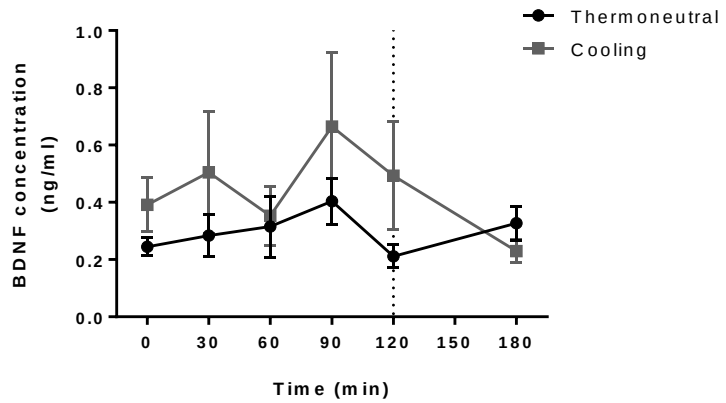
Thermoneutral
Cooling
BDNF concentration (ng/ml)
1.0
0.8
0.6
0.4
0.2
0.0
0 30 60 90 120 150 180
Time (min)

(c)

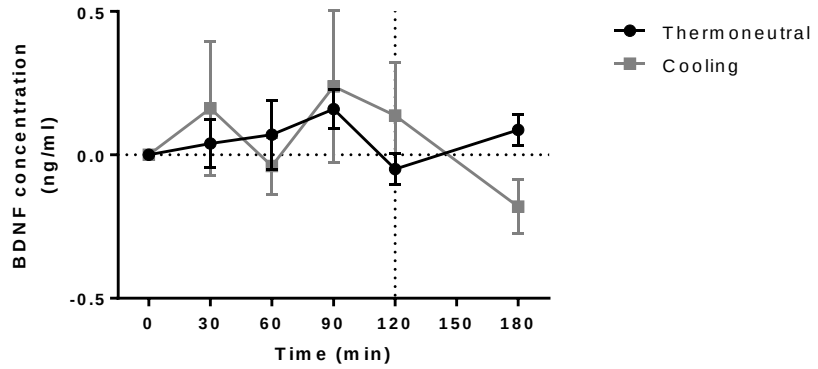
Thermoneutral
Cooling
BDNF concentration (ng/ml)
0.5
0.0
-0.5
0 30 60 90 120 150 180
Time (min)

(d)

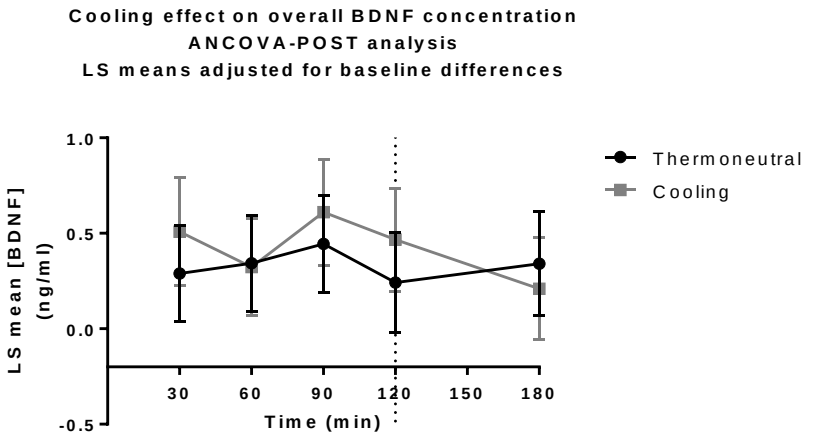

(e)

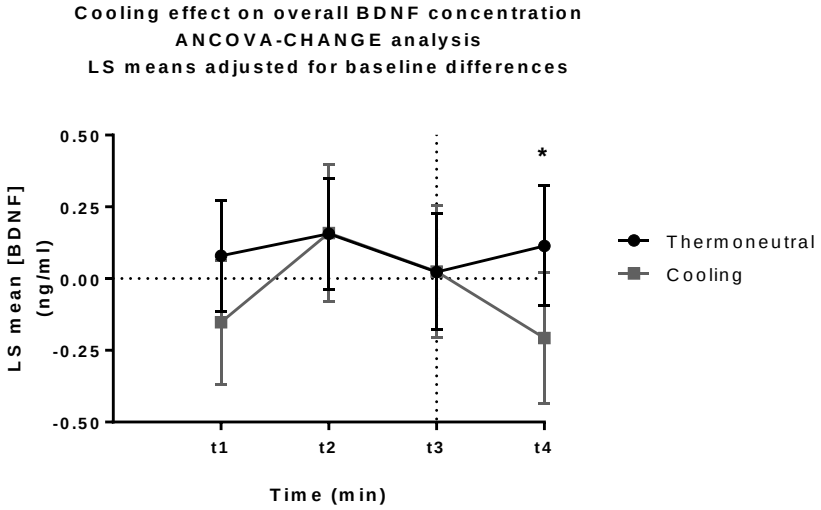

Figure 23. Effect of temperature intervention on BDNF concentration. Complete data was available on 14 participants. (a) All data points measured with horizontal means shown at each time point. (b) Group means with error bars (SEM). (c) Group means of gain scores with error bars (SEM). (d) Least squares means with error bars (SEM 95% CI) derived from ANCOVA-POST analysis that adjusts for baseline differences. This model was found to be invalid due to statistically significant group differences in pre-test scores (see main text). (e) Least squares means with error bars (SEM 95% CI) derived from ANCOVA-CHANGE analysis, which was found to be a valid model but also did not show any statistically significant group effect. There was a nominally significant group difference at the t4 time point ($p = 0.049$).

4.4.3.3. Glucose homeostasis

4.4.3.3.1. Glucagon

Plasma glucagon concentration was measured before and after the temperature intervention at t_0 and t_{120}. There was significant overlap in glucagon concentrations between groups (figure 24a), but there appeared to be a trend for an increase in glucagon concentration over time in the thermoneutral group and a decrease in the cooling group (figure 24b), but a two-tailed paired t test at 120 minutes was not significant nor when using a change score. ANCOVA analysis did not show any statistically significant group or time effect, although there is a downward trend with cooling (figure 24c).

(a)

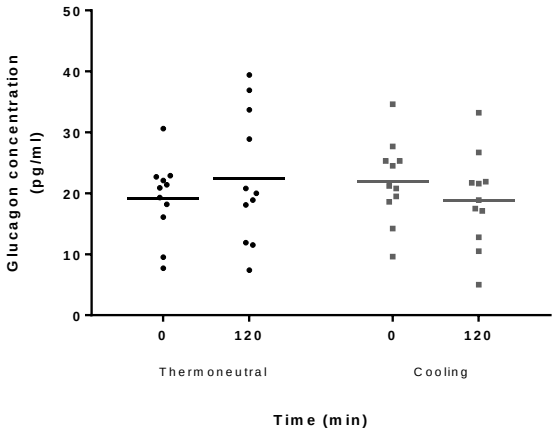

(b)

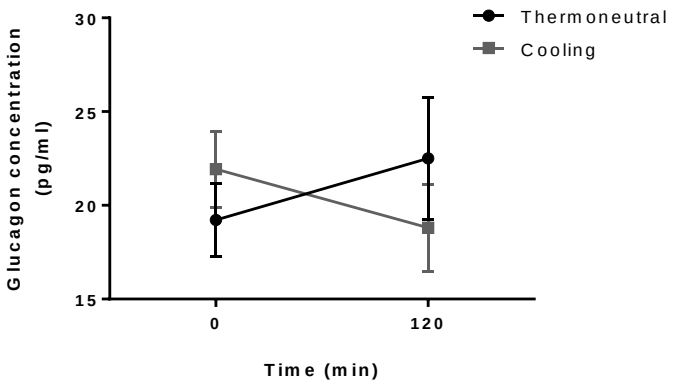

(c)

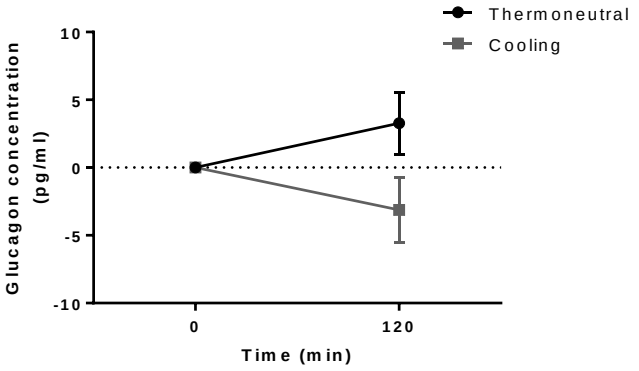

(d)

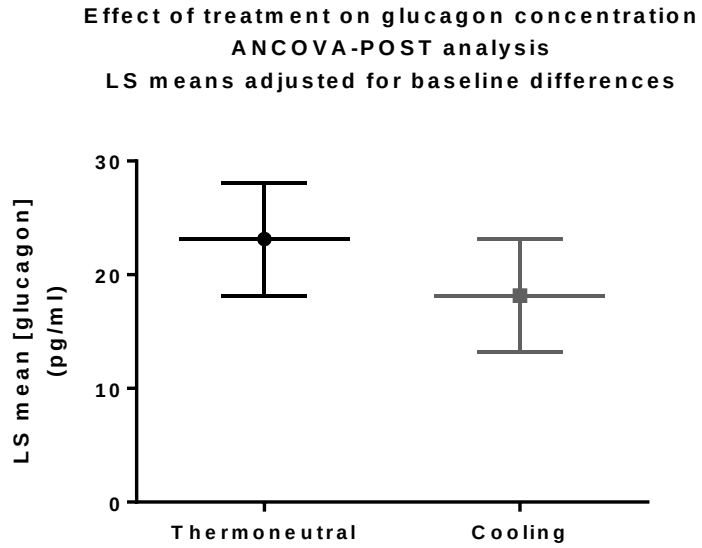

Figure 24. Effect of temperature intervention on glucagon concentration. Complete data was available on 11 participants. (a) All data points measured with horizontal means shown at each time point. (b) Group means with error bars (SEM). (c) Group means of gain scores with error bars (SEM). (d) Least squares means with error bars (SEM 95% CI) derived from ANCOVA-POST analysis that adjusts for baseline differences. ANOCVA-POST modelling did not show any group effect and there were no statistically different group differences at any time point for (b) - (d) using multiple two-tailed paired t tests. Note temperature intervention stopped at 120 minutes and no readings after this are available.

4.4.3.3.2. Glucose

Blood glucose concentration was also measured before and after the temperature intervention at t_0 and t_{120}. There was no statistically significant difference in means and change score means (figure 25b), and ANCOVA analysis showed no significant change in least squares means or group effect (figure 25c).

(a)

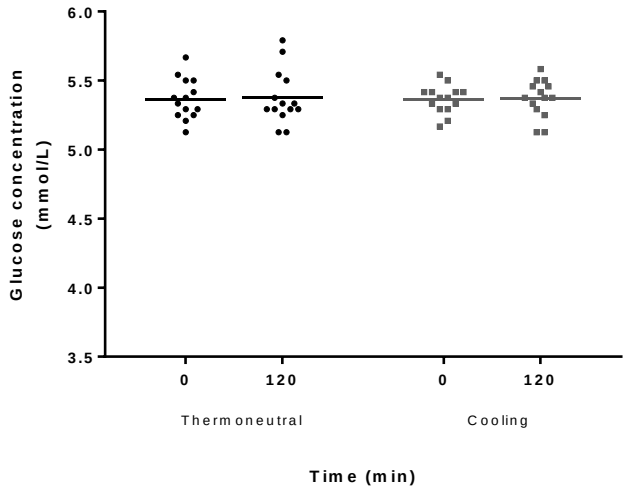

(b)

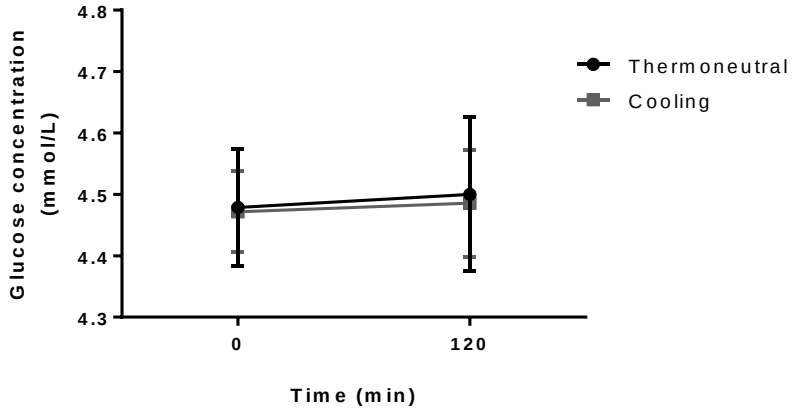

(c)

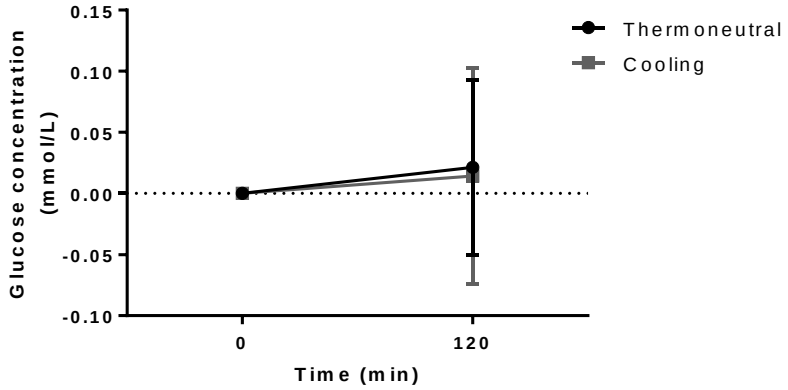

(d)

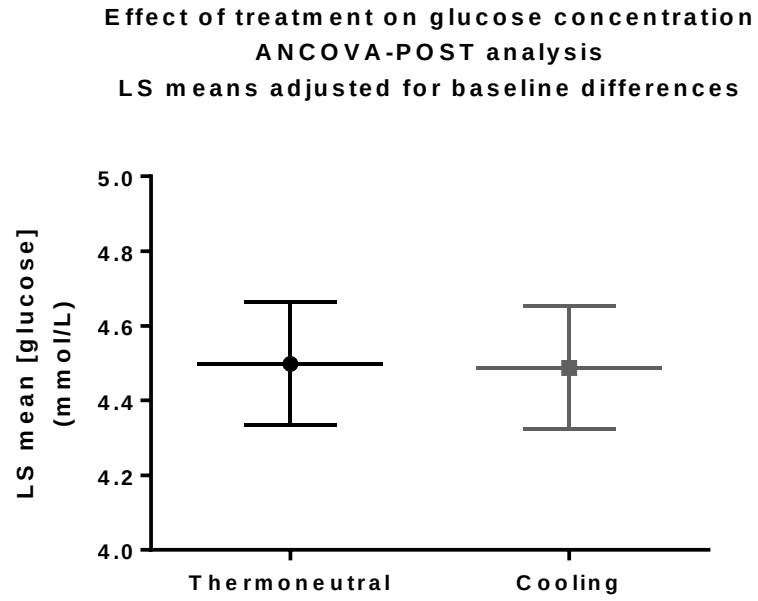

Figure 25. Effect of temperature intervention on glucose concentration. Complete data was available on 14 participants. (a) All data points measured with horizontal means shown at each time point. (b) Group means with error bars (SEM). (c) Group means of gain scores with error bars (SEM). (d) Least squares means with error bars (SEM 95% CI) derived from ANCOVA-POST analysis that adjusts for baseline differences. ANOCVA-POST modelling did not show any group effect and there were no statistically different group differences at any time point for (b) - (d) using multiple two-tailed paired t tests. Note temperature intervention stopped at 120 minutes and no readings after this are available.

4.4.3.3.3. Insulin

Plasma insulin was measured before the temperature intervention, every 30 minutes during it, and 60 minutes afterwards (as per leptin and BDNF). Raw data suggested an initial downward trend in insulin concentration with both treatment groups followed up an upward trend after intervention cessation. However, two-tailed paired t tests on means were not significant (figure 26b). Adjusting for baseline differences, ANCOVA-POST analysis gave an R^2 value of 0.618 meaning 62% of the variance was explained by the covariates. Most of this came from the pre-test values predicting the post-test values ($p < 0.0001$), but also the effect of time ($p = 0.002$). Grouping did not affect the post-test scores ($p = 0.574$) and there was no group effect over time (group*time interaction, $p = 0.819$).

(a)

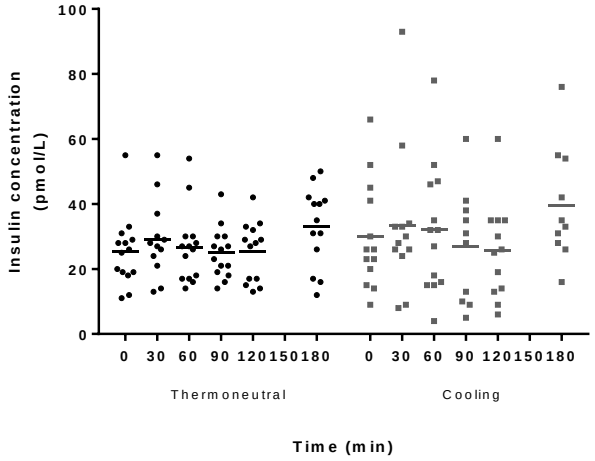

(b)

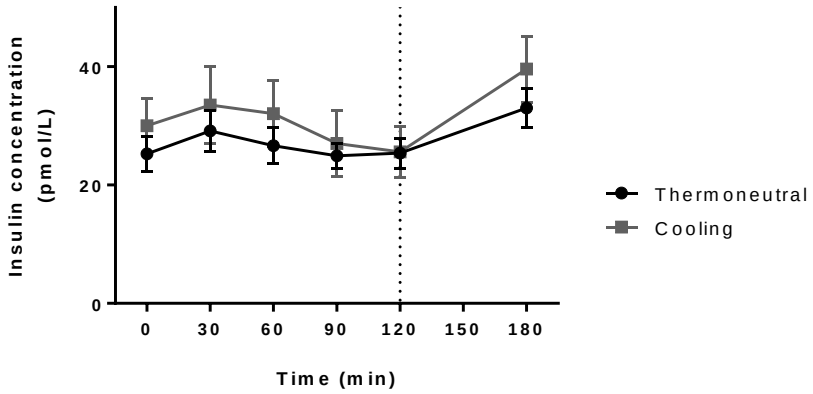

(c)

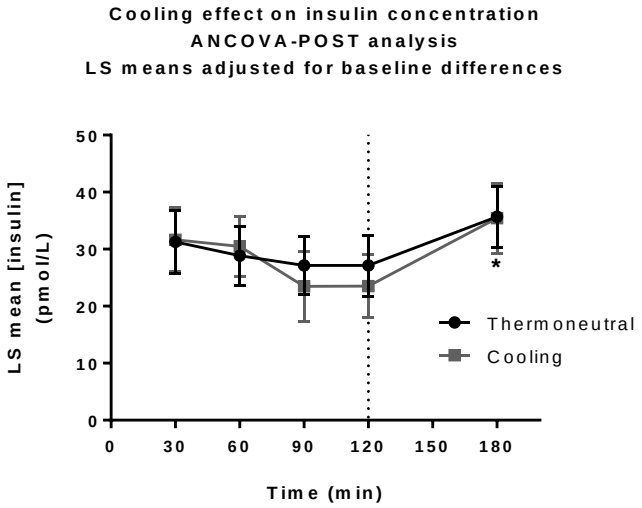

Figure 26. Effect of temperature intervention on insulin concentration. Complete data was available on 14 and 13 subjects in the thermoneutral and cooling groups, respectively. (a) All data points measured with horizontal means shown at each time point. (b) Group means with error bars (SEM). (c) Least squares means with error bars (SEM 95% CI) derived from ANCOVA-POST analysis that adjusts for baseline differences. Data shows an upward trend after the temperature intervention cessation but this was not statistically significant. No group differences at any time point was significant for (b) - (c) using multiple two-tailed paired t tests. Vertical dotted lines denote treatment cessation at t_{120}.

4.4.3.4. Cortisol

Serum cortisol was measured before the temperature intervention, every 30 minutes during, and 60 minutes afterwards (as per leptin and insulin). Raw data suggested an overall downward trend in cortisol concentration, with a greater negative effect with the cooling group (figures 27a and 27b). However, two-tailed paired t tests on means at each time point were not significant. Adjusting for baseline differences, ANCOVA-POST analysis gave an R^2 value of only 0.219, and the analysis of variance showed that the validity of the model was not hugely significant ($p = 0.006$). Nonetheless, the type II and III sum of squares analysis did show there was a marginal overall effect from the pre-test scores, but none from the time or group covariates. Due to these atypical results, the assumptions of the ANCOVA model were subsequently tested firstly by running an ANOVA to check that there were no significant differences in the pre-test values between groups, and secondly running an ANCOVA on post-test scores using pre-test and group covariates to check that the group*time interaction had no

significant between-subject effects (thereby testing the assumption of homogeneity of regression correlation). The first test did show that there were between-group differences in pre-test scores ($p = 0.016$), but the second test showed that the assumption of homogeneity was valid.

As there were significant overall differences in the pre-test scores between groups, running these checks on a gain score transformation of the data set (figure 27d) showed that there were no differences between groups in the pre-test scores ($p = 0.457$) and also that the assumption of homogeneity was valid in this data format. An ANCOVA-CHANGE analysis was therefore performed and showed that the R^2 value was better at 0.528, and the validity of the model was highly significant ($p < 0.0001$). However, this analysis showed that there were indeed no significant effects of group or time on cortisol levels. The least squares means derived from this analysis did not show individual statistical significance at any individual time frame (figure 27e).

(a)

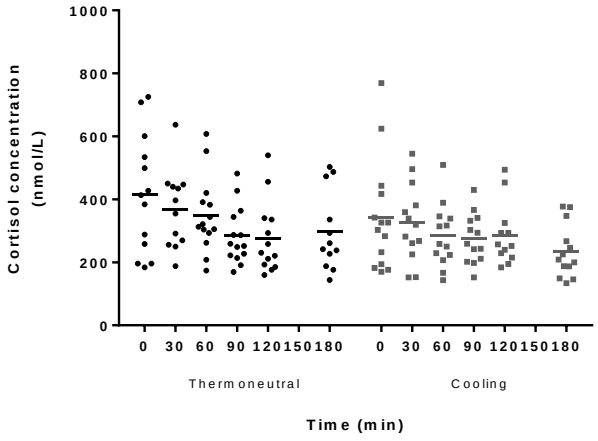

(b)

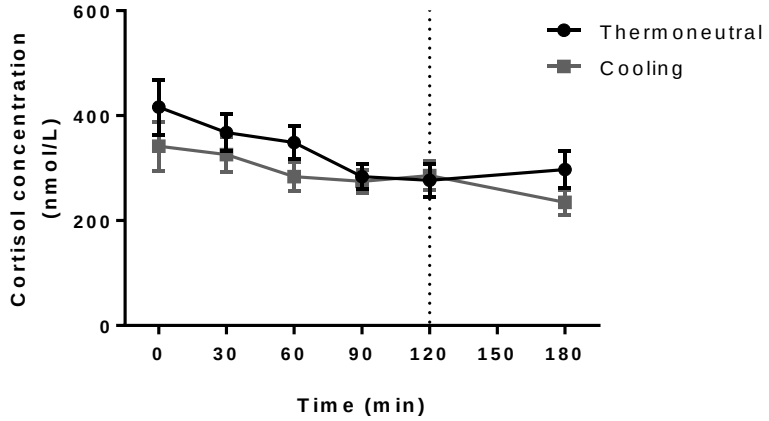

(c)

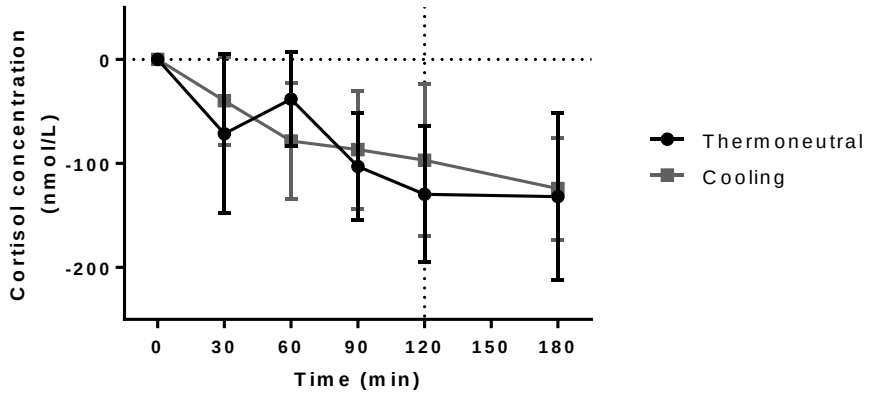
Cortisol concentration (nmol/L)
0
-100
-200
0
30
60
90
120
150
180
Time (min)
Thermoneutral
Cooling

(d)

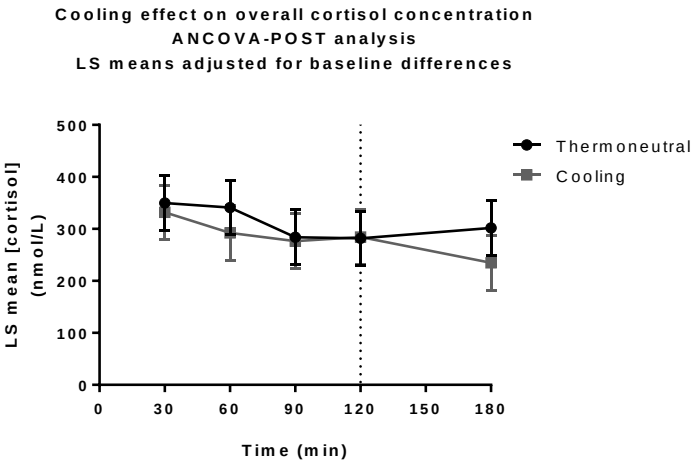
Cooling effect on overall cortisol concentration
ANCOVA-POST analysis
LS means adjusted for baseline differences
LS mean [cortisol] (nmol/L)
500
400
300
200
100
0
0
30
60
90
120
150
180
Time (min)
Thermoneutral
Cooling

(e)

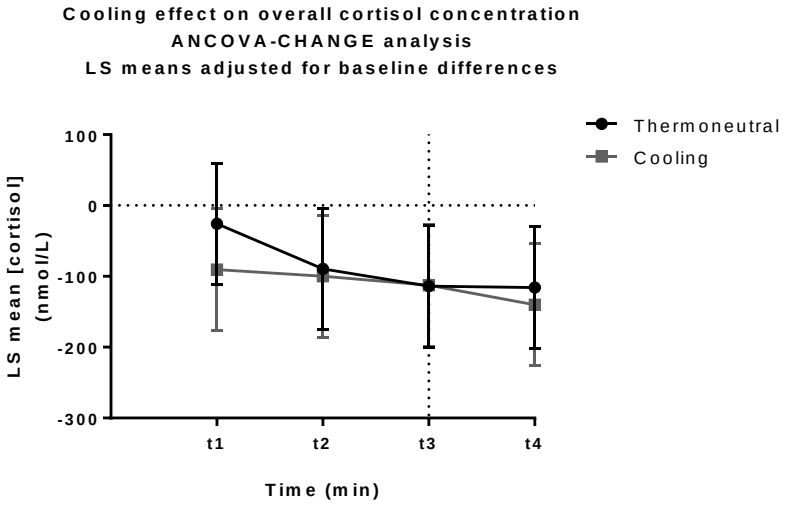
Cooling effect on overall cortisol concentration
ANCOVA-CHANGE analysis
LS means adjusted for baseline differences
LS mean [cortisol] (nmol/L)
100
0
-100
-200
-300
t1
t2
t3
t4
Time (min)
Thermoneutral
Cooling

Figure 27. Effect of temperature intervention on cortisol concentration. Complete data was available on 14 participants. (a) All data points measured with horizontal means shown at each time point. (b) Group means with error bars (SEM). (c) Group means of gain scores with error bars (SEM). (d) Least squares means with error bars (SEM 95% CI) derived from ANCOVA-POST analysis that adjusts for baseline differences. This model was found to be invalid due to statistically significant group differences in pre-test scores (see main text). (e) Least squares means with error bars (SEM 95% CI) derived from ANCOVA-CHANGE analysis, which was found to be a valid model but also did not show any statistically significant group effect. No group differences at any time point was significant for (b) - (e) using multiple two-tailed paired t tests. Vertical dotted lines denote treatment cessation at t_{120}.

4.4.3.5. Thyroid function

Thyroid function was measured before the temperature intervention, every 30 minutes during, and one hour after its cessation. There was no significant difference between the two intervention groups in thyroid function, measured using the assay platform Advia Centaur.

4.4.2.5.1. Thyroid stimulating hormone (TSH)

The cooling group appears to have higher TSH levels compared to thermoneutral, but that both decrease during intervention before returning to their baseline 60 minutes after treatment cessation (figure 28b). These differences were not statistically significant at each time point when evaluating t test scores on the ordinary means. When baseline differences are adjusted for using ANCOVA-POST analysis (R^2 = 0.921 and analysis of variance model p <0.0001) there is a nominally significant group effect seen (p = 0.052) on type I sum of squares (SS) analysis, but this is not significant on type II (p = 0.974) and type III (p = 0.954) SS analysis, and so should be discounted. A plot of derived LS means is shown in figure 28c, and there are no significant differences between groups at any time point.

(a)

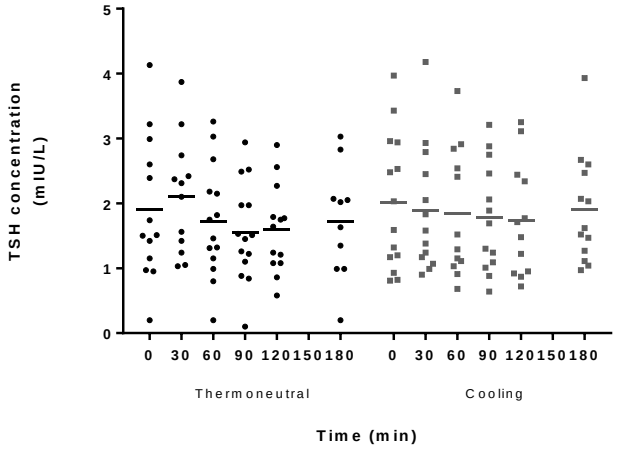
TSH concentration (mIU/L)
0
1
2
3
4
5
0 30 60 90 120 150 180 0 30 60 90 120 150 180
Thermoneutral
Cooling
Time (min)

(b)

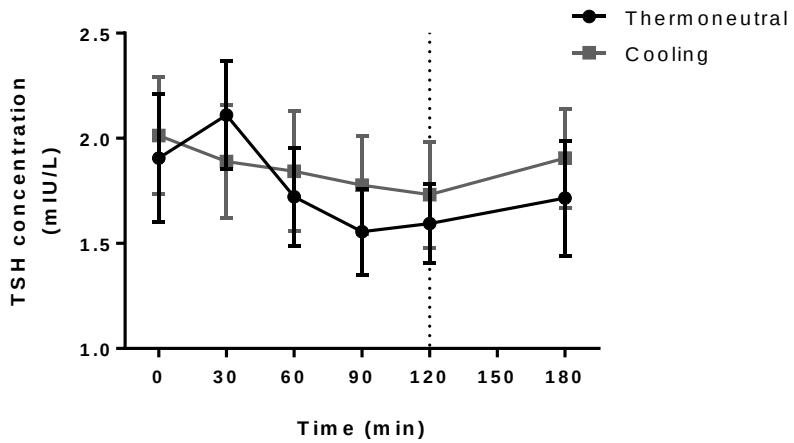
Thermoneutral
Cooling
TSH concentration (mIU/L)
1.0
1.5
2.0
2.5
0 30 60 90 120 150 180
Time (min)

(c)

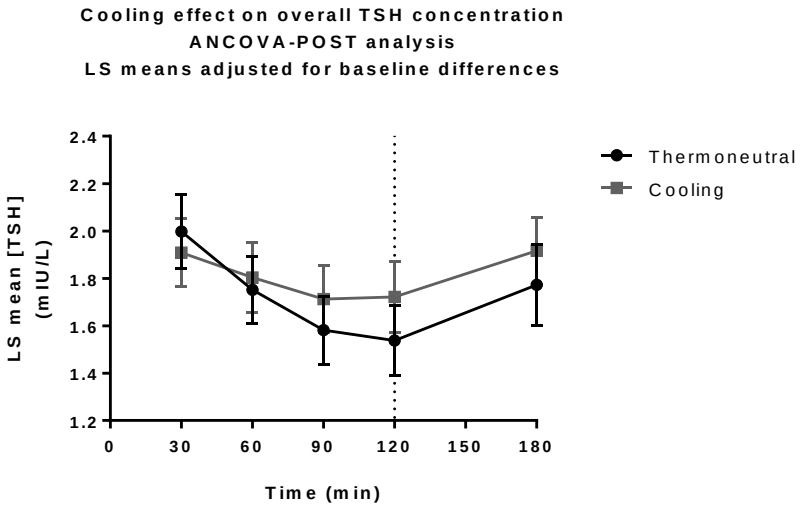
Cooling effect on overall TSH concentration
ANCOVA-POST analysis
LS means adjusted for baseline differences
Thermoneutral
Cooling
LS mean [TSH] (mIU/L)
1.2
1.4
1.6
1.8
2.0
2.2
2.4
0 30 60 90 120 150 180
Time (min)

Figure 28. Effect of temperature intervention on TSH concentration. Complete data was available on 14 subjects in each group. (a) All data points measured with horizontal means shown at each time point. (b) Group means with error bars (SEM). (c) Least squares means with error bars (SEM 95% CI) derived from ANCOVA-POST analysis that adjusts for baseline differences. Data shows an upward trend after the temperature intervention cessation but this was not statistically significant. No group differences at any time point was significant for (b) - (c) using multiple two-tailed paired t tests. Vertical dotted lines denote treatment cessation at t_{120}.

4.4.2.5.2. Free thyroxine hormone (fT4)

The cooling group appears to have lower fT4 levels at all time points (figure 29b), and a statistically significant difference is seen when comparing the overall means of the two groups unadjusted for baseline, (not shown). However, when baseline differences are adjusted for using ANCOVA-POST analysis (R^2 = 0.848 and analysis of variance model p <0.0001) no difference is seen. Type I, II, and III sum of squares analysis shows that only the pre-test scores have an effect on post-test scores, and not group or time factors. A chart of derived LS means is shown in figure 29c, and there are no significant differences between groups at any time point.

(a)

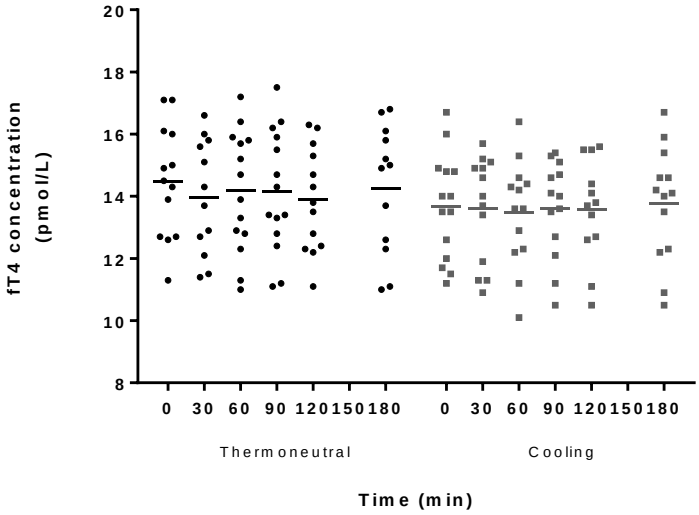

(b)

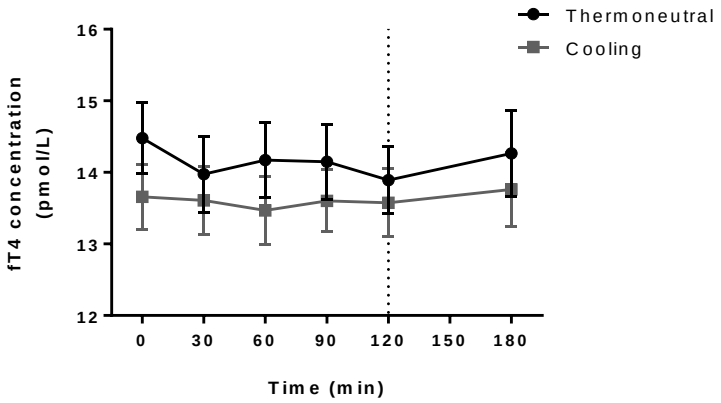

(c)

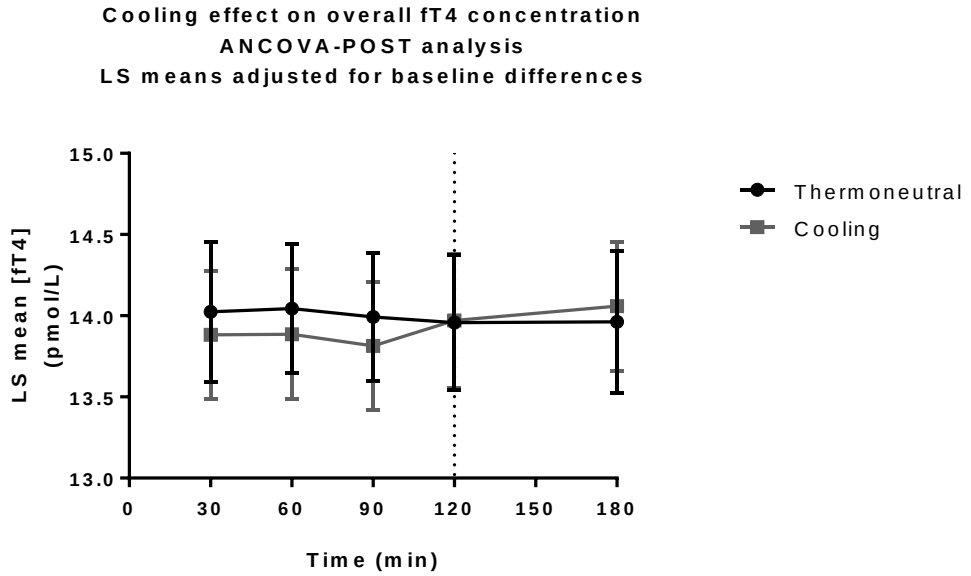

Figure 29. Effect of temperature intervention on fT4 concentration. Complete data was available on 14 subjects in each group. (a) All data points measured with horizontal means shown at each time point. (b) Group means with error bars (SEM). (c) Least squares means with error bars (SEM 95% CI) derived from ANCOVA-POST analysis that adjusts for baseline differences. Data shows an upward trend after the temperature intervention cessation but this was not statistically significant. No group differences at any time point was significant for (b) - (c) using multiple two-tailed paired t tests. Vertical dotted lines denote treatment cessation at t_{120}.

4.4.2.5.3. Free triiodothyronine (fT3)

In the unadjusted data, there appeared to be a trend for lower fT3 concentration means in the cooling group (figure 30b), but this apparent trend was lost after adjustment for baseline differences using ANCOVA-POST analysis ($R^2 = 0.776$ and analysis of variance model $p < 0.0001$). Type I, II, and III sum of squares analysis shows that only the pre-test scores have an effect on post-test scores, and not group or time factors, although the group factor approached significance ($p = 0.074$). A chart of derived LS means is shown in figure 30c, and there are no significant differences between groups at any time point.

(a)

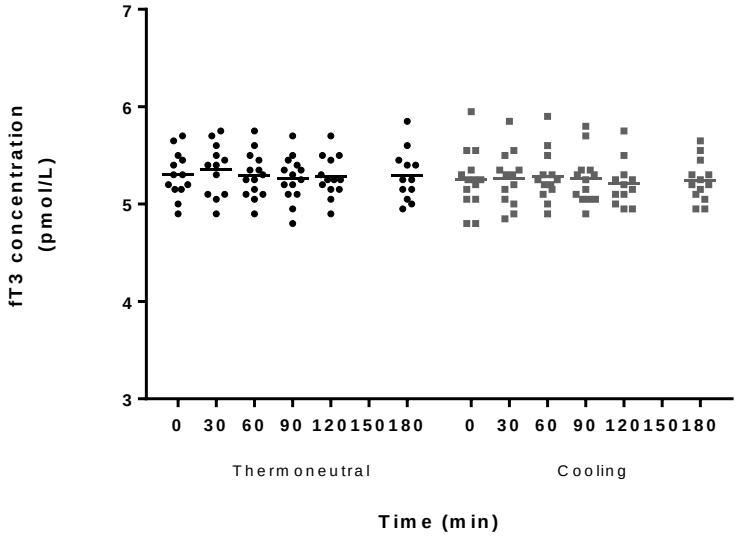

(b)

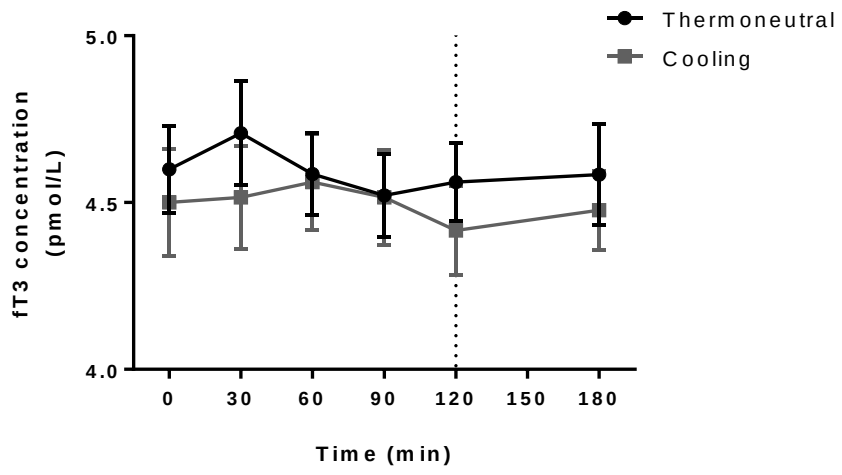

(c)

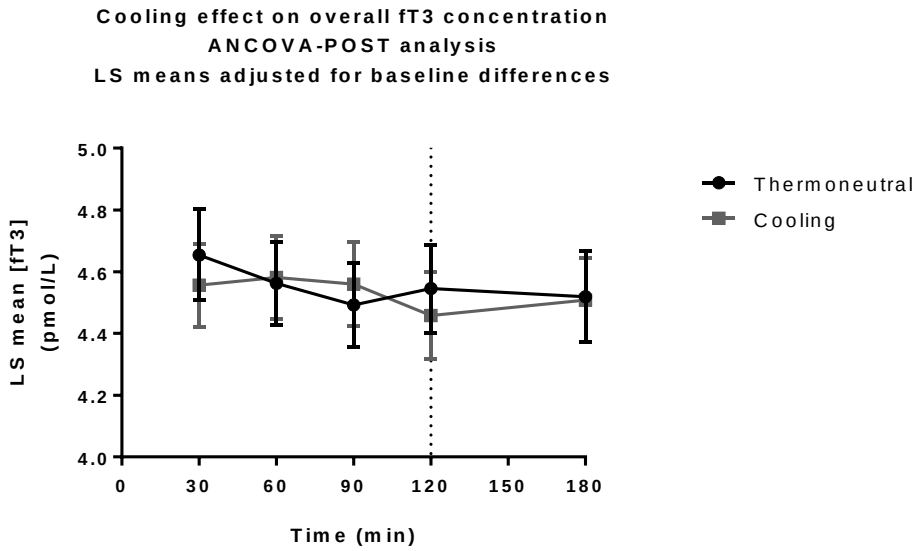

Figure 30. Effect of temperature intervention on fT3 concentration. Complete data was available on 14 subjects in each group. (a) All data points measured with horizontal means shown at each time point. (b) Group means with error bars (SEM). (c) Least squares means with error bars (SEM 95% CI) derived from ANCOVA-POST analysis that adjusts for baseline differences. No group differences at any time point was significant for (b) - (c) using multiple two-tailed paired t tests. Vertical dotted lines denote treatment cessation at t_{120}.

4.4.4. Energy expenditure response to cooling

4.4.4.1. Energy expenditure

A gas exchange monitor was used to measure energy expenditure (EE) and respiratory quotient (RQ). Measurements were taken after 60 minutes at a thermoneutral temperature (Tn60, just before the temperature intervention, referred to here as 'pre-test'), and after 2 hours of the temperature intervention (at Ti120, referred to here as 'post-test'). Measurements were taken under controlled conditions in a quiet, dimly lit room, and the participant was closely observed to ensure they did not fall asleep. At the time of recording consecutive time epochs were examined. When the difference between consecutive epochs was <10%, a five minute period of data was taken and averaged for each of the 15 participants. As the participants were starved, energy expenditure in the above conditions is considered equivalent to the basal metabolic rate (BMR).

The raw plots shows a trend for an increase in energy expenditure mean pre- and post-test for both temperature intervention groups, with higher values for the cooling group (31a and 31b). However, the differences in gain scores ('delta-test') do not show any statistically different results with a two-tailed paired t test (p = 0.33, figure 31c), and although the baseline-adjusted least squares means derived from ANCOVA modelling also show a trend for greater EE with cooling (figure 31d), this also did not reach significance (R^2 = 0.612, p = 0.32).

(a)

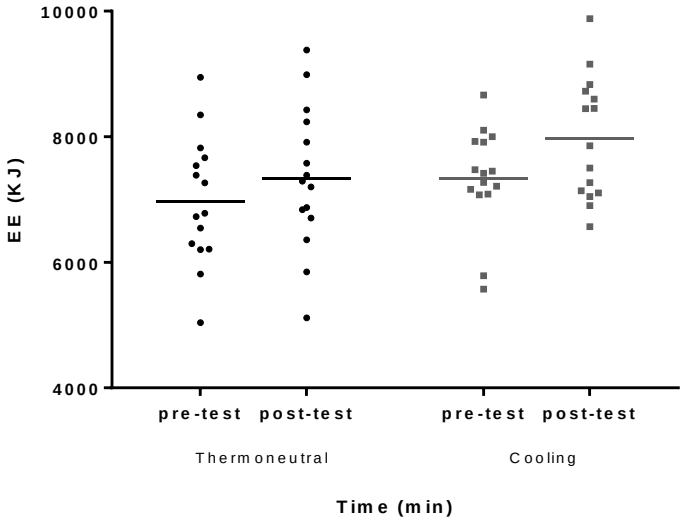

(b)

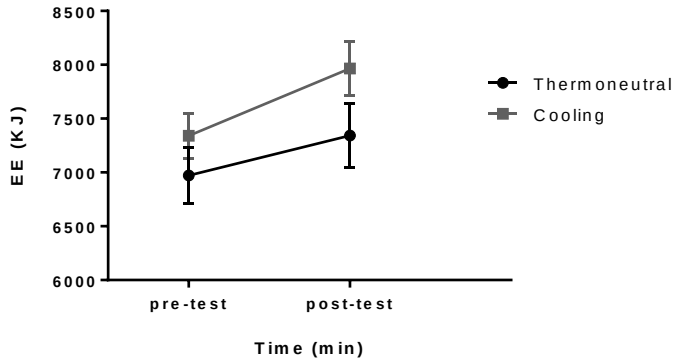

(c)

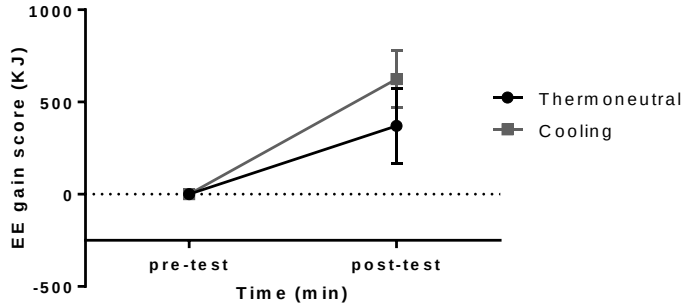

(d)

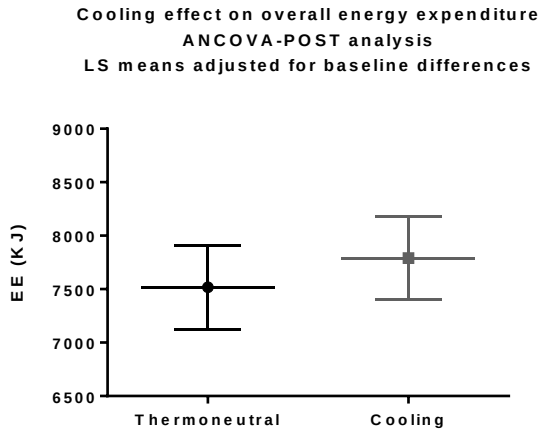

Figure 31. Effect of temperature intervention on energy expenditure. Complete data was available on 15 participants. (a) All data points with means pre-test and post-test. (b) Group means with error bars (SEM). (c) Group means of gain scores with error bars (SEM). (d) Least squares means with error bars (SEM 95% CI) derived from ANCOVA-POST analysis, which did not show any group effect.

4.4.4.2. Energy expenditure and correlation with body fat

It was not possible to set up an ANCOVA model that adjusted for baseline using pre-test scores as a quantitative covariate for the dependent variable of post-test scores, whilst also using percentage body fat as another quantitative covariate, and so three separate ANCOVA models were performed using percentage body fat as the covariate for either pre-test, post-test, or delta-test (the gain score of post-test minus pre-test) as the dependant variable, with the temperature intervention group added as a qualitative covariate. Percentage body fat did not appear to affect any of the dv (type III sum of squares analysis showed p values of 0.163, 0.461, and 0.493, respectively), and there were no %fat*group interactions seen. Correlation between pre-test, post-test, and delta-test values against percentage body fat, total mass, and height, was also assessed individually using a linear regression model, and no correlations were found although a non-significant trend was seen for greater EE with increasing percentage body fat (figure 32 and table 11).

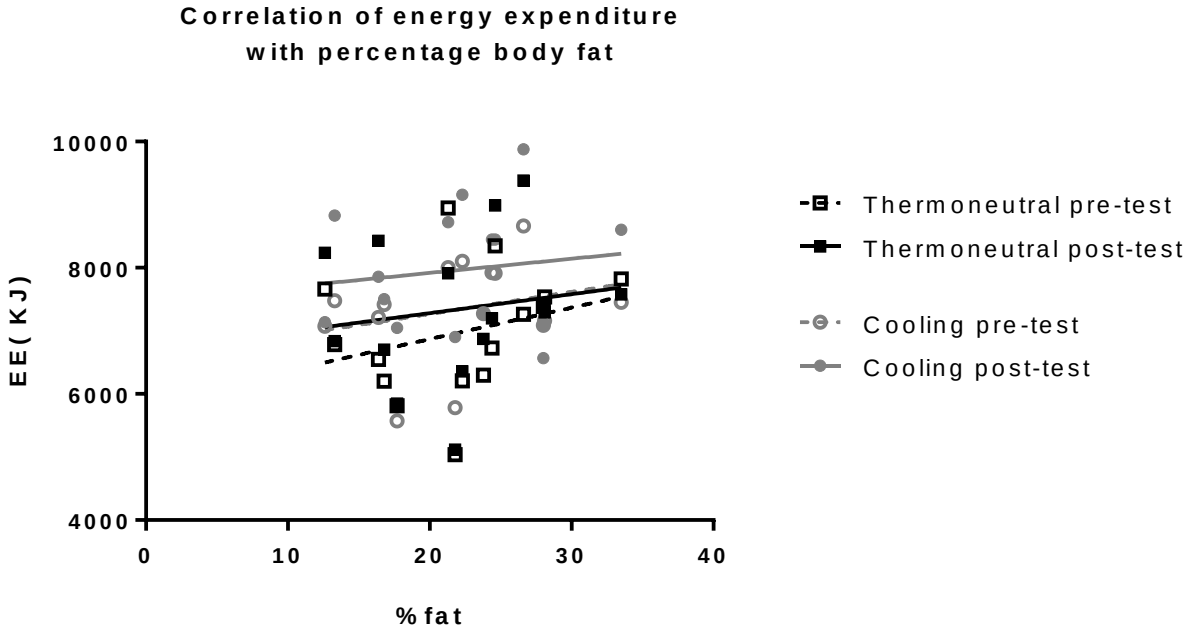

Figure 32. Correlation between percentage body fat and energy expenditure. Scatter plot for four groups of data (pre-test and post-test scores for thermoneutral and cooling groups. Linear trend lines were drawn, and although each appears to have a pattern for greater EE with increasing body fat, these were not significant, as shown by then linear regression model results shown in table 11.

		Thermoneutral			Cooling		
		Pre-test	Post-test	Delta-test	Pre-test	Post-test	Delta-test
R^2		0.353	0.567	0.267	0.268	0.097	0.069
F		1.999	4.805	1.339	1.341	0.394	0.271
P value		0.173	0.022	0.312	0.311	0.760	0.845
Height	F	0.396	0.041	0.980	1.021	0.638	0.005
	Pr>F	0.542	0.842	0.343	0.334	0.441	0.947
Mass	F	2.536	3.006	0.000	0.017	0.155	0.220
	Pr>F	0.140	0.111	0.998	0.898	0.702	0.648
% Fat	F	0.188	0.816	0.230	0.458	0.320	0.009
	Pr>F	0.673	0.386	0.641	0.513	0.583	0.926

Table 11. Correlation of height, mass, and percentage body fat with energy expenditure. Pre-test, post-test, and delta-test (gain score) for the thermoneutral and cooling groups. Linear regression lines shown on a scatter plot for all 15 participants. No correlation is seen between any of the groups or factors assessed. Calculated using XLSTAT package for Microsoft Excel. All data sets passed tests of normality.

4.4.4.3. Respiratory quotient

The respiratory quotient (RQ), calculated by dividing the volume of carbon dioxide eliminated by the amount of oxygen consumed, provides a measure of the primary substrate utilised as an energy source by the body. Respiratory quotients of 1 represent carbohydrate utilisation, whereas those of 0.7 represent fat. The RQ was measured before and after the temperature intervention under resting, fasted conditions in a dimly lit, quiet room. The same five minute period of data used for BMR calculation was averaged for each of the 15 participants.

There appeared to be a lower RQ in the cooling group of the study (figure 33a and 33b) but this trend reversed when plotting the gain score (figure 33c) and a two-tailed paired t test show no significant differences between means ($p = 0.21$). The baseline-adjusted least squares means derived from ANCOVA modelling show no group differences ($R^2 = 0.245$, $p = 0.774$, figure 32d).

(a)

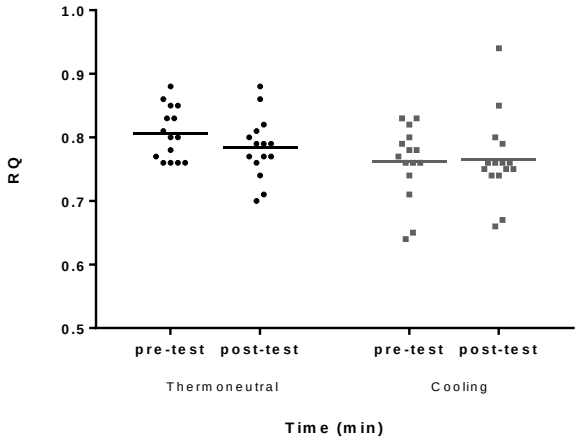
1.0
0.9
0.8
0.7
0.6
0.5
RQ
pre-test
post-test
pre-test
post-test
Thermoneutral
Cooling
Time (min)

(b)

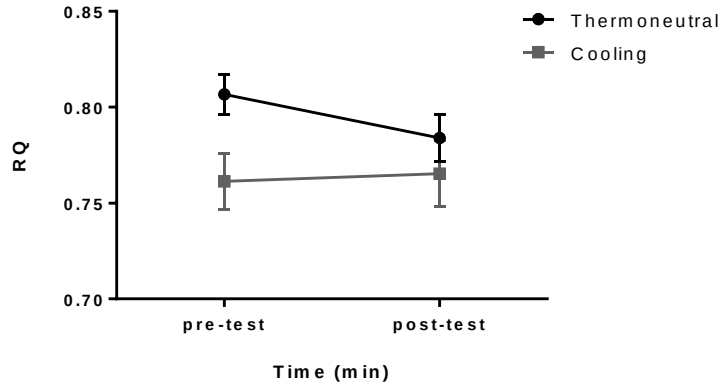
0.85
0.80
0.75
0.70
RQ
Thermoneutral
Cooling
pre-test
post-test
Time (min)

(c)

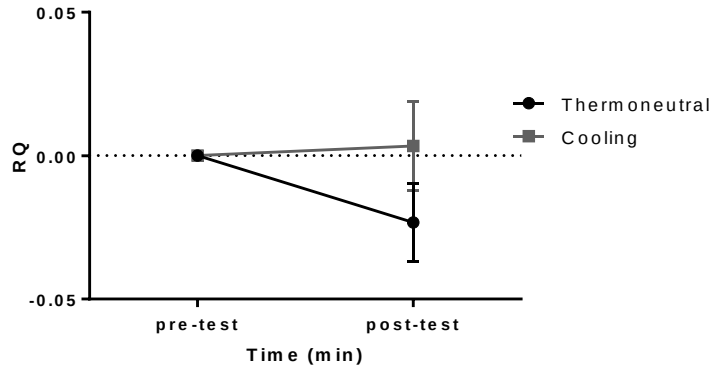
0.05
0.00
-0.05
RQ
Thermoneutral
Cooling
pre-test
post-test
Time (min)

(d)

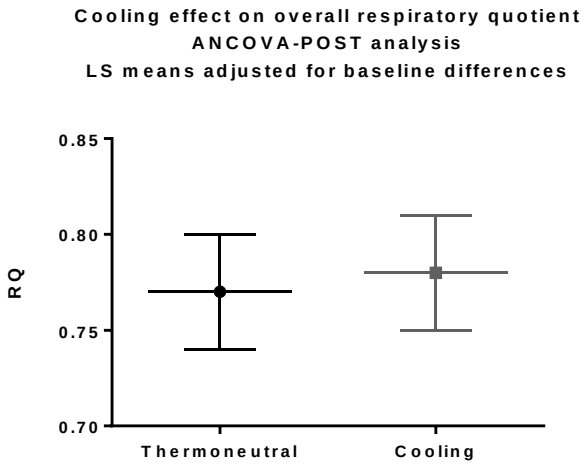

Figure 33. Effect of temperature intervention on respiratory quotient. Complete data was available on 15 participants. (a) All data points measured with means shown at pre-test and post-test. (b) Group means with error bars (SEM). (c) Group means of gain scores with error bars (SEM). (d) Least squares means with error bars (SEM 95% CI) derived from ANCOVA-POST analysis that adjusts for baseline differences. ANOCVA-POST modelling did not show any group effect and there were no statistically different group differences at any time point for (b) - (d) using multiple two-tailed paired t tests.

4.4.4.4. Respiratory quotient and correlation with body fat

As per analysis for energy expenditure, three separate ANCOVA models were performed using percentage body fat as the covariate for either pre-test, post-test, or delta-test (the gain score of post-test minus pre-test) as the dependant variable, with the temperature intervention group added as a qualitative covariate. Percentage body fat did not appear to affect any of the dv (type III sum of squares analysis showed p values of 0.524, 0.332, and 0.666, respectively), and there were no %fat*group interactions seen.

Correlation between pre-test, post-test, and delta-test values against percentage body fat, total mass, and height, was also assessed individually using a linear regression model, and no correlations were found with percentage body fat, but as one might expect here was correlation with RQ and mass, and RQ and height for some of the factors (figure 34 and table 12).

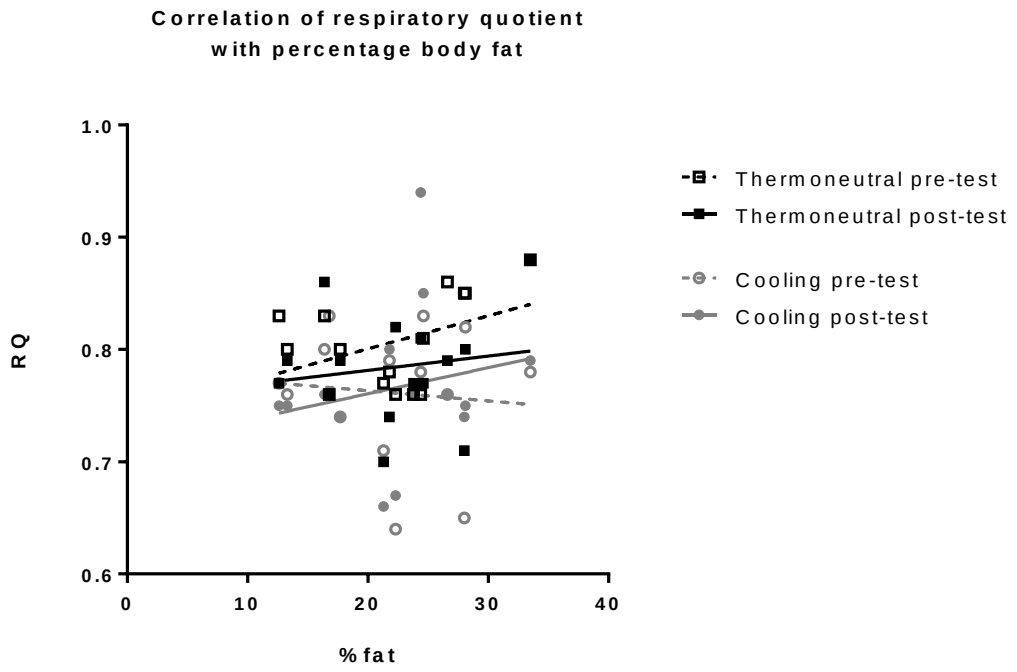

Figure 34. Correlation between percentage body fat and respiratory quotient. Scatter plot for four groups of data (pre-test and post-test scores for thermoneutral and cooling groups. Linear trend lines shown, none statistically significant.

		Thermoneutral			Cooling		
		Pre-test	Post-test	Delta-test	Pre-test	Post-test	Delta-test
R^2		0.628	0.072	0.354	0.524	0.194	0.205
F		6.186	0.285	2.014	4.036	0.883	0.945
Pr > F		0.010	0.836	0.171	0.037	0.480	0.452
Height	F	6.151	0.205	4.183	6.626	0.411	1.460
	Pr>F	**0.031**	0.659	**0.066**	**0.026**	0.535	0.252
Mass	F	12.417	0.017	5.512	1.049	0.014	0.797
	Pr>F	**0.005**	0.899	**0.039**	0.328	0.908	0.391
% Fat	F	1.252	0.238	1.513	0.092	0.120	0.024
	Pr>F	0.287	0.635	0.244	0.768	0.736	0.879

Table 12. Correlation of height, mass, and percentage body fat with the respiratory quotient. Pre-test, post-test, and delta-test (gain score) for the thermoneutral and cooling groups. Linear regression lines drawn on a scatter plot for all 15 participants. No correlation is seen between any of the groups or factors assessed. All data sets passed tests of normality.

4.4.4.5. Energy intake and fat preference

Energy intake was assessed one hour after the cessation of the temperature intervention. We used a paradigm that we had previously developed where subjects were given a 15g anonymised taste sample of the three test meals (20, 40 and 60% fat content, meals identical in appearance, mouth-feel and taste) and asked a visual analogue score was performed for each to assess how much the participant "liked" it. The three test meals were then provided and subjects were then allowed to eat *ad libitum*, and total consumption of each was measured by weight. The visual analogue scales were then repeated in an identical manner. This paradigm has been previously used to show that patients with disrupted leptin-melanocortin signalling (from MC4R mutations) eat more high fat food, without any change in their "liking" ratings, indicating that this may be a subconscious biological effect.

Meal	Fat (%)	Protein (%)	Carbohydrate (%)	Caloric density (kcal g^{-1})
Low fat	20	25	56	1.1
Medium fat	40	19	42	1.5
High fat	60	13	28	2.0

Table 13. Macronutrient composition of the meals used in the fat preference test. Percentage of energy derived from each macronutrient is shown. Kcal=Calories.

(a)

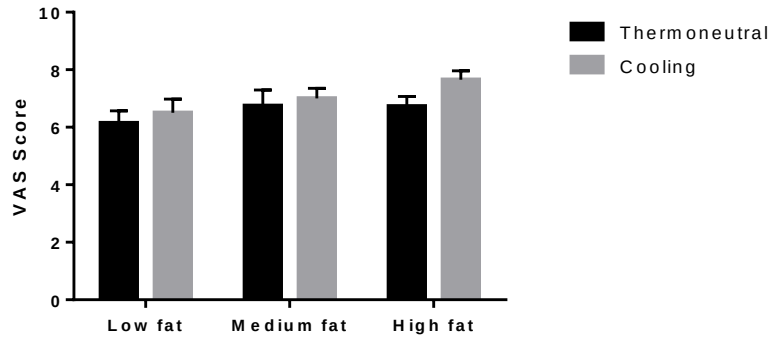

(b)

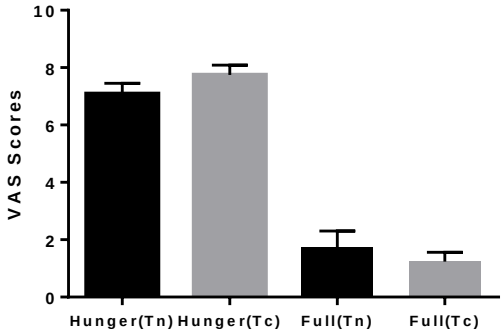

(c)

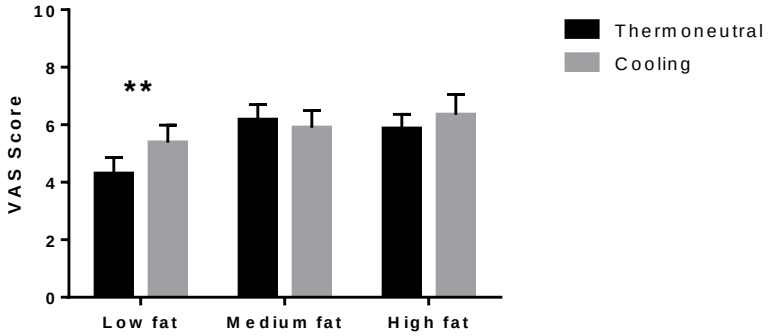

(d)

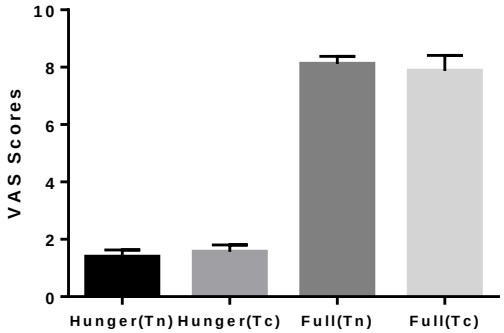

Figure 35. Likings ratings for the fat preference meals premeal (a) and postmeal (b). Results show mean with standard error of mean. Likings ratings in the premeal VAS scores did not reach significance, although showed a trend towards preference for the high fat meal in the cooling study arm. The post-meal VAS scores showed a significant preference for the low fat meal in the cooling arm of the study when a two-tailed paired t-test was applied ($p = 0.009$), but there was no significant difference for the other two test meals. Hunger and fullness was additionally assessed before and after the fat preference meal. Premeal measurements showed a trend for participants to be more hungry and less

full in the cooling study arm, this did not reach statistical significance when a paired t test was applied (p = 0.0561 and 0.32, respectively). Postmeal hunger and fullness scores did not show any difference between the two study arms.

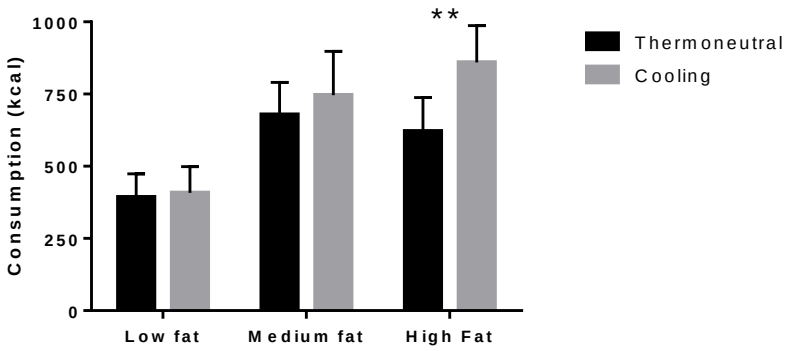

Figure 36. Total intake of low, medium and high fat meals following temperature intervention.
Results show mean consumption (kCal) with standard error of mean. A two-tailed paired t test was applied and showed a significant increase in consumption of the high fat meal in the cooling arm of the study (p = 0.0048). There was no significant difference in consumption of the low and medium fat meals between the two study arms.

4.4.5. Neurocognitive response to cooling

4.4.5.1. Perception of neurocognition

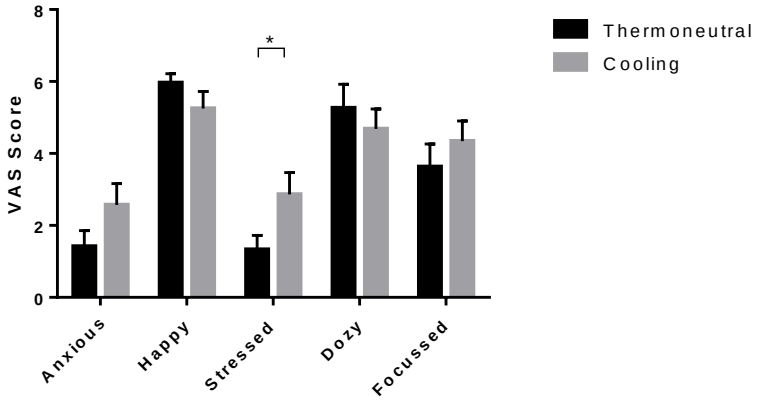

Figure 37. Changes in perception of neurocognition as measured by visual analogue scale. A visual analogue scale was performed before and after the temperature intervention to assess the subject's perception of their neurocognitive state. A paired t test showed that the subjects in the cooling arm felt significantly more stressed than in the thermoneutral arm ($p = 0.0428$), but other parameters did not reach significance.

4.4.5.2. Changes in neurocognitive tasks in response to cooling

4.4.5.2.1. Rey auditory verbal learning test (RAVLT) test

The RAVLT test evaluates a wide diversity of functions: short-term auditory-verbal memory, rate of learning, learning strategies, retroactive and proactive interference, presence of confabulation and confusion in memory processes, information retention and differences between learning and retrieval. Participants are given a list of 15 unrelated words repeated over five different trials. Another list is of 15 unrelated words are given and the client must again repeat the original list of 15 words then and again after 20 minutes. There was no difference in score between the two study intervention arms.

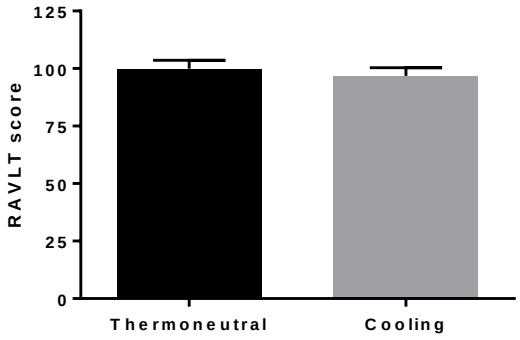

Figure 38. RAVLT scores in the thermoneutral and cooling study intervention arms. There was no difference between the two study arms (n = 14, paired t test, p = 0.4194).

4.4.5.2.2. Verbal fluency

The verbal fluency test is a short test of verbal functioning. The test used in this study was of letter fluency; subjects were given a letter and asked to list as many words as they could beginning with that letter in one minute. The letter used was changed each time to limit any learning-related improvement in the task. It tests verbal ability and executive control. Participants in the cooling arm of the study were able to generate significantly more words in one minute than they were after two hours at a thermoneutral temperature.

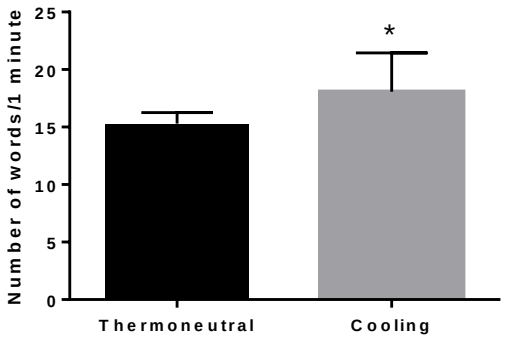

Figure 39. Post temperature intervention verbal fluency. Subjects in the cooling arm of the study were able to generate significantly more words than in the thermoneutral arm (n = 14). Data shown is mean with standard error of mean. A paired t test showed significance (p = 0.0126).

4.4.5.2.3. Digit span

The digit span is a test where participants are asked to repeat number sequences of increasing length. This is followed by a similar test where participants are asked to repeat number sequences in reverse. The first element tests short term memory and the second working memory. The scores for the two tests are then added together to give an overall score. Participants in the cooling arm scored significantly more highly in the cooling arm than the thermoneutral arm of the study.

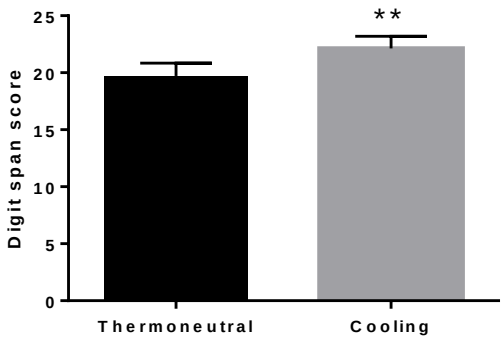

Figure 40. Digit span scores in response to cooling. Participants in the cooling arm were significantly better at the digit span test than those exposed to two hours at a thermoneutral temperature. Data shown is mean with standard error of mean and was available of 14 subjects. A paired t test demonstrated significance ($p = 0.0048$).

4.4.5.2.4. Hayling test

The Hayling test is a measure of response initiation and response suppression. Subjects are asked to complete a list of fifteen sentences with the last word missing. They are then given a second set of sentences missing the last word and are asked to complete the sentences with a word missing with a word that is completely unrelated to the sentence in every way. The time taken for both of these responses is measured. The first part of the test measures response initiation time, and the second, response suppression (a frontal lobe function) and thinking time. A composite score is awarded based on the two test elements. There was no significant difference between the two study arms in the response to the Hayling test.

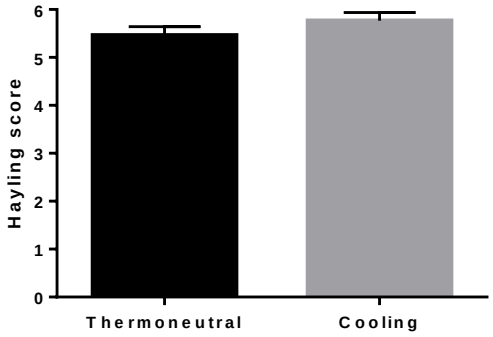

Figure 41. Effect of cooling on the Hayling test. Complete data was available on 14 participants. A paired t test showed that there was no significant difference between the two study arms (p = 0.2188).

4.4.5.2.5. Trail making test

The trail making test examines visual attention and task switching. It consists of two parts; in the first part (A) the subject is instructed to connect a set of 25 numbered dots as quickly as possible, while still maintaining accuracy. In the second part (B) the numbers are interspersed with letters. The test can provide information about visual search speed, scanning, speed of processing, mental flexibility, as well as executive functioning. While there was a trend towards higher scores in the cooling arm of the study for the second part of the test, this did not reach significance.

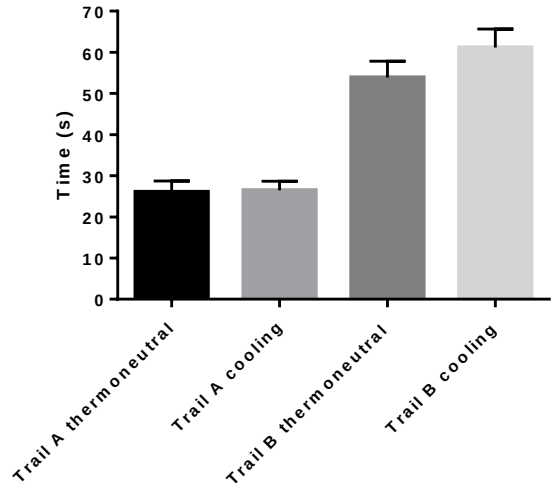

Figure 42. Effect of cooling on the trail making test. Data was available on 14 participants, and shows mean with standard error of mean. A paired t test was applied separately to both parts of the test, but it did not show significance (Trail making part A, p = 0.9035, trail making part B, p = 0.1198)

4.4.5.2.6. Rey diagram

The Rey diagram requests subjects to reproduce a complex line drawing, first by copying it freehand (recognition), and then by drawing it from memory after a time period of three minutes (recall). It tests many different elements of cognition, including visuospatial abilities, memory, attention, planning and working memory. No difference in time taken for task completion was seen for wither study arm.

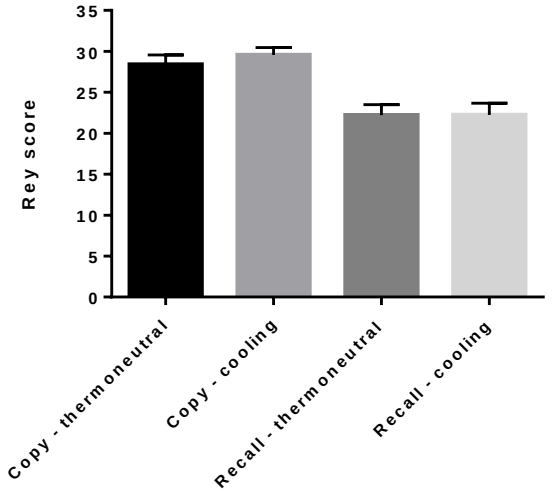

Figure 43. Effect of cooling on Rey diagram completion. Data was available on 14 subjects. No significant difference was observed between the two study arms in either the copying or recall elements of the task when a paired t test was applied ($p = 0.2025$ and $p = 0.9817$, respectively).

4.5 Discussion

The neurobiological response to cold is complex. Environmental cooling is detected by skin thermoreceptors, which signal via the lateral parabrachial nucleus to the median preoptic nucleus, which then relays via the lateral preoptic area to the dorsomedial hypothalamus. This signals via the sympathetic premotor neurons in the rostral raphe pallidus to spinal intermediolateral nucleus, to stimulate brown adipose tissue. The sympathetic response also drives peripheral vasoconstriction and piloerection to reduce heat loss. Communication with higher centres drives behavioural change to minimise heat loss. If these mechanisms are insufficient to maintain body temperature and there is continued exposure to cold then a shivering response is induced. This is a process with several stages; initially muscle tone increases, followed by sporadic muscle twitches, before rhythmic muscular contraction begins. The shivering threshold varies between individuals, and is affected by adiposity, gender, lean muscle mass and length of cold exposure. Shivering is a very energy intensive process, and any assessment of energy expenditure would therefore be uninterpretable if the shivering threshold were breached. In this study, the temperature of the cooling intervention was thus chosen to activate brown adipose tissue while avoiding shivering. To ensure that the participants did not shiver we performed an electromyogram (EMG) during the temperature intervention, which confirmed that none of the participants shivered during the intervention.

In the present study we have performed a randomised crossover trial of cooling for two hours at 16^{o}C versus two hours at thermoneutrality (25^{o}C) to explore the physiological, biochemical and neurocognitive effects of cooling. Past studies (Chen, Cypess et al. 2016) have indicated that this degree of cooling is sufficient to induce activation of brown adipose tissue in adults.

4.5.1 Evidence of cooling

Different research paradigms have been proposed for the study of cooling on humans. Environmental cooling, by decreasing the air temperature in sealed calorimetry room has been explored (Langeveld, Tan et al. 2016). They took healthy, normal weight adults (5 males, 5 females)and exposed them to either thermoneutrality (24°C) or mild cooling (18°C) for 2.5 hours after an overnight stay at thermoneutrality, measuring skin temperature, blood biochemistry, cold and hunger scores, and metabolic rate were measured every 30 minutes during the temperature intervention. They used a thermography camera to assess for possible brown adipose tissue activation in the supraclavicular fossa and the sternal area for comparison. They showed that at thermoneutrality the temperature of

both remained stable. The temperature of both areas increased in response to mild cold, and the temperature drop was greater in the sternal area than in the supraclavicular fossa. Other groups have similarly used the controlled temperature of indirect calorimetry rooms to explore the effects of mild cold. However we chose a protocol constructed by collaborators in Germany (Iwen, Backhaus et al. 2017), that had previously been shown to result in ^{18}FDG-PET-proven BAT activation.

Our study protocol was designed in accordance with the BARCIST 1.0 report (Chen, Cypess et al. 2016) written to standardise the approach to the study of BAT activation. Thus subjects were screened for recent cold exposure, fasted, wore standardised clothing under a cooling suit, and subjects were cold-exposed for two hours (BARCIST guidelines recommend minimal cold exposure of 1 hour). A fixed-temperature approach (rather than a personalised protocol where a subject is cooled to a temperature a set number of degrees above their shivering threshold) was used as the study group was standardised and not heterogeneous. It is reasonable to assume that exposure to temperatures of 16^{o}C for two hours is sufficient to activate brown adipose tissue as this similar protocols have been effective at doing so, as shown by ^{18}FDG-PET scans (van Marken Lichtenbelt, Schrauwen et al. 2002, Bredella, Fazeli et al. 2012).

Skin temperature, measured digitally by ibuttons, demonstrated that while cooling reduced peripheral skin temperature, it did not reduce the temperature of the skin overlying the supraclavicular fossa. Retrospectively, if this study could be performed again, placing the iButtons over the inter-scapular region might provide a more reliable measure of BAT activation as it is located away from major blood vessels and so may be more representative of BAT activation, rather than just core temperature. However, this approach was used as it was consistent with protocols used by other study groups who had demonstrated ^{18}FDG-PET-proven activation of BAT. Further analysis was conducted to see if this represented a central-peripheral gradient, or whether the temperature of the supraclavicular fossa was maintained over-and-above the surrounding area, which might constitute an indication of brown adipose tissue activation in this region. Whilst the recorded temperatures in the chest region were higher than those recorded peripherally, it was still significantly lower than those taken from the supraclavicular fossa. This indicates that while peripheral vasoconstriction in response to cold exposure contributes to the marked drop seen in peripheral temperatures, the supraclavicular fossa temperatures appear to be protected above those taken in the region. This may indicate heat generation from brown adipose tissue activation. Core body temperature was not affected.

This data is consistent with the findings of other study groups. Van der Lans and colleagues demonstrated that subjects exposed to either thermoneutral temperatures (25.6^{o}C) or air cooling (15.8^{o}C) for 60 minutes found that the temperature of the skin overlying the supraclavicular fossa

dropped significantly less (-0.9 ± 0.6°C) than peripheral skin temperature (-3.8°C ± 0.6°C) when measured by the same methods used here (van der Lans, Vosselman et al. 2016).

There was a wide inter-individual range of response to cooling; some subjects underwent a marked vasoconstriction on exposure to cold, whereas others did not. This limited the number of blood samples that were collected as for some subjects the vasoconstriction was so profound that it was not possible to draw blood. The reasons for this individual variation were not clear.

4.5.2 Mechanisms mediating the thermogenic response

Mitochondrial uncoupling in BAT is mediated by uncoupling protein-1 (ucp1), a 32 kDa protein expressed in the inner membrane of the mitochondria, which dissipates the proton gradient of the inner mitochondrial membrane without ADP phosphorylation. Brown adipose tissue is activated by sympathetic efferents from the rostral raphe pallidus (Cao and Morrison 2006). It is therefore reasonable to expect that participants in the cooling arm of the study will show other markers of sympathetic drive, relative to the thermoneutral arm. Mean heart rate, measure by actiheart, was not significant in the cooling arm of the study, nor were pulse rate measurements taken at 30 minute intervals during the study. Systolic blood pressure was significantly elevated in the cooling arm of the study, indicating that the cooling intervention was sufficient to increase sympathetic tone.

Studies in rodents and humans have shown that BAT thermogenesis is activated by noradrenaline and thyroid hormone, and inhibited by corticosteroids. Both noradrenaline and thyroid hormone stimulate lipolysis and increase BAT uptake of free fatty acids. Mice with triple KO of all three B adrenoceptors have defective cold-induced BAT thermogenesis (Jimenez, Leger et al. 2002). Hypothyroid mammals may develop hypothermia because they are resistant to noradrenaline-induction of BAT thermogenesis.

Disruption of the *Dio2* (*dio2-/-),* the gene encoding the thioredoxin-fold-containing selenoenzyme that converts the prohormone thyroxine to the active hormone tri-iodothyronine, results in brown-adipose-specific hypothyroidism, in an otherwise euthyroid animal. Cold exposure in these animals results in hyperadrenergic stimulation of BAT, resulting in increased lipolysis, and expression of ucp-1 and PPAR-γ mRNA. This exaggerated response suppresses the stimulation of BAT lipogenesis that is normally seen after 24-48h in mice. The availability of free fatty acids is therefore rapidly exhausted, and impairs the thermogenic response of BAT (Fonseca, Werneck-De-Castro et al. 2014) . Thyroid hormone signalling, and in particular induction of deiodinase 2 enzymes, additionally play a central

role in BAT adipogenesis in vitro, and BAT development in mouse embryos (Bianco AC, Lancet Diabetes Endocrinol, 2013).

Expression of *Dio 2* is dependent on cAMP. Thus BAT stimulation with noradrenaline creates a state of localised thyrotoxicosis within brown adipocytes. Saturation of thyroid hormone receptors with T3 results in *Ucp-1* induction (Lee, Takahashi et al. 2012). Therefore on cold stimulation it might be anticipated that there would be an increase in noradrenaline-mediated sympathetic drive, with resulting deiodinase 2 stimulated conversion of T4 to T3. No significant effects on thyroid hormone levels were observed.

4.5.3 Cooling and the stress response

On cooling, there was no significant difference in pulse rate between the two study arms, but systolic blood pressure was significantly increased in the cooling arm of the study. This is consistent with an increase in sympathetic drive, and previously published literature on cooling.

The interplay between the acute and chronic stress response is complex and has significant inter-individual variability. The central sympathetic nervous system comprises of catecholaminergic, norephinephrine-synthesizing cell groups in the pons and medulla and the locus coeruleus. These form a complex stimulatory and inhibitory network with multiple sites of interaction with the CRH neurons located in the paraventricular nucleus of the hypothalamus. CRH secretion is stimulated by the action of norepinephrine on the a1-noradrenergic receptors. There are also autoregulatory negative feedback loops that exist in both the PVN, CRH and brainstem catecholaminergic neurons, which inhibit the corresponding presynaptic CRH and a2-noradrenergic receptors. Additionally there are multiple regulatory inputs from the seratonergic and cholinergic system, inhibitory input from the GABA/BDZ system and the opioid neuronal system of the brain. Glucocorticoids also have an inhibitory effect (Herman 2018). Secretion of CRH results in the breakdown of POMC, releasing ACTH which subsequently releases cortisol from the adrenal glands. Additionally B endorphin is released, resulting in an analgesic effect, and AVP is released, further contributing to blood pressure effects. One of the key net outputs of activation of the stress response is to stimulate an adaptive redirection of energy, with increased gluconeogenesis and lipolysis to mobilise fuel stores to allow for a 'fight or flight' response. Thus the characteristic tightly controlled pulsatile release of CRH is disrupted by stress; during acute stress the amplitude and synchronicity of both CRH and AVP increase. Glucocorticoids are the final hormone effectors of the HPA axis. The inactive glucocorticoid receptor resides in the cytosol as a hetero-oligomer with heat shock proteins. Upon ligand binding the receptors dissociate and homodimerise, translocating to the nucleus where they interact with specific glucocorticoid response elements of the DNA to transactivate or repress target genes (Savory, Prefontaine et al. 2001). Most adverse effects are mediated by transactivation, whereas transrepression is thought to control many of the anti-inflammatory effects of glucocorticoids via suppression of inflammatory pathways e.g. AP-1, NF-kB. Glucocorticoids have a negative feedback effect on both CRH and ACTH secretion.

Physiological stress results in a peak cortisol response by 120 minutes. We might therefore expect an increase in serum cortisol levels in the cooling arm of the study relative to the thermoneutral arm.

However, this was not observed, and while there was a downward trend for cortisol in the cooling intervention, there was no significant difference between the two study arms.

4.5.4 Effect of cooling on glucose, insulin and glucagon

An increase in sympathetic drive results in a mobilisation of fuel reserves to allow for a "fight or flight" response. It might therefore be expected that cooling results an initial increase in glucagon to liberate glucose from glycogen, and that insulin is suppressed. However, no significant difference was observed between the study arms for these measures. This may reflect the timing of the samples: the described response is an acute one, taking place in the initial minutes following exposure to a stressor. Glucose and glycogen samples were taken before, and 120 minutes after initiation of cooling, and the first insulin samples were taken at 30 minutes.

4.5.5. Leptin

Cooling is known to reduce *ob* gene expression in the white adipose tissue on mice (Trayhurn P, Biochem J, 1995) and there is limited data to suggest that cooling also reduces circulating leptin levels in humans (Ricci, Fried et al. 2000). Reducing the amount of circulating leptin in effect creates a state of partial leptin deficiency. We confirmed these findings in this study, and a significant percentage reduction in leptin was seen in the cooling arm of the study. This is intriguing, and may indicate that leptin is a master regulator of response to energy deficit, irrespective of cause.

4.5.6. Energy expenditure and respiratory quotient

Reductions in circulating leptin have a powerful orexigenic effect. Leptin is additionally known to drive thermogenesis and energy expenditure via its action on PrRP-containing neurons in the dorsomedial hypothalamus (Dodd, Worth et al. 2014). It is reasonable to hypothesise that cooling will therefore lower circulating leptin levels, resulting in an increase in hunger and a reduction in energy expenditure. However, acting contrary to this is the effect of brown adipose tissue activation on energy expenditure. The net effect we observed was an increase in basal metabolic rate with the cooling intervention.

Respiratory quotient is calculated by the volume of carbon dioxide eliminated divided by the amount of oxygen consumed. It provides a measure of substrate utilisation; a respiratory quotient of 1 indicates a carbohydrate energy source, whereas a respiratory quotient of 0.7 indicates a fat source. The mean respiratory quotient found in the thermoneutral arm of the study was significantly higher than in the cooling arm (0.78 and 0.75, respectively). This is in keeping with an increase in fat utilisation in the cooling arm of the study and is in keeping with published literature on substrate utilisation in cooling (Cannon and Nedergaard 2004).

4.5.7. Food intake and fat preference

Impairment of leptin-melanocortin drives a preference for high fat food an avoidance of high sucrose food (van der Klaauw, Keogh et al. 2016). We therefore hypothesised that cooling, a state of partial leptin deficiency, would result in an increased preference for high fat food. Whilst we did not observe any significant differences in visual analogue scales assessing “liking” of high, medium or low fat food, we did see a significant increase in the amount of high fat food consumed in the cooling arm of the study. This is in keeping with our previous findings of fat preference in patients with MC4R mutations and further corroborates the importance of leptin-melanocortin circuitry in fat preference. In future studies it would be interesting to see if there was a decrease in the amount of high sucrose food in a sucrose-preference test after cooling, as this is also reduced in patients with MC4R mutations.

Brain-derived neurotrophic factor (BDNF) is a protein that acts to support the maintenance and survival of existing neurons and encourages the growth and differentiation of new neurons. It is active in brain areas associated with memory and neurocognition, including the hippocampus, basal forebrain and cortex. It is upregulated exercise and fasting (Szuhany, Bugatti et al. 2015) and central administration of BDNF reduces food intake, leptin and insulin levels and decreases fat mass (Noble,

Billington et al. 2011). We did not find a statistically significant difference in BDNF between the two study arms. It would be interesting to investigate this in a larger study sample as this might provide an interesting mechanistic insight into the links between negative energy balance and neurocognition.

4.5.8. Cooling results in an improvement in attention on neurocognitive testing

Prior to the administration of the neurocognitive tests there was an increase in the subject's perception of anxiety on the visual analogue scale score. This could be in keeping with the increase in sympathetic tone previously described.

There was a significant improvement in both the verbal fluency and digit span tests after the subjects had been cooled. Both these tests assess executive control, with the verbal fluency additionally assessing verbal ability, and the digit span short term and working memory. There was no difference between the two study arms in the RAVLT, Hayling, trail-making or Rey diagram tests. In some cases, for instance with the RAVLT test, this may be because most of the subjects scored highly, and the test was therefore not discriminating. The Hayling test is a test of response initiation and suppression (a frontal lobe function), and there seemed to be no effect of cooling on these functions, nor on the visuospatial skills required for the Rey diagram completion. With the trail making test there was a trend towards improvement in the second part of the study, which tests mental flexibility and executive function. It may be that this is within the variation that may normally be seen within testing, or that the trend shows that the study is underpowered.

Whether the improvements seen represent a genuine improvement in some elements of neurocognition, or whether they simply represent an increase in attention due to the increased sympathetic drive is not possible to deduce from these data.

4.6. Conclusions

Here we present data illustrating the physiological effects of mild cooling on humans. We confirm, in keeping with previous studies, that cooling results in an increase in sympathetic drive, and that skin temperature overlying BAT deposits is maintained, relative to skin temperature in other regions. We confirm that cooling increases energy expenditure and reduces respiratory quotient, driving substrate utilisation towards fat. Collectively it is probable that these data represent activation of brown adipose tissue, and similar paradigms have shown ^{18}-FDG-PET confirmed confirmation of this.

We show that cooling results in significant reductions in circulating leptin levels with a resulting increase in fat preference. This is important as it provides evidence of leptin acting as a central regulator of cooling-induced energy deficit. There was no statistically significant difference between the cooling and thermoneutral interventions in BDNF concentration. It would be interesting to explore the effects of cooling on BDNF in a larger data set as this could provide an enticing explanation for our leptin data.

We have shown that some neurocognitive tests improve with cooling, and did not show any evidence of torpor. It is not possible to discriminate whether these improvements were secondary to an increase in sympathetic drive, or due to a genuine alteration in neurocognition.

CHAPTER FIVE: THE EFFECTS OF COOLING ON THE METABOLOMIC PROFILE OF HEALTHY MEN

5.1. Summary

We conducted a randomised cross over trial of two hours of cooling (16^{o}C) versus two hours at thermoneutrality (25^{o}C) to investigate the metabolic effects of mild cold exposure on human physiology. The cooling temperature was chosen as existing literature indicated that this would be sufficient to result in brown adipose tissue activation, without inducing shivering. We were interested in exploring the effects of cold exposure on substrate utilisation and in comparing this data to that obtained during caloric restriction. We hypothesised that the response to calorie deficit, whether from cold exposure or secondary to caloric restriction, is regulated by central leptin-mediated mechanisms and sought to employ a metabolomics approach to address this question.

Metabolomics, the measurement of hundreds of small molecule metabolites, their precursors, derivatives, and degradation products, has emerged as a useful tool for the study of physiology and disease. We used liquid chromatography-tandem mass spectrometry (LC-MS) methods to characterize changes in carbohydrates, lipids, amino acids, and steroids in eight normal weight heathy men at baseline, every 30 minutes during a temperature intervention, and one hour after cessation of the temperature intervention. We compared the metabolomics profiles of subjects in the two temperature intervention study arms (thermoneutral at 25^{o}C versus cooling at 16^{o}C).

We found that the differences between participants were greater than any change caused by the temperature intervention. We therefore took a paired intra-individual approach to analysis to look for cooling-triggered metabolomics changes. One key finding was that lysophosphatidylethanolamines, lipids that are derived from the plasma membrane increased in the cooling arm of the study suggesting an increase in lipid turnover. Additionally an increase in the fatty acid (22:6), docosahexaenoic acid, was seen. This is an arachidonic acid-derived omega-3 polyunsaturated fatty acid, which is associated with a neuroprotective effect (Kim 2014). This finding is of particular interest, given the RBM-3 mediated link between cooling and neuroprotection and the improvements in cognitive function observed in the data presented in Chapter 4. Further studies with larger sample sizes will be needed to test this hypothesis more fully.

5.2. Introduction

Cold exposure has been shown to activate brown adipose tissue in adult humans (Cypess, Lehman et al. 2009), resulting in increased insulin sensitivity and an increase in lipid metabolism. In lean healthy humans acute cold-induced BAT activation has been associated with elevated appearance rates of free fatty acids (Locke, Kahali et al. 2015) from the lipolysis of white adipose tissue (WAT) and increased uptake of free fatty acids into BAT depots (Ouellet, Labbe et al. 2012, Blondin, Tingelstad et al. 2017). Furthermore, prolonged cold exposure (5-8 hours) increased whole-body lipolysis, FFA cycling and FFA oxidation in obese human males (Chondronikola, Volpi et al. 2016). Collectively these studies indicate that BAT activation signals to the white adipose tissue to trigger mobilisation of energy substrates via lipolysis and β-oxidation of FFA. Non-shivering thermogenesis predominantly utilises free fatty acids, with low levels of glucose use, mainly utilised for the synthesis of glycerol-3-phosphate and triglycerides, and *de novo* synthesis of free fatty acids (Cannon and Nedergaard 2004, Virtanen, Lidell et al. 2009). Cumulatively these observations are likely to explain improvements in lipid metabolism and insulin sensitivity that have been observed in clinical studies (Festuccia, Blanchard et al. 2011, Ouellet, Labbe et al. 2012, Chondronikola, Volpi et al. 2016).

However, to date, the detailed biochemical mechanisms that mediate the effects of cold-induced BAT activation are not fully understood.

We have collaborated with our colleague Prof. Sebastian Schmid and his team (University of Lubeck) for the design of this study. His team have demonstrated that acute cold exposure increases the expression of selected genes involved in lipolysis and FA-oxidation measured in human peripheral blood using a similar paradigm and an identical water-perfused suit. They additionally performed Botnia clamps (an intravenous oral glucose tolerance test followed by a euglycaemic, hyperinsulinaemic clamp) to determine whole body glucose utilisation and insulin sensitivity in cooling relative to thermoneutrality. Furthermore they demonstrated ^{18}-FDG-PET proven brown adipose tissue activation in two participants undergoing this protocol (under review).

Metabolomics, the systematic study of small-molecule products of biochemical pathways by mass spectrometry, has offered a sensitive technique to allow new insights into the dynamics of metabolism, and has proved a useful technique to dissect out the effects on molecular pathways caused by a specific perturbation. The metabolomic profile at a given time point represents the cumulative effects of the diet, genome, transcriptome, proteome, and gut microbiome–host interaction on small molecule metabolites whose concentrations change rapidly (Guo, Milburn et al. 2015). This has allowed new methods to predict, diagnose and discover several metabolic disorders.

Metabolomics has shown that elevated levels of specific branched-chain amino acids (isoleucine, leucine, valine) are strongly associated with the development of type 2 diabetes mellitus, and that prediction of progression to disease could be made on the basis of elevations in a combination of these amino acids, with a fivefold increase in risk for subjects with values in the top quartile (Wang, Larson et al. 2011). A systematic review of metabolomics studies in obese children identified changes in amino acid metabolism that were associated with obesity. They also found increases in branched chain amino acids, aromatic amino acids and acylcarnitines were predictors of insulin resistance (Zhao, Gang et al. 2016). We were interested in exploring the effects of cooling on the metabolomic profile of lipids and amino acids in fasting healthy young men with cold-activated brown adipose tissue, relative to thermoneutral conditions.

Metabolomics has been previously used to define a unique profile associated with acute calorie restriction (participants received 10% of total daily energy requirement for 48 hours), which highlighted the expected shift from carbohydrate to fat metabolism, with an increase in lipolysis and β-oxidation of fatty acids (Collet, Sonoyama et al. 2017). There was decrease in specific antioxidants (plasmalogen phosphatidylethanolamines) and an increase in branched chain amino acids and dehydroxyepiandrosterone sulphate. As caloric restriction and cold exposure both result in a net calorie deficit, we were interested in comparing the results of these two studies, to test if there were common metabolic processes involved.

We performed a carefully controlled experimental study to directly examine the effects of cold exposure in eight normal weight young men housed in a clinical research facility where diet, fluid intake, timing of meals, and sleep were precisely controlled and standardised. Fasting blood samples were obtained at the following time points: baseline (after an overnight fast), 30, 60, 90 and 120 minutes into the temperature intervention, and 1 hour after cessation of the temperature intervention. We used a high throughput IDQP180 Biocrates panel for our metabolomics assay employing using liquid chromatography-tandem mass spectrometry methods to measure small molecule metabolites involved in carbohydrate, fat, protein, and steroid metabolism. Additional lipid measurements were made by an in-house assay. By measuring the metabolome in the same individuals during two study arms which were identical, with the exception of the temperature intervention, our aim was to identify the metabolites that change significantly with cooling. Both study arms are performed after an overnight fast as food given prior to the temperature interventions would have made the results difficult to interpret.

5.3. Methods

From the 15 participants who undertook the complete study protocol, eight subjects were identified where samples across all time points were of sufficient quality with no haemolysis to perform metabolomics. These samples were taken forward for analysis. The AbsoluteIDQ® Biocrates p180 Kit (Biocrates Life Sciences AG, Innsbruck, Austria).was used to measure 175 metabolites across six compound classes (hexoses, amino acids, biogenic amines, acylcarnitines, glycerophospholipids and sphingolipids). Additional analysis of lipid samples were conducted on an in-house assay by the NIHR BRC metabolomics and lipidomics facility. Blood samples from 8 individuals were taken at baseline (Tn60), 30 minutes, 60 minutes, 90 minutes, and 120 minutes after the start of (Ti30, Ti60, Ti90 and Ti120, respectively), and 60 minutes after the end of the intervention (Group A = thermoneutral condition; Group B = cooling condition). Metabolomic measurements for all the above samples were performed at the Department of Biochemistry, the University of Cambridge, using AbsoluteIDQ® Biocrates p180 Kit (Biocrates Life Sciences AG, Innsbruck, Austria) (Amino Acid panel). An additional in-house lipid panel was performed that had been developed using a method for open profiling of lipids by DIHRMS (Han and Gross 2003, Graessler, Schwudke et al. 2009). The relative quantity of metabolites was obtained by normalization of the metabolite signal intensity to that of an internal standard. The combined results comprised: 20 amino acids, 24 amino acid derivatives, 13 cholesteryl esters (Locke, Kahali et al.), 16 ceramides (Cer), 14 diacylglycerols (DAGs), 2 monoacylglycerols (MAGs), 30 free fatty acids (FFAs), 5 fatty acid ester of hydroxyl fatty acids (FAHFAs), 48 lysoglycerophospholipids, 201 glycerophopholipids, 42 sphingomyelins, and 70 triacylglycerols (TAGs). The metabolites of Tp60 from one individual (CS001192) in thermoneutral condition (Group A) were haemolysed and unable to be processed as were the metabolites in lipid panel in Tp60 from another individual (CS01176). They were therefore excluded from the relevant analyses. The other missing values were imputed by replacing them by half of the minimum positive value in the original date in each metabolite.

5.4. Results

Cluster analysis was performed separately for the metabolites in the two panels (Amino Acid panel and Lipid panel) from the two conditions (Group A and B), based on the Euclidean distance, where each sample is a vector with all of the metabolite values, using the online software, Metaboanalyst (http://www.metaboanalyst.ca/faces/home.xhtml). In all four time-group combinations, the samples from the same individuals tended to cluster together regardless of the time-points (Figure 44), suggesting that the inter-personal differences were greater than the impact of the intervention.

5.4.1. Hierarchical clustering of the metabolome across participants

We first examined large scale changes across the samples in the study. Hierarchical clustering of metabolomics data was performed using Metabolanalyst, an online program that ascribes each sample a vector value and clusters samples based on Euclidean distance. The samples are then grouped based on their similarity, generating a heat map. From this analysis we can see that samples largely cluster according to participant, and not intervention. This indicates that the difference between participants was greater that the any difference caused by the intervention (figure 44).

A.

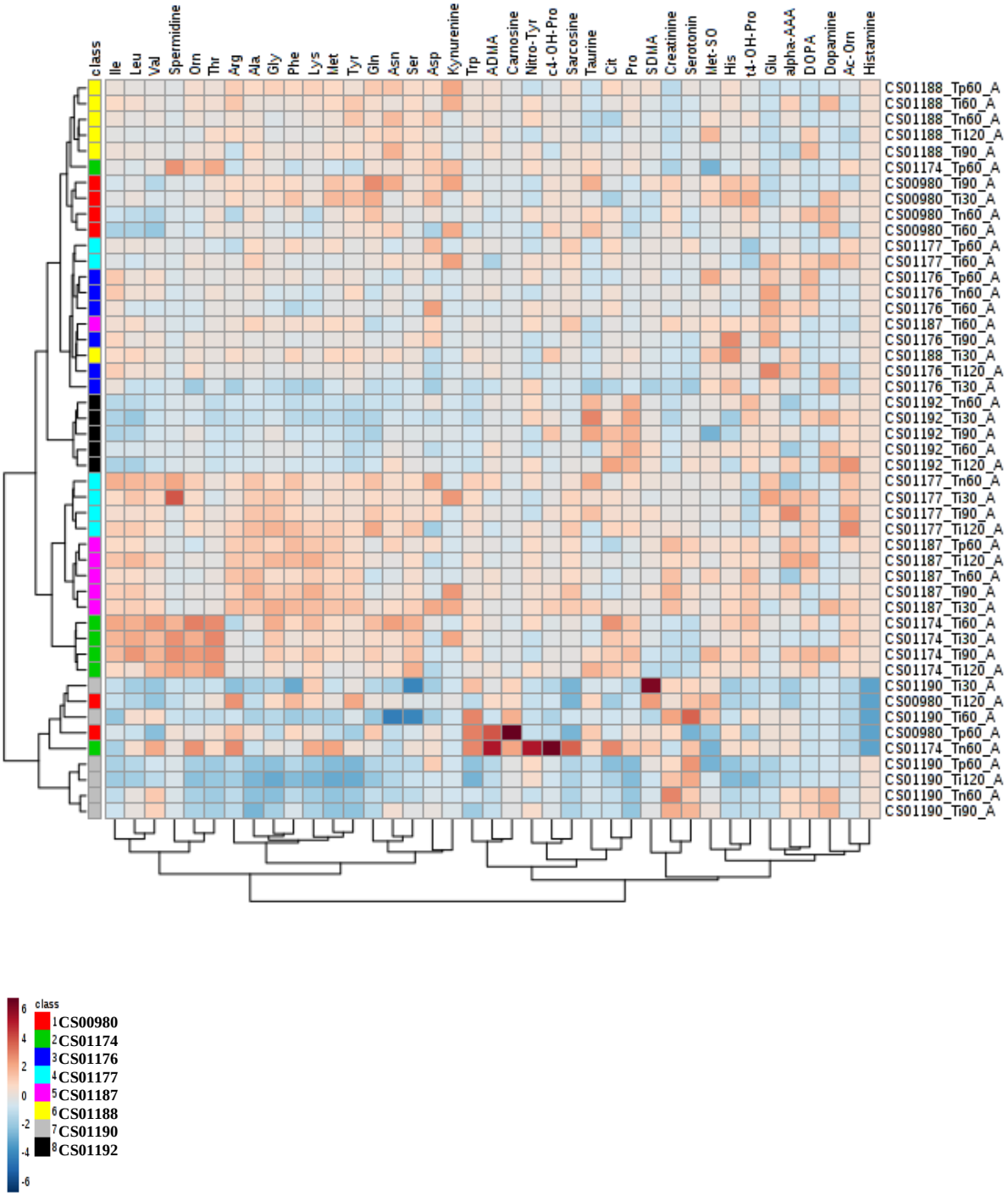
class
Ile
Leu
Val
Spermidine
Orn
Thr
Arg
Ala
Gly
Phe
Lys
Met
Tyr
Gln
Asn
Ser
Asp
Kynurenine
Trp
ADMA
Carnosine
Nitro-Tyr
c4-OH-Pro
Sarcosine
Taurine
Cit
Pro
SDMA
Creatinine
Serotonin
Met-SO
His
t4-OH-Pro
Glu
alpha-AAA
DOPA
Dopamine
Ac-Orn
Histamine
CS01188_Tp60_A
CS01188_Ti60_A
CS01188_Tn60_A
CS01188_Ti120_A
CS01188_Ti90_A
CS01174_Tp60_A
CS00980_Ti90_A
CS00980_Ti30_A
CS00980_Tn60_A
CS00980_Ti60_A
CS01177_Tp60_A
CS01177_Ti60_A
CS01176_Tp60_A
CS01176_Tn60_A
CS01176_Ti60_A
CS01187_Ti60_A
CS01176_Ti90_A
CS01188_Ti30_A
CS01176_Ti120_A
CS01176_Ti30_A
CS01192_Tn60_A
CS01192_Ti30_A
CS01192_Ti90_A
CS01192_Ti60_A
CS01192_Ti120_A
CS01177_Tn60_A
CS01177_Ti30_A
CS01177_Ti90_A
CS01177_Ti120_A
CS01187_Tp60_A
CS01187_Ti120_A
CS01187_Tn60_A
CS01187_Ti90_A
CS01187_Ti30_A
CS01174_Ti60_A
CS01174_Ti30_A
CS01174_Ti90_A
CS01174_Ti120_A
CS01190_Ti30_A
CS00980_Ti120_A
CS01190_Ti60_A
CS00980_Tp60_A
CS01174_Tn60_A
CS01190_Tp60_A
CS01190_Ti120_A
CS01190_Tn60_A
CS01190_Ti90_A
6
4
2
0
-2
-4
-6
class
1 CS00980
2 CS01174
3 CS01176
4 CS01177
5 CS01187
6 CS01188
7 CS01190
8 CS01192

B.

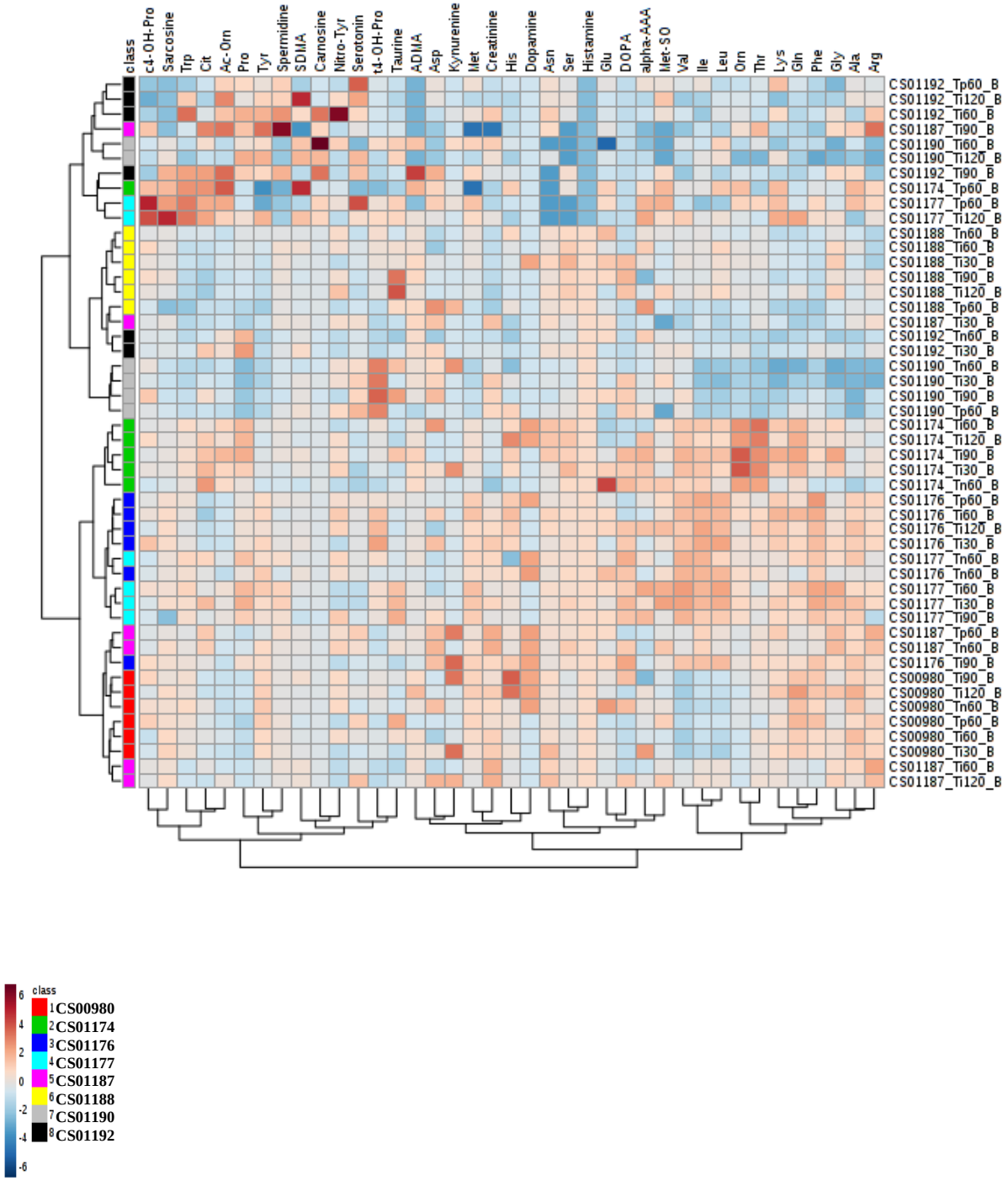
class
c4-OH-Pro
Sarcosine
Trp
Cit
Ac-Orn
Pro
Tyr
Spermidine
SDMA
Carnosine
Nitro-Tyr
Serotonin
t4-OH-Pro
Taurine
ADMA
Asp
Kynurenine
Met
Creatinine
His
Dopamine
Asn
Ser
Histamine
Glu
DOPA
alpha-AAA
Met-SO
Val
Ile
Leu
Orn
Thr
Lys
Gln
Phe
Gly
Ala
Arg
CS01192_Tp60_B
CS01192_Ti120_B
CS01192_Ti60_B
CS01187_Ti90_B
CS01190_Ti60_B
CS01190_Ti120_B
CS01192_Ti90_B
CS01174_Tp60_B
CS01177_Tp60_B
CS01177_Ti120_B
CS01188_Tn60_B
CS01188_Ti60_B
CS01188_Ti30_B
CS01188_Ti90_B
CS01188_Ti120_B
CS01188_Tp60_B
CS01187_Ti30_B
CS01192_Tn60_B
CS01192_Ti30_B
CS01190_Tn60_B
CS01190_Ti30_B
CS01190_Ti90_B
CS01190_Tp60_B
CS01174_Ti60_B
CS01174_Ti120_B
CS01174_Ti90_B
CS01174_Ti30_B
CS01174_Tn60_B
CS01176_Tp60_B
CS01176_Ti60_B
CS01176_Ti120_B
CS01176_Ti30_B
CS01177_Tn60_B
CS01176_Tn60_B
CS01177_Ti60_B
CS01177_Ti30_B
CS01177_Ti90_B
CS01187_Tp60_B
CS01187_Tn60_B
CS01176_Ti90_B
CS00980_Ti90_B
CS00980_Ti120_B
CS00980_Tn60_B
CS00980_Tp60_B
CS00980_Ti60_B
CS00980_Ti30_B
CS01187_Ti60_B
CS01187_Ti120_B
6
4
2
0
-2
-4
-6
class
1 CS00980
2 CS01174
3 CS01176
4 CS01177
5 CS01187
6 CS01188
7 CS01190
8 CS01192

C.

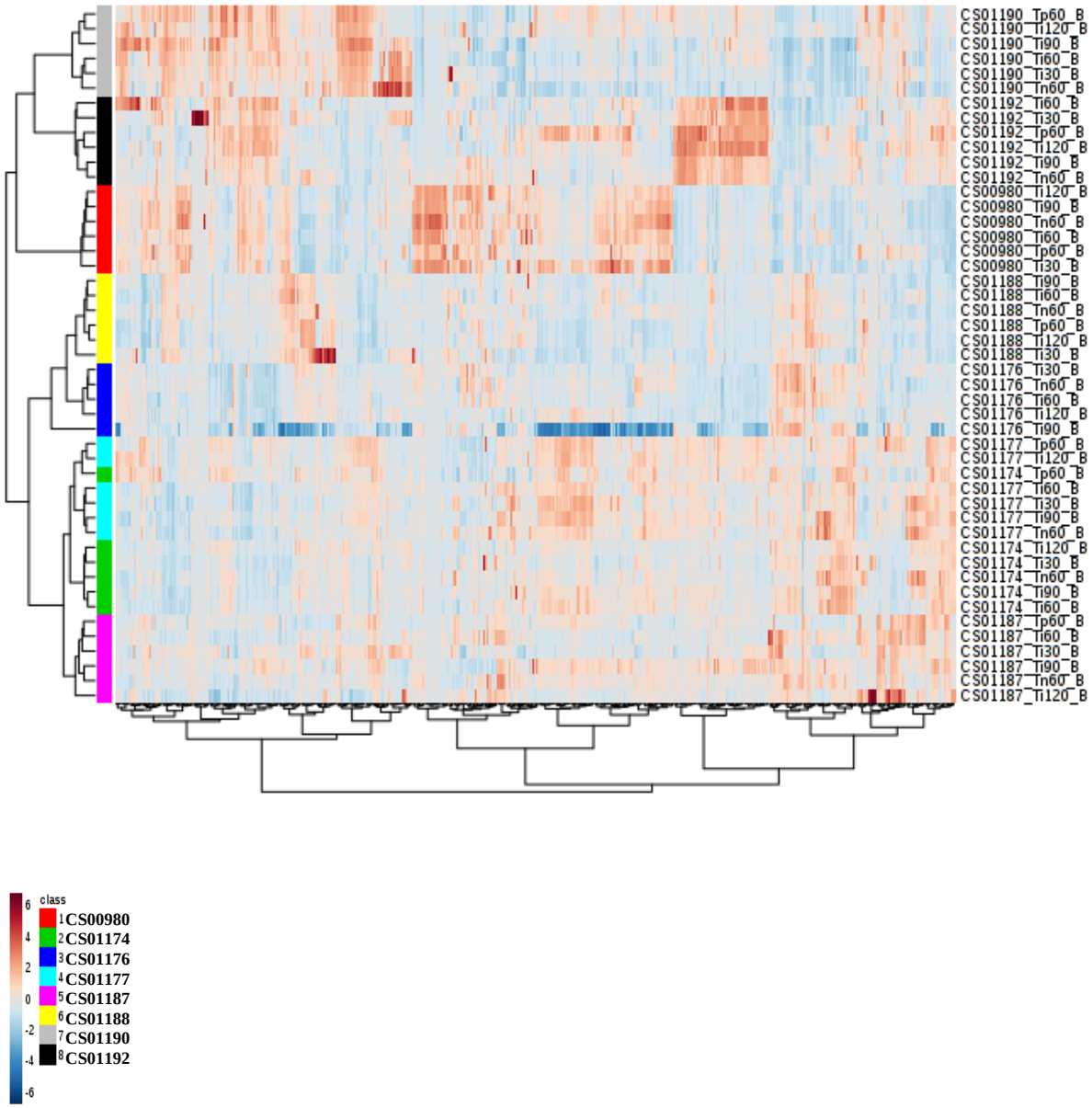
CS01190_Tp60_B
CS01190_Ti120_B
CS01190_Ti90_B
CS01190_Ti60_B
CS01190_Ti30_B
CS01190_Tn60_B
CS01192_Ti60_B
CS01192_Ti30_B
CS01192_Tp60_B
CS01192_Ti120_B
CS01192_Ti90_B
CS01192_Tn60_B
CS00980_Ti120_B
CS00980_Ti90_B
CS00980_Tn60_B
CS00980_Ti60_B
CS00980_Tp60_B
CS00980_Ti30_B
CS01188_Ti90_B
CS01188_Ti60_B
CS01188_Tn60_B
CS01188_Tp60_B
CS01188_Ti120_B
CS01188_Ti30_B
CS01176_Ti30_B
CS01176_Tn60_B
CS01176_Ti60_B
CS01176_Ti120_B
CS01176_Ti90_B
CS01177_Tp60_B
CS01177_Ti120_B
CS01174_Tp60_B
CS01177_Ti60_B
CS01177_Ti30_B
CS01177_Ti90_B
CS01177_Tn60_B
CS01174_Ti120_B
CS01174_Ti30_B
CS01174_Tn60_B
CS01174_Ti90_B
CS01174_Ti60_B
CS01187_Tp60_B
CS01187_Ti60_B
CS01187_Ti30_B
CS01187_Ti90_B
CS01187_Tn60_B
CS01187_Ti120_B
6
4
2
0
-2
-4
-6
class
1 CS00980
2 CS01174
3 CS01176
4 CS01177
5 CS01187
6 CS01188
7 CS01190
8 CS01192

D.

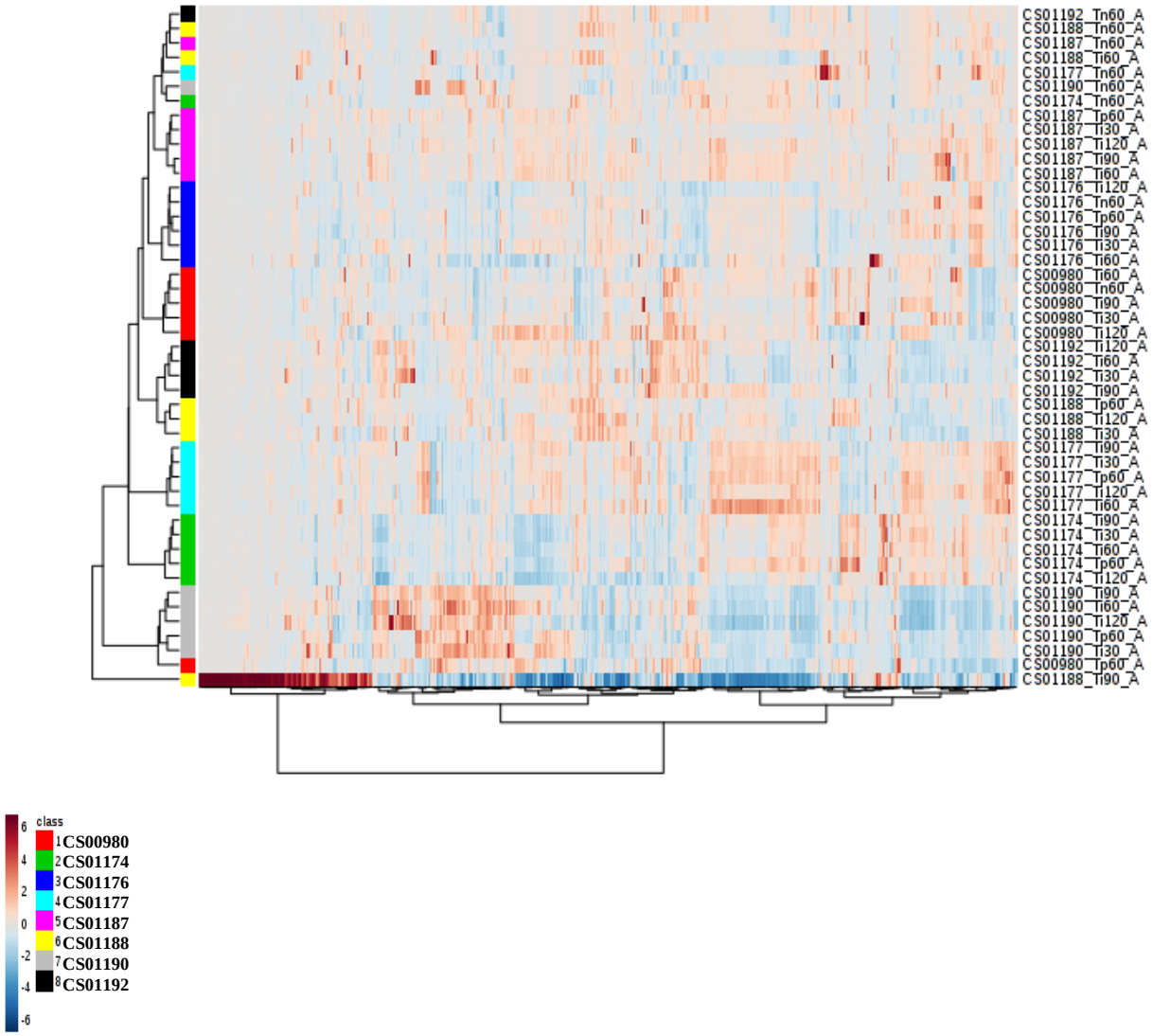

Figure 44. A heat map derived from hierarchical clustering of the metabolomic data. Clustering was performed using complete linkage and Euclidean distance, where each sample is a vector with all of the metabolite values. The colour scale correlates with relative metabolite abundance across the samples: the white indicates median value, red an elevation above the median, and blue a decrease below the median. These panels were created using Metaboanalyst, a program to order the samples based on their similarity to each other. Figures (a) and (b) show the results of the amino acid panel in the thermoneutral arm and cooling arm of the study, respectively. Figures (c) and (d) show the results of the lipid panel in the thermoneutral and cooling study arms, respectively. The patient's unique identifier, time point and study arm (A, thermoneutral; B, cooling) are listed on the right.

5.4.2. Large scale changes with cooling intervention across participants

Amino acid and lipid changes were analysed separately as there is established software available for pathway analysis of amino acid data (KEGG), whereas the analysis of lipidomic data is less standardised.

5.4.2.1. Cooling-induced changes in amino acids

The AbsoluteIDQ® Biocrates p180 Kit measures 21 amino acids and 21 biogenic amines. A full list of metabolites is provided by Biocrates (http://www.biocrates.com/products/research-products/absoluteidq-p180-kit).

Using KEGG pathway analysis, the data on amino acids measured during the thermoneutral and cooling arms of the study were compared. This analysis revealed that whilst for some participants the cooling intervention resulted in changes to specific metabolites, these were not consistent and did not reach statistical significance after Benjamini-Hochberg correction.

However, general trends in the data were observed. When compared to the thermoneutral arm of the study the cooling arm was enriched for increases in nitrogen, arginine and proline metabolism. Additionally there were increases in aminoacyl tRNA synthesis. These are enzymes that attach the appropriate amino acid onto the tRNA strand by catalyzing the esterification of a specific cognate amino acid or its precursor to one of all its compatible cognate tRNAs to form an aminoacyl-tRNA. Collectively these results indicate an increase in protein synthesis in the cooling arm of the study (Figure 45).

Directly comparing the metabolomics data from the cooling study to the previously performed caloric restriction study (Collet, Sonoyama et al. 2017) is challenging, as the effect size of the cooling intervention was much smaller than that of the caloric restriction. Additionally, the sampling time points of the two studies were very different, which is a significant limitation when trying to understand the complexities of such a dynamic process. However, taking into account these limitations, we can make some observations. In the caloric restriction study there was an increase in the glucogenic amino acids. In the cooling study these were not universally elevated; in common with calorie restriction cooling caused an increase in alanine. The other glucogenic amino acids did not increase in the cooling study, and glutamate and serine paradoxically decreased. The ketogenic branched chain amino acid leucine increased in both, whereas isoleucine, which increased with caloric

restriction did not change during cooling. These findings suggest that, in line with data in animals (Blouet, Jo et al. 2009), leucine is the most sensitive marker of negative energy balance.

Changes were also seen in other amino acid breakdown products (figure 45). Histamine, a biogenic amine derived from the breakdown of histidine plays a pivotal role in the acute allergic response, and in chronic inflammatory reactive diseases such as asthma. It was reduced in the cooling arm of the study, but did not change in the thermoneutral arm. The relevance of this finding is unclear but central histaminergic signalling is known to play a role in energy homeostasis.

Serotonin is a tryptophan-derived monoamine neurotransmitter. Approximately 90% of the body's serotonin is found in the enterochromaffin cells of the gastrointestinal tract where it plays a key role in gut motility. Additionally it has important central roles in regulation of mood, appetite and sleep. Increases in serotonin were seen on cooling. Further studies will be needed to investigate this finding.

A

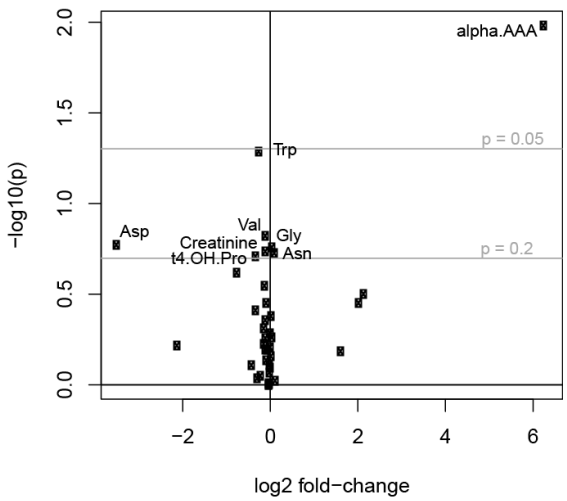
Arm A: Ti120 vs Tn60
alpha.AAA
Trp
p = 0.05
Asp
Val
Gly
Creatinine
Asn
t4.OH.Pro
p = 0.2
−log10(p)
log2 fold−change

B

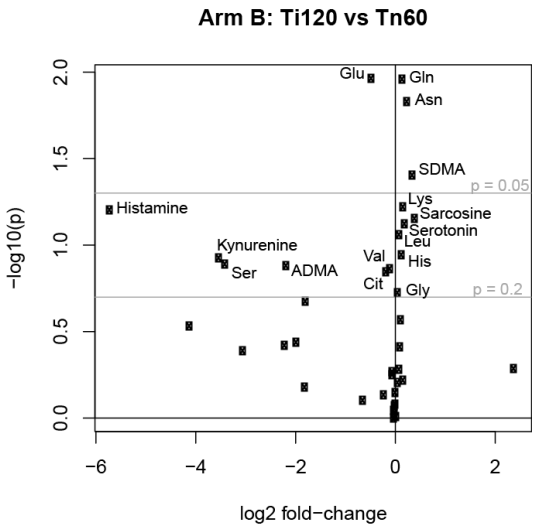
Arm B: Ti120 vs Tn60
Glu
Gln
Asn
SDMA
p = 0.05
Histamine
Lys
Sarcosine
Serotonin
Leu
Kynurenine
Ser
ADMA
Val
His
Cit
Gly
p = 0.2
−log10(p)
log2 fold−change

C

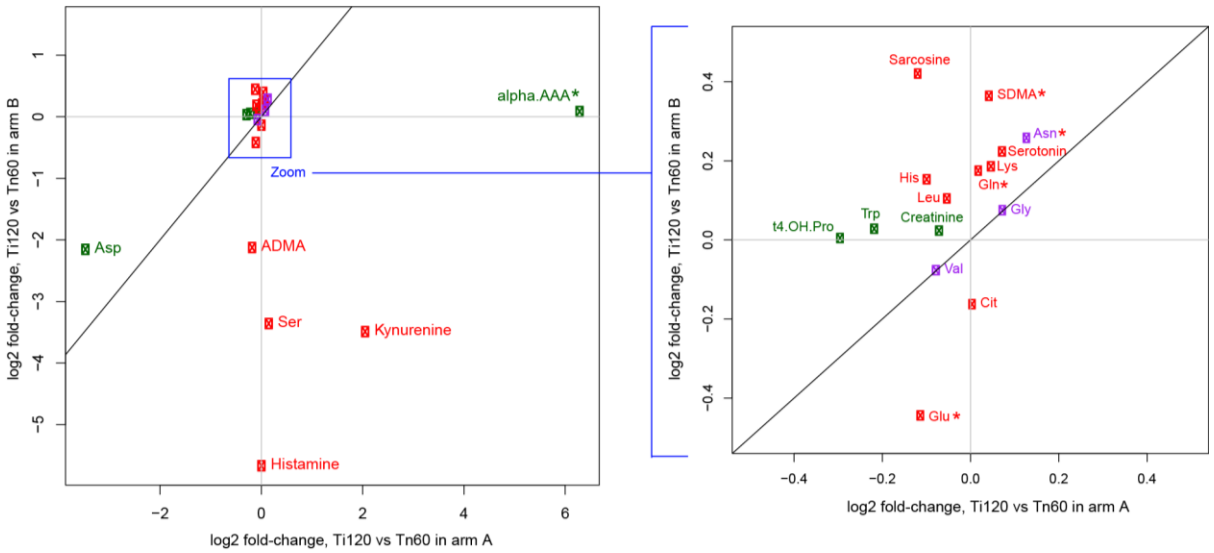
alpha.AAA*
Zoom
Asp
ADMA
Ser
Kynurenine
Histamine
log2 fold-change, Ti120 vs Tn60 in arm B
log2 fold-change, Ti120 vs Tn60 in arm A
Sarcosine
SDMA*
Asn*
Serotonin
Lys
His
Gln*
Leu
Gly
Trp
Creatinine
t4.OH.Pro
Val
Cit
Glu*

D

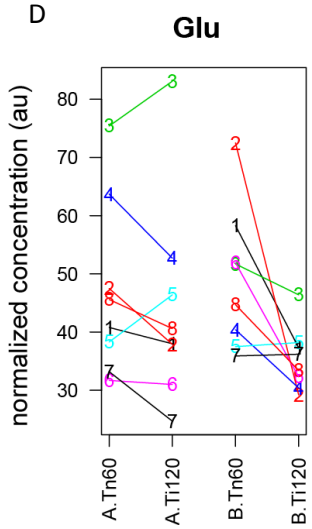
Glu
normalized concentration (au)
A.Tn60
A.Ti120
B.Tn60
B.Ti120

E

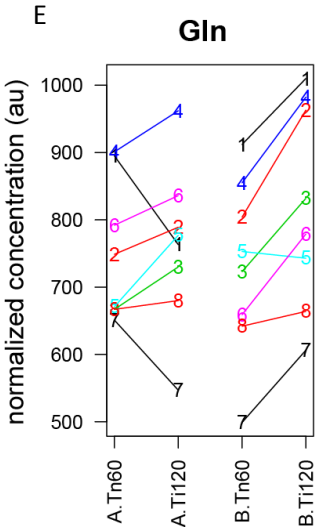
Gln
normalized concentration (au)
A.Tn60
A.Ti120
B.Tn60
B.Ti120

Figure 45. Differential concentrations of amino acids & derivatives. Ti120 vs Tn60 within each arm. LIMMA, a program that was devised to fit linear models to microarray data, was used to fit a linear model (~subjectID+{A.Tn60, A. Ti120, B.Tn60, B.Ti120}) and two different contrasts inspected: (A.Ti120 vs A.Tn60) and (B.Ti120 vs B.Tn60); *see Methods*.

A. Volcano plot for arm A; **B.** Volcano plot for arm B; **C.** For species with (Locke, Kahali et al.) p<0.2, the fold-change within A is compared to the fold-change within B. (Left: the largest fold-changes are driven by 0's in the original units, right: zoomed in to the centre). Names: Red: p<0.2 in B, p>0.2 in A, green: p>0.2 in B, p<0.2 in A, purple: p<0.2 in both A and B. Asterisks indicate p<0.05: Red: p<0.05 in B, p>0.05 in A, green: p>0.05 in B, p<0.05 in A, purple: p<0.05 in both A and B. **D.** Examples shown as paired scatter plots. Left, Glutamic acid (Glu), identified as down in B only (raw p<0.05). Right, Glutamine (Gln), identified as up in B only (raw p<0.05).

A

	Cooling: Ti120 - Tn60				Thermoneutral: Ti120 - Tn60			
species.idx	logFC.B	AveExpr.B	P.Value.B	adj.P.Val.B	logFC.A	AveExpr.A	P.Value.A	adj.P.Val.A
Glu	-0.449	5.397	0.011	0.192	-0.114	5.397	0.487	0.985
Gln	0.170	9.561	0.011	0.192	0.017	9.561	0.783	0.999
Asn	0.253	5.652	0.015	0.192	0.126	5.652	0.188	0.955
SDMA	0.360	-1.703	0.040	0.367	0.042	-1.703	0.802	0.999
Lys	0.181	7.885	0.060	0.367	0.046	7.885	0.618	0.985
Histamine	-5.696	-3.794	0.062	0.367	0.003	-3.794	0.999	0.999
Sarcosine	0.415	4.047	0.070	0.367	-0.120	4.047	0.594	0.985
Serotonin	0.219	-0.539	0.075	0.367	0.072	-0.539	0.548	0.985
Leu	0.101	7.241	0.087	0.373	-0.053	7.241	0.352	0.985
His	0.149	6.457	0.114	0.373	-0.099	6.457	0.283	0.985

B

Label	Query	Match	HMDB	PubChem	KEGG
Gln	Glutamine	L-Glutamine	HMDB00641	5961	C00064
His	His	L-Histidine	HMDB00177	6274	C00135
Leu	Leu	L-Leucine	HMDB00687	6106	C00123
Lys	Lys	L-Lysine	HMDB00182	5962	C00047
Sarcosine	Sarcosine	Sarcosine	HMDB00271	1088	C00213
SDMA	SDMA	Symmetric dimethylarginine	HMDB03334	169148	
Serotonin	Serotonin	Serotonin	HMDB00259	5202	C00780

C

KEGG Pathway	Total	Expected	# Hits	Raw p	FDR	Hits
Aminoacyl-tRNA biosynthesis	75	0.187	4	1.25E-05	0.001	L-Histidine; L-Glutamine; L-Lysine; L-Leucine
Nitrogen metabolism	39	0.0972	2	0.00368	0.1474	L-Glutamine; L-Histidine
Arginine and proline metabolism	77	0.1919	2	0.01394	0.3717	L-Glutamine; Sarcosine

D

Metaboanalyst pathways	total	expected	# hits	Raw p	FDR	Hits
Ammonia Recycling	18	0.153	2	0.0089	0.703	L-Histidine; L-Glutamine

Table 14. Analysis of the effect of cooling on amino acid metabolomics profile. A. LIMMA results for the contrasts (B.Ti120 vs B.Tn60) and (A.Ti120 vs A.Tn60) after fitting to the linear model with design. **B.** Species with $p<0.2$ in the cooling arm only (red points with $y>0$ in Fig 45C) and used for pathway analysis. **C.** Metaboanalyst KEGG pathway enrichments. **D.** Enrichment for Metaboanalyst curated pathways (via HMDB identifiers).

5.4.2.2. Cooling-induced changes in lipids

The AbsoluteIDQ® Biocrates p180 Kit measures 90 species of glycerophospholipids and 15 species of sphingolipids. A full list of lipid species measured is provided (http://www.biocrates.com/products/research-products/absoluteidq-p180-kit). An additional in-house panel of lipid measurements was performed to allow the analysis of additional species to provide a comprehensive panel.

There is no pathway analysis equivalent to KEGG for lipids, and analysis of lipidomics usually depends on in-house expertise, rather than a consortium-recognised approach. We were interested in examining the lipids that changed most significantly in the two study groups, and in comparing the effect on lipids of cooling with those of caloric restriction. This data was analysed by looking at fold change of lipid species in both study arms, and then examining the species that reached an (uncorrected) p value of <0.2 and <0.05. We then looked in more detail at the lipid species that increased most significantly.

The top ten lipid species (Table 14, ordered by p value) highlight the species that changed more in cooling than the thermoneutral study arm. We can see that half of these species are lysophosphatidylethanolamines, lipids that are derived from the plasma membrane. They result from the hydrolysis of phosphatidylethanolamine, a reaction catalysed by phospholipase A2. Little is known about the role of these species in human plasma, however, lower levels of LPE have been found in the lipidomic studies of diseased coronary arteries (Kurano, Kano et al. 2017)(Kurano M, J Lipid Res, 2017). The increase of these, in addition to the lysophosphatidylcholines and glycerophosphoserines in the cooling arm of the study may indicate an increase in lipid turnover. Cooling may affect the structure of the lipid bilayer in cell membranes (Bazinet and Laye 2014).

Additionally an increase in the fatty acid (22:6), docosahexaenoic acid, was seen. This is an arachidonic acid-derived omega-3 polyunsaturated fatty acid, which is associated with a neuroprotective effect, including for Alzheimer's disease (Freund LY, J Int Med, 2014; Hashimoto M, J Neurochem, 2002). It has additionally been associated with improvements in synaptic plasticity (Jump DB, J Biol Chem, 2002), and dietary supplementation with DHA increases BDNF levels in rodents (Wu A, Cell Neurosci, 2008). This finding is of particular interest, given the RBM-3 mediated link between cooling and neuroprotection described by our collaborator Prof Mallucci (Peretti D, Nature 2015) and the improvements in cognitive function observed in the data presented in Chapter 4.

A

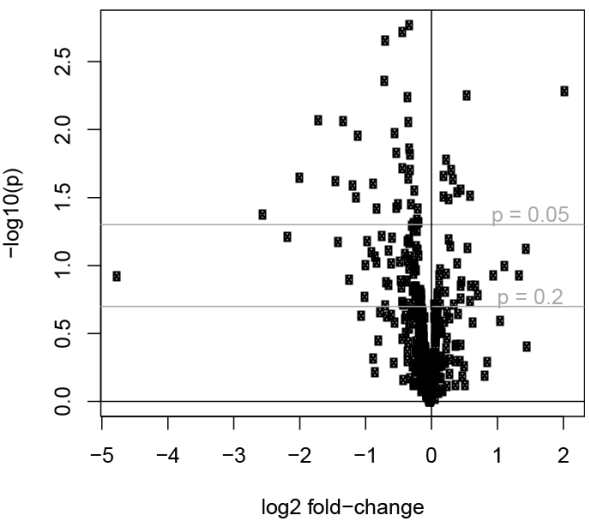
Arm A: Ti120 vs Tn60
−log10(p)
log2 fold−change
p = 0.05
p = 0.2

B

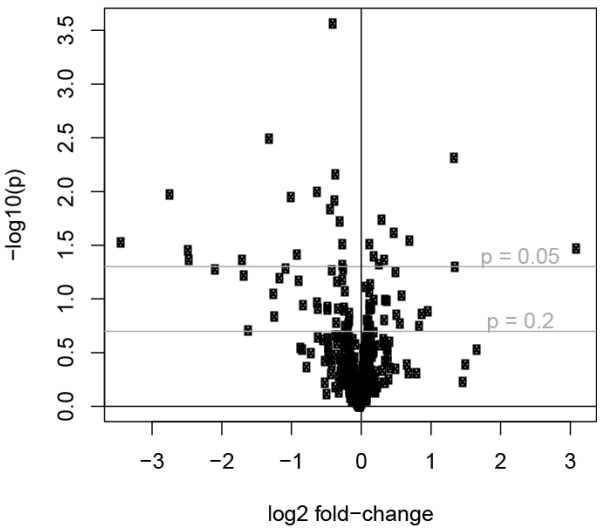
Arm B: Ti120 vs Tn60
−log10(p)
log2 fold−change
p = 0.05
p = 0.2

C

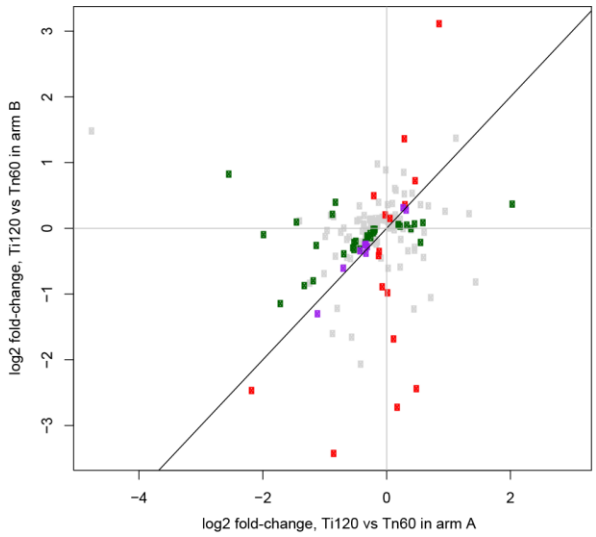
log2 fold-change, Ti120 vs Tn60 in arm B
log2 fold-change, Ti120 vs Tn60 in arm A

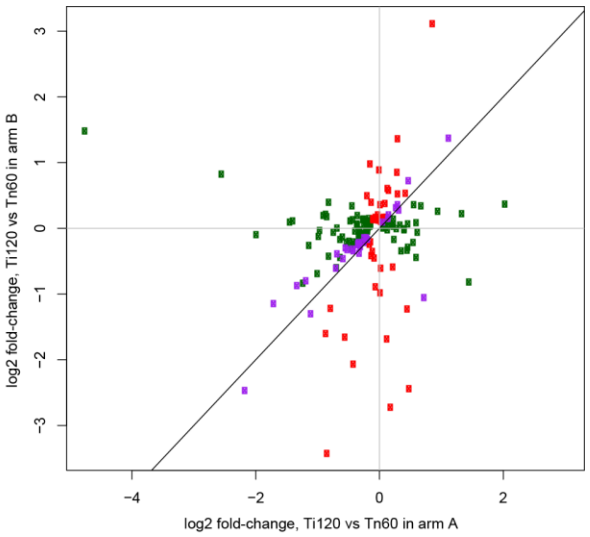
log2 fold-change, Ti120 vs Tn60 in arm B
log2 fold-change, Ti120 vs Tn60 in arm A

Figure 46. Differential concentrations (Ti120 vs Tn60, within each arm) of lipids. LIMMA was used to fit a linear model (~subjectID + {A.Tn60,A. Ti120, B. Tn60, B. Ti120}) and two different contrasts inspected: (A.Ti120 vs A.Tn60) and (B.Ti120 vs B.Tn60); see Methods. A. Volcano plot for arm A. B. Volcano plot for arm B. C. For species with (Locke, Kahali et al.) p<0.2, the fold-change within A is compared to the fold-change within B. Left, colours: Grey: 0.05<p<0.2 in either A or B or both, red: p<0.05 in B, p>0.05 in A, green: p>0.05 in B, p<0.05 in A, purple: p<0.05 in both A and B. Right, colours: Red: p<0.2 in B, p>0.2 in A, green: p>0.2 in B, p<0.2 in A, purple: p<0.2 in both A and B.

			Cooling: Ti120-Tn60				Thermoneutral: Ti120-Tn60			
Name	Prefix	Class	LogFC	Ave exp	P	Adj p	LogFC	Ave Expr	P	Adj p
LPE_18:2_[M-H]1-	LPE	Lysophosphatidylethanolamines	-0.376	-4.399	0.0003	0.127	-0.311	-4.399	0.002	0.342
BA(DCA)_[M-H]1-	BA	Bile acid derivatives	-1.300	-8.277	0.003	0.708	-1.092	-8.277	0.011	0.430
MG_18:1_[M+NH4]1+	MG	Monoradylglycerols	1.363	-8.449	0.005	0.708	0.308	-8.449	0.488	0.823
LPE_20:2_[M-H]1-	LPE	Lysophosphatidylethanolamine	-0.346	-1.688	0.007	0.708	-0.409	-1.688	0.002	0.342
LPE_18:2_[M+H]1+	LPE	Lysophosphatidylethanolamine	-0.606	-8.178	0.010	0.708	-0.684	-8.178	0.004	0.383
PS-P_30:1_[M+H]1+	PS-P	Phosphatidylserine	-2.727	-11.034	0.011	0.708	0.192	-11.034	0.846	0.962
LPS-O_18:0_[M+H]1+	LPS-O	Glycerophosphoserines	-0.984	-10.843	0.011	0.708	0.035	-10.843	0.922	0.982
LPE_20:4_[M-H]1-	LPE	Lysophosphatidylethanolamine	-0.355	-4.228	0.012	0.708	-0.097	-4.228	0.464	0.823
LPC_15:1_[M+H]1+ / LPE_18:1_[M+H]1+	LPC/LPE	Lysophosphatidylcholine /Lysophosphatidylethanolamine	-0.415	-8.469	0.015	0.755	-0.112	-8.469	0.485	0.823
FA(22:6)_[M-H]1-	FA	Fatty acyls (docoshexaenoic acid)	0.317	-2.901	0.018	0.801	0.284	-2.901	0.032	0.458

Table 15. LIMMA results for the contrasts (B.Ti120 vs B.Tn60) and (A.Ti120 vs A.Tn60). After fitting to the linear model with design (~subjectID+{A.Tn60, A. Ti120, B. Tn60, B. Ti120}). This table shows the top 10 ordered by (Locke, Kahali et al.) p for the "B" contrast (B.Ti120 vs B.Tn60).

5.4.3. Power calculations

Due to the novel nature of this experiment, pre-test power calculations were problematic to calculate as the potential effect size of the results were not known. As can be seen from the data, these did in fact vary substantially depending on the amino acid or lipid protein investigated, and also between individuals. Some differences within and between arms were as great as 50 per cent, and others much smaller.

A linear regression model was applied to calculate the necessary number of observations associated with an R^2 that is statistically significant from zero, using the XLSTAT statistical package for Excel. For each experiment there is only one independent variable; time (when comparing the effect within each temperature intervention arm) or temperature (when comparing between arms). The power required was conservatively set at 0.9 (1-beta, where beta is the type II error). Calculation of the number of subjects required tested three different effect sizes: 0.10, 0.30, and 0.50. Alpha (type II error) was set at 0.05. A simulation plot was also generated to show the range of sample sizes needed to achieve a power between 0.80 and 0.95. Naturally, the larger the effect size, the smaller the sample size needed to achieve the desired power. Figure 47 shows that the sample sizes required to achieve a power of 0.9 were 107, 37, and 23 for effect sizes of 0.10, 0.30, and 0.50, respectively.

Effect size	0.10	0.30	0.50
Power	0.9	0.9	0.9
alpha	0.05	0.05	0.05
Sample size	**107**	**37**	**23**

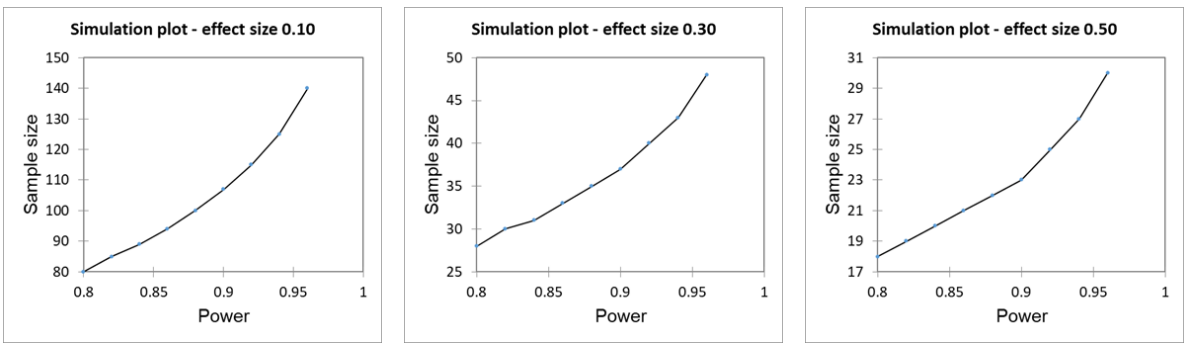

Figure 47. Power calculations with respect to the effect size. Above, table of sample sizes required to achieve a power of 0.9 depending on the effect size. Below, simulation plots showing sample size needed dependant on the effect size and desired power (between 0.8 and 0.95).

5.5. Conclusions

In this study we sought to dissect the metabolomic changes that occur in response to cooling. There have been several factors that limited the conclusions that can be drawn from this data. Firstly, the effect size of the cooling intervention was small. The temperature of the cooling intervention was carefully chosen, as other studies have shown that this is sufficient to activate brown adipose tissue, without initiating shivering within the given timeframe (Chen, Cypess et al. 2016). However, as participants were only exposed to mild cold for a relatively short period of time, the effect size of the metabolomics change was small. This is also reflected in some of the biochemical data; the effect size for many of the measured parameters was small. There was also considerable variability between individuals, both in their response to cold, and the changes in metabolomic profile. The Metaboanalyst derived-data demonstrates that differences between individuals were greater than the effect of the temperature intervention. Although a paired approach to analysis was taken, the study was underpowered.

Metabolomics has been previously used to examine the metabolic effects of acute caloric restriction (Collet, Sonoyama et al. 2017). In this study metabolomics were performed on the samples of eight normal weight healthy men. Baseline samples were compared with those taken after 48 hours of calorie restriction (10% of total daily energy needs), and after a further 48 hours of eating *ad libitum.* The effect size of this intervention was much greater than that of cooling. Comparison between the two studies is additionally limited because the platforms used for the two studies were different; the caloric restriction study was performed by the company Metabolon, which tests a much broader range of metabolites and break down products (770 in total).

There are some limitations to the metabolomics panels we chose for analysis in this study. There is no examination of glycolysis or the citric acid cycle, and it is therefore not possible to compare our study results with those of the caloric restriction study for these elements, where we demonstrated a decrease in pyruvate. However, despite these limitations it is possible to comment on some general trends seen within the data. While it is not possible to comment on directly on glycolysis, citrate was measured, and increased in both studies, and this might represent a decrease in flux of the TCA in both studies.

In the caloric restriction study there was an increase in the glucogenic and branched chain amino acids. In the cooling study these were not universally elevated, but in common with calorie restriction cooling resulted in elevated alanine and leucine levels. The other glucogenic amino acids did not

increase on cooling, with decreases in glutamate and serine seen, in addition to a drop in the ketogenic branched chain amino acid isoleucine.

In short, there are some differences and some similarities between the two studies. This may be due to differences in effect size; the effect of reducing a participant's calories to 10% of those required for 48 hours is inevitably much larger than exposure to mild cold for two hours. Furthermore, the markedly different time courses between the two studies make it hard to draw comparisons, as the processes under study are all highly dynamic. It is therefore difficult to draw firm conclusions about shared biology between the two studies. Both arms of the cooling study were performed following an overnight fast, so there were features consistent with fasting in both study arms. Additionally, as none of the corrected p values reach statistical significance, a larger sample size will need to be studied to more fully explore the metabolomics changes associated with cooling.

CHAPTER SIX: DISCUSSION

This thesis focuses on further understanding the mechanisms involved in thermogenesis in humans. I have taken two approaches to this problem. Firstly, I have undertaken studies in healthy male volunteers, where they have undergone an experimental manipulation in the form of mild cold exposure to examine the physiological and metabolic changes with cooling. Secondly, I have characterised the first rare human variants in a gene known to be involved in thermogenesis in animals, GPR10.

6.1. Cooling as an experimental manipulation

The experimental paradigm of two hours of exposure to a temperature of 16^{o}C was chosen on the basis of published evidence that a similar degree of cooling leads to brown adipose tissue activation as measured by ^{18}FDG-PET CT. In the original NEJM issue of articles demonstrating the presence of BAT in adult humans (2009), Van Marken Lichtenbelt demonstrated active BAT in healthy young men exposed to temperatures of 16^{o}C via a climatic chamber for two hours (van Marken Lichtenbelt, Schrauwen et al. 2002), whilst Orava used a similar paradigm of air exposure to 17^{o}C in a chilled room to demonstrate BAT activation (Orava, Nuutila et al. 2011). There is little published literature on the use of cooling via a cooling suit. However, our colleague Dr Sebastian Schmid, Lubeck Germany has used identical suits for a cooling study, and has demonstrated activation of BAT using an ^{18}FDG-PET CT (Iwen, Backhaus et al. 2017). We can therefore have confidence that our paradigm is likely to activate brown adipose tissue.

On cooling we observed a significant drop in peripheral skin temperature, an increase in systolic blood pressure, compatible with an increased sympathetic drive. The gas exchange monitor demonstrated a trend towards an increase in resting metabolic rate compared to the thermoneutral arm, with a shift towards fatty acid oxidation shown by a reduction in respiratory quotient, but this did not reach significance. Differences in thyroid function were not significant, nor was serum cortisol. Leptin levels reduced significantly more in the cooling study arm. In common with our previously reported findings on increased preference for high fat foods in patients with disrupted leptin-melanocortin signalling, we have found that the partial state of leptin deficiency resulting from cooling is also reflected by a significant increase in preference for high fat food on the fat preference meal (van der Klaauw, Keogh et al. 2016). Changes in BDNF levels did not reach significance. There was an improvement in some neurocognitive tests; the verbal fluency and digit span tests significantly improved.

Although there were clear physiological changes induced by the temperature intervention, we have not been able to show significant changes in the metabolome, although the study was underpowered

to detect an effect. Metabolomics has been previously used to examine the effects of 48 hours of calorie restriction (10% of daily energy needs) in healthy normal weight men. In that study we observe an increase in branched chain amino acids, increased lipolysis of triglycerides, acylcarnitines, ketone bodies, 3-OH fatty acids, sphingolipids and endocannabinoids, and a decrease in phospholipids and plasmalogens. None of the results in the cooling study reached statistical significance after Benjamini-Hochberg correction to control for false discovery rate. This is probably because the effect size of 48 hours of calorie restriction is much greater than two hours of mild cooling; a greater effect size may have been seen if participants were cooled to a lower temperature and for longer. However, we were concerned that this would result in the adaptive response of shivering with resulting increases in energy expenditure, and that this might confound our interpretation of results.

6.2. The effect of chronic cold exposure and acclimatisation on thermogenesis

There have been several previous studies examining acclimatisation to chronic cold exposure. Population studies show that indigenous black Africans have reduced shivering thermogenesis in the cold and less cold induced vasodilation in fingers and toes compared to Caucasians and Inuit (Daanen and Van Marken Lichtenbelt 2016). These findings are in keeping with others that show that both males and females from circumpolar regions have basal metabolic rates between 3-19% higher than would be predicted on the basis of people from temperate zones (Leonard, Sorensen et al. 2002). However, other groups have shown that both black and white people living in subtropical zones have the same amounts of brown adipose tissue, indicating that it is exposure to extreme temperatures, rather than innate ethnic differences that explain these findings (Perkins, Mshelia et al. 2013).

Together, these findings demonstrate that while people who are habituated to a cold environment may have an increased basal metabolic rate, it is unclear whether this is secondary to ethnic differences in the amount or activity of brown adipose tissue, or whether it is simply due to environmental conditioning.

Brown adipose tissue is activated by cold, increased sympathetic drive and thyroid hormones. It has been hypothesised that cold adaptation might result in changes in thyroid activity and that this is essential in Arctic and cold-exposed populations. This theory was supported by the finding that serum thyroglobulin was highest amongst Arctic hunters and settlement dwellers who were markedly cold exposed. They additionally had the lower measurements of T3; TSH was not affected (Andersen, Kleinschmidt et al. 2012). These findings are consistent with an increase in consumption of thyroid hormone, and a higher thyroid hormone turnover.

6.3. Other approaches to the study of energy expenditure

There are other experimental approaches to studying energy expenditure. Just as changes with thyroid hormone have been observed in cold-acclimatised populations, studies on the action of thyroid hormone on brown adipose tissue have yielded new insights on its biology. Induction of the deiodinase 2 enzyme results in BAT adipogenesis *in* vitro and its development in mice embryos. Brown adipocytes express high levels of deiodinase II and low levels of deiodinase 3, resulting in high rates of conversion of thyroxine to triiodothyronine, and low levels of inactive reverse T3. Enhanced thyroid hormone signalling results in the activation of several genes, including *PPARγ1α* and *ucp1.*

The effects of thyroid hormone on BAT activation have been explored in patients with thyroid carcinoma, before and after the initiation of TSH-suppressive thyroxine therapy following surgery, with ^{18}FDG-PET imaging. These case reports have shown improvements in metabolic markers and glycaemic control with increasing levels of BAT activation (Skarulis, Celi et al. 2010, Broeders, Vijgen et al. 2016). No data from human clinical trials of THRb stimulation have been reported, but both mouse and primate models suggest that THRb selectively stimulates BAT and promotes adaptive thermogenesis. (Grover, Mellstrom et al. 2003).

While collectively these studies demonstrate a role for thyroid hormone in the activation of brown adipose tissue, administration of levothyroxine is not a “clean” method of investigating brown adipose tissue biology; thyroid hormone, acting via its nuclear receptors THRa and THRb, activates in excess of 200 different genes. The effects of levothyroxine are therefore wide-ranging, and will not allow the examination of BAT in isolation. Additionally, administration of thyroid hormone as a weight loss tool is likely to be of very limited potential due to the negative cardiovascular profile and effects on bone density.

6.4. Insights from the genetics of energy expenditure in humans

The heritability of energy expenditure has been illustrated by seminal studies examining the effects of overfeeding in monozygotic twin pairs. Twelve adult pairs of monozygotic twins were overfed by ~1000 kcal per day, six days per week for a total of 84 out of 100 consecutive days. The total excess consumption was 83,000 kcal. They demonstrated that weight gain was highly variable, ranging from 4.4 to 13.3kg, with a mean weight gain of 8.3kg. There was a significant similarity within each twin pair in the amount of weight gained, with approximately three times more variance between twin pairs than within twin pairs (Bouchard, Tremblay et al. 1990).

There are no described cases of human monogenic obesity resulting from rare mutations in molecules known to be involved in human thermogenesis, for instance *ucp-1* or the β3 adrenergic receptor. However, a common polymorphism in *ucp-1* has been described; the Trp64Arg polymorphism of ADRβ3 generates less cyclic AMP in response to adrenergic agonists than does the wild-type receptor, and lowers the response to β3 adrenergic agonists in transfected 3T3-L1 preadipocytes. Also described is a common polymorphism in the DIO2 enzyme (Thr92Ala) that is associated with type 2 diabetes. Individuals possessing both variants, have a propensity to obesity (Kimura, Sasaki et al. 2000). Additionally, rare human mutations in *KSR2* (kinase suppressor of Ras 2), an intracellular scaffolding pathway with effects on multiple pathways, that impair cellular fatty acid oxidation and glucose oxidation *in vitro*. Affected patients have a low basal metabolic rate and heart rate, in addition to severe childhood hyperphagia, weight gain and insulin resistance (Pearce, Atanassova et al. 2013).

GPR10 is known to be downstream of leptin and is important for its thermogenic effects (Dodd, Worth et al. 2014). There is therefore there is a clear rationale for studying human mutations that may affect its function, and this thesis describes the first rare human mutations in this molecule that are obesity associated.

6.5. Rare variant analysis and establishing causality

Establishing whether variants contribute to a person's obesity can be challenging. We planned to perform a detailed clinical phenotyping of the patients, but this was difficult as many of them were not available for study. We have studied variants found in both cases and controls, and have performed a thorough functional characterisation and have demonstrated a dominant negative effect of the mutant receptor on the wild type, in cells cotransfected with both. We explored the use of *C. elegans* in demonstrating the association of mutations in GPR10 with obesity by using CARS microscopy; these efforts were frustrated by the degree of variability in fat content in both wild type and *npr-6* null worms. We are therefore in the process of creating a heterozygous mouse of the P193S mutation – one of the three mutations that demonstrate an *in vitro* loss of function and a dominant negative effect on the wild type receptor, in collaboration with Professor Simon Luckman, who has contributed much of the rodent work conducted on GPR10 signalling. The phenotype of the heterozygous mouse will hopefully help to elucidate whether this human mutation can cause obesity.

Whilst human studies are very challenging, and there are many potential pitfalls to the approach we have taken, we know that drugs that act on targets validated by studies resulting from human genetic data have a much greater chance of reaching the market (Nelson, Tipney et al. 2015). Whilst the

challenge of neuropeptides as a potential treatment for obesity is creating drugs that can be peripherally administered and cross the blood brain barrier, there has been much industry work on creating lipidised versions of PrRP that have therapeutic potential (Maletinska, Nagelova et al. 2015). This work contributes to the evidence necessary to support their rational use in humans.

References

Addinsoft (2017). "XLSTAT 2017: Data analysis and Statistical Solution for Microsoft Excel." Addinsoft, Paris, France.

Ahima, R. S., D. Prabakaran, C. Mantzoros, D. Qu, B. Lowell, E. Maratos-Flier and J. S. Flier (1996). "Role of leptin in the neuroendocrine response to fasting." Nature **382**(6588): 250-252.

Allison, D. B., J. Kaprio, M. Korkeila, M. Koskenvuo, M. C. Neale and K. Hayakawa (1996). "The heritability of body mass index among an international sample of monozygotic twins reared apart." Int J Obes Relat Metab Disord **20**(6): 501-506.

Alonso, L. G. and T. H. Maren (1955). "Effect of food restriction on body composition of hereditary obese mice." Am J Physiol **183**(2): 284-290.

Andersen, S., K. Kleinschmidt, B. Hvingel and P. Laurberg (2012). "Thyroid hyperactivity with high thyroglobulin in serum despite sufficient iodine intake in chronic cold adaptation in an Arctic Inuit hunter population." Eur J Endocrinol **166**(3): 433-440.

Bazinet, R. P. and S. Laye (2014). "Polyunsaturated fatty acids and their metabolites in brain function and disease." Nat Rev Neurosci **15**(12): 771-785.

Bechtold, D. A. and S. M. Luckman (2006). "Prolactin-releasing Peptide mediates cholecystokinin-induced satiety in mice." Endocrinology **147**(10): 4723-4729.

Bechtold, D. A. and S. M. Luckman (2007). "The role of RFamide peptides in feeding." J Endocrinol **192**(1): 3-15.

Bhattacharyya, S., J. Luan, B. Challis, C. Schmitz, P. Clarkson, P. W. Franks, R. Middelberg, J. Keogh, I. S. Farooqi, C. Montague, J. Brennand, N. J. Wareham and S. O'Rahilly (2003). "Association of polymorphisms in GPR10, the gene encoding the prolactin-releasing peptide receptor with blood pressure, but not obesity, in a U.K. Caucasian population." Diabetes **52**(5): 1296-1299.

Bjursell, M., M. Lenneras, M. Goransson, A. Elmgren and Y. M. Bohlooly (2007). "GPR10 deficiency in mice results in altered energy expenditure and obesity." Biochem Biophys Res Commun **363**(3): 633-638.

Bland, J. M. and D. G. Altman (1994). "Regression towards the mean." BMJ **308**(6942): 1499.

Blondin, D. P., H. C. Tingelstad, C. Noll, F. Frisch, S. Phoenix, B. Guerin, E. E. Turcotte, D. Richard, F. Haman and A. C. Carpentier (2017). "Dietary fatty acid metabolism of brown adipose tissue in cold-acclimated men." Nat Commun **8**: 14146.

Blouet, C., Y. H. Jo, X. Li and G. J. Schwartz (2009). "Mediobasal hypothalamic leucine sensing regulates food intake through activation of a hypothalamus-brainstem circuit." J Neurosci **29**(26): 8302-8311.

Bouchard, C., A. Tremblay, J. P. Despres, A. Nadeau, P. J. Lupien, G. Theriault, J. Dussault, S. Moorjani, S. Pinault and G. Fournier (1990). "The response to long-term overfeeding in identical twins." N Engl J Med **322**(21): 1477-1482.

Bredella, M. A., P. K. Fazeli, L. M. Freedman, G. Calder, H. Lee, C. J. Rosen and A. Klibanski (2012). "Young women with cold-activated brown adipose tissue have higher bone mineral density and lower Pref-1 than women without brown adipose tissue: a study in women with anorexia nervosa, women recovered from anorexia nervosa, and normal-weight women." J Clin Endocrinol Metab **97**(4): E584-590.

Broeders, E. P., G. H. Vijgen, B. Havekes, N. D. Bouvy, F. M. Mottaghy, M. Kars, N. C. Schaper, P. Schrauwen, B. Brans and W. D. van Marken Lichtenbelt (2016). "Thyroid Hormone Activates Brown Adipose Tissue and Increases Non-Shivering Thermogenesis--A Cohort Study in a Group of Thyroid Carcinoma Patients." PLoS One **11**(1): e0145049.

Calebiro, D., T. de Filippis, S. Lucchi, C. Covino, S. Panigone, P. Beck-Peccoz, D. Dunlap and L. Persani (2005). "Intracellular entrapment of wild-type TSH receptor by oligomerization with mutants linked to dominant TSH resistance." Hum Mol Genet **14**(20): 2991-3002.

Cannon, B. and J. Nedergaard (2004). "Brown adipose tissue: function and physiological significance." Physiol Rev **84**(1): 277-359.

Cao, W. H. and S. F. Morrison (2006). "Glutamate receptors in the raphe pallidus mediate brown adipose tissue thermogenesis evoked by activation of dorsomedial hypothalamic neurons." Neuropharmacology **51**(3): 426-437.

Castellano, J. M., V. M. Navarro, R. Fernandez-Fernandez, R. Nogueiras, S. Tovar, J. Roa, M. J. Vazquez, E. Vigo, F. F. Casanueva, E. Aguilar, L. Pinilla, C. Dieguez and M. Tena-Sempere (2005). "Changes in hypothalamic KiSS-1 system and restoration of pubertal activation of the reproductive axis by kisspeptin in undernutrition." Endocrinology **146**(9): 3917-3925.

Chan, J. L., K. Heist, A. M. DePaoli, J. D. Veldhuis and C. S. Mantzoros (2003). "The role of falling leptin levels in the neuroendocrine and metabolic adaptation to short-term starvation in healthy men." J Clin Invest **111**(9): 1409-1421.

Chen, K. Y., A. M. Cypess, M. R. Laughlin, C. R. Haft, H. H. Hu, M. A. Bredella, S. Enerback, P. E. Kinahan, W. Lichtenbelt, F. I. Lin, J. J. Sunderland, K. A. Virtanen and R. L. Wahl (2016). "Brown Adipose Reporting Criteria in Imaging STudies (BARCIST 1.0): Recommendations for Standardized FDG-PET/CT Experiments in Humans." Cell Metab **24**(2): 210-222.

Chondronikola, M., E. Volpi, E. Borsheim, C. Porter, M. K. Saraf, P. Annamalai, C. Yfanti, T. Chao, D. Wong, K. Shinoda, S. M. Labbe, N. M. Hurren, F. Cesani, S. Kajimura and L. S. Sidossis (2016). "Brown Adipose Tissue Activation Is Linked to Distinct Systemic Effects on Lipid Metabolism in Humans." Cell Metab **23**(6): 1200-1206.

Collet, T. H., T. Sonoyama, E. Henning, J. M. Keogh, B. Ingram, S. Kelway, L. Guo and I. S. Farooqi (2017). "A Metabolomic Signature of Acute Caloric Restriction." J Clin Endocrinol Metab **102**(12): 4486-4495.

Cousin, B., S. Cinti, M. Morroni, S. Raimbault, D. Ricquier, L. Penicaud and L. Casteilla (1992). "Occurrence of brown adipocytes in rat white adipose tissue: molecular and morphological characterization." J Cell Sci **103 (Pt 4)**: 931-942.

Cypess, A. M., S. Lehman, G. Williams, I. Tal, D. Rodman, A. B. Goldfine, F. C. Kuo, E. L. Palmer, Y. H. Tseng, A. Doria, G. M. Kolodny and C. R. Kahn (2009). "Identification and importance of brown adipose tissue in adult humans." N Engl J Med **360**(15): 1509-1517.

Daanen, H. A. and W. D. Van Marken Lichtenbelt (2016). "Human whole body cold adaptation." Temperature (Austin) **3**(1): 104-118.

Davis, T. R. and J. Mayer (1954). "Imperfect homeothermia in the hereditary obese-hyperglycemic syndrome of mice." Am J Physiol **177**(2): 222-226.

Dib, B., P. P. Rompre, S. Amir and P. Shizgal (1994). "Thermogenesis in brown adipose tissue is activated by electrical stimulation of the rat dorsal raphe nucleus." Brain Res **650**(1): 149-152.

Dodd, G. T., A. A. Worth, N. Nunn, A. K. Korpal, D. A. Bechtold, M. B. Allison, M. G. Myers, Jr., M. A. Statnick and S. M. Luckman (2014). "The thermogenic effect of leptin is dependent on a distinct population of prolactin-releasing peptide neurons in the dorsomedial hypothalamus." Cell Metab **20**(4): 639-649.

Ellacott, K. L., C. B. Lawrence, N. J. Rothwell and S. M. Luckman (2002). "PRL-releasing peptide interacts with leptin to reduce food intake and body weight." Endocrinology **143**(2): 368-374.

Enriori, P. J., P. Sinnayah, S. E. Simonds, C. Garcia Rudaz and M. A. Cowley (2011). "Leptin action in the dorsomedial hypothalamus increases sympathetic tone to brown adipose tissue in spite of systemic leptin resistance." J Neurosci **31**(34): 12189-12197.

Fan, W., B. A. Boston, R. A. Kesterson, V. J. Hruby and R. D. Cone (1997). "Role of melanocortinergic neurons in feeding and the agouti obesity syndrome." Nature **385**(6612): 165-168.

Farooqi, I. S., G. Matarese, G. M. Lord, J. M. Keogh, E. Lawrence, C. Agwu, V. Sanna, S. A. Jebb, F. Perna, S. Fontana, R. I. Lechler, A. M. DePaoli and S. O'Rahilly (2002). "Beneficial effects of leptin on obesity, T cell hyporesponsiveness, and neuroendocrine/metabolic dysfunction of human congenital leptin deficiency." J Clin Invest **110**(8): 1093-1103.

Festuccia, W. T., P. G. Blanchard and Y. Deshaies (2011). "Control of Brown Adipose Tissue Glucose and Lipid Metabolism by PPARgamma." Front Endocrinol (Lausanne) **2**: 84.

Fonseca, T. L., J. P. Werneck-De-Castro, M. Castillo, B. M. Bocco, G. W. Fernandes, E. A. McAninch, D. L. Ignacio, C. C. Moises, A. R. Ferreira, B. Gereben and A. C. Bianco (2014). "Tissue-specific

inactivation of type 2 deiodinase reveals multilevel control of fatty acid oxidation by thyroid hormone in the mouse." Diabetes **63**(5): 1594-1604.

Frayling, T. M., N. J. Timpson, M. N. Weedon, E. Zeggini, R. M. Freathy, C. M. Lindgren, J. R. Perry, K. S. Elliott, H. Lango, N. W. Rayner, B. Shields, L. W. Harries, J. C. Barrett, S. Ellard, C. J. Groves, B. Knight, A. M. Patch, A. R. Ness, S. Ebrahim, D. A. Lawlor, S. M. Ring, Y. Ben-Shlomo, M. R. Jarvelin, U. Sovio, A. J. Bennett, D. Melzer, L. Ferrucci, R. J. Loos, I. Barroso, N. J. Wareham, F. Karpe, K. R. Owen, L. R. Cardon, M. Walker, G. A. Hitman, C. N. Palmer, A. S. Doney, A. D. Morris, G. D. Smith, A. T. Hattersley and M. I. McCarthy (2007). "A common variant in the FTO gene is associated with body mass index and predisposes to childhood and adult obesity." Science **316**(5826): 889-894.

Galgani, J. E., F. L. Greenway, S. Caglayan, M. L. Wong, J. Licinio and E. Ravussin (2010). "Leptin replacement prevents weight loss-induced metabolic adaptation in congenital leptin-deficient patients." J Clin Endocrinol Metab **95**(2): 851-855.

Gavrilova, O., L. R. Leon, B. Marcus-Samuels, M. M. Mason, A. L. Castle, S. Refetoff, C. Vinson and M. L. Reitman (1999). "Torpor in mice is induced by both leptin-dependent and -independent mechanisms." Proc Natl Acad Sci U S A **96**(25): 14623-14628.

Geiser, F. and G. Heldmaier (1995). "The impact of dietary fats, photoperiod, temperature and season on morphological variables, torpor patterns, and brown adipose tissue fatty acid composition of hamsters, Phodopus sungorus." J Comp Physiol B **165**(5): 406-415.

Giralt, M. and F. Villarroya (2013). "White, brown, beige/brite: different adipose cells for different functions?" Endocrinology **154**(9): 2992-3000.

Graessler, J., D. Schwudke, P. E. Schwarz, R. Herzog, A. Shevchenko and S. R. Bornstein (2009). "Top-down lipidomics reveals ether lipid deficiency in blood plasma of hypertensive patients." PLoS One **4**(7): e6261.

Grover, G. J., K. Mellstrom, L. Ye, J. Malm, Y. L. Li, L. G. Bladh, P. G. Sleph, M. A. Smith, R. George, B. Vennstrom, K. Mookhtiar, R. Horvath, J. Speelman, D. Egan and J. D. Baxter (2003). "Selective thyroid hormone receptor-beta activation: a strategy for reduction of weight, cholesterol, and lipoprotein (a) with reduced cardiovascular liability." Proc Natl Acad Sci U S A **100**(17): 10067-10072.

Gu, W., B. J. Geddes, C. Zhang, K. P. Foley and A. Stricker-Krongrad (2004). "The prolactin-releasing peptide receptor (GPR10) regulates body weight homeostasis in mice." J Mol Neurosci **22**(1-2): 93-103.

Guo, L., M. V. Milburn, J. A. Ryals, S. C. Lonergan, M. W. Mitchell, J. E. Wulff, D. C. Alexander, A. M. Evans, B. Bridgewater, L. Miller, M. L. Gonzalez-Garay and C. T. Caskey (2015). "Plasma metabolomic profiles enhance precision medicine for volunteers of normal health." Proc Natl Acad Sci U S A **112**(35): E4901-4910.

Halaas, J. L., K. S. Gajiwala, M. Maffei, S. L. Cohen, B. T. Chait, D. Rabinowitz, R. L. Lallone, S. K. Burley and J. M. Friedman (1995). "Weight-reducing effects of the plasma protein encoded by the obese gene." Science **269**(5223): 543-546.

Hall, W. D., C. M. Ferrario, M. A. Moore, J. E. Hall, J. M. Flack, W. Cooper, J. D. Simmons, B. M. Egan, D. T. Lackland, M. Perry, Jr. and E. J. Roccella (1997). "Hypertension-related morbidity and mortality in the southeastern United States." Am J Med Sci **313**(4): 195-209.

Han, X. and R. W. Gross (2003). "Global analyses of cellular lipidomes directly from crude extracts of biological samples by ESI mass spectrometry: a bridge to lipidomics." J Lipid Res **44**(6): 1071-1079.

Hausberg, M., D. A. Morgan, J. L. Mitchell, W. I. Sivitz, A. L. Mark and W. G. Haynes (2002). "Leptin potentiates thermogenic sympathetic responses to hypothermia: a receptor-mediated effect." Diabetes **51**(8): 2434-2440.

Heldmaier, G., S. Ortmann and R. Elvert (2004). "Natural hypometabolism during hibernation and daily torpor in mammals." Respir Physiol Neurobiol **141**(3): 317-329.

Hendricks, A. E., E. G. Bochukova, G. Marenne, J. M. Keogh, N. Atanassova, R. Bounds, E. Wheeler, V. Mistry, E. Henning, A. Korner, D. Muddyman, S. McCarthy, A. Hinney, J. Hebebrand, R. A. Scott, C. Langenberg, N. J. Wareham, P. Surendran, J. M. Howson, A. S. Butterworth, J. Danesh, B. G. Nordestgaard, S. F. Nielsen, S. Afzal, S. Papadia, S. Ashford, S. Garg, G. L. Millhauser, R. I. Palomino, A. Kwasniewska, I. Tachmazidou, S. O'Rahilly, E. Zeggini, I. Barroso and I. S. Farooqi (2017). "Rare Variant Analysis of Human and Rodent Obesity Genes in Individuals with Severe Childhood Obesity." Sci Rep **7**(1): 4394.

Herman, J. P. (2018). "Regulation of Hypothalamo-Pituitary-Adrenocortical Responses to Stressors by the Nucleus of the Solitary Tract/Dorsal Vagal Complex." Cell Mol Neurobiol **38**(1): 25-35.

Hinuma, S., Y. Habata, R. Fujii, Y. Kawamata, M. Hosoya, S. Fukusumi, C. Kitada, Y. Masuo, T. Asano, H. Matsumoto, M. Sekiguchi, T. Kurokawa, O. Nishimura, H. Onda and M. Fujino (1998). "A prolactin-releasing peptide in the brain." Nature **393**(6682): 272-276.

Horiuchi, J., T. Saigusa, N. Sugiyama, S. Kanba, Y. Nishida, Y. Sato, S. Hinuma and J. Arita (2002). "Effects of prolactin-releasing peptide microinjection into the ventrolateral medulla on arterial pressure and sympathetic activity in rats." Brain Res **958**(1): 201-209.

Illig, T., C. Gieger, G. Zhai, W. Romisch-Margl, R. Wang-Sattler, C. Prehn, E. Altmaier, G. Kastenmuller, B. S. Kato, H. W. Mewes, T. Meitinger, M. H. de Angelis, F. Kronenberg, N. Soranzo, H. E. Wichmann, T. D. Spector, J. Adamski and K. Suhre (2010). "A genome-wide perspective of genetic variation in human metabolism." Nat Genet **42**(2): 137-141.

Ingalls, A. M., M. M. Dickie and G. D. Snell (1950). "Obese, a new mutation in the house mouse." J Hered **41**(12): 317-318.

Iwen, K. A., J. Backhaus, M. Cassens, M. Waltl, O. C. Hedesan, M. Merkel, J. Heeren, C. Sina, L. Rademacher, A. Windjager, A. R. Haug, F. W. Kiefer, H. Lehnert and S. M. Schmid (2017). "Cold-Induced Brown Adipose Tissue Activity Alters Plasma Fatty Acids and Improves Glucose Metabolism in Men." J Clin Endocrinol Metab **102**(11): 4226-4234.

Jimenez, M., B. Leger, K. Canola, L. Lehr, P. Arboit, J. Seydoux, A. P. Russell, J. P. Giacobino, P. Muzzin and F. Preitner (2002). "Beta(1)/beta(2)/beta(3)-adrenoceptor knockout mice are obese and cold-sensitive but have normal lipolytic responses to fasting." FEBS Lett **530**(1-3): 37-40.

Kavaliers, M. and M. Hirst (1985). "FMRFamide suppresses kappa opiate induced feeding in the mouse." Peptides **6**(5): 847-849.

Kim, H. Y. (2014). "Neuroprotection by docosahexaenoic acid in brain injury." Mil Med **179**(11 Suppl): 106-111.

Kimura, K., N. Sasaki, A. Asano, J. Mizukami, S. Kayahashi, T. Kawada, T. Fushiki, M. Morimatsu, T. Yoshida and M. Saito (2000). "Mutated human beta3-adrenergic receptor (Trp64Arg) lowers the response to beta3-adrenergic agonists in transfected 3T3-L1 preadipocytes." Horm Metab Res **32**(3): 91-96.

King, A., Q. Yang, S. Huesman, T. Rider and C. C. Lo (2015). "Lipid transport in cholecystokinin knockout mice." Physiol Behav **151**: 198-206.

Kurano, M., K. Kano, T. Dohi, H. Matsumoto, K. Igarashi, M. Nishikawa, R. Ohkawa, H. Ikeda, K. Miyauchi, H. Daida, J. Aoki and Y. Yatomi (2017). "Different origins of lysophospholipid mediators between coronary and peripheral arteries in acute coronary syndrome." J Lipid Res **58**(2): 433-442.

Kuri-Morales, P., J. Emberson, J. Alegre-Diaz, R. Tapia-Conyer, R. Collins, R. Peto and G. Whitlock (2009). "The prevalence of chronic diseases and major disease risk factors at different ages among 150,000 men and women living in Mexico City: cross-sectional analyses of a prospective study." BMC Public Health **9**: 9.

Labadi, A., E. S. Grassi, B. Gellen, G. Kleinau, H. Biebermann, B. Ruzsa, G. Gelmini, O. Rideg, A. Miseta, G. L. Kovacs, A. Patocs, E. Felszeghy, E. V. Nagy, E. Mezosi and L. Persani (2015). "Loss-of-Function Variants in a Hungarian Cohort Reveal Structural Insights on TSH Receptor Maturation and Signaling." J Clin Endocrinol Metab **100**(7): E1039-1045.

Labbe, S. M., M. Mouchiroud, A. Caron, B. Secco, E. Freinkman, G. Lamoureux, Y. Gelinas, R. Lecomte, Y. Bosse, P. Chimin, W. T. Festuccia, D. Richard and M. Laplante (2016). "mTORC1 is Required for Brown Adipose Tissue Recruitment and Metabolic Adaptation to Cold." Sci Rep **6**: 37223.

Langeveld, M., C. Y. Tan, M. R. Soeters, S. Virtue, G. K. Ambler, L. P. Watson, P. R. Murgatroyd, V. K. Chatterjee and A. Vidal-Puig (2016). "Mild cold effects on hunger, food intake, satiety and skin temperature in humans." Endocr Connect **5**(2): 65-73.

Langmead, C. J., P. G. Szekeres, J. K. Chambers, S. J. Ratcliffe, D. N. Jones, W. D. Hirst, G. W. Price and H. J. Herdon (2000). "Characterization of the binding of [(125)I]-human prolactin releasing peptide (PrRP) to GPR10, a novel G protein coupled receptor." Br J Pharmacol **131**(4): 683-688.

Laurent, P., J. A. Becker, O. Valverde, C. Ledent, A. de Kerchove d'Exaerde, S. N. Schiffmann, R. Maldonado, G. Vassart and M. Parmentier (2005). "The prolactin-releasing peptide antagonizes the opioid system through its receptor GPR10." Nat Neurosci **8**(12): 1735-1741.

Lawrence, C. B., F. Celsi, J. Brennand and S. M. Luckman (2000). "Alternative role for prolactin-releasing peptide in the regulation of food intake." Nat Neurosci **3**(7): 645-646.

Lawrence, C. B., K. L. Ellacott and S. M. Luckman (2002). "PRL-releasing peptide reduces food intake and may mediate satiety signaling." Endocrinology **143**(2): 360-367.

Lawrence, C. B., Y. L. Liu, M. J. Stock and S. M. Luckman (2004). "Anorectic actions of prolactin-releasing peptide are mediated by corticotropin-releasing hormone receptors." Am J Physiol Regul Integr Comp Physiol **286**(1): R101-107.

Lee, J. Y., N. Takahashi, M. Yasubuchi, Y. I. Kim, H. Hashizaki, M. J. Kim, T. Sakamoto, T. Goto and T. Kawada (2012). "Triiodothyronine induces UCP-1 expression and mitochondrial biogenesis in human adipocytes." Am J Physiol Cell Physiol **302**(2): C463-472.

Leonard, W. R., M. V. Sorensen, V. A. Galloway, G. J. Spencer, M. J. Mosher, L. Osipova and V. A. Spitsyn (2002). "Climatic influences on basal metabolic rates among circumpolar populations." Am J Hum Biol **14**(5): 609-620.

Li, Y. Q., Y. Shrestha, M. Pandey, M. Chen, A. Kablan, O. Gavrilova, S. Offermanns and L. S. Weinstein (2016). "G(q/11)alpha and G(s)alpha mediate distinct physiological responses to central melanocortins." J Clin Invest **126**(1): 40-49.

Lin, S. H., A. C. Arai, R. A. Espana, C. W. Berridge, F. M. Leslie, J. R. Huguenard, M. Vergnes and O. Civelli (2002). "Prolactin-releasing peptide (PrRP) promotes awakening and suppresses absence seizures." Neuroscience **114**(1): 229-238.

Locke, A. E., B. Kahali, S. I. Berndt, A. E. Justice, T. H. Pers, F. R. Day, C. Powell, S. Vedantam, M. L. Buchkovich, J. Yang, D. C. Croteau-Chonka, T. Esko, T. Fall, T. Ferreira, S. Gustafsson, Z. Kutalik, J. Luan, R. Magi, J. C. Randall, T. W. Winkler, A. R. Wood, T. Workalemahu, J. D. Faul, J. A. Smith, J. H. Zhao, W. Zhao, J. Chen, R. Fehrmann, A. K. Hedman, J. Karjalainen, E. M. Schmidt, D. Absher, N. Amin, D. Anderson, M. Beekman, J. L. Bolton, J. L. Bragg-Gresham, S. Buyske, A. Demirkan, G. Deng, G. B. Ehret, B. Feenstra, M. F. Feitosa, K. Fischer, A. Goel, J. Gong, A. U. Jackson, S. Kanoni, M. E. Kleber, K. Kristiansson, U. Lim, V. Lotay, M. Mangino, I. M. Leach, C. Medina-Gomez, S. E. Medland, M. A. Nalls, C. D. Palmer, D. Pasko, S. Pechlivanis, M. J. Peters, I. Prokopenko, D. Shungin, A. Stancakova, R. J. Strawbridge, Y. J. Sung, T. Tanaka, A. Teumer, S. Trompet, S. W. van der Laan, J. van Setten, J. V. Van Vliet-Ostaptchouk, Z. Wang, L. Yengo, W. Zhang, A. Isaacs, E. Albrecht, J. Arnlov, G. M. Arscott, A. P. Attwood, S. Bandinelli, A. Barrett, I. N. Bas, C. Bellis, A. J. Bennett, C. Berne, R. Blagieva, M. Bluher, S. Bohringer, L. L. Bonnycastle, Y. Bottcher, H. A. Boyd, M. Bruinenberg, I. H. Caspersen, Y. I. Chen, R. Clarke, E. W. Daw, A. J. M. de Craen, G. Delgado, M. Dimitriou, A. S. F. Doney, N. Eklund, K. Estrada, E. Eury, L. Folkersen, R. M. Fraser, M. E. Garcia, F. Geller, V. Giedraitis, B. Gigante, A. S. Go, A. Golay, A. H. Goodall, S. D. Gordon, M. Gorski, H. J. Grabe, H. Grallert, T. B. Grammer, J. Grassler, H. Gronberg, C. J. Groves, G. Gusto, J. Haessler, P. Hall, T. Haller, G. Hallmans, C. A. Hartman, M. Hassinen, C. Hayward, N. L. Heard-Costa, Q. Helmer, C. Hengstenberg, O. Holmen, J. J. Hottenga, A. L. James, J. M. Jeff, A. Johansson, J. Jolley, T. Juliusdottir, L. Kinnunen, W. Koenig, M. Koskenvuo, W. Kratzer, J. Laitinen, C. Lamina, K. Leander, N. R. Lee, P. Lichtner, L. Lind, J. Lindstrom, K. S. Lo, S. Lobbens, R. Lorbeer, Y. Lu, F. Mach, P. K. E. Magnusson, A. Mahajan, W. L. McArdle, S. McLachlan, C. Menni, S. Merger, E. Mihailov, L. Milani, A. Moayyeri, K. L. Monda, M. A. Morken, A. Mulas, G. Muller, M. Muller-Nurasyid, A. W. Musk, R. Nagaraja, M. M. Nothen, I. M. Nolte, S. Pilz, N. W. Rayner, F. Renstrom, R. Rettig, J. S. Ried, S. Ripke, N. R. Robertson, L. M. Rose, S. Sanna, H.

Scharnagl, S. Scholtens, F. R. Schumacher, W. R. Scott, T. Seufferlein, J. Shi, A. V. Smith, J. Smolonska, A. V. Stanton, V. Steinthorsdottir, K. Stirrups, H. M. Stringham, J. Sundstrom, M. A. Swertz, A. J. Swift, A. C. Syvanen, S. T. Tan, B. O. Tayo, B. Thorand, G. Thorleifsson, J. P. Tyrer, H. W. Uh, L. Vandenput, F. C. Verhulst, S. H. Vermeulen, N. Verweij, J. M. Vonk, L. L. Waite, H. R. Warren, D. Waterworth, M. N. Weedon, L. R. Wilkens, C. Willenborg, T. Wilsgaard, M. K. Wojczynski, A. Wong, A. F. Wright, Q. Zhang, E. P. Brennan, M. Choi, Z. Dastani, A. W. Drong, P. Eriksson, A. Franco-Cereceda, J. R. Gadin, A. G. Gharavi, M. E. Goddard, R. E. Handsaker, J. Huang, F. Karpe, S. Kathiresan, S. Keildson, K. Kiryluk, M. Kubo, J. Y. Lee, L. Liang, R. P. Lifton, B. Ma, S. A. McCarroll, A. J. McKnight, J. L. Min, M. F. Moffatt, G. W. Montgomery, J. M. Murabito, G. Nicholson, D. R. Nyholt, Y. Okada, J. R. B. Perry, R. Dorajoo, E. Reinmaa, R. M. Salem, N. Sandholm, R. A. Scott, L. Stolk, A. Takahashi, F. M. van 't Hooft, A. A. E. Vinkhuyzen, H. J. Westra, W. Zheng, K. T. Zondervan, A. C. Heath, D. Arveiler, S. J. L. Bakker, J. Beilby, R. N. Bergman, J. Blangero, P. Bovet, H. Campbell, M. J. Caulfield, G. Cesana, A. Chakravarti, D. I. Chasman, P. S. Chines, F. S. Collins, D. C. Crawford, L. A. Cupples, D. Cusi, J. Danesh, U. de Faire, H. M. den Ruijter, A. F. Dominiczak, R. Erbel, J. Erdmann, J. G. Eriksson, M. Farrall, S. B. Felix, E. Ferrannini, J. Ferrieres, I. Ford, N. G. Forouhi, T. Forrester, O. H. Franco, R. T. Gansevoort, P. V. Gejman, C. Gieger, O. Gottesman, V. Gudnason, U. Gyllensten, A. S. Hall, T. B. Harris, A. T. Hattersley, A. A. Hicks, L. A. Hindorff, A. D. Hingorani, A. Hofman, G. Homuth, G. K. Hovingh, S. E. Humphries, S. C. Hunt, E. Hypponen, T. Illig, K. B. Jacobs, M. R. Jarvelin, K. H. Jockel, B. Johansen, P. Jousilahti, J. W. Jukema, A. M. Jula, J. Kaprio, J. J. P. Kastelein, S. M. Keinanen-Kiukaanniemi, L. A. Kiemeney, P. Knekt, J. S. Kooner, C. Kooperberg, P. Kovacs, A. T. Kraja, M. Kumari, J. Kuusisto, T. A. Lakka, C. Langenberg, L. L. Marchand, T. Lehtimaki, V. Lyssenko, S. Mannisto, A. Marette, T. C. Matise, C. A. McKenzie, B. McKnight, F. L. Moll, A. D. Morris, A. P. Morris, J. C. Murray, M. Nelis, C. Ohlsson, A. J. Oldehinkel, K. K. Ong, P. A. F. Madden, G. Pasterkamp, J. F. Peden, A. Peters, D. S. Postma, P. P. Pramstaller, J. F. Price, L. Qi, O. T. Raitakari, T. Rankinen, D. C. Rao, T. K. Rice, P. M. Ridker, J. D. Rioux, M. D. Ritchie, I. Rudan, V. Salomaa, N. J. Samani, J. Saramies, M. A. Sarzynski, H. Schunkert, P. E. H. Schwarz, P. Sever, A. R. Shuldiner, J. Sinisalo, R. P. Stolk, K. Strauch, A. Tonjes, D. A. Tregouet, A. Tremblay, E. Tremoli, J. Virtamo, M. C. Vohl, U. Volker, G. Waeber, G. Willemsen, J. C. Witteman, M. C. Zillikens, L. S. Adair, P. Amouyel, F. W. Asselbergs, T. L. Assimes, M. Bochud, B. O. Boehm, E. Boerwinkle, S. R. Bornstein, E. P. Bottinger, C. Bouchard, S. Cauchi, J. C. Chambers, S. J. Chanock, R. S. Cooper, P. I. W. de Bakker, G. Dedoussis, L. Ferrucci, P. W. Franks, P. Froguel, L. C. Groop, C. A. Haiman, A. Hamsten, J. Hui, D. J. Hunter, K. Hveem, R. C. Kaplan, M. Kivimaki, D. Kuh, M. Laakso, Y. Liu, N. G. Martin, W. Marz, M. Melbye, A. Metspalu, S. Moebus, P. B. Munroe, I. Njolstad, B. A. Oostra, C. N. A. Palmer, N. L. Pedersen, M. Perola, L. Perusse, U. Peters, C. Power, T. Quertermous, R. Rauramaa, F. Rivadeneira, T. E. Saaristo, D. Saleheen, N. Sattar, E. E. Schadt, D. Schlessinger, P. E. Slagboom, H. Snieder, T. D. Spector, U. Thorsteinsdottir, M. Stumvoll, J. Tuomilehto, A. G. Uitterlinden, M. Uusitupa, P. van der Harst, M. Walker, H. Wallaschofski, N. J. Wareham, H. Watkins, D. R. Weir, H. E. Wichmann, J. F. Wilson, P. Zanen, I. B. Borecki, P. Deloukas, C. S. Fox, I. M. Heid, J. R. O'Connell, D. P. Strachan, K. Stefansson, C. M. van Duijn, G. R. Abecasis, L. Franke, T. M. Frayling, M. I. McCarthy, P. M. Visscher, A. Scherag, C. J. Willer, M. Boehnke, K. L. Mohlke, C. M. Lindgren, J. S. Beckmann, I. Barroso, K. E. North, E. Ingelsson, J. N. Hirschhorn, R. J. F. Loos and E. K. Speliotes (2015). "Genetic studies of body mass index yield new insights for obesity biology." Nature **518**(7538): 197-206.

Maalouf, M., J. M. Rho and M. P. Mattson (2009). "The neuroprotective properties of calorie restriction, the ketogenic diet, and ketone bodies." Brain Res Rev **59**(2): 293-315.

Maletinska, L., V. Nagelova, A. Ticha, J. Zemenova, Z. Pirnik, M. Holubova, A. Spolcova, B. Mikulaskova, M. Blechova, D. Sykora, Z. Lacinova, M. Haluzik, B. Zelezna and J. Kunes (2015). "Novel lipidized analogs of prolactin-releasing peptide have prolonged half-lives and exert anti-obesity effects after peripheral administration." Int J Obes (Lond) **39**(6): 986-993.

Mantzoros, C. S., M. Ozata, A. B. Negrao, M. A. Suchard, M. Ziotopoulou, S. Caglayan, R. M. Elashoff, R. J. Cogswell, P. Negro, V. Liberty, M. L. Wong, J. Veldhuis, I. C. Ozdemir, P. W. Gold, J. S. Flier and J. Licinio (2001). "Synchronicity of frequently sampled thyrotropin (TSH) and leptin concentrations in healthy adults and leptin-deficient subjects: evidence for possible partial TSH regulation by leptin in humans." J Clin Endocrinol Metab **86**(7): 3284-3291.

Maruyama, M., H. Matsumoto, K. Fujiwara, C. Kitada, S. Hinuma, H. Onda, M. Fujino and K. Inoue (1999). "Immunocytochemical localization of prolactin-releasing peptide in the rat brain." Endocrinology **140**(5): 2326-2333.

Milligan, G., S. Wilson and J. F. Lopez-Gimenez (2005). "The specificity and molecular basis of alpha1-adrenoceptor and CXCR chemokine receptor dimerization." J Mol Neurosci **26**(2-3): 161-168.

Minokoshi, Y., Y. B. Kim, O. D. Peroni, L. G. Fryer, C. Muller, D. Carling and B. B. Kahn (2002). "Leptin stimulates fatty-acid oxidation by activating AMP-activated protein kinase." Nature **415**(6869): 339-343.

Mochiduki, A., T. Takeda, S. Kaga and K. Inoue (2010). "Stress response of prolactin-releasing peptide knockout mice as to glucocorticoid secretion." J Neuroendocrinol **22**(6): 576-584.

Montague, C. T., I. S. Farooqi, J. P. Whitehead, M. A. Soos, H. Rau, N. J. Wareham, C. P. Sewter, J. E. Digby, S. N. Mohammed, J. A. Hurst, C. H. Cheetham, A. R. Earley, A. H. Barnett, J. B. Prins and S. O'Rahilly (1997). "Congenital leptin deficiency is associated with severe early-onset obesity in humans." Nature **387**(6636): 903-908.

Nelson, M. R., H. Tipney, J. L. Painter, J. Shen, P. Nicoletti, Y. Shen, A. Floratos, P. C. Sham, M. J. Li, J. Wang, L. R. Cardon, J. C. Whittaker and P. Sanseau (2015). "The support of human genetic evidence for approved drug indications." Nat Genet **47**(8): 856-860.

Noble, E. E., C. J. Billington, C. M. Kotz and C. Wang (2011). "The lighter side of BDNF." Am J Physiol Regul Integr Comp Physiol **300**(5): R1053-1069.

Orava, J., P. Nuutila, M. E. Lidell, V. Oikonen, T. Noponen, T. Viljanen, M. Scheinin, M. Taittonen, T. Niemi, S. Enerback and K. A. Virtanen (2011). "Different metabolic responses of human brown adipose tissue to activation by cold and insulin." Cell Metab **14**(2): 272-279.

Osugi, T., K. Ukena, S. A. Sower, H. Kawauchi and K. Tsutsui (2006). "Evolutionary origin and divergence of PQRFamide peptides and LPXRFamide peptides in the RFamide peptide family. Insights from novel lamprey RFamide peptides." FEBS J **273**(8): 1731-1743.

Ouellet, V., S. M. Labbe, D. P. Blondin, S. Phoenix, B. Guerin, F. Haman, E. E. Turcotte, D. Richard and A. C. Carpentier (2012). "Brown adipose tissue oxidative metabolism contributes to energy expenditure during acute cold exposure in humans." J Clin Invest **122**(2): 545-552.

Ozata, M., I. C. Ozdemir and J. Licinio (1999). "Human leptin deficiency caused by a missense mutation: multiple endocrine defects, decreased sympathetic tone, and immune system dysfunction indicate new targets for leptin action, greater central than peripheral resistance to the effects of

leptin, and spontaneous correction of leptin-mediated defects." J Clin Endocrinol Metab **84**(10): 3686-3695.

Pearce, L. R., N. Atanassova, M. C. Banton, B. Bottomley, A. A. van der Klaauw, J. P. Revelli, A. Hendricks, J. M. Keogh, E. Henning, D. Doree, S. Jeter-Jones, S. Garg, E. G. Bochukova, R. Bounds, S. Ashford, E. Gayton, P. C. Hindmarsh, J. P. Shield, E. Crowne, D. Barford, N. J. Wareham, S. O'Rahilly, M. P. Murphy, D. R. Powell, I. Barroso and I. S. Farooqi (2013). "KSR2 mutations are associated with obesity, insulin resistance, and impaired cellular fuel oxidation." Cell **155**(4): 765-777.

Pelleymounter, M. A., M. J. Cullen, M. B. Baker, R. Hecht, D. Winters, T. Boone and F. Collins (1995). "Effects of the obese gene product on body weight regulation in ob/ob mice." Science **269**(5223): 540-543.

Peretti, D., A. Bastide, H. Radford, N. Verity, C. Molloy, M. G. Martin, J. A. Moreno, J. R. Steinert, T. Smith, D. Dinsdale, A. E. Willis and G. R. Mallucci (2015). "RBM3 mediates structural plasticity and protective effects of cooling in neurodegeneration." Nature **518**(7538): 236-239.

Perkins, A. C., D. S. Mshelia, M. E. Symonds and M. Sathekge (2013). "Prevalence and pattern of brown adipose tissue distribution of 18F-FDG in patients undergoing PET-CT in a subtropical climatic zone." Nucl Med Commun **34**(2): 168-174.

Rahman, M., S. Muhammad, M. A. Khan, H. Chen, D. A. Ridder, H. Muller-Fielitz, B. Pokorna, T. Vollbrandt, I. Stolting, R. Nadrowitz, J. G. Okun, S. Offermanns and M. Schwaninger (2014). "The beta-hydroxybutyrate receptor HCA2 activates a neuroprotective subset of macrophages." Nat Commun **5**: 3944.

Redman, L. M., L. K. Heilbronn, C. K. Martin, L. de Jonge, D. A. Williamson, J. P. Delany and E. Ravussin (2009). "Metabolic and behavioral compensations in response to caloric restriction: implications for the maintenance of weight loss." PLoS One **4**(2): e4377.

Rezai-Zadeh, K., S. Yu, Y. Jiang, A. Laque, C. Schwartzenburg, C. D. Morrison, A. V. Derbenev, A. Zsombok and H. Munzberg (2014). "Leptin receptor neurons in the dorsomedial hypothalamus are key regulators of energy expenditure and body weight, but not food intake." Mol Metab **3**(7): 681-693.

Ricci, M. R., S. K. Fried and K. D. Mittleman (2000). "Acute cold exposure decreases plasma leptin in women." Metabolism **49**(4): 421-423.

Rosenbaum, M., M. Sy, K. Pavlovich, R. L. Leibel and J. Hirsch (2008). "Leptin reverses weight loss-induced changes in regional neural activity responses to visual food stimuli." J Clin Invest **118**(7): 2583-2591.

Ruf, T. and F. Geiser (2015). "Daily torpor and hibernation in birds and mammals." Biol Rev Camb Philos Soc **90**(3): 891-926.

Samson, W. K., Z. T. Resch and T. C. Murphy (2000). "A novel action of the newly described prolactin-releasing peptides: cardiovascular regulation." Brain Res **858**(1): 19-25.

Savory, J. G., G. G. Prefontaine, C. Lamprecht, M. Liao, R. F. Walther, Y. A. Lefebvre and R. J. Hache (2001). "Glucocorticoid receptor homodimers and glucocorticoid-mineralocorticoid receptor heterodimers form in the cytoplasm through alternative dimerization interfaces." Mol Cell Biol **21**(3): 781-793.

Schwartz, M. W., R. J. Seeley, S. C. Woods, D. S. Weigle, L. A. Campfield, P. Burn and D. G. Baskin (1997). "Leptin increases hypothalamic pro-opiomelanocortin mRNA expression in the rostral arcuate nucleus." Diabetes **46**(12): 2119-2123.

Simonds, S. E., J. T. Pryor, E. Ravussin, F. L. Greenway, R. Dileone, A. M. Allen, J. Bassi, J. K. Elmquist, J. M. Keogh, E. Henning, M. G. Myers, Jr., J. Licinio, R. D. Brown, P. J. Enriori, S. O'Rahilly, S. M. Sternson, K. L. Grove, D. C. Spanswick, I. S. Farooqi and M. A. Cowley (2014). "Leptin mediates the increase in blood pressure associated with obesity." Cell **159**(6): 1404-1416.

Skarulis, M. C., F. S. Celi, E. Mueller, M. Zemskova, R. Malek, L. Hugendubler, C. Cochran, J. Solomon, C. Chen and P. Gorden (2010). "Thyroid hormone induced brown adipose tissue and amelioration of diabetes in a patient with extreme insulin resistance." J Clin Endocrinol Metab **95**(1): 256-262.

Smith, C. A., E. J. Want, G. O'Maille, R. Abagyan and G. Siuzdak (2006). "XCMS: processing mass spectrometry data for metabolite profiling using nonlinear peak alignment, matching, and identification." Anal Chem **78**(3): 779-787.

Sorensen, T. I., C. Holst and A. J. Stunkard (1998). "Adoption study of environmental modifications of the genetic influences on obesity." Int J Obes Relat Metab Disord **22**(1): 73-81.

Sunter, D., A. K. Hewson, S. Lynam and S. L. Dickson (2001). "Intracerebroventricular injection of neuropeptide FF, an opioid modulating neuropeptide, acutely reduces food intake and stimulates water intake in the rat." Neurosci Lett **313**(3): 145-148.

Szuhany, K. L., M. Bugatti and M. W. Otto (2015). "A meta-analytic review of the effects of exercise on brain-derived neurotrophic factor." J Psychiatr Res **60**: 56-64.

Takayanagi, Y., H. Matsumoto, M. Nakata, T. Mera, S. Fukusumi, S. Hinuma, Y. Ueta, T. Yada, G. Leng and T. Onaka (2008). "Endogenous prolactin-releasing peptide regulates food intake in rodents." J Clin Invest **118**(12): 4014-4024.

Takayasu, S., T. Sakurai, S. Iwasaki, H. Teranishi, A. Yamanaka, S. C. Williams, H. Iguchi, Y. I. Kawasawa, Y. Ikeda, I. Sakakibara, K. Ohno, R. X. Ioka, S. Murakami, N. Dohmae, J. Xie, T. Suda, T. Motoike, T. Ohuchi, M. Yanagisawa and J. Sakai (2006). "A neuropeptide ligand of the G protein-coupled receptor GPR103 regulates feeding, behavioral arousal, and blood pressure in mice." Proc Natl Acad Sci U S A **103**(19): 7438-7443.

Tan, K., I. D. Pogozheva, G. S. Yeo, D. Hadaschik, J. M. Keogh, C. Haskell-Leuvano, S. O'Rahilly, H. I. Mosberg and I. S. Farooqi (2009). "Functional characterization and structural modeling of obesity associated mutations in the melanocortin 4 receptor." Endocrinology **150**(1): 114-125.

Tartaglia, L. A., M. Dembski, X. Weng, N. Deng, J. Culpepper, R. Devos, G. J. Richards, L. A. Campfield, F. T. Clark, J. Deeds, C. Muir, S. Sanker, A. Moriarty, K. J. Moore, J. S. Smutko, G. G. Mays, E. A. Wool,

C. A. Monroe and R. I. Tepper (1995). "Identification and expression cloning of a leptin receptor, OB-R." Cell **83**(7): 1263-1271.

Toien, O., J. Blake, D. M. Edgar, D. A. Grahn, H. C. Heller and B. M. Barnes (2011). "Hibernation in black bears: independence of metabolic suppression from body temperature." Science **331**(6019): 906-909.

Trayhurn, P., M. E. Thomas, J. S. Duncan and D. V. Rayner (1995). "Effects of fasting and refeeding on ob gene expression in white adipose tissue of lean and obese (oblob) mice." FEBS Lett **368**(3): 488-490.

Trayhurn, P., P. L. Thurlby and W. P. James (1977). "Thermogenic defect in pre-obese ob/ob mice." Nature **266**(5597): 60-62.

Twisk, J. W. R., L. Bosman, H. T, R. J, W. M and H. M (2018). "Different ways to estimate treatment effects in randomised controlled trials." Contemp Clin Trials Commun **10**: 80-85.

Uchida, K., D. Kobayashi, G. Das, T. Onaka, K. Inoue and K. Itoi (2010). "Participation of the prolactin-releasing peptide-containing neurones in caudal medulla in conveying haemorrhagic stress-induced signals to the paraventricular nucleus of the hypothalamus." J Neuroendocrinol **22**(1): 33-42.

van der Klaauw, A. A., J. M. Keogh, E. Henning, C. Stephenson, S. Kelway, V. M. Trowse, N. Subramanian, S. O'Rahilly, P. C. Fletcher and I. S. Farooqi (2016). "Divergent effects of central melanocortin signalling on fat and sucrose preference in humans." Nat Commun **7**: 13055.

van der Lans, A. A., M. J. Vosselman, M. J. Hanssen, B. Brans and W. D. van Marken Lichtenbelt (2016). "Supraclavicular skin temperature and BAT activity in lean healthy adults." J Physiol Sci **66**(1): 77-83.

van Marken Lichtenbelt, W. D., P. Schrauwen, S. van De Kerckhove and M. S. Westerterp-Plantenga (2002). "Individual variation in body temperature and energy expenditure in response to mild cold." Am J Physiol Endocrinol Metab **282**(5): E1077-1083.

Virtanen, K. A., M. E. Lidell, J. Orava, M. Heglind, R. Westergren, T. Niemi, M. Taittonen, J. Laine, N. J. Savisto, S. Enerback and P. Nuutila (2009). "Functional brown adipose tissue in healthy adults." N Engl J Med **360**(15): 1518-1525.

Walsh, B. H., D. I. Broadhurst, R. Mandal, D. S. Wishart, G. B. Boylan, L. C. Kenny and D. M. Murray (2012). "The metabolomic profile of umbilical cord blood in neonatal hypoxic ischaemic encephalopathy." PLoS One **7**(12): e50520.

Wang, T. J., M. G. Larson, R. S. Vasan, S. Cheng, E. P. Rhee, E. McCabe, G. D. Lewis, C. S. Fox, P. F. Jacques, C. Fernandez, C. J. O'Donnell, S. A. Carr, V. K. Mootha, J. C. Florez, A. Souza, O. Melander, C. B. Clish and R. E. Gerszten (2011). "Metabolite profiles and the risk of developing diabetes." Nat Med **17**(4): 448-453.

Wardle, J., S. Carnell, C. M. Haworth and R. Plomin (2008). "Evidence for a strong genetic influence on childhood adiposity despite the force of the obesogenic environment." Am J Clin Nutr **87**(2): 398-404.

Watanabe, A., S. Okuno, M. Okano, S. Jordan, K. Aihara, T. K. Watanabe, Y. Yamasaki, H. Kitagawa, K. Sugawara and S. Kato (2007). "Altered emotional behaviors in the diabetes mellitus OLETF type 1 congenic rat." Brain Res **1178**: 114-124.

Webb, G. P., S. A. Jagot and M. E. Jakobson (1982). "Fasting-induced torpor in Mus musculus and its implications in the use of murine models for human obesity studies." Comp Biochem Physiol A Comp Physiol **72**(1): 211-219.

Yamada, T., A. Mochiduki, Y. Sugimoto, Y. Suzuki, K. Itoi and K. Inoue (2009). "Prolactin-releasing peptide regulates the cardiovascular system via corticotrophin-releasing hormone." J Neuroendocrinol **21**(6): 586-593.

Yen, K., T. T. Le, A. Bansal, S. D. Narasimhan, J. X. Cheng and H. A. Tissenbaum (2010). "A comparative study of fat storage quantitation in nematode Caenorhabditis elegans using label and label-free methods." PLoS One **5**(9).

Young, P., J. R. Arch and M. Ashwell (1984). "Brown adipose tissue in the parametrial fat pad of the mouse." FEBS Lett **167**(1): 10-14.

Zhang, Y., R. Proenca, M. Maffei, M. Barone, L. Leopold and J. M. Friedman (1994). "Positional cloning of the mouse obese gene and its human homologue." Nature **372**(6505): 425-432.

Zhao, X., X. Gang, Y. Liu, C. Sun, Q. Han and G. Wang (2016). "Using Metabolomic Profiles as Biomarkers for Insulin Resistance in Childhood Obesity: A Systematic Review." J Diabetes Res **2016**: 8160545.